THE UNIVERSITY
of EDINBURGH

Role of the Arabidopsis Glucose Sensor Hexokinase1 (HXK1) in Seedling Establishment

Ashwin L. Ganpudi

Thesis submitted for the Doctor of Philosophy degree

School of Biological Science

The University of Edinburgh

(2018)

Success is a science.

If you have the conditions, you get the result.

Oscar Wilde

Abstract

Light energy serve as primary substrates for photosynthetic sugar production in plant metabolic maintenance. In addition, light also functions as a crucial environmental cue initiating a series of signal transduction cascades downstream to the photoreceptors. Limited knowledge exists on the molecular connections integrating the metabolic and photoreceptor signalling pathways.

The primary focus of this thesis is the plant glucose receptor Hexokinase1 (HXK1). Arabidopsis HXK1 performs a dual function 1) an enzymatic role in glycolysis catalysing glucose phosphorylation to generate glucose-6-phosphate (G6P) and 2) a transcriptional repressor role in response to exogenous sugar. While the enzymatic role required for ATP production during respiration is conserved across biological systems, the sugar induced nuclear signalling role has only been identified in yeast and Arabidopsis.

In this thesis, I show that HXK1 operates during nutrient limiting conditions such as extended periods of darkness or suboptimal light in seedlings. A first-ever RNAseq enabled us to gain insights into the mutant transcriptome. Energy demanding pathways were downregulated and carbon starvation induced Branched Chain Amino Acid (BCAA) degradation pathway is upregulated as an alternate energy source. Supplying Glucose-6-Phosphate (G6P – HXK1 enzymatic endproduct) restored the mutant phenotype and the C starvation response during nutrient limited conditions. This highlights the requirement of HXK1 enzyme rather than the signalling component during seedling establishment. Nuclear HXK1 operates as a transcriptional repressor in response to exogenous sugar. It is postulated to function during feedback inhibition

of photosynthetic genes. However, our data indicates that this does not appear to be the case when endogenous sugars are naturally elevated in seedlings.

Further, I present preliminary data on the potential feedback regulation by HXK1Overpression (HXK1OX) in blue and red light signalling pathway. HXK1 exerts a negative control on blue light mediated photomorphogenesis. Red light negates this effect in a PHYB dependent manner. Although the transcriptomes are reflective of the phenotype, the molecular mechanism behind this response is unknown. Taken together, my thesis discovers novel facets of HXK1 during seedling establishment

Acknowledgements

Big thanks to my inspiring and dynamic advisor Dr. Karen Halliday for her immense intellectual support and guidance throughout the programme. Thank you for putting up with me.

Thanks to all the members of the Halliday lab (past and present) - Andrew, Johanna, Karine, James, Ammad, Ejas, Uriel, Gabi, Deyue, Kelly, Eve and Daniel for all their invaluable help, advice and friendship. I wish to thank all my other friends, both on and off -campus for making my stay memorable and enjoyable.

Indebted to the Darwin Trust of Edinburgh for strong financial support. Will dearly miss vibrant Edinburgh and its trademark dreich weather.

Thanks to my parents, family members and all my friends back home for their support.

Declarations

This thesis contains original data based on following publications:

- Krahmer J, **Ganpudi A**, Abbas A, Romanowski A, Halliday KJ (2018) Phytochrome, Carbon Sensing, Metabolism, and Plant Growth Plasticity. Plant Physiol. 176(2):1039-1048

- Seaton D, Toledo-Ortiz G, **Ganpudi A**, Kubota A, Imaizumi T, Halliday KJ (2018) Dawn and photoperiod sensing by phytochrome A. Proc. Natl. Acad. Sci. USA *(in press)*

I hereby declare that this thesis is my own work except where explicitly stated.
No part of this thesis has been submitted for a professional qualification or a degree at the University of Edinburgh or any other university.

Ashwin Ganpudi

(August 2018)

Table of Contents

Abstract……II
Acknowledgements…….....IV
Declarations……V
List of Figures……IX

CHAPTER I - Introduction

1.1. Light – A crucial cue for sustenance……..1
1.2. Light signalling mediated seedling establishment…….2
1.2.1. Molecular description of red light photoreceptors – Phytochromes……2
1.2.2. Phytochrome – Phytochrome Interacting Factor (PIF) signalling……...5
1.2.3. Role of COP1-SPA and DET1 during seedling photomorphogenesis…….8
1.2.4. Positive regulators of light signalling……11
1.2.5. Other key signalling components mediating seedling establishment……12
1.3. Energy mediated seedling establishment…….18
1.4. Glucose signalling……19
1.4.1. Hexokinase1 – An introduction to the glucose sensor……...21
1.4.2. SnRK1 and TOR Kinase.……...24
1.4.3. Role of HXK1, SnRK1 and TOR in seedling establishment…….26
1.5. Light-sugar signalling interface……...27
1.6. Aims of the thesis…….30

CHAPTER 2 - Experimental Protocols

2.1. Plant materials and growth conditions…….33
2.2. Seedling and adult plant growth parameter…….33
2.3. Gene expression analysis…….34
2.3.1. qRT-PCR……...34
2.3.2. RNAseq analysis……35
2.3.3. DNA microarrays analysis…….35

2.4. Protein extraction and immunoblots……36
2.5. Starch and sugar quantification……37

CHAPTER 3 - Critical role of Hexokinase1 (HXK1) during seedling establishment

3.1.Introduction……...39
3.2. Results……..42
3.2.1. HXK1 Operates in the Dark and Low Light in Seedlings – Continuous light…….……...42
3.2.2. HXK1 Operates in the Dark and Low Light in Seedlings – Photoperiods…44
3.2.3. RNAseq - HXK1 is required for nutrient resource management……...46
3.2.3.1 RNAseq analysis reveals down regulation of energy demanding processes in *gin2*……49
3.2.3.2. RNAseq analysis – C starvation response is upregulated in the *gin2* mutants…….....51
3.2.4. The enzymatic and not the signalling role of HXK1 is required for seedling establishment……..54
3.2.5. Glucose-6-Phosphate (G6P) application rescues *gin2* starvation response...57
3.2.6. 94% of the chloroplast transcriptome is altered in *gin2* mutants……...58
3.2.7. Effect of photosynthetic Inhibition in *gin2* mutants……..60
3.2.8. Hexokinase1 operates independent of the PIFs during seedling establishment……..61
3.2.9. HXK1 is not required for feedback mediated photosynthetic inhibition…...67
3.3. Discussion……70

CHAPTER 4 - Effect of HXK1 overexpression in light signalling

4.1. Introduction……..76
4.2. Results……..78
4.2.1. Effect of monochromatic light on HXK1 during seedling photomorphogenesis……..78

4.2.2. Effect of B and R light on HXK1 transcript and protein abundance…….81
4.2.3. HXK1OX transcriptome in B and B+R…….82
4.2.4. Transcriptome clustering……...87
4.2.3.1. Cluster analysis……90
4.2.5. Effect of PHYB loss in HXK1OX…….....92
4.3. Discussion……96

CHAPTER 5 - A role for Constitutive Photomorphogenic1 (COP1) and De- etiolated1 (DET1) in sugar signalling

5.1. Introduction – COP1 and DET1……101
5.2. Results……104
5.2.1. *cop1* and *det1* mutant seedlings are sugar insensitive……104
5.2.2. *cop1* and *det1* adult mutant plants are sugar hypersensitive ……...105
5.2.3. *cop1/det1* sugar hypersensitivity is mimicked under increased light conditions……112
5.2.4. Metabolite analysis in adult mutants……113
5.3. Discussion……..114

CHAPTER 6 - Summary and general discussion……121

CHAPTER 7 – References……127

Appendix ……139

List of Figures

CHAPTER 1

Fig.1.1: Absorption spectra for the three classes of Arabidopsis light photoreceptors……..3
Fig.1.2: Simplified illustration of phytochrome activation and inactivation…….....4
Fig.1.3: Molecular components and processes during dark to light transition. ……...16
Fig.1.4: Regulatory pathways of photosynthesis derived sugars……..20
Fig.1.5: Dual role of Arabidopsis Hexokinase1……..….23

CHAPTER 3

Fig.3.1: Seedling morphology of the HXK1 family – Dark and continuous light…….....43
Fig.3.2: Seedling morphology of the HXK1 family – Photoperiods…….45
Fig.3.3: HXK1 diurnal transcript and protein abundance…….46
Fig.3.4: RNAseq Analysis – Down regulated genes……49
Fig.3.5: Glucose content and etiolated hypocotyl epidermal cell length/cell number……..50
Fig.3.6: RNAseq Analysis – Upregulated genes…….....52
Fig.3.7: Comparison between *gin2* upregulated genes and C starvation genes……....53
Fig.3.8: Phenotypic analysis of *gin2* mutants to glucose and G6P…….....56
Fig.3.9: G6P application rescues *gin2* starvation response……..……...58
Fig.3.10: 94% of the chloroplast transcriptome is upregulated in *gin2* mutants……..…59
Fig.3.11: Effect of photosynthetic inhibition in *gin2* mutants – DCMU application……..61
Fig.3.12: Phenotypic analysis of *pifQ* and *gin2* mutants…….....62
Fig.3.13: Molecular analysis of *pifQ* and *gin2* mutants…….……..64
Fig.3.14: Comparison between the *gin2* transcriptome and direct PIF targets……....66
Fig.3.15: HXK1 is not required for feedback mediated photosynthetic inhibition……69

CHAPTER 4

Fig.4.1: Effect of monochromatic light on HXK1 mutants and OX…….80
Fig.4.2: HXK1 transcript and protein abundance in various light treatments……...81
Fig.4.3: Genes differentially altered in transcript expression in the HXK1OX……82

Fig.4.4: Gene Ontology (GO) – Up and downregulated genes in B……..……...….83
Fig.4.5: Gene Ontology (GO) – Up and downregulated genes in B+R…….……84
Fig.4.6: Comparison between genes regulated by CRY and HXK1OX in B……85
Fig.4.7: Comparison between B and B+R and CRY regulated genes.……..86
Fig.4.8: Pictorial representation of gene clustering……..88
Fig.4.9: Graphical representation of LogFC expression levels of individual cluster genes…..89
Fig.4.10: Energy demanding pathways significantly altered in B is restored to Wt in B+R….91
Fig.4.11: Effect of PhyB loss in HXK1OX: B, R and B+R…….93
Fig.4.12: Genetic analysis of phyb-9 35S:HXK1…….....95
Fig.4.13: Model depicting HXK1 action on B light signalling. R light negates that effect…...97

CHAPTER 5

Fig.5.1: COP1 and DET1 involvement in multiple signalling pathways……....103
Fig.5.2: *cop1/det1/pifQ* seedling response to sugar……105
Fig.5.3: *cop1/det1* adult plant response to sucrose – Growth response…….....107
Fig.5.4: *cop1/det1* adult plant response to sucrose – Leaf development…….108
Fig.5.5: *cop1/det1* adult plant response to glucose…….....110
Fig.5.6: *pifQ* adult plant response to sugar (sucrose and glucose)……..…111
Fig.5.7: *cop1/det1/pifQ* adult plant response to increasing light intensities……...113
Fig.5.8: Metabolite levels in wildtype, *cop1, det1* and *pifQ* mutants……..114
Fig.5.9: Speculative working model……..120

CHAPTER I- INTRODUCTION

Light mediated photoreceptor and metabolic signal transduction

In the following section, I summarise briefly, literature pertaining to light mediated photoreceptor and photosynthate sugar signalling. Its interface with other endogenous and exogenous signals with particular emphasis during seedling establishment is introduced. Finally, I conclude this chapter by highlighting recent emerging data on the cross talk between both these light dependent pathways and outline the goals of this study.

1.1. Light – A crucial cue for sustenance

Rooted firmly to the soil, plants have acquired a high degree of developmental plasticity to optimise and fine-tune growth and reproduction in response to their ambient environment. Plants employ a range of sensory systems to perceive and transduce external signals. Light, in particular functions as one such crucial environmental cue. In addition to being the primary substrate for photosynthesis, light regulates multiple developmental processes such as seed germination, seedling establishment, meristem activation for leaf and root development, leaf expansion, stem elongation, phototropism, neighbour detection, biological clock, flowering time, etc (Li et al. 2011). The duration and intensity of light also enables plants to sense seasons via temperatures and photoperiods thereby accordingly strategizing growth and reproduction. The most dramatic response to light is observed at a young stage when seedlings transition from below soil surface to above. Under sub-optimal light conditions in the soil, seedlings exhibit an etiolated growth pattern characterized by an

elongated hypocotyl, undeveloped cotyledons and a limited root system (skotomorphogenesis). On perceiving sunlight, hypocotyl growth ceases, cotyledons expand to photosynthesise and stem cell populations at root and shoot apices are activated (photomorphogenesis) (Arsovski et al. 2012; Nemhauser, 2008). This photoreceptor dependent switch from skotomorphogenic to photomorphogenic growth massively re-programmes the *Arabidopsis* transcriptome (Ma et al. 2001). In this brief time, a plant matures from a seed reserve-dependent embryo to a self-sufficient photoautotroph. The Arabidopsis seedling hypocotyl growth pattern has emerged as an exemplary phenotypic readout to elucidate molecular signalling events in response to the external environment (particularly light and temperature) or endogenous cues. Plant photoreceptors are implicated in inhibition of hypocotyl elongation during photomorphogenesis and the confluence of complex pathways from light perception, signal transduction to downstream gene transcription and posttranslational events regulating this phenotype are well characterised.

1.2. Light signalling mediated seedling establishment

1.2.1. Molecular description of red light photoreceptors - Phytochromes

Plants are sophisticatedly equipped to monitor quality, quantity, duration and direction of the incoming light signals to accordingly alter their genetic programmes. Light is perceived by a complex array of photoreceptors defined by the colours of light they absorb. In Arabidopsis cryptochromes (Cry1–2), phototropins (Phot1–2), three ZTL-type receptors absorb blue/UV-A light (320-500 nm), the more recently discovered UVR8 absorbs UV-B light (280 – 320 nm) and the phytochromes (PhyA–E) absorb red/far-red light (600-750 nm) (Fig1.1). Genetic, biochemical and molecular

analysis of these 13 photoreceptor genes indicate that they share complex synergistic, antagonistic, and redundant relationships (Li et al. 2011).

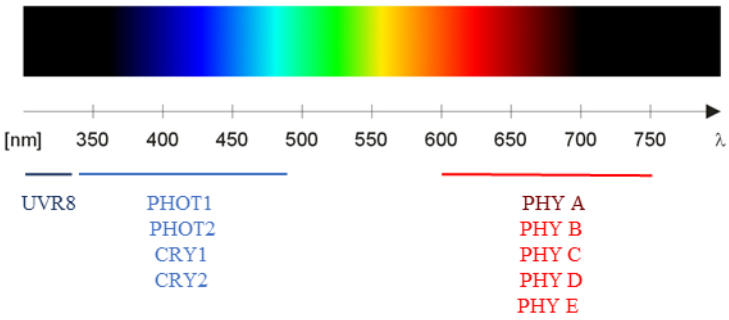

Fig1.1: Absorption spectra for the three classes of *Arabidopsis* light photoreceptors. UV-B absorbing UVR8, UV-A/blue light absorbing cryptochromes/phototropins and red/far-red absorbing phytochromes.

There are five distinct phytochromes in Arabidopsis, designated PHYTOCHROMEA (PHYA) to PHYE. PHYA, the type I far-red light photoreceptor is light labile and PHYB – PHYE, the type II red light photoreceptors are light stable. PHYA is most abundant in dark/far-red grown seedlings and its protein levels drop rapidly on exposure to red or white light. In light grown plants, PHYB is the most abundant phytochrome, whereas PHYC – PHYE are less abundant (Li et al. 2011). Phytochromes are soluble homodimers synthesized in the cytosol in their inactive form. The molecular mass of the apoprotein monomer is approximately 125 kDa. Phytochrome apoproteins are synthesized in the cytosol, where they assemble with a linear tetrapyrrole chromophore, phytochromobillin. The phytochrome molecule comprise of an N-terminal domain (~70 kDa) and a C-terminal domain (~55 kDa), connected by a flexible hinge region.

Phytochromes are synthesized in the Pr form that has the peak of absorption in red light. Phytochromes can interconvert between two relatively stable conformers: a

Red (R) light-absorbing inactive Pr form (λmax = 660) and a Far-Red (FR) light-absorbing active Pfr form (λmax = 730). Upon light irradiation, phytochromes are converted to the biologically active Pfr form and translocate to the nucleus. Under saturating light, a photoequilibrium is established between Pr and Pfr and the proportion of Pfr depends on the R:FR. Provision of a far-red supplement to rapidly convert Pfr to Pr has been exploited extensively as an experimental tool in labs to inactivate phytochrome activity. In addition, the thermally unstable Pfr can be reversed back to Pr in a light-independent relaxation process called dark reversion (Li et al. 2011; Viczian et al. 2016).

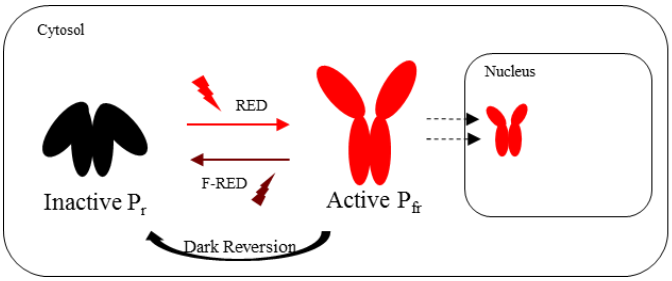

Fig1.2: Simplified illustration of phytochromes activation by red and inactivation by Far-red light and dark. Activated Pfr form translocate to the nucleus from the cytosol.

Type I photoreceptor PhyA mediates two types of responses: very low fluence response (VLFR < 1µmol m^{-2} s^{-1}) detecting low light conditions that type II phytochromes cannot distinguish from darkness, and the high irradiance response (HIR) requiring continuous high photon fluence of far-red light. Since PHYA functions as an FR and dim light sensor, it shares little functional redundancy with the other phytochromes. Type II photoreceptors (predominantly PHYB) mediate the Low Fluence Response (LFR 10–1000µmol m^{-2} s^{-1}) which is characterized by its red (R)/far-red (FR) reversibility and requires red light for induction (Li et al. 2011; Viczian et al. 2016).

1.2.2. Phytochrome – Phytochrome Interacting Factor (PIF) signalling

Upon light induced nuclear import, the phytochromes localize to discrete sub nuclear foci, called nuclear bodies (NB) or speckles. The pattern of NB formation is highly dynamic and directly regulated by light quality, quantity and temperature. Early NBs are predominant degradation sites of Phytochrome Interacting Factors (PIFs) whereas the 'late' NBs determine the PHYB mediated signal transduction. These 'late' photobodies comprise predominantly of PHYB-E (as PHYA is light labile and rapidly degraded). Interestingly, the size and number of these 'late' NBs depend on the fluence rate of red light. Under high-intensity red light, active PHYB Pfr appears to be localized exclusively to a few large photobodies with diameters between 1 and 2μm (Chen et al., 2003). In contrast, under dim R light or light with a low R-to-FR ratio, where more PHYB reverts to the inactive Pr form, PHYB tends to localize as many smaller NBs or localizes diffusely in the nucleoplasm (Chen, 2008). The formation of large PHYB NBs correlates tightly with the light-dependent hypocotyl inhibition response, larger the NBs (low to negligible PIF activity) shorter the hypocotyl and smaller the NBs (elevated PIF activity) longer the hypocotyl.

PIFs (Phytochrome Interacting Factors) belong to the basic helix-loop-helix (bHLH) family of transcription factors. There are seven Phytochrome Interacting Factors (PIF1,3,4,5,6,7,8) in Arabidopsis that function in a partially differential to a largely overlapping manner to regulate multiple pathways (Leivar and Monte, 2014; de Lucas and Prat, 2014). All the PIFs interact with the Pfr forms of PHYB through the N-terminal APB (active phytochrome B binding) with exceptions of PIF1 and PIF3 capable of also binding to PHYA via the APA (active phytochrome A binding) domain. Except PIF7, direct physical interaction between the PIFs and photoactive

phytochromes in Nuclear Bodies (NB) leads to the phosphorylation followed by ubiquitination and subsequent degradation by the 26S proteasome (Leivar and Quail, 2011; Leivar and Monte, 2014; de Lucas and Prat, 2014).

Only recently, the kinase (Photoregulatory Protein Kinases PPK1-4) and the E3 ubiquitin ligase LRB (Light Response Bric-a-Brack/Tramtrack/Broad) responsible for PIF3 phosphorylation and ubiquitination was identified (Ni et al. 2014; 2017). In addition to light dependent phytochrome induced degradation of PIFs in NBs, PHYB is capable of sequestering PIFs at the target promotors to inhibit its DNA binding activity (Park et al. 2012).

Mutating the PIF family of genes - *PIF* quadruple mutant *pif1 pif3 pif4 pif5* (or *pifQ*) result in seedlings exhibiting a photomorphogeneic phenotype (short hypocotyl/open cotyledon) in the dark (Leivar et al, 2008) thereby establishing PIFs as pivotal components operating redundantly in photomorphogenic repression in dark. In contrast to single *pif* mutants, the transcriptomic profile of *pif quadruple (pifQ)* mutants in the dark largely resemble that of wild-type seedlings grown in the light (Leivar et al. 2009; Zhang et al. 2013). PIFs function as either transcriptional activators or repressors. Extensive transcriptomics and biochemical studies have identified genes in multiple pathways directly targeted by PIFs. The defined PIF binding sites on target gene promotors are strongly enriched in the DNA motif G-box (CACGTG) and the E-box variant (CACATG and CATGTG) that has been called the PBE-box (for PIF binding E-box) (Leivar and Monte, 2014).

Apart from seedling de-etiolation, much work has been published on the involvement of PIFs as system integrators during seed germination, shade avoidance, thermal growth, hormonal pathways and the circadian clock (Leivar and Monte, 2014).

PIFs mediate the shade avoidance response, which is initially perceived by the photoreceptors through changes in light quality. Intensity of blue light decreases (Low Blue Light LBL) and ratio of red (R) to far-red (FR) decreases under foliar shade/close parallel neighbour proximity as green leaves absorb R and reflect FR (Casal, 2012). In plants, shade avoidance response triggers elongated hypocotyls – stems – petioles – internodes / hyponastic leaves with reduced leaf lamina area and early flowering. Amongst the PIF family members - PIF4, PIF5, and PIF7 play important roles in shade avoidance. Auxin levels rise rapidly after the onset of low R:FR in the cotyledons (sites of shade perception) and subsequently transported down to the hypocotyl/petioles or stems to induce cell elongation (Procko et al. 2014; Tao et al. 2008). Joanne Chory's lab identified the missing links between shade signals (low R:FR and LBL) and auxin metabolism and auxin -dependent /-independent changes to plant architecture. Li et al. (2012) identified PIF7 as the direct master regulator of auxin biosynthesis under low R:FR conditions. Whereas, Pedmale et al. (2016) identified PIF4 and PIF5 to function exclusively under LBL conditions downstream of cryptochrome (CRY1 and CRY2) to modulate growth in an auxin independent manner. CRY1 and CRY2 interact with PIF4 and PIF5 to regulate the expression of several thousand cell wall modifying genes aiding in elongation. Auxin biosynthetic rates or auxin biosynthetic/responsive/signalling genes do not appear to be induced under exclusive LBL conditions. Hence, taken together shade conditions (naturally characterised by low R:FR and LBL) appear to elicit multiple growth programmes via the PIF family for structural alterations.

These 'shade signals' are routinely used in research laboratories (by artificially supplying Far-Red light) to induce rapid Pfr PhyB inactivation for enhanced PIF

activity. Interestingly, increased duration or enhanced intensity of FR can superactivate PHYA, a potent suppressor of hypocotyl elongation. Hence, under natural conditions PHYA functions to buffer exaggerated PIF activity thereby ensuring an optimum balance in growth. To circumvent PHYA super activation, a so-called End of Day Far-Red (EoD FR) short pulse is sufficient to only inactivate PHYB Pfr for maximal effect (Roig-Villanova and Martínez-García, 2016)

1.2.3. Role of COP1-SPA and DET1 during seedling photomorphogenesis

As mentioned above, light-induced translocation of Phy Pfr from the cytosol into the nucleus is an early and indispensable step in phytochrome signalling for PIF inactivation and photomorphogenesis promotion. In addition, both photoreceptors (PHY and CRYPTOCHROMES) promote photomorphogenesis by inhibiting the COP1/SPA E3 ligase complex. In the dark COP1-SPA complex target a myriad of positive regulators of photomorphogenesis for Ub mediated proteosomal turnover. Cryptochromes (Liu et al. 2011; Lian et al. 2011) and Pfr phytochrome A and B interact directly with SPA1 (Sheerin et al. 2015), to reorganize and inhibit COP1-SPA E3 ligase complex activity (Fig1.3). The photoactivated phytochromes and cryptochromes disrupt the direct interaction of COP1 and SPA proteins provides a mechanistic model to explain the fast inactivation of the COP1-SPA complex in the light to promote seedling photomorphogenesis. In addition to the COP1-SPA E3 ligase and the PIF family of transcription factors, De-Etiolated1 (DET1) also functions as a negative regulator of photomorphogenesis. Seedlings mutated in the *COP1, DET1* or the *PIF* family locus exhibit a light grown (photomorphogenic as opposed to skotomorphogenic) phenotype even in the dark. However, the precise role and target

substrates of DET1 E3 ligase complex in photomorphogenesis repression and light driven inactivation is completely unknown.

COP1-SPA: an E3 ubiquitin ligase complex at the heart of light signalling:

COP1 is a 76kDa RING E3 ligase and contains three protein–protein interaction domains: an N-terminal RING-finger region, a coiled-coil domain and seven WD40 repeats at its C terminus. The RING-finger motif mediates the interaction with Ub-conjugating enzymes (E2s), and the coiled-coil region of COP1 allows the formation of homodimers or heterodimers with members of the SPA protein family and the WD40 repeats function as the substrate interaction domain (Lau and Deng 2012). The SPA family (SPA1-4) of proteins has been established as core components of the COP1 complex important for COP1 E3 ligase activity. In *spa quadruple* mutants, at least two COP1 direct targets – HY5 and HFR1 protein (positive regulators of photomorphogenesis) accumulate at higher levels. *COP1* and *SPA1* interact genetically, and the quadruple *spa* mutant displays a striking constitutive photomorphogenic phenotype similar to strong *cop1* mutants in the dark (Hoecker, 2017). In the dark or during skotomorphogenesis, COP1 targets a myriad of key positive regulators of photomorphogenesis such as Elongated Hypocotyl 5 (HY5), Long After Far-Red light 1 (LAF1) and Long Hypocotyl in Far Red (HFR1) for ubiquitination and subsequent proteosomal degradation, leading to a complete suppression of photomorphogenesis (Lau and Deng, 2012). In light, COP1 nuclear activity is inhibited by its export from the nucleus (a slow inactivation mechanism) and direct inactivation of the COP1-SPA complex by photoreceptors phytochromes and cytochromes (a fast inactivation mechanism) thereby relieving the repression on

the positive regulators of photomorphogenesis (Liu et al. 2011; Lian et al. 2011; Sheerin et al. 2015) (Fig. 3).

DET1: An unconventional E3 ligase and a transcriptional regulator:

DET1, the first photomorphogenic repressor to be identified (Chory et al. 1989) is a highly enigmatic, less studied protein with no recognizable domains besides two nuclear localization signals (Pepper et al. 1994). The discovery that DET1 complexes with COP10 and DDB1 (a CUL4 core adaptor) as a CDD complex, has implicated DET1 in the E3 ligase machinery (Yanagawa et al. 2004). Similar to *cop1* and *pif* family mutants, *det1* mutant seedlings also exhibits a light grown phenotype in the dark, however no positive regulators of photomorphogenesis have been identified as direct targets of the CDD complex in the dark. The PIF family transcription factors binds to thousands of skotomorphogenesis promoting genes in the dark. Dong et al. (2014) recently demonstrated physical protein interactions between DET1 and PIFs and that PIF protein levels are depleted in the *det1* mutant. Hence, DET1 positively stabilizes PIF protein levels in the dark thereby promoting skotomorphogenesis through the PIFs. This study provides one potential mechanism by which DET1 represses photomorphogenesis in the dark. COP1 was also shown to positively stabilise dark PIF protein levels (Baur et al. 2004; Ling et al. 2017) (Fig. 3). Another mechanism of DET1 repression on photomorphogenesis via PIFs appears to be partly through the gibberellic acid (GA) pathway. Seedlings deficient in GA exhibit a partially de-etiolated phenotype in dark. All of these partial photomorphogenic phenotypes could be suppressed by the lack of DELLA family proteins, the negative regulators of PIFs. DELLAs can directly interact and inhibit PIF activity by

sequesteration (Feng et al. 2008; de Lucas et al. 2008). Li et al. (2016) report that DET1 negatively regulates DELLA protein abundance in the dark to relieve repression on the PIFs. These results suggest that DET1 represses photomorphogenesis by stabilizing PIF proteins and negatively regulating the repressive action of DELLAs on the PIFs (Fig1. 3).

1.2.4. Positive regulators of light signalling

The positive regulators of photomorphogenesis functioning downstream to the photoreceptors include: B-box zinc-finger transcription factors (BBXs), bZIP transcription factors HY5 and HYH, bHLH transcription factor HFR1, and other transcription factors such as LAF1, PIL, PAR, GATA family, Z box Binding TFs, etc (Xu et al. 2015) (Fig1.3).

Elongated Hypocotyl 5 (HY5), a constitutively nuclear bZIP protein is the first known and most extensively studied transcription factor involved in promoting photomorphogenesis downstream to the phytochromes, cryptochromes and the UV-B photoreceptors. The abundance of HY5 protein is directly correlated to light quantity (Osterlund et al. 2000). Incremental increase in light fluences enhances HY5 protein abundance ultimately resulting in complete suppression of the seedling hypocotyl elongation. Hence, the *hy5* mutant seedlings exhibit an elongated hypocotyl response. In the dark, HY5 is turned over by the COP1-SPA E3 ligase to repress photomorphogenesis (Osterlund et al. 2000). Interestingly, the phosphorylation status of HY5 crucially contributes to its stability and activity during photomorphogenesis transition (Hardtke et al. 2000). Chromatin immunoprecipitation (ChIP) - chip studies reveal that HY5 binds directly to a large number of genes (~3000) involved in multiple

pathways (Lee et al. 2007; Zhang et al. 2011). A detailed list of in vivo confirmed HY5 target genes have been compiled by Gangappa and Botto, (2016). HY5 has been shown to bind to multiple promotor response elements such as G-box, T/G-box, E-box, GATA-box, ACE-box, Z- and C- boxes (Gangappa and Botto, 2016). HY5 and its working partner HY5 Homolog (HYH) can physically interact with PIF's to form dimers and antagonistically (in-competition) regulate common target genes (Chen et al. 2013; Toledo-Oritz et al. 2014).

1.2.5. Other key signalling components mediating seedling establishment

Under continuous dark conditions, seedlings exhibit a skotomorphogenic growth phenotype. As outlined above, skotomorphogenesis is mediated by the PIF family of transcription factors and the Cullin4 based COP1-SPA and DET1-COP10 E3 ligase activity. However, even under photomorphogenic, diurnal conditions (light-dark photoperiods) the hypocotyl length of seedlings or the stem length of adult plants continue to be regulated by these factors.

Both, the circadian clock and light signalling pathways co-regulate hypocotyl/stem elongation with maximal growth rate at the End of Night (EON – a dark window period before dawn) (Nozue et al. 2007). Signals from both the clock and light pathways converge on PIF4 and PIF5. While PIF4 and PIF5 protein abundance is post-translationally suppressed by phytochromes during the day (reviewed previously), the Evening Complex (EC) suppresses *PIF4* and *PIF5* transcription from late evening to mid-night until the EON. As the level of the EC decreases as dawn approaches (EON), transcriptional suppression of PIF4/PIF5 is released and hypocotyl growth is promoted (Nusinow et al. 2011). Hence the hypocotyl length of seedlings

grown in Short Day (SD) photoperiods (8L: 16D) is more enhanced than seedlings grown under Long Day photoperiods (16L: 8D) due to the extended dark periods of PIF activity. PIF1 and PIF3 also contribute to hypocotyl elongation as an End of Day (EOD) Far-Red pulse (required for rapid PHYB inactivation and subsequent PIF accumulation) resulted in a shorter than wildtype hypocotyl phenotype in *pif1*, *pif3* single mutants and more enhanced in *PIF quadruple* mutant (*pifQ* - *pif1pif3pif4pif5*) (Soy et al. 2012; 2014). However, the gene expression pattern of PIF1/3 does not appear similar to PIF4/5 suggesting the absence of Evening Complex (EC) influence on transcriptional regulation.

Phytohormones Gibberellic acid (GA), auxin and Brassinosteriods (BR) play major roles during both skotomorphogenesis and diurnal regulation of hypocotyl growth. In the dark, GAs accumulate and DELLA activity is supressed whereas the converse occurs in the presence of light. Two papers demonstrate PIF sequestration directly by DELLAs thereby functioning as another negative regulator of PIF activity in the light (Feng et al. 2008; de Lucas et al. 2008) (Fig1.3).

Recent papers for Zhiyong Wang's lab draws a more complex picture between light/dark – Brassinosteroid (BR) – Auxin and GA hormone co-ordination in regulating hypocotyl growth (Oh et al. 2012; 2014; Bai et al. 2012). Brassinosteroids are a class of steroid hormones that negatively regulate photomorphogenesis. Brassinosteroid biosynthetic and signalling mutants exhibit de-etiolated phenotypes in the dark. When brassinosteroid levels are low, BZR1, a key signalling component is inactivated by phosphorylation (mediated by BIN2 kinase), whereas increasing concentration of brassinosteroids inactivates BIN2, promotes BZR1 dephosphorylation and subsequent binding to BR responsive target genes (Clouse,

2011; Kutschera and Wang, 2012). Darkness induces the dephosphorylation while light promotes the phosphorylation of BZR1. Oh et al. (2012) demonstrated direct interaction between BZR1 and PIF4. They immunoprecipitated the chromatin of transgenic Arabidopsis lines expressing both BZR1–myc and PIF4–YFP to reveal that both BZR1 and PIF4 co-occupy the promoter of atleast 2000 common target genes in vivo. Two years later they identified a new addition to this complex, Auxin Responsive Factor 6 (ARF6) – a direct interactor of BZR1 and PIF4 (Oh et al. 2014). Hence, ARF6-BZR1-PIF4 interdependently activate shared target genes to synergistically promote hypocotyl growth. GA regulates cell elongation through the degradation of DELLA proteins. DELLAs have been identified to sequester BZR1 (Bai et al. 2012), PIF3/4 (Feng et al. 2008; de Lucas et al. 2008) and ARF6 (Oh et al. 2014) thereby negatively regulating ARF6-BZR1-PIF complex activity in promoting hypocotyl length in the light. These results demonstrate that GA releases DELLA-mediated inhibition of the complex, and that the DELLA-BZR1-PIF4-ARF6 interaction defines a core transcription module that mediates coordinated growth regulation by hormone and light signals.

Interestingly, even the phosphatase BIN2 has also been implicated in skotomorphogenesis, besides inactivating BZR1, BIN2 is shown to phosphorylate the PIFs for proteolysis in the light (Bernardo-García et al. 2014). In dark, the COP1-SPA complex sequester BIN2 to repress this activity thereby contributing to PIF stabilization and skotomorphogenesis promotion. Light destabilises COP1-SPA activity and release the repressive effects on BIN2 (Fig. 3) (Ling et al. 2017).

Another phytohormone, ethylene has also been implicated in photomorphogenesis repression via the master signalling component Ethylene

Insensitive3 (EIN3). EIN3 prevents the opening and expansion of cotyledons and promote apical hook formation to maintain skotomorphogenesis. COP1 positively promotes EIN3 stability in the dark by degrading EBF1/EBF2 (negative regulators of EIN3). Overexpression of EIN3 in the *cop1* mutant restored the *cop1* open cotyledon defect to Wt in the dark. Under light conditions, COP1 is inactivated and PHYB directly targets EIN3 protein for rapid degradation (Shi et al. 2016a, 2016b) thereby promoting photomorphogenesis (Fig1.3).

A great deal has been published on the molecular mechanisms of light signalling and light mediated hormonal control on seedling skotomorphogenesis/photomorphogenesis. However, it is not clear as to how exactly sugar or metabolic components feeds into this complex network to regulate seedling establishment.

Dark Promoted Skotomorphogenesis

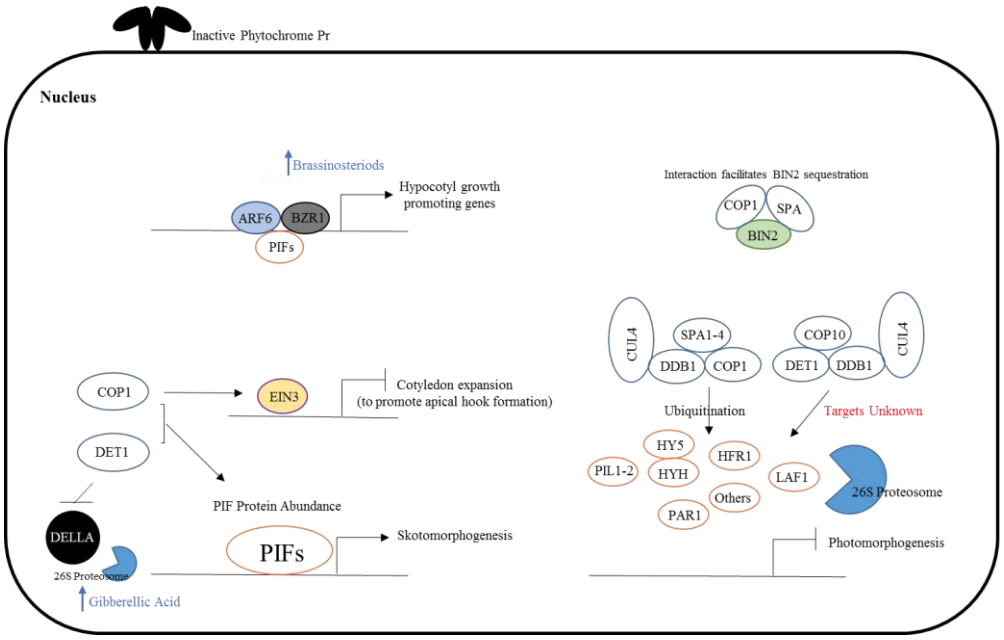

Light Induced Photomorphogenesis

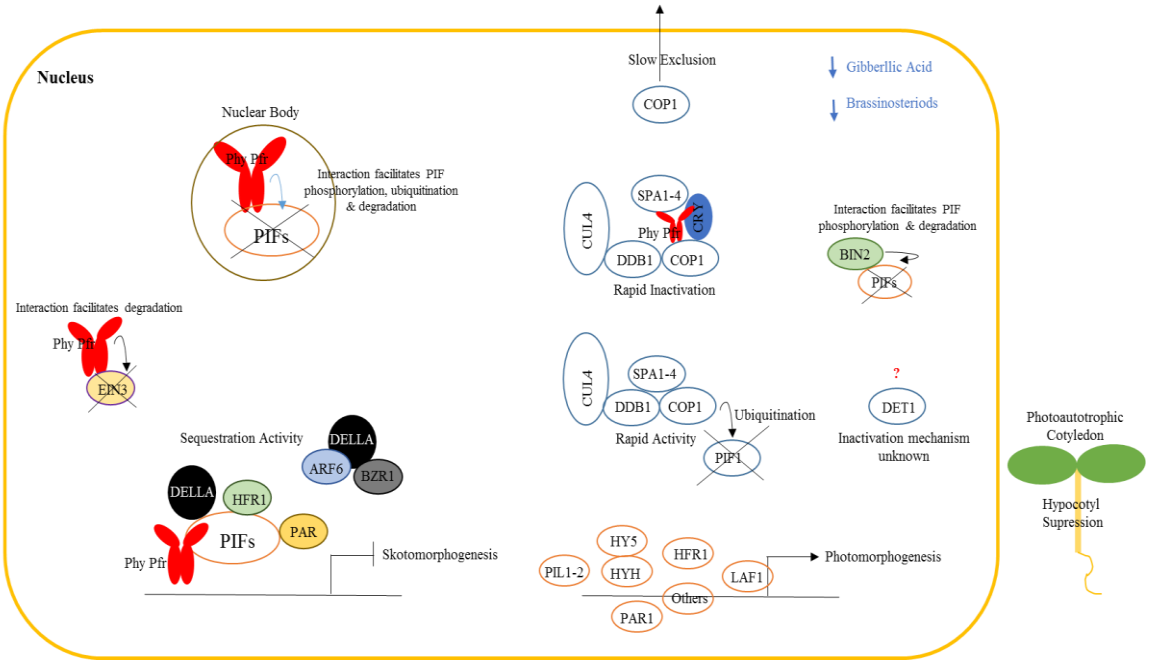

Fig1.3: Molecular components and processes during dark to light transition.
Dark (Skotomorphogenesis): Phytochromes are inactive and cytosol localized. The COP1-SPA (and DET1-COP10) based E3 ligase complex target multiple positive regulators of photomorphogenesis for degradation. COP1 and DET1 positively regulate the abundance of Phytochrome Interacting Factors (PIFs). The PIFs regulate the expression of thousands of skotomorphogenesis promoting genes independently and in concert with BZR1 and ARF6 (reviewed in section below). DET1 and elevated gibberellic acid levels negatively regulate DELLA protein abundance thereby releasing the repressive effects of DELLAs on the skotomorphogenesis promoting PIFs-BZR1-ARF6 complex. COP1-SPA promotes accumulation of EIN3 (to repress cotyledon expansion) and sequester BIN2 (negative regulator of PIFs) to stabilize PIF protein levels.

Light (Photomorphogenesis): Photoactivated phytochromes translocate to the nucleus to target PIFs for degradation (in nuclear bodies) or sequestration to inhibit PIF activity. Phytochromes interact with EIN3 and catalyse its turnover. Low levels of brassinosteroids reduce BZR1 activity and low levels of GA enhances DELLA protein abundance. DELLAs sequesters PIFs and ARF6/BZR1 from target promotors thereby repressing skotomorphogenesis. BIN2 is released from COP1-SPA complex and catalyse PIF turnover. In rapid response to light, COP1-SPA E3 ligase complex catalyse PIF1 turnover while the photoreceptors (Phytochrome (Phy) and Cryptochrome (Cry)) disassociate this E3 ligase complex by inhibiting COP1-SPA interactions. COP1 is slowly excluded from the nucleus. Protein levels of COP1 targets (HY5-HYH, HFR1, LAF1 and more) accumulate to positively promote photomorphogenesis.

1.3. Energy mediated seedling establishment

During the day, photosynthesis derived energy and carbon (C) support growth and metabolism, whilst at night, the accumulated C reserve function as fuel. Several studies have demonstrated that starch synthesis and degradation is tightly linked to photoperiods. Starch is synthesised during the day and degraded at night in a linear fashion. This pattern of starch turnover is remarkably robust against changes in the environment. When less C is available (e.g. short days or low light), a larger proportion of the photosynthate accumulates as starch (in the day) and degraded more slowly during the nigh ensuring that reserves last until dawn. Starch degradation is timed such that starch is exhausted at dawn as anticipated by the clock (Graf et al. 2010).

However, the growth measurements in adult plants are not correlative or entirely consistent with seedling hypocotyl elongation from an energy standpoint. Leaf growth in adult plants is maximal several hours after dawn, requires light and is regulated by daylength (Dornbusch et al. 2014). In contrast, seedling hypocotyl elongation is also photoperiodic with maximal growth occurring during the End of Night (EoN) dark phase. Although the role of PIF signalling in hypocotyl elongation is well established, how metabolic signals regulate the PIF network in diurnal conditions largely remains unknown.

For seedlings grown in complete darkness, energy balance is key to etiolated hypocotyl elongation as growth is exclusively seed reserve dependent. In Arabidopsis, the primary energy source for etiolated growth is derived from fatty acids stored in the embryo and endosperm. Mutations in two enzymes involved in mobilizing energy stores in the seed, *phosphoenolpyruvate carboxykinase 1 (pck1)* and *isocitrate lyase (icl)* display inhibition of hypocotyl growth particularly in the dark. Both enzymes are

key components for catabolizing fatty acids to produce sugars by gluconeogenesis and the glyoxylate cycle respectively. Both, *pck1* and *icl* mutants exhibit strong defects in etiolated hypocotyl elongation. The provision of exogenous sugars rescue this growth deficiency. An interesting discovery is that gluconeogenesis in the seed endosperm is required for PCK1 dependent skotomorphogenic growth. Removal of endosperms result in short etiolated hypocotyls in Wt with further enhancement in *pck1* mutants compared to intact seedlings. Glyoxylate cycle on the other hand can be compensated by photosynthesis during post-germinative growth. Hence, seedling establishment is compromised in the *icl* mutants only when light intensity or day length is decreased but exhibits a Wt phenotype at high light or long days. (Eastmond et al. 2000; Penfield et al. 2004). Detailed investigation between metabolic, light and hormonal components potentially working in co-operation during seedling established is required.

1.4. Glucose signalling

A number of genes involved in sugar sensing and signalling have been identified in mutant screens for altered responses to exogenous sugars during seed germination and early seedling growth in Arabidopsis. For example, glucose insensitive (*gin*) mutants fail to undergo growth arrest in the presence of inhibitory levels of glc, exhibiting normal hypocotyl elongation, cotyledon greening, and expansion. Independent screens for other sugar response phenotypes revealed that certain sucrose uncoupled (*sun*), sugar insensitive (*sis*), and/or impaired sucrose induction (*isi*) mutations were allelic to *gin* loci, suggesting that these genes may function at the interface of different sugar signalling pathways (Eveland and Jackson, 2012). Sugar-based signalling pathways cross talk with various hormones to modulate

critical aspects of plant growth. In general, plants defective in abscisic acid (ABA) and/or ethylene perception and signalling tend to display altered sugar response phenotypes. However, additional connections between sugars and other plant hormones, such as auxin/BR, have emerged, and some evidence suggests potential sugar–hormone regulation of specific developmental processes

Master glucose regulated signalling components that modulate plant growth are Hexokinase1 (HXK) glucose sensor, Trehalose 6-Phosphate (T6P) signal, Target of Rapamycin (TOR) kinase and the SNF1-related Protein Kinase1 (SnRK1) (Sheen, 2014; Li and Sheen, 2016) (Fig1.4). SnRK1 and TOR kinases sense opposite energy levels and govern highly overlapping transcriptional networks. However, little is known about the glucose receptor HXK1 and its role in plant growth and development at the molecular level. The role of these master regulators during seedling establishment will be introduced with strong emphasis on Hexokinase 1, the primary component of this thesis.

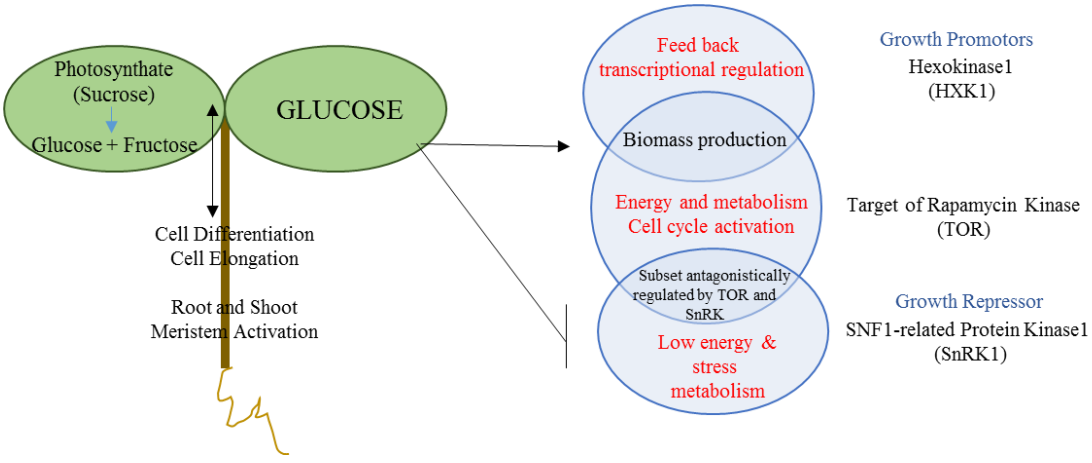

Fig1.4: Regulatory pathways of photosynthesis derived sugars. Sucrose is actively transported to the sink tissues to promote growth and maintain energy and metabolic homeostasis. The regulatory mechanisms and functions of three master regulators - HXK1, TOR and SnRK1 modulated by sugar availability is depicted.

1.4.1. Hexokinase1 – An introduction to the glucose sensor

Photosynthesis derived carbohydrates (glucose) is utilized via aerobic (or anaerobic) respiration to yield ATP energy molecules. The first respiratory pathway - Glycolysis is a sequence of enzymatic reactions that catabolize one molecule of glucose to yield two molecules of pyruvate. Glucose enters the cell and is irreversibly phosphorylated by the enzyme Hexokinase1 (HXK1). The enzymatic role of HXK1 in glycolysis is highly conserved. The HXK1 catalysed Glucose-6-Phosphate (G6P) is 'trapped' within the cell due to its negative charge thereby inhibiting diffusion back to the plasma membrane.

Hexokinase1 (HXK1) is the first demonstrated intracellular glucose sensors in plants. Plant genomes encode multiple hexokinases (HXKs) and HXK-like (HKL) proteins with overlapping and distinct functions. The Arabidopsis genome encodes three HXKs and three HXK-like (HKL) genes. While all three HXKs bind and phosphorylate glucose, HKL genes are predicted to bind glucose with a relatively lower affinity and lack phosphorylation ability. HKLs likely have only regulatory functions (Karvae et al. 2008). In the 90s, Jang and Sheen (1997) suggested that, in addition to their conserved enzymatic role in glycolysis, plant Hexokinase (HXK) may function as a sugar sensor and as a sugar-signalling component in transcriptional regulation. They observed anti-sense HXK1 seedlings to be glucose insensitive and that HXK1 is required to supress nuclear photosynthetic genes in response to glucose. These functions of HXK1 was confirmed when the catalytic and the signalling activities of HXK1 were uncoupled a few years later.

Moore et al. (2003) performed a forward genetic screen on 6% glucose to identify glucose insensitive (gin) mutants that overcome seedling developmental arrest.

Thus, the *gin2* (a missense mutation in Arabidopsis HXK1 locus) mutant was identified as the putative glucose sensor from this study as the seedlings developed normally under physiologically toxic levels of glucose. HXK1 performs dual roles – enzymatic role in glycolysis and the proposed nuclear signalling role (Fig1.5). The highlight of Moore et al. (2003) is uncoupling the two role. They generated two catalytically inactive HXK1 alleles with an amino acid substitution in the catalytic domains (G104D and S177A). Both lines exhibit decreased glucose phosphorylation activity as interaction with ATP is inhibited. However, the G6P levels and the sugar phosphorylation activity measured in the *gin2* mutant and the point mutants (S177A/G104D) is only reduced by around 40% (Moore et al. 2003; Bruggeman et al. 2016) suggesting compensatory roles. Under exogenous glucose treated conditions, repression of photosynthetic genes (*CAB2, CAA*) is observed in wildtype and catalytically inactive HXK1 lines but not in the *gin2* mutant. Cho et al. (2007) detected HXK1 protein in both nuclear and cytoplasmic fractions. However, the ratio between nucleus:cytoplasm is approximately 1:105. Hence, HXK1 is not a nuclear abundant protein. A MALDI-TOF mass-spectrometry was performed on highly enriched nuclear fractions of HXK1 and identified two interactor proteins: a scaffold vacuolar H+ ATPase B1 subunit (VHAB1) and a subunit of the 19S regulatory particle of proteasome (RPT5B). *In vivo* CO-IPs confirmed the interaction between the three proteins in the nucleus. Further, they postulate that HXK1 and its partner proteins are required for glucose induced gene repression. The glucose induced repression of two photosynthetic genes *CAB2* and *CAA* was absent in the *gin2*, *vhab1* and *rpt5b* mutant. This mechanism is postulated as a negative feedback mechanism to shut down

photosynthesis. Further, using ChIP-qPCR, HXK1 enrichment was observed on the *CAB2* promotor proximal to the transcriptional start site.

However, contradicting Cho et al. (2007) and Yanagasawa et al. (2003), Balasubramanium et al. (2007) were unable to detect GFP tagged HXK1 in the nuclear fraction of Arabidopsis or pea leaves or visualize nuclear localization in response to sugar/light/dark treatment. However, this experiment was performed in Arabidopsis protolasts and not in planta as Cho et al. (2007). Hence, how sugar precisely facilitates HXK1 nuclear localization or complex assembly at the chromatin is unknown.

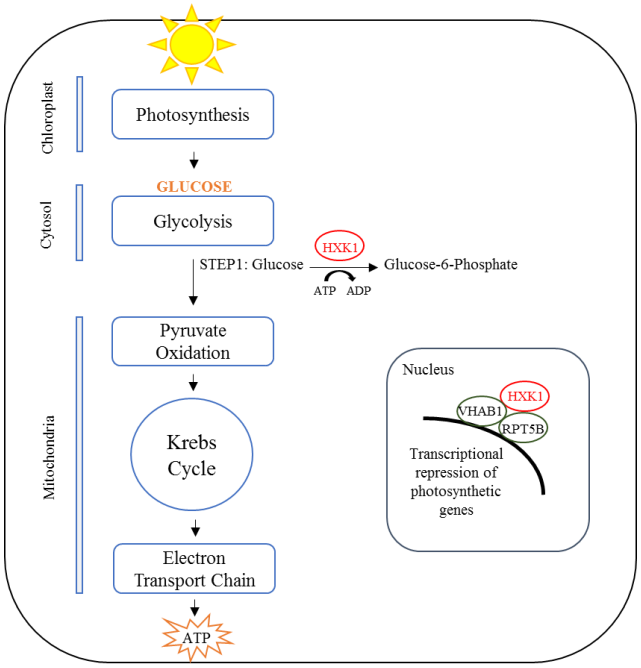

Fig1.5: HXK1 dual role
HXK1 catalyse glucose phosphorylation in glycolysis. In response to sugar, HXK1 assemble as a nuclear signalling complex to repress photosynthetic genes.

HXK1 is required for sugar induced stomatal closure and sugar mediated transcriptional repression of atleast 10 aquaporin genes (Li et al. 2018; Kelly et al. 2017). Apart from photosynthesis associated genes, HXK1 also appears to function as an added sugar mediated transcriptional repressor of miR156 (Yang et al. 2013), certain 'sugar responsive' genes (Kunz et al. 2015) and N transporter NRT2.1 (de Jong et al. 2014). Beyond transcriptional control, HXK1 signalling is required for glucose-

mediated turnover of EIN3 protein, a key ethylene-signalling regulator in the nucleus via unknown mechanisms (Yanagisawa et al. 2003). HXK1 also appears to be somehow required for glucose induced auxin biosynthesis (Sairanen et al. 2012). The hexokinase1 mutant (*gin2*) has a lower basal level of IAA and a reduced capacity for induction of IAA biosynthesis by glc relative to Wt. Sairanen et al. (2012) suggests that the phosphorylation status of the sugars is important for their capacity to induce IAA biosynthesis, however this has to be tested.

The catalytic role of HXK1 is involved in programmed cell death. Myo-inositol is synthesised from G6P by the enzyme Myo-Inositol 1-Phosphate Synthase (MIPS1). *mips1* mutants exhibit spontaneous lesions on leaves. To understand how MIPS1 negatively regulates cell death Bruggemann et al. (2016) performed a suppression screen. Mutations of *HXK1* in the *mips1* background result in lesion free plants. In the *mips1* mutant, the induction of cell death was attributed to the reduced accumulation of myo-inositol and galactinol, which accumulated to Wt levels in the *mips hxk1* double mutants via unclear mechanisms. Role of G6P in this process is unknown.

Taken together, HXK1 appears to be multi-dimensional component required for various biological processes in plants.

1.4.2. SnRK1 and TOR Kinase:

SnRK1 (Snf1-related protein kinase 1) and TOR (target of rapamycin) are evolutionarily conserved protein kinases that lie at the heart of energy sensing, playing antagonistic roles in the regulation of metabolism and gene expression. SnRK1 is activated in response to declining energy supplies triggering the repression of energy-

consuming anabolic processes and growth. Conversely, TOR promotes growth in response to energy availability (Baena-González et al. 2007; Xiong et al. 2013) .

Promoter analysis of strong SnRK1 activated carbon (C) starvation genes (DIN6/ETFQO) have defined a specific G-box DNA motif to be responsible for its transcriptional activation synergistically with bZIP transcription factors. SnRK1 triggers phosphorylation of bZIP to facilitate heterodimer formation to directly control transcription via binding to G-box promoter elements (Baena-González et al. 2007; Lorenzo Pedrotti et al. 2018).

Arabidopsis TOR is an exceptionally large protein kinase (2481 amino acids) with multiple repeats and regulatory domains in the N-terminus and an evolutionarily conserved Ser/Thr protein kinase domain at the C-terminus. Mutating any of these conserved domains on the TOR locus result in embryo lethality (Ren et al. 2011). From sequence similarity searches and subsequent molecular characterization, mammalian TORC components and downstream effectors have been identified in Arabidopsis such as RAPTOR1-2, LST8, S6K1-2, RPS6a/b and TAP46 (Sheen, 2014; Xiong and Sheen, 2013). Arabidopsis TOR kinase is modulated by diverse upstream signals (sugar/hormones/light/macronutrients) and operate in concert with regulatory partners (Raptor and LST8) to phosphorylate S6K1,2, TAP46, E2FA, E2FB, LIPIN and ATG1. These activated components trigger a suite of signal transduction cascades in the nucleus, nucleolus and cytosol to control massive transcriptome reprogramming, meristem activation, cell cycle, endocycle, rRNA transcription, ribosome biogenesis, translation, primary and secondary metabolism - all pivotal to cell proliferation and overall growth (Xiong et al. 2013). Hence, both kinases exert their function through wide-ranging transcriptional reprogramming and metabolic readjustments.

1.4.3. Role of HXK1, SnRK1 and TOR in seedling establishment

Previous studies have implicated HXK1, SnRK1 and TOR kinase in seedling establishment. Moore et al. (2003) uncoupled the enzymatic from the proposed signalling role of HXK1 by point mutating ATP binding sites in the catalytic domain. Hence, $HXK1^{S177A}$ and $HXK1^{G104D}$ are lines impaired in HXK1 catalytic activity with intact signalling function. They observe that HXK1 mutant *gin2* exhibit a small seedling stature (short hypocotyl/small cotyledon) in sugar free media at low light fluences. Further, this phenotype is rescued in $HXK1^{S177A}$ and $HXK1^{G104D}$ lines suggesting the involvement of nuclear HXK1 for seedling establishment via unknown mechanisms (Moore et al. 2003). However, in response to exogenous sugar, the *gin2* mutant exhibit a Wt hypocotyl enhancement suggesting a HXK1 independent sugar signalling pathway (Simon et al. 2018; Sing et al. 2017; Zhang et al. 2016).

While SnRK1 mutant seedlings exhibit no obvious phenotype under nutrient sufficient conditions, the effect of SnRK1 in nutrient limiting conditions has only been investigated in the adult stage (Baena-González et al. 2007). However, SnRK1 appears to be required for sugar mediated hypocotyl growth as the SnRK1OX appears insensitive to exogenous supply (Simon et al. 2018).

TOR kinase on the other hand is crucially required for post germinative seedling growth. Oestradiol (*es*) induced *tor* mutant seedlings display growth retardation despite supplying CO_2, light or sugar. This highlights the crucial requirement of TOR for meristematic cell cycle activation and respiration mediated energy production (Xiong et al. 2013). Wt seedlings phenocopying a *tor-es* mutant when treated with TOR inhibitor AZD-8055 (Pfeiffer et al. 2016). TOR kinase also

appears to be required for sugar mediated seedling hypocotyl growth in dark through the BR signalling pathway by stabilizing BZR1, a key TF (Zhang et al. 2016).

Based on these datasets, the master glucose regulators HXK1, SnRK1 and TOR kinase are required for seedling growth.

1.5. Light-sugar signalling interface

Contribution published in Krahmer et al. (2018)

Although a solid body of research exists separately on light signal transduction - photosynthesis and central metabolic signalling, only recently, molecular connections between the pathways have gained momentum (Krahmer et al. 2018). Amongst the first few reports, Fox et al. (2015) identified *phyAphyBcry1cry2* quadruple mutants to have reduced net CO_2 uptake (~70%), chlorophyll levels and RuBisCO protein levels thereby implicating photoreceptors to photosynthetic efficiency. Yang et al. (2016) further employed a Gas Chromatography – Mass Spectrometry (GC-MS) analytical approach to gain a broader view of phytochrome impact on primary metabolism. They observed elevated levels of metabolizible sugars, starch, multiple TCA cycle organic acids and specific amino acids in the phytochrome multiple knock out mutant. These results highlight a hitherto unknown function of phytochrome signalling in metabolism.

Among the myriad of signalling components functioning downstream to the phytochromes, HY5 and PIFs have emerged as the first few players potentially linking light signal transduction to carbon sensing/signalling and metabolism. Earlier ChIP-chip analysis identified >3500 direct HY5 target genes with a significant enrichment in metabolic, nutrient signalling and photosynthetic genes (Lee et al. 2007). HY5 was

subsequently shown to regulate the expression of chlorophyll biosynthesis and photosynthesis-related genes through direct binding to G-box promoter elements (Toledo-Ortiz *et al*. 2014). More recently, HY5 has been shown to directly enhance the expression of TREHALOSE-6-PHOSPHATE SYNTHASE 1 (*TPS1),* and the sucrose efflux transporters SWEET11, and SWEET12. TPS1 elevates levels of trehalose-6-phosphate (T6P), a metabolic signalling molecule that controls growth, flowering and shoot-to-root transport of sucrose (Chen *et al*. 2016). However, HY5 action is not confined to the shoot, a series of elegant grafting experiments demonstrate its translocation to the root to induce the expression of root located *HY5*, which in turn activates *NRT2.1* transcription and root nitrate uptake. Furthermore, the HY5-induced *NRT2.1* expression in the root appears to be dependent on the shoot metabolic carbon status. Thus, HY5 appears to play a pivotal role in co-ordinating carbon uptake and growth in the shoot with nitrogen uptake in roots (Chen et al. 2016). COP1 E3 ligase activity appears to be sucrose regulated: COP1-SPA mediated proteolysis of photoreceptor PHYA was shown to be impaired by sucrose application (Debrieux et al. 2013). It will be interesting to establish if other COP1 targets such as HY5 are regulated by internal carbon status.

The other family of light signalling transcription factors - PIFs have also been implicated in sugar signalling. Sucrose induced hypocotyl elongation appears to be PIF dependent and this response is abolished in the *pifQuadruple (pif1pif3pif4pif5)* mutant (Stewart et al. 2011). Although sucrose only moderately alters PIF transcription, PIF5 protein was shown to accumulate in response to sucrose (Stewart et al. 2011). A different study by Shor et al. (2017) did not observe sucrose effects on the protein stability of PIF1,3,4 and 5, but demonstrated through ChIP-qPCR that sucrose

enhances PIF enrichment at the promoters of clock genes *LHY* and *CCA1*. This sucrose-dependent regulation appears to enhance the peak of *LHY* and *CCA1* expression at dawn. The authors propose that this mechanism may allow PIFs to participate in sucrose entrainment of the oscillator. PIFs have also been shown to be required for sugar regulated auxin biosynthesis and signalling (Sairanen et al. 2012; Lilley-Steward et al. 2012).

PIF interacting proteins DELLA and BZR1, master regulators in the gibberellic acid (GA) and brassinosteroid (BR) pathways, respectively, have also been implicated in sugar responses. DELLAs are potent growth suppressors that are known to operate, in part, by directly sequestering PIFs and BZR1 from target promoters (Davière and Achard, 2016). Recently, sucrose (and not glucose) was shown to stabilise the DELLA protein - RGA and inhibits its GA mediated turnover. This stabilised DELLA is necessary for both sucrose-induced upregulation of the anthocyanin biosynthetic genes and sucrose induced hypocotyl growth repression in dark grown seedlings (Li et al. 2014). A separate study using PAC treatment (a GA biosynthesis inhibitor) implicated GA in sucrose induction of hypocotyl elongation in dark adapted seedlings (Zhang 2010). The BR regulated transcription factor BZR1 has also been implicated in this dark dependent sucrose response (Zhang et al. 2015). Zhang et al. (2016) demonstrated that sucrose increased the stability of BZR1 in a mechanism proposed to involve Target of Rapamycin (TOR) kinase. Inhibiting TOR activity results in growth arrest and reduced expression of BR responsive genes (Zhang et al, 2016). Hence, carbon availability controls a growth programme through a TOR-dependent BZR1 pathway. TOR has also been implicated in the integration of carbon and light signalling in the control of leaf initiation at the shoot apical meristem (SAM). Light promotes leaf

initiation and meristematic activity by triggering localisation of the polar auxin transporter PIN1 and cytokinin signalling (Yoshida et al. 2011). Two recent reports (Pfeiffer et al. 2016; Li et al. 2017) further demonstrate mechanistic insights on light and sugar interface on TOR kinase activity to initiate shoot/root meristematic growth. TOR appears to activate WUSCHEL (master stem cell activator) through cytokinin and the GTPase Rho-related protein 2 (ROP2) through auxins for cell cycle activation at the meristematic region. Both these processes act upstream to light and sugar signals. Interestingly, neither light nor glucose alone can efficiently activate TOR kinase in the shoot apex, but a combination of both signals is required for maximal TOR activity.

Hence, taken together, these finding has advanced our thinking on how light, hormone and metabolic/sugar signalling pathways jointly coordinate at multiple levels to regulate plant growth and development thereby opening new line of thoughts in plant molecular research.

1.6. Aims of the thesis

Molecular connections between phytochrome signalling, carbon metabolism and sugar signalling are being explored in the Halliday lab (Yang et al. 2016) and several other labs. However, the precise co-ordination between the signalling networks remain unclear. The glucose sensor HXK1 mutant *gin2* has a short hypocotyl (Moore et al. 2003) that is reminiscent of the light signalling *pif* mutant (Gommers and Monte, 2018). Further, in response to sugar, nuclear HXK1 is required for the transcriptional repression of photosynthetic genes (*CAB2/CAA*). Cho et al. (2007) identified HXK1 enrichment at the *CAB2* promotor encompassing a G box cis- element. This element is crucially required for light mediated *CAB2* direct activation by HY5 (Andronis et al.

2008). Hence, *CAB2* regulation appears to be a convergence point for light and HXK1 mediated sugar signalling. My thesis explores the role of HXK1 in skoto- and photomorphogenic seedling development. It uncovers an important role for HXK1 in seed resource utilization during limited nutrient conditions and it identifies a potent feedback regulation that most likely blocks blue light signalling.

CHAPTER 3: Here, I provide evidence that HXK1 performs an important metabolic role for seedling sustenance during nutrient limiting conditions. The transcriptome reflects the mutant phenotype. Energy -demanding and –deficit pathways down- and up -regulated respectively. Supplying G6P (HXK1 enzymatic end product) rescued this response. Our results indicate that the enzymatic role of HXK1 rather than the signalling function as previously described (Moore et al. 2003) is required for seedling establishment. HXK1 negatively regulates the plastome in the dark and largely operate independent to PIF signalling during skotomorphogenesis. Further, we also show discrepancies concerning the sugar mediated HXK1 nuclear function in photosynthetic gene repression (Cho et al. 2007; Moore et al. 2003). Taken together, this chapter highlights novel insights into the role of HXK1 during seedling establishment.

CHAPTER 4: Here, I present data on the potential feedback regulation by the HXK1Overpressor (HXK1OX) in different light quality. HXK1OX inhibits blue light mediated seedling photomorphogenesis. Red light inhibits HXK1OX action in blue. Genetic evidence indicate PHYB signalling requirement for this red light mediated

suppression. The transcriptome is reflective of the HXK1OX phenotype in both light conditions. However, this study requires mechanistic understanding of HXK1 integration in the two light pathways.

CHAPTER 5: Here, I introduce novel preliminary data on potential involvement of light signalling components Constitutive Photomorphogenic1 (COP1) and De-etiolated1 (DET1) in sugar sensing and signalling. The role of COP1 and DET1 in response to sugar switch between the developmental stages (seedlings and adult plants). Based on published findings, I speculate a working model to support the conditional phenotype.

CHAPTER 6: The chapter comprises of general discussions pertaining to the thesis, highlighting the various questions raised from the project with perspectives of possible future work, and a brief conclusion of the findings and significance of this study.

APPENDIX: I state experimental contributions towards a publication (Seaton et al. 2018, *under revision*) highlighting PhytochromeA as a dawn and photoperiodic sensor.

CHAPTER 2

EXPERIMENTAL PROTOCOLS

2.1. Plant materials and growth conditions

The wild-type *Arabidopsis thaliana* ecotypes used in this study are *Landsberg erecta* (*Ler*) and *Columbia-0* (*Col*). The mutant alleles described are: *gin2* (Moore et al. 2003, *hxk1-3* (CS861759) (Huang et al. 2015), the phytochrome single mutant *phyB-9* (Reed et al. 1998), *pifQ* (*pif1-1, pif3-3, pif4-2, pif5-3* (Leivar et al. 2008), *cop1-4* (Deng et al. 1991) and *det1-1* (Chory et al. 1989). The transgenic lines used in this study are 35S:HXK1 (Kelly et al. 2012) and 35S:HXK1-FLAG (Cho et al. 2006). *gin2* and *35S:HXK1-FLAG* are in the *Ler* background, all other mentioned lines are in the Col-0 background. *35S:HXK1 phyB-9* double mutants were obtained by standard genetic crossing (Weigel and Glazebrook, 2002) and the double mutant obtained through screening and genotyping. For all experiments, seeds were surface-sterilized as described in Fankhauser and Casal (2004), sown on 1/2 MS (Duchefa Biochemie, basal salt mixture) and stratified in darkness for 2-3 days at 4°C. Specific details on growth conditions, photoperiods and white/mono-chromatic light intensities are mentioned in the respective figure legends. For Glucose-6-Phosphate (G6P) and DCMU treatment: Filter sterilized stocks of 100 mM G6P (Sigma) in water and 10mM DCMU (Sigma) in ethanol was directly added to cooled sterilized media according to desired concentration and seedlings directly sown.

2.2. Seedling and adult plant growth parameter

NIH ImageJ was used to quantify hypocotyl length from photographed images of seedlings laid flat on media. Adobe Photoshop C86 was used to quantify cotyledon area from photographed images of seedlings with full cotyledon exposure. For adult biomass quantifications, leaf rosettes were harvested from 4-wk-old plants and weighed immediately (before dehydration) using a precision balance. The plant materials were then dried at 80°C for 10 days to obtain dry biomass. Leaf number was manually counted and rosette diameter/area measured using NIH ImageJ. Specific light treatments and intensities are mentioned in respective figure legends. For epidermal cell length/number of etiolated hypocotyls, seedling were cleared o/n in chlorohydrate as described in Weigel and Glazebrook (2002), mounted on slides and visualized using DIC microscopy. Individual cell length from each frame of the hypocotyl (basal, middle, upper) was measured using image J and cell number manually counted per file.

2.3. Gene expression analysis

2.3.1. qRT-PCR

For qRT-PCR experiments, seedlings harvested in liquid nitrogen was ground into fine powder. RNA was extracted using the RNeasy Plant Mini Kit (Qiagen) with on-column DNase digestion. cDNA synthesis was performed using the qScript cDNA SuperMix (Quanta Biosciences) as described by the manufacturer. The qRT-PCR was set up as a 10µL reaction using SYBR Green (Roche) in a 384-well plate, performed with a Lightcycler 480 system (Roche). Results were analysed using the Light Cycler 480 software. The primers used in this study are listed in Table1.

2.3.2. RNAseq analysis:

RNAseq was performed on 4 day old etiolated Ler and *gin2* seedlings (biological duplicates) grown at 18C. RNA was extracted using the RNeasy Plant Mini Kit (Qiagen) with on-column DNase digestion, quality control checked and sent to Edinburgh Genomics for sequencing.

Dr. Andrew Romanowski (Halliday lab) performed raw data analysis. Libraries were prepared following the TruSeq RNA v2 Sample Preparation Guide (Illumina). The multiplexed samples were loaded onto Illumina HiSeq 2500 sequencer, providing 100-bp single-end reads. Reads were quality-filtered using the standard Illumina process and demultiplexed with two allowed barcode mismatches. Sequence files were generated in FASTQ format. Read counts were calculated for genes, exon bins, AS bins and intron bins with the ASpli package (cita ASPli) using custom scripts written in R. Histograms showing the depth of sequencing coverage were generated using the IGB Browser (CITA IGB). Detection of cycling was performed using JTK_Cycle (Hughes et al., 2010) implemented in R (64-bit, version 2.12.1). Relative amplitude estimates were calculated by dividing the subtraction of the absolute peak expression and through levels, by the sum of through level plus one (to avoid divisions by zero). Heat maps were generated using scripts for R. PSI/PIR indexes were calculated as previously described (cita PSI/PIR) using custom scripts written in R.

2.3.3. DNA microarrays analysis:

Whole transcriptome analysis was performed on 4 day old Col and *35S:HXK1* seedlings (biological triplicates) grown in continuous blue light (10μM m^{-2} s^{-1}) and

blue + red light (10 + 40μM m^{-2} s^{-1}) at 18C. RNA was extracted using the RNeasy Plant Mini Kit (Qiagen) with on-column DNase digestion and shipped to Nottingham Arabidopsis Stock Centre (NASC) on dry ice. RNA integrity was confirmed using an Agilent 2100 Bioanalyzer with the RNA 6000 Nano Kit (Agilent Technologies). Whole transcriptome analysis was conducted by hybridizing total RNA of three independent biological replicates for each line to Affymetrix Arabidopsis Gene 1.1 ST Array Strips (Affymetrix). Gene expression data were analyzed using Partek Genomics Suite 6.6 software (Partek).

Gene Ontology (GO) analyses derived from both RNAseq and Affymetrix data were performed with the VirtualPlant web service (Katari et al. 2010). The overrepresented pathways tabulated has a p-value cut-off of 0.01 (Fisher Exact Test).

2.4. Protein extraction and immunoblots

Plant tissue was harvested in liquid nitrogen and ground into fine powder. Total protein was extracted using extraction buffer (100mM Tris-HCL(pH 8), 50mM EDTA, 0.25M NaCl, 0.7%SDS and 1mM DDT (freshly added)) (Duek et al. 2004). Samples were incubated at 65°C for 10 min before centrifuging at the highest speed for 10 min. Supernatant was collected into a new tube, and protein was quantified using Pierce BCA kit according to the manufacturer's instructions. 50-100 μg of each sample suspended in 4X Lamelli buffer + β-mercaptoethanol was loaded on a 12% SDS-PAGE, followed by a wet transfer to a polyvinylidene fluoride (PVDF) membrane. The FLAG tag was detected by probing the membrane with a rat anti-FLAG monoclonal antibody (BioRad MCA4764P) at a dilution of 1:5000. Loading was checked by directly reprobing membranes using a mouse monoclonal anti-Actin antibody (Sigma A0480)

at a dilution of 1:5000 followed by a HRP-conjugated anti-mouse (Bio-Rad) at a dilution of 1:5000. Signals were detected using the Amersham ECL kit as instructed by the manufacturer. ImageJ was used for band quatification to calculate relative abundance.

2.6. Starch and sugar quantification

Plant tissues (seedlings/whole rosettes – where applicable) was collected and ground to a fine powder in liquid nitrogen. 20mg powder was weighed into a tube. 250µl of 80% ethanol was added to the sample powder, vortexed and incubated at 80°C for 20 min. Then the samples were centrifuged at 14000 rpm for 5 min and supernatant transferred to a separate tube. This process is repeated again by adding 150 µl 80% ethanol and 250 µl 50% ethanol to the pellet. The supernatants collected in the tube will be used for glucose and sucrose quantification, while the pellet is used for starch and protein measurments. The detailed protocol is published in Hendriks et al. (2003).

Sugar extraction and determination: Solution mix for 1 microplate: 15.5 ml HEPES/KOH (1M) $MgCl_2$ (30mM) pH7 buffer, 480µl ATP, 480µl NADP, 80µl G6PDH

Determination: Per well, disposed in duplicates: 20 µl ethanolic extract + 160 µl Mix

Read at 340 nm (1 measurement every min), after OD stabilised, successively added the following enzymes: 1µl Hexokinase (after OD stabilised) add 1µl Phosphoglucose isomerase (after OD stabilised) add 1 µl Invertase.

Calculations: Use following equation: µmol NADPH = OD/(2.85*6.22)

Starch Determination: Solutions: Acetate/NaOH (0.5M) pH4.9 buffer, HCl (0.5M) + acetate/NaOH (0.1M) pH4.9 buffer, Amyloglucosidase, Amylase, HEPES/KOH (0.1M) $MgCl_2$ (3mM) pH7 buffer, 480µl ATP, 480µl NADP, 80µl G6PDH

Starch degradation mix (25 ml): 3 ml amyloglucosidase + 30 µl α-amylase together

To the initial pellet, added 400µl NaOH (0.1 M), and heated at 95°C for 30 min. To hydrolyse starch, add 80µl HCl (0.5 M) acetate/NaOH (0.1M) pH 4.9 and 100µl starch degradation mix.

Incubate overnight at 37°C. Plate is setup and glucose (hydrolysed starch) is determined by adding hexokinase enzyme using the formula mentioned above.

CHAPTER 3

Critical role of Hexokinase1 (HXK1) during seedling establishment

3.1. Introduction

Successful germination and seedling establishment rely upon the presence and utilization of sufficient reserves (Baud et al. 2008). Arabidopsis seeds contain a significant portion of stored carbon and energy as Triacylglycerols (TAG) and Seed Storage Proteins (SSR) in addition to minute quantities of sucrose within the cotyledons of the mature embryo. After germination in the dark, stored nutrients are invested in hypocotyl elongation at the expense of root and cotyledon development (skotomorphogenesis). The TAG energy reserves in the endosperm are critical for skotomorphogenic growth. Mutations in *phosphoenolpyruvate carboxykinase 1 (pck1)* and *isocitrate lyase (icl)* display inhibition of etiolated hypocotyl growth. Both enzymes are key components for catabolizing reserve fatty acids to produce sugars by gluconeogenesis and the glyoxylate cycle respectively (Eastmond et al. 2000; Penfield et al. 2004). Skotomorphogenesis is also regulated by multiple signalling components (Chaiwanon et al. 2016; Seluzicki et al. 2017). On light perception, seedling switch to the photomorphogenic programme characterized by hypocotyl repression and cotyledon expansion to facilitate photosynthetic vegetative growth. In addition to fuelling energy and carbon skeleton supply, photosynthate sugars are widely considered to function as signalling molecules. Evolutionary conserved regulatory pathways functioning in plant sugar sensing and signalling have been identified and characterized (Li and Sheen, 2016; Sheen, 2014).

Hexokinase 1 (HXK1) is the first demonstrated intracellular glucose receptor in plants. Arabidopsis HXK1 performs a dual function: a mitochondrial bound enzymatic and a nuclear signalling role. HXK1 enzyme catalyses the first glycolytic step of glucose phosphorylation to generate glucose-6-phosphate (G6P), a highly conserved role across evolutionary systems (Cárdinas et al. 1998) One molecule of glucose yields 30-32 ATP energy molecules during aerobic respiration to fuel plant growth and metabolic maintenance. Cho et al. (2007) also proposed a signalling role for Arabidopsis HXK1. They demonstrate nuclear HXK1 in complex with partner proteins RPT5B and VHAB1 to directly repress photosynthetic genes in the presence of exogenous glucose. Using ChIP-qPCR, they observed strong HXK1 enrichment on the *CAB2* promotor region that encompasses characterized cis-elements including a previously characterized G box (Andronis et al. 2008; Maxwell et al. 2003). This sugar-dependent HXK1 nuclear regulatory role is postulated to function as a negative feedback photosynthetic inhibitory mechanism (Cho et al. 2007).

Moore et al. (2003) generated lines harbouring point mutations in the catalytic domain of HXK1 to uncouple the enzymatic from the proposed signalling role. Hence, $HXK1^{S177A}$ and $HXK1^{G104D}$ have reduced glucose phosphorylation activity but intact signalling function. They show certain conditional phenotypes wherein the *HXK1* mutant *gin2* (*glucose insensitive 2*) is insensitive to elevated glucose (6%) mediated germination inhibition. The *gin2* mutant exhibit a small seedling stature at low light on sugar free media. Interestingly, $HXK1^{S177A}$ and $HXK1^{G104D}$ could restore the impaired phenotypes to wildtype. This highlights the crucial requirement of HXK1 signalling function rather than the enzymatic role for seedling development.

In this study, our genetic data highlight HXK1 requirement during nutrient reserve dependent conditions for seedling establishment. Based on the mutant phenotypes, HXK1 predominantly operates during nutrient limited conditions such as periods of darkness or low light. RNAseq analysis enabled us to gain unprecedented insights into the *gin2* transcriptome. Key energy -demanding and –deficit pathways are altered in the mutant suggesting energy deprivation. Supplying glucose-6-phosphate (HXK1 enzymatic endproduct) rescues both the *gin2* starvation response and the mutant phenotype to Wt. This indicates that the enzymatic role of HXK1 rather than the signalling function as previously described (Moore et al. 2003) is crucially required for seedling establishment. We also show that HXK1 negatively regulates the plastome in the dark and largely operate independent to PIF signalling during skotomorphogenesis. Further, by enhancing endogenous sugar levels rather than exogenous supply, we show that HXK1 is not required for photosynthetic gene repression in seedlings as previously described (Cho et al. 2007; Moore et al. 2003). Taken together, we highlight multiple facets of the glucose sensor HXK1 during seedling establishment.

3.2. Results

3.2.1. HXK1 Operates in the Dark and Low Light in Seedlings – Continuous Light

The seedling developmental transition from skotomorphogenic growth (elongated hypocotyl/closed cotyledons) to light induced photomorphogenic growth (hypocotyl growth suppression and cotyledon expansion) is orchestrated by multiple signalling components including the PIF family of transcription factors (Gommers and Monte, 2018). PIFs promote hypocotyl elongation and are active in the dark, light inhibits PIF activity via multiple mechanisms and subsequently hypocotyl elongation in a fluence dependent manner. Hence, the PIF quadruple mutants (*pifQ*) exhibit a short hypocotyl in the dark and at continuous low light fluences (Leivar et al. 2012; Xin et al. 2017). I found that the *hexokinase1* mutants *gin2* (Ler background) and *hxk1-3* (Col background) exhibit a similar response as detailed below and shown in Fig. 1.

The HXK1 mutants (*gin2* and *hxk1-3*), overexpressor (HXK1OX) and relevant Wt controls were grown in the dark and increasing fluences of white light on sugar free media. As observed in Fig. 1A, *gin2 a*nd *hxk1-3* mutants exhibit a short etiolated hypocotyl while a subtle enhancement is observed in the overexpressor relative to wildtype indicating a potential role for HXK1 in the dark during skotomorphogenesis. While a standard light fluence dependent photomorphogenic response is observed in wildtype, a marked short hypocotyl and small cotyledon phenotype is observed in the hexokinase1 mutants *gin2* and *hxk1-3* exclusively under low light fluences (Fig. 1A,B). However, under high light intensities the mutant hypocotyl length and cotyledon area appear wildtype suggesting a less dominatant role for HXK1 in these conditions. Hence, the mutants appear to undergo photomorphogenesis more rapidly and is required during low light fluences.

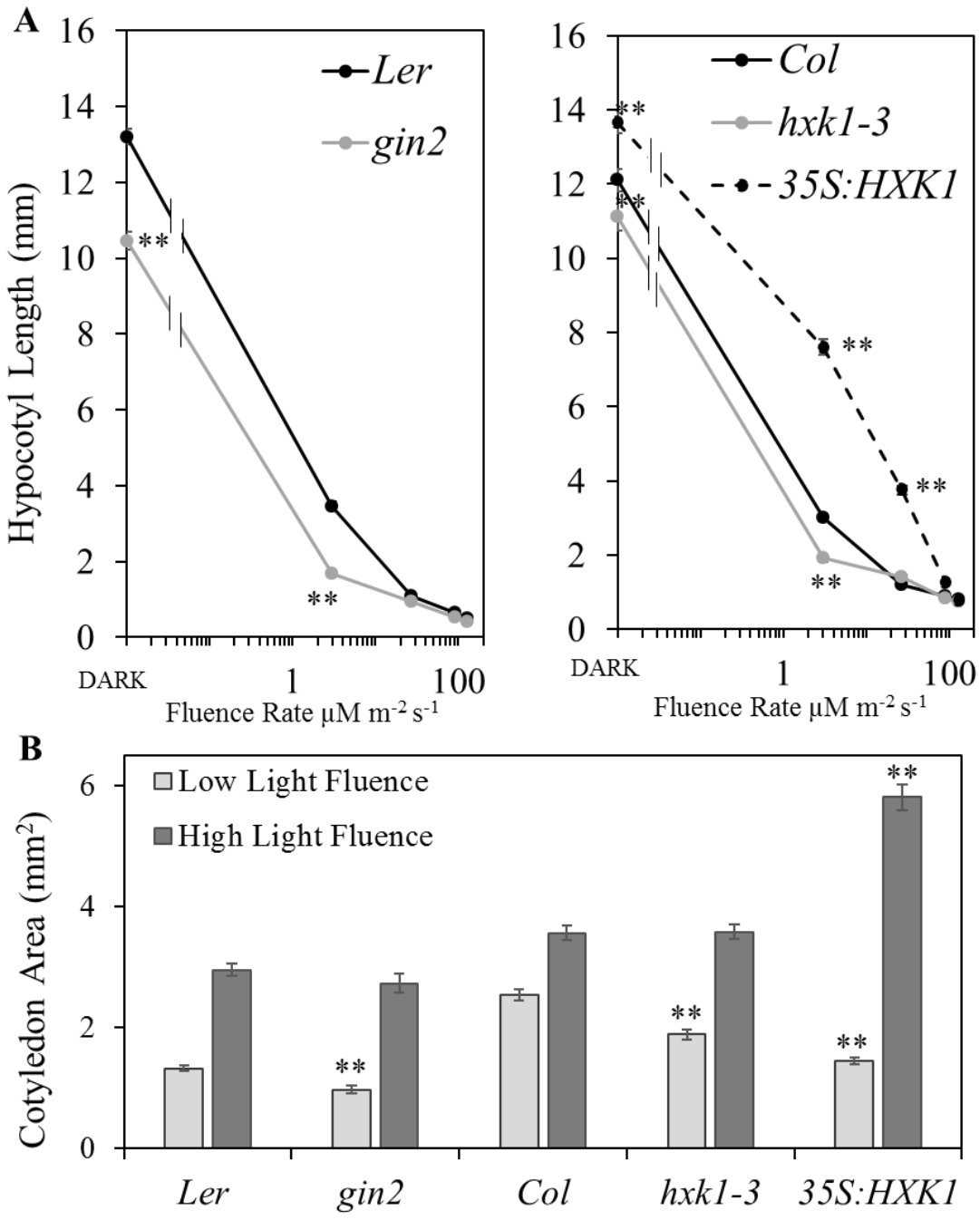

Fig4.1: Seedling morphology of the HXK1 family – Dark and continuous light.
A) Hypocotyl length (in Dark, 3, 27, 90, 130µmol m^{-2} s^{-1} white light) and B) cotyledon area (in 3µmol m^{-2} s^{-1} and 130µmol m^{-2} s^{-1} white light) of 7 day old Wt, *gin2, hxk1-3* and *35S:HXK1* seedlings grown in continuous light at 18°C. Error bars indicate ±SEM; and **P⩽ 0.01 of *gin2, hxk1-3* and *35S:HXK1* relative to respective Wt in each condition (Student's t-test).

In contrast, *HXK1OX* exhibits an etiolated phenotype at low light fluence (elongated hypocotyl and small cotyledon) while high light completely supresses hypocotyl elongation and significantly enhances cotyledon area. Although the HXK1 mutants phenocopy the PIF mutants, the HXK1OX appear phenotypically different to a PIFOX. The PIFOX exhibits an elongated hypocotyl/small cotyledon even at high light fluences (Johansson et al. 2014; our data – not shown). Taken together, HXK1 appears to operate in the dark/low light fluences and is required for normal seedling photomorphogenesis.

3.2.2. HXK1 Operates in the Dark and Low Light in Seedlings – Photoperiods

The PIF family of TFs govern photoperiodic control of hypocotyl length (Huang and Nusinow, 2016). To test if the HXK1 mutants phenocopy the PIF mutants under various photoperiods, we grew the seedlings under Short Day (SD 8:16), 12:12 and Long Day (LD 16:8) conditions under 100µmol m^{-2} s^{-1} light (Fig4.2). As observed, Wt seedlings exhibit a dramatic suppression of hypocotyl length as the photoperiodic increases, a well-characterized Evening Complex (EC) regulated PIF dependent mechanism (Fig4.2) (Nusinow et al. 2011). The hexokinase1 mutants *gin2* and *hxk1-3* exhibit a marked short hypocotyl phenotype under Short Day (SD) photoperiods, as light duration lengthens (12:12 to LD), the hypocotyl length of the mutants appear wildtype (a trend similar to *pif* mutants, Gommers and Monte, 2018*)*. In contrast to the mutants, HXK1OX exhibits an opposite hypocotyl enhancement phenotype which is more prevalent in SD (2.2 fold enhancement) than LD (1.4 fold enhancement). As the fluence rate data (Fig4.1) indicated that the HXK1 mutant phenotype was more obvious at low light fluences, we wanted to establish whether the abolition of the

mutant/ox phenotype in LD is simply due to extended high light exposure. Hence, the experiment was repeated in LD conditions but under low light (5µM m^{-2} s^{-1}) which is still sufficient to entrain the clock. This downward shift in light restored the HXK1 mutant/Ox phenotype. Hence, HXK1 appears to operate under periods of extended darkness (SD) or limited light (SD and LD (5µM m^{-2} s^{-1}) consistent to our findings described in Fig. 1.

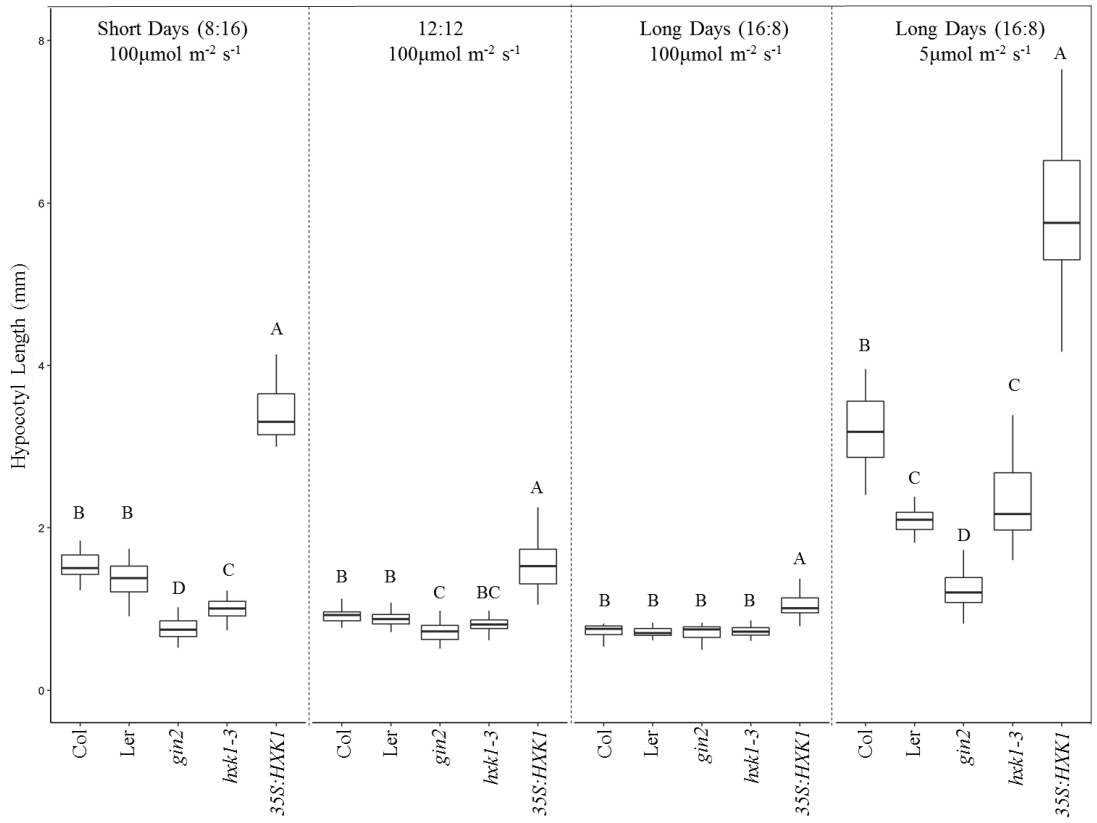

Fig4.2: Seedling morphology of the HXK1 family – Photoperiods
Hypocotyl length of 7 day old seedlings grown in various photoperiods (SD/12:12/LD) at 100µmol $m^{-2}s^{-1}$ and LD conditions at 5µmol $m^{-2}s^{-1}$ at 18°C. Horizontal bars, boxes, and whiskers show medians, interquartile ranges (IQR), and dataranges, respectively. Different letters denote statistical differences ($P > 0.05$) among samples as assessed by one-factorial ANOVA and Tukey HSD.

We were interested to check if HXK1 is transcriptionally or post transcriptionally regulated like the PIFs as the *HXK1* mutants phenocopy the *PIF*

mutants in photoperiods. As observed in Fig. 3, *HXK1* transcription does not appear to be regulated by the Evening Complex (EC) as the *HXK1* transcript levels are more or less similar under both photoperiodic conditions (Fig4.3A). Similarly, HXK1 proteins levels (35S:HXK1-FLAG) appear similar between EOD/EON time points at SD or LD. However, HXK1 shows a photoperiodic regulation at the posttranslational level since HXK1-FLAG accumulates 2 folds higher in LD than SD (Fig4.3B). Hence, HXK1 transcript or protein levels in SD and LD do not appear to be regulated in a similar fashion to the PIFs.

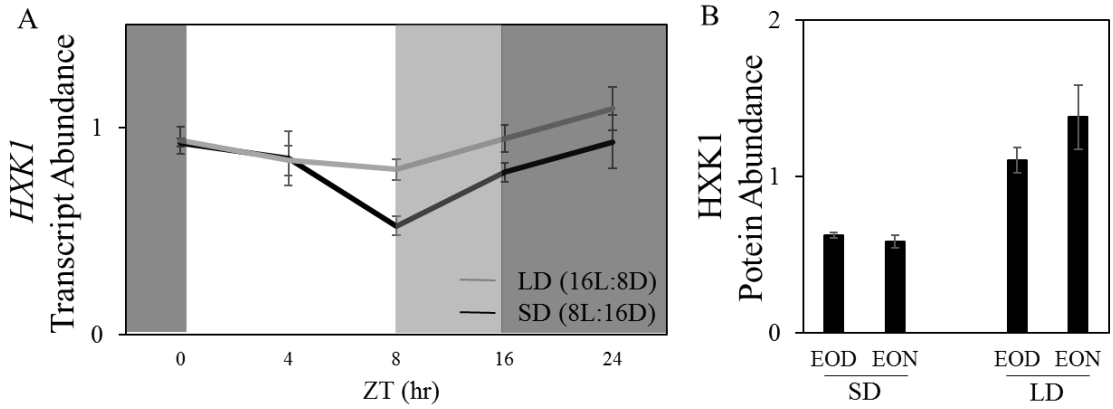

Fig4.3: HXK1 diurnal transcript and protein abundance. A) HXK1 transcript abundance relative to PP2A in 7-day-old Wt seedlings in LD and SD and B) HXK1 protein levels relative to GAPDH in 7-day-old 35S:HXK1-FLAG seedlings grown in SD and LD in 100µmol $m^{-2}s^{-1}$ at 18°C. Error bars indicate ±SEM from three biological replicates.

3.2.3. RNAseq analysis - HXK1 is required for nutrient resource management

As the effects of the *gin2* mutation is evident during periods of extended darkness, an RNAseq was performed on 4-day-old etiolated *gin2* mutant seedlings. This would enable us to understand the underlying mutant transcriptome and the molecular interdependency with the PIF transcription factor family during

skotomorphogenesis. In the *gin2* mutants, 2353 genes were misregulated - 1276 genes was downregulated (< -1.5 FC) and 1077 genes was upregulated (> 1.5 FC).

3.2.3.1 RNAseq analysis reveals down regulation of energy demanding processes in *gin2*

Amongst the down-regulated class of genes (1276 with ≤ -1.5 FC), the enriched Gene Ontology (GO) terms are ATP energy demanding pathways. A large number of microtubules, kinesins, myosins, cytoskeletal motor proteins, certain ribosomal and several storage protein encoding genes are down regulated in the *gin2* mutants (Fig4. 4A,B).

Cytoskeletal motor proteins utilise ATP to move along the cytoskeletal elements -microtubules (kinesins) and microfilaments (myosins). Cytoskeletal motor proteins directly mobilize the organization of various cytoskeletal arrays during cell division, cell expansion and cell growth in plant tissues. They are also responsible for the motility of molecules, organelles and chromosomal segregation apart from spindle organization during mitosis and meiosis (Hashimoto, 2015).

Signal converging genes responsible for hypocotyl elongation include expansins, extensins, Xyloglucan endoTransglucosylase/Hydrolase (XTHs) and the Paclobutrazol REsistant (PREs). Disruption of microtubules leads to reduced XTH activity in cell elongation (Sasidaran et al. 2014). Interestingly, connecting this linkage, only the XTH family of genes appear downregulated (-2 to -4 fold decrease) in the *gin2* mutants (Fig4.4C). XTHs promote cell wall loosening by either re-joining xyloglucan (xyloglucan endotransglucosylase activity) or hydrolyse xyloglucan (xyloglucan hydrolase activity). Hence, the downregulation of certain *XTHs* may

contribute to reduced hypocotyl elongation in the *gin2* mutants primarily due to predominantly reduced microtubular activity. Among other downregulated genes are core cell cycle genes predominantly of the CYC-B subfamily class (-1.6 to -3 fold decrease) and certain cyclin dependent kinase and cyclin family proteins (Fig4.4D).

Other notable gene families among the downregulated class are seed storage proteins and storage facilitating proteins (cruciferins, albumins, cupins, oleosins (-2 to -12 fold decrease)) (Fujiwara et al. (2002), certain ribosomal proteins and ribosome biogenesis encoding genes (Fig4.4E). However, on measuring total protein content, no difference was observed in the *gin2* mutants relative to Wt (data not shown) suggesting a potential compensation. Hence, taken together, transcript levels of genes involved in energy demanding process such as cell division, expansion, cytoskeletal and microtubular organization, storage and certain ribosomal proteins is downregulated in the *gin2* mutants. This data suggests that the enzymatic role of HXK1 required for glucose phosphorylation and subsequently ATP generation may be required during nutrient reserve dependent conditions.

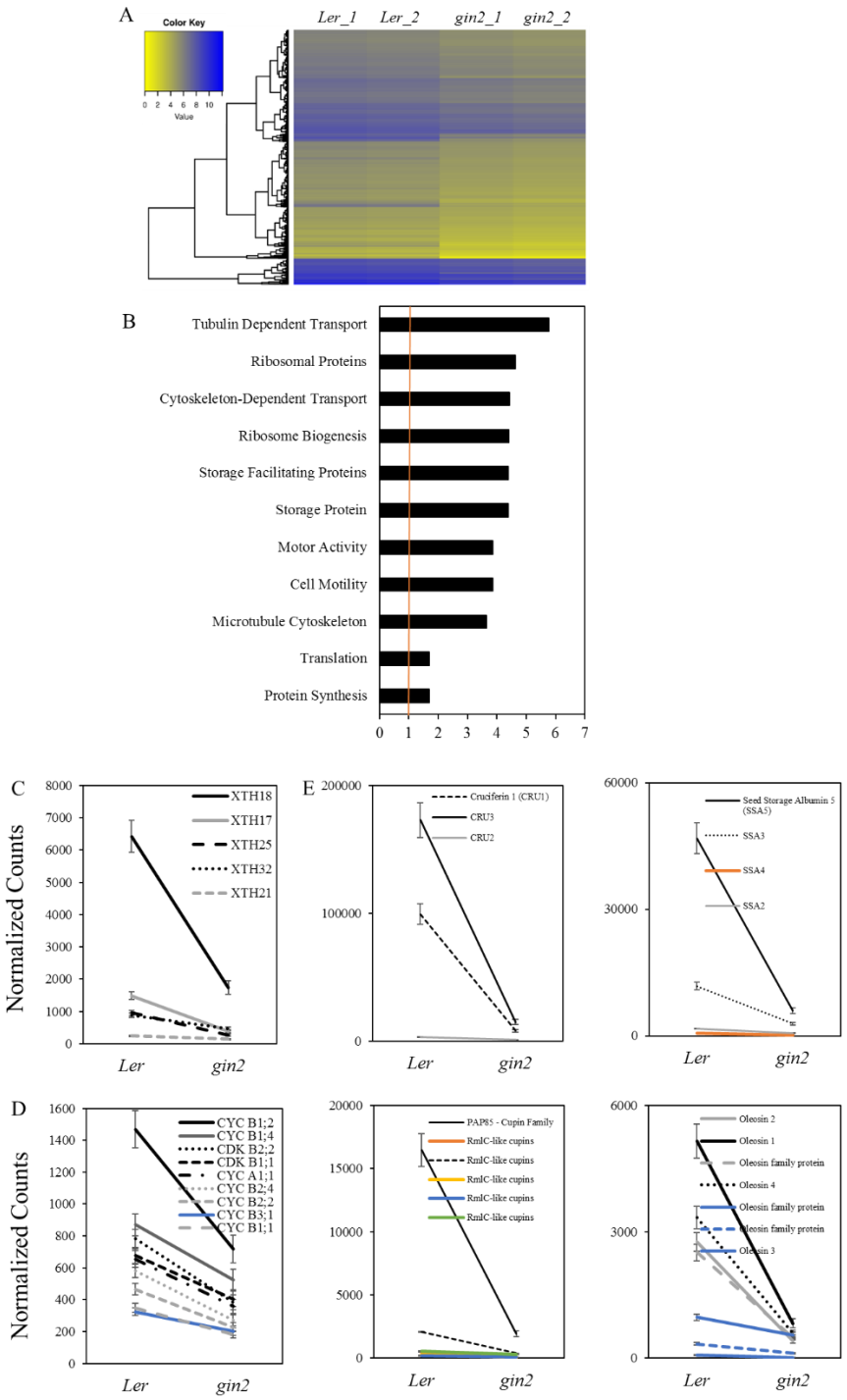

Fig4.4: RNAseq Analysis – Down regulated genes
A) Hierarchical clustering of downregulated genes in 4-day-old etiolated Ler and *gin2* biological duplicates. B) Gene Ontology (GO) analysis of downregulated genes (derived from Virtual Plant public database) depict pathway enrichment. Pathways with a statistically significant enrichment (>1 (orange line), $p \leq 0.01$) are shown. mRNA expression pattern of normalised counts of C) XTH gene family D) core cell cyclin B type genes E) seed storage proteins derived from RNAseq data. Error bars indicate ±SE.

I reasoned that the down-regulation of energy-demanding processes may be due to energy deprivation because of inefficient mobilisation of seed reserves. To test whether the *gin2* mutants are experiencing energy deprivation, I measured glucose levels. Indeed, a 55% increase in the mutants relative to Wt was observed (Fig4.5A). The enhanced glucose level reiterates the requirement of HXK1 mediated metabolic glucose processing for ATP production to fuel energy demanding biological activities. As a simple read-out to confirm that cytoskeleton dependent cell division and expansion activity are altered in the *gin2* mutants, I measured both, epidermal cell length at the basal/middle/upper regions of the hypocotyl and epidermal cell number of the entire file (Fig4.5 B,C). In the Wt as well as *gin2* (Fig4.5B), epidermal cells at the basal region are more expanded than cells at the actively dividing upper region proximal to the apical hook. However, within each of these regions, the *gin2* mutants have shorter cells than Wt (17% decrease in basal region, 26% decrease in the middle region and 34% in the upper region). In addition, a 34% reduction in cell number was observed in the *gin2* mutants relative to Wt (Fig4.5C). Taken together, cell division and expansion are reduced in the *gin2* mutants, which are energy-demanding processes and may therefore be the result of low ATP availability.

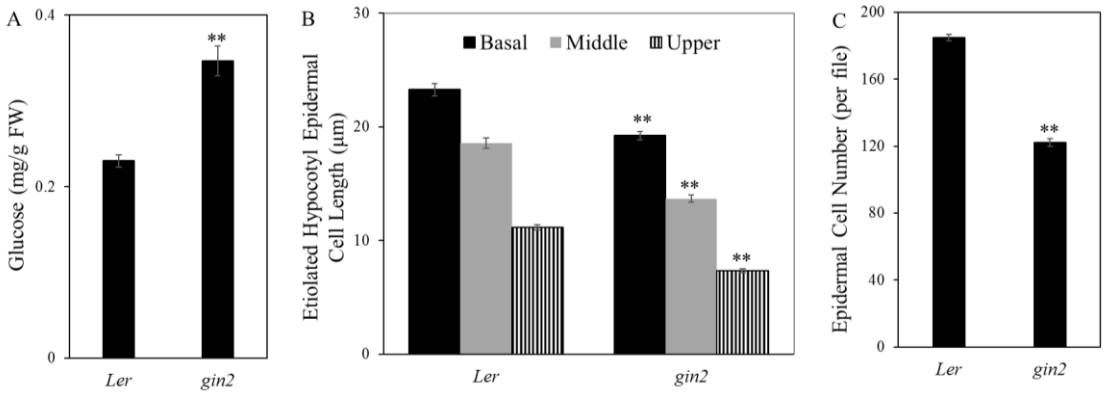

Fig4.5: A) Glucose levels (mg/g FW) in 4-day-old etiolated Ler and *gin2* seedlings grown at 18C. B) Epidermal hypocotyl cell length (μm) at the basal, middle and upper region and C) epidermal cell number (per file) of 4-day-old etiolated hypocotyls. Error bars indicate ±SEM, **P≤ 0.01 of *gin2* relative to Ler (Student's t-test).

3.2.3.2. RNAseq analysis – C starvation response is predominantly upregulated in the *gin2* mutants

Amongst the upregulated subset of transcripts in the RNAseq, transcript levels of genes involved in various metabolic pathways and starvation markers appear to be enhanced in the *gin2* mutant according to GO analysis (Fig4.6A,B). This suggests direct or indirect negative action of HXK1 on such pathways. The three most enriched pathways in the upregulated subset have catabolic functions – they include genes involved in the degradation of the Branched Chain Amino Acids (BCAA) – Leu, Ile and Val (Fig4.6C). In addition to functioning as building blocks for protein biosynthesis, amino acids play pivotal roles during signalling and stress response. BCAA degradation is an evolutionary conserved process occurring in the mitochondria induced by carbon starvation. Interestingly, BCAA degradation pathway genes are diurnally regulated with enhanced transcriptional induction at night (Peng et al, 2015). The branched-chain amino acid transaminase (BCATs) family of enzymes is particularly critical for the last step of synthesis and the initial step of degradation of these amino acids

Oxidation of BCAAs directly feeds electrons into the electron transport chain. The carbon skeletons are further converted to precursors of the tricarboxylic acid (TCA) cycle through a series of biochemical steps for subsequent ATP production (Fig. 6C). ATP generation from the BCAA catabolic pathway is particularly high: Ile, Leu and Val yield 29, 32 and 24 ATP molecules respectively (Binder, 2010; Hildebrandt et al.

2015). Hence, it appears that the HXK1 mutant *gin2* employ the BCAA pathway to support cellular respiration, energy production and subsequently growth under periods of prolonged darkness or suboptimal light levels.

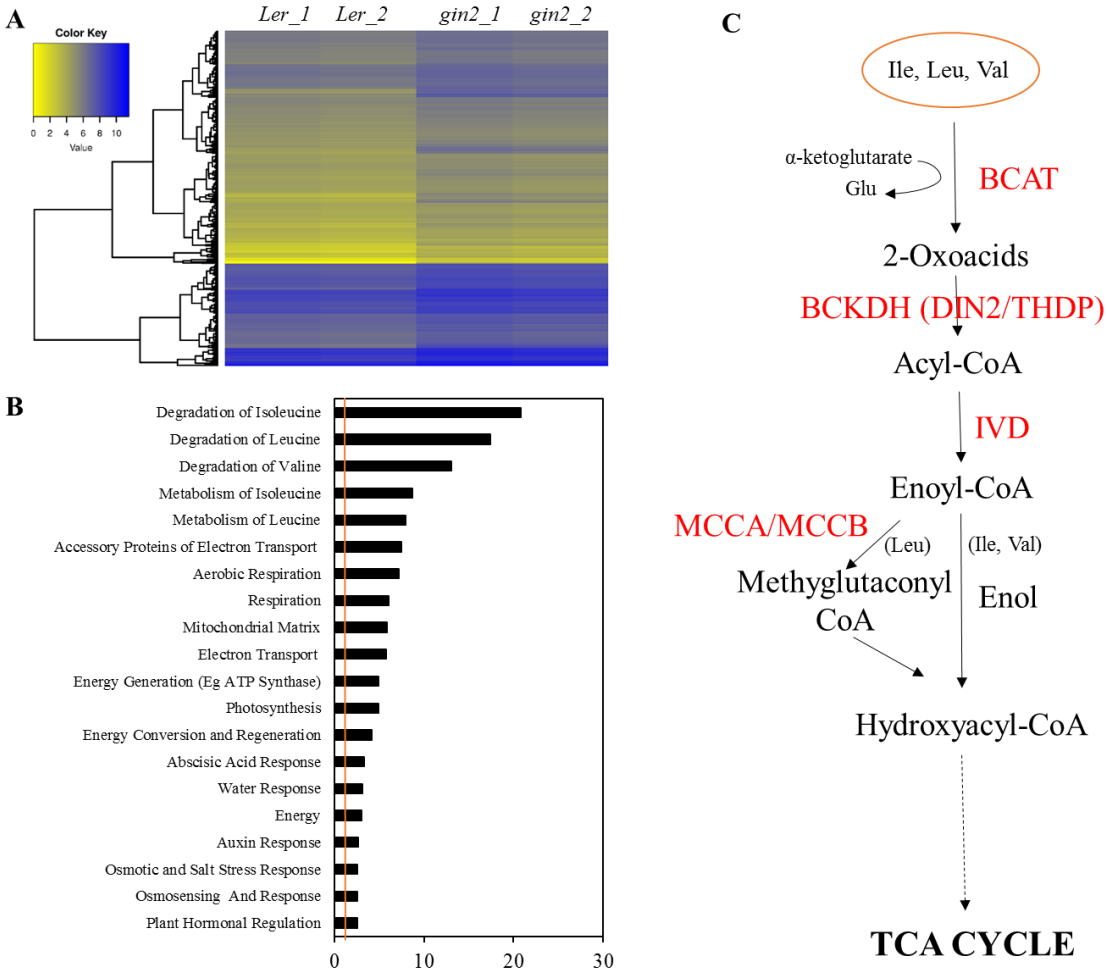

Fig4.6: RNAseq Analysis – Upregulated genes
A) Hierarchical clustering of downregulated genes in 4-day-old etiolated Ler and *gin2* biological duplicates. B) Gene Ontology (GO) analysis of downregulated genes (derived from Virtual Plant public database) depict pathway enrichment. Pathways with a statistically significant enrichment (>1 (orange line), $p \leq 0.01$) are shown. C) Diagrammatic representation of the BCAA catabolic pathway yielding TCA cycle substrates.

The upregulated genes in the *gin2* mutants were compared with two published C starvation induced gene lists to obtain the degree of overlap. Fig4.7A is a comparison with C starvation induced genes in light grown Arabidopsis seedlings (Cookson et al. 2016) and Fig4.7B is a comparison with SnRK1/KIN10 regulated C starvation genes in light grown Arabidopsis protoplasts (Baena-González et al, 2007). The growth conditions of my data and these published resources are not identical as the published data is derived from light grown conditions and our RNAseq data from dark grown seedlings. However, as observed in Fig4.7, although only a small percentage of genes overlap with the *gin2* mutant between both gene lists, the subsets are strongly enriched in the BCAA degradation pathway.

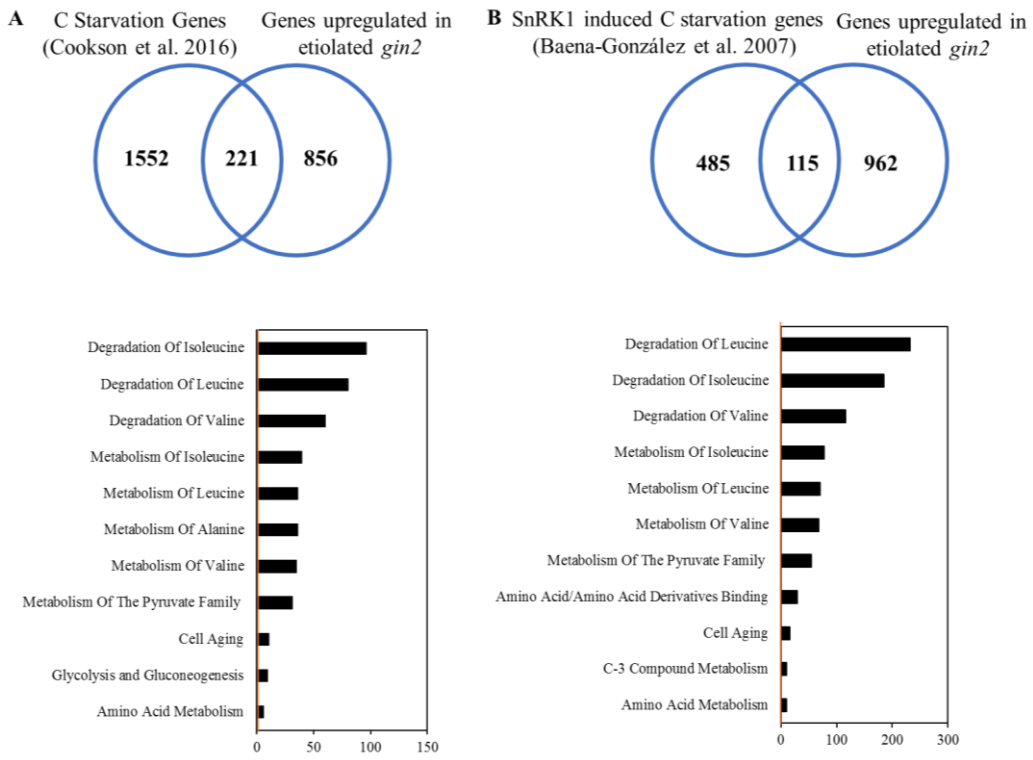

Fig4.7: Comparison between genes upregulated in the *gin2* mutants with A) C starvation induced genes (Cookson et al. 2016) and B) SnRK1 regulated C starvation genes (Baena-Gonzalez et al. 2007) with respective GO analysis of common gene subset. GO terms derived from VirtualPlant database depict ratio enrichment (observed/expected value). Pathways with a statistically significant enrichment (>1 (orange line), $p \leq 0.01$) are shown.

To summarise, HXK1 operates particularly during nutrient limited conditions (Fig4.1,4.2). The RNAseq data gives us novel insights into the mutant transcriptome. Energy –demanding and –deficit pathways are down and up -regulated respectively. The *gin2* mutants are impaired in glucose phosphorylation and the ability to generate energy to fuel these biological processes. However, under photosynthetically active high light conditions, HXK1 activity appears to be compensated potentially by other HXKs thereby restoring normal glycolytic activity and respiration. Taken together, it appears that the enzymatic role of HXK1 rather than the signalling role is critical for nutrient reserve management during nutrient limiting conditions.

3.2.4. The enzymatic and not the signalling role of HXK1 is required for seedling establishment

As the carbon starvation induced BCAA catabolic pathway is triggered as an energy source (Binder, 2010) we hypothesised that the enzymatic role rather than the nuclear signalling role of HXK1 is required for seedling establishment during nutrient limiting conditions.

To test this, we grew the *gin2* mutants in the absence and presence of 27mM (0.5%w/v) glucose (HXK1 substrate) or 5 or 10mM Glucose-6-Phosphate (G6P, HXK1 enzymatic endproduct to bypass HXK1 enzymatic function). As shown, in Fig. 8A, Wt and *gin2* etiolated seedlings were unresponsive to glucose but 5 and 10mM G6P was sufficient to elongate *gin2* mutants to Wt length. In low light grown seedlings (Fig4.8B), glucose stimulated hypocotyl elongation in Wt and *gin2*. This observation is consistent with published results indicating a HXK1 signalling independent role in

sugar mediated hypocotyl elongation (Simon et al. 2018; Sing et al. 2017; Zhang et al. 2016). Interestingly, while Wt seedlings were insensitive to G6P treatment, it again completely restored the short *gin2* hypocotyl to Wt length. Analogous responses were recorded for cotyledon area in response to glucose and G6P treatments (Fig4.8B). G6P application also rescued the *gin2* short hypocotyl phenotype when grown in Short Days (SD) (100μmol m^{-2} s^{-1}) or low light fluences in Long Days (LD) (5μmol m^{-2} s^{-1}) (Data not shown).

Taking these results together, it is evident that the reason for the *gin2* small seedling stature phenotype during nutrient limiting conditions (periods of extended darkness/low light/short days) is due to G6P deficit and the BCAA catabolic pathway is likely activated as an alternative energy source. By bypassing HXK1 enzymatic activity through G6P application, energy production is restored and the *gin2* mutants exhibit a Wt seedling phenotype.

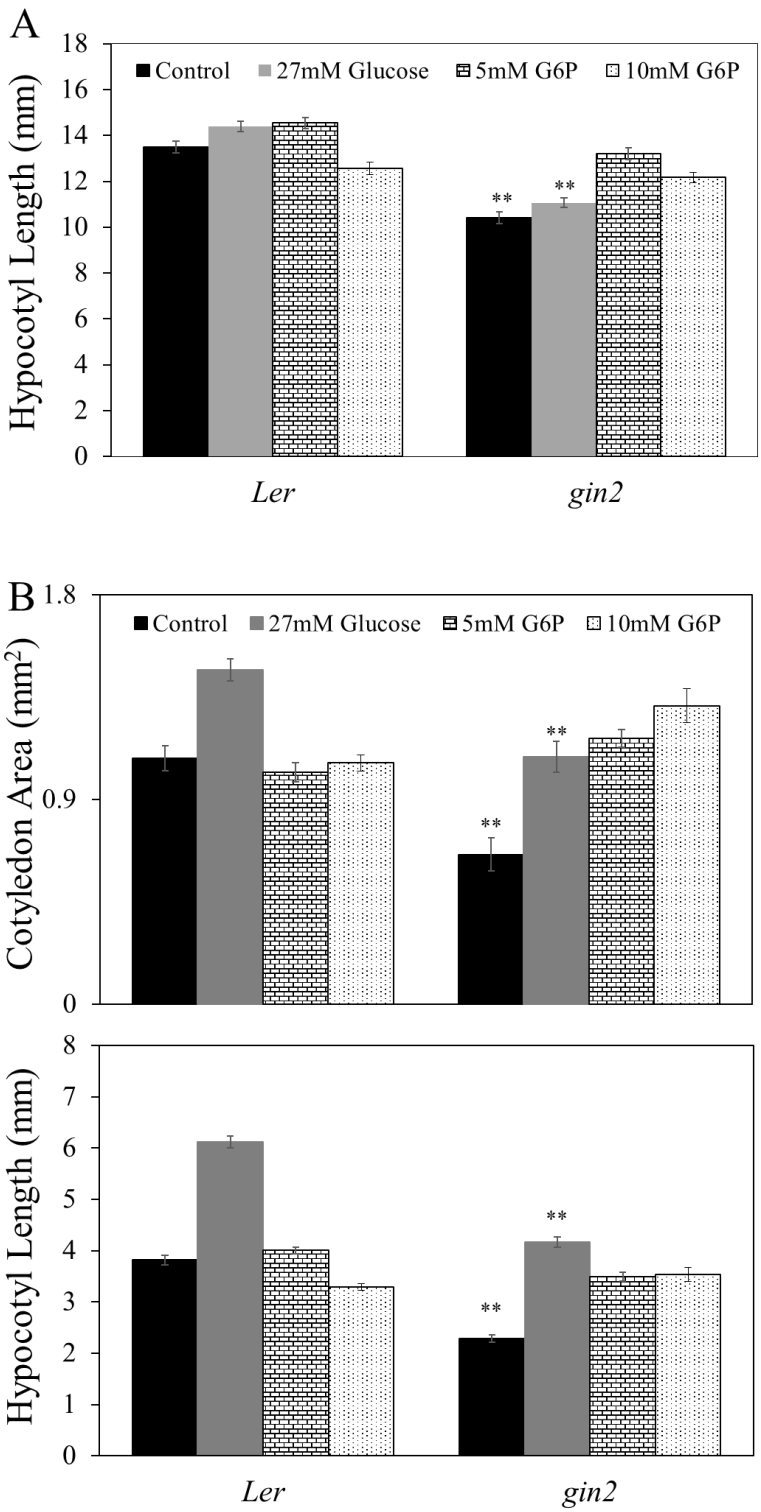

Fig4.8: Phenotypic analysis of 7 day old Ler and *gin2* seedlings grown in control conditions and in the presence of 27mM glucose or 5 and 10mM G6P. A) Hypocotyl length of etiolated seedlings and B) Cotyledon area and hypocotyl length of seedlings grown under continuous low light fluence (3μmol m^{-2} s^{-1}). Error bars indicate ±SE; and **P≤ 0.01 of *gin2* relative to Ler in each treatment (Student's t-test).

3.2.5. Glucose 6 Phosphate (G6P) application rescues *gin2* starvation response

To test if glucose and G6P application also rescues the *gin2* starvation response, I measured the transcript abundance of highly upregulated BCAA pathway genes (Fig4. 6) by qPCR. Validating the RNAseq data, under control conditions, six BCAA catabolic genes (*BCAT2 / DIN2 / THDP / IVD / MCCA / MCCB*) are highly upregulated in the *gin2* mutant relative to Wt (3 to 8 fold increase) (Fig4.9). All six genes are SnRK1/KIN10 regulated and strongly supressed by exogenous sugar application (Baena-González et al. 2007). As expected, glucose application (3mM glucose) strongly supressed the expression of these starvation genes as observed in Wt seedlings. Although the sugar-induced suppression is also observed in the *gin2* mutant, these genes are upregulated relative to Wt (2.2 to 3.8 fold increase). The effect of sugar is consistent with the seedling hypocotyl phenotype (Fig4.8B). Hence, glucose does not entirely rescue the starvation response due to *HXK1* deficiency. Mechanistically there are two possibilities for the increased starvation marker expression in *gin2:* Either HXK1 is required for sugar mediated transcriptional repression of these starvation genes or the energy deficit in the *gin2* mutants triggers this induction independently of HXK1.

G6P, although ineffective in Wt, strongly repressed the transcript abundance of all six carbon starvation induced BCAA degradation genes to Wt levels in the *gin2* mutants (Fig4.9). Hence, by bypassing HXK1 metabolic role and restoring respiration for energy production, G6P application rescued both the *gin2* mutant phenotype and starvation response. This data supports the crucial role of HXK1 enzymatic function in seedling establishment during nutrient limiting conditions.

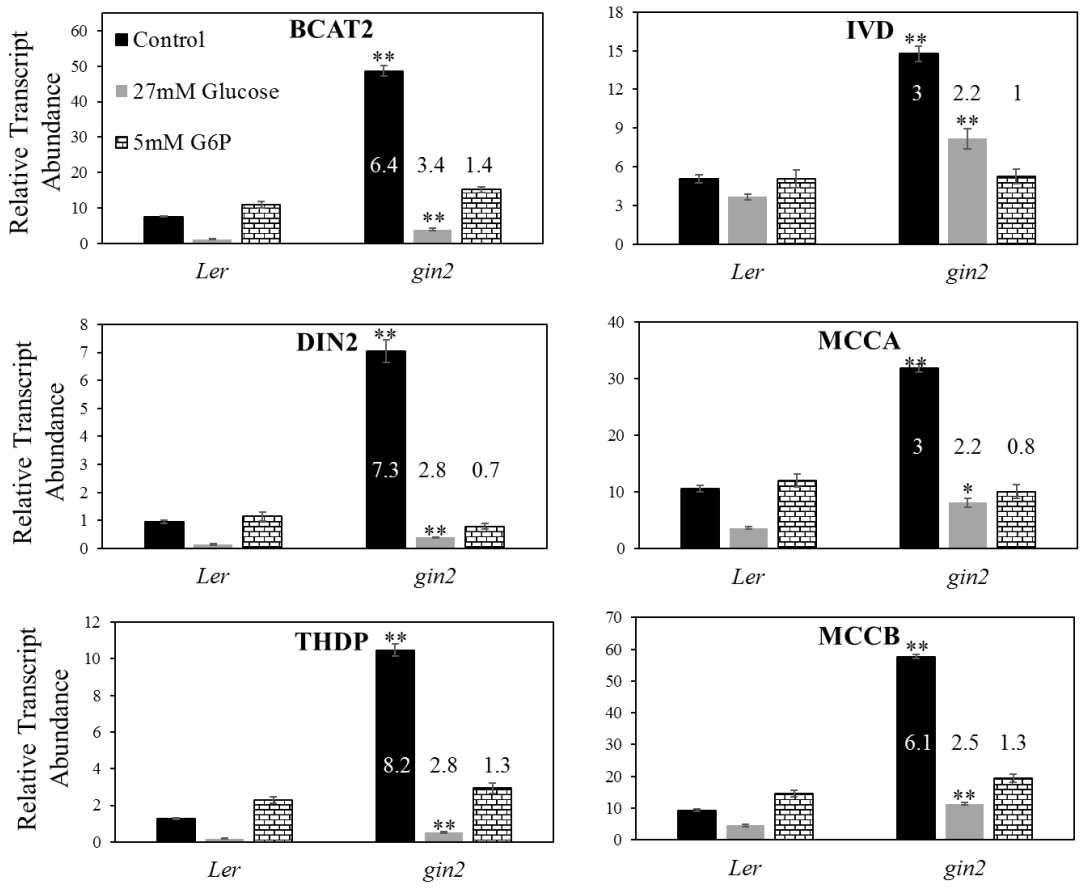

Fig4.9: Transcript abundance of six BCAA degradation pathway genes normalized to PP2A in 4-day-old etiolated Ler and *gin2* seedlings grown in the absence and presence of 27mM glucose and 5mM G6P. Error bars indicate ±SE; Fold Change (FC) increase depicted and **P≤ 0.01 of *gin2* relative to respective Ler in each treatment (Student's t-test).

3.2.6. 94% of the chloroplast transcriptome is altered in *gin2* mutants

Chloroplasts are chlorophyll containing green-pigmented plastid family organelles responsible for photosynthetic reactions. In response to developmental or environmental cues, plastids convert to different forms. Although the plastome (plastid genome) encodes 133 genes, more than 2000-3000 nuclear encoded proteins are imported in for functional requirements. Etioplasts form in the dark and differentiate into chloroplasts upon illumination (Jarvis and López-Juez, 2014). During chloroplast

biogenesis, plastid gene transcription involves two types of RNA polymerase: Nuclear Encoded Polymerase (*RPO* gene family) and Plastid Encoded Polymerase (SIG gene family) (Hajdukiewicz et al. 1997). The nuclear encoded SIG family initiates transcription of plastid housekeeping genes. This includes the RPO family, which thereafter drives the expression of the plastome. An interesting revelation from our RNAseq is that 94% of the plastome is upregulated in dark grown *gin2* mutants (Fig 4.10). While the transcript levels of the SIG gene family are unaltered in the *gin2* mutants, all four RPO subunits (*RPOA, RPOB, RPOC1, RPOC2*) are severely upregulated. If HXK1 exerts a direct/indirect negative control over the plastome or exclusively over RPO activity which inturn govern the plastome is unknown. Transcript levels of TFs and certain key nuclear encoded proteins (*GLK2 / PIFs / HY5 / GUNs / HEMA1 / PORA,B / TOC159 / GLK1 / ARRs / EIN3 / LHC* gene family) Jarvis and López-Juez, (2014) required during chloroplast biogenesis is unaltered in the *gin2* mutants according to my RNAseq data. This could be the reason why the etiolated *gin2* mutants do not have open cotyledons in the dark but HXK1 somehow exclusively controls the plastome. However, detailed investigation into this novel observation is required to understand the underlying mechanism.

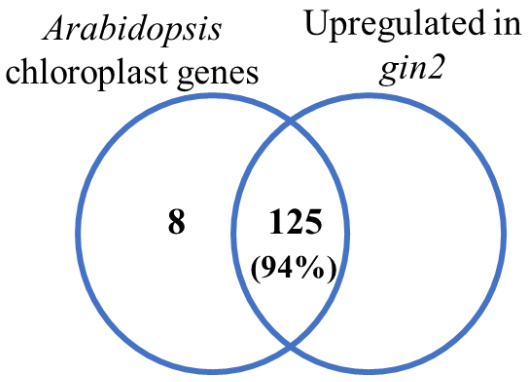

Fig4.10: Venn diagram depicting percentage overlap between Arabidopsis chloroplast encoding genes and chloroplast genes upregulated in the *gin2* mutants.

3.2.7. Effect of Photosynthetic Inhibition in *gin2* Mutants

Based on the above conclusion that the *gin2* mutants has a low energy mobilisation due to its metabolic incapacity, we hypothesised that *gin2* may be less effective in resource allocation by blocking photosynthate production. To test this, I grew the *gin2* mutants and Wt under low and high light in the absence and presence of the photosynthetic inhibitor DCMU (3-(3,4-dichlorophenyl)-1,1-dimethylurea) and quantified cotyledon area and hypocotyl length. DCMU blocks electron flow from photosystem II thereby inhibiting the Electron Transport Chain (ETC) and subsequently photosynthate production. Photosynthate sugars are transported across the phloem from source to sink tissues to meet energy demands. During suboptimal light levels, limited C fixed in seedling cotyledons (source) is transported to the sink hypocotyl tissues to support growth at the expense of cotyledon expansion. In contrast, high light supress hypocotyl growth and facilitate cotyledon expansion (source and sink tissue) for enhanced photosynthetic capture (Kircher and Schopfer, 2012; Kohnen et al. 2016)

As observed in Fig4.11A, under suboptimal light conditions *gin2* mutants exhibit a small seedling stature (small cotyledon area, short hypocotyl) relative to Wt. Although 5 and 10μM DCMU application had no effects on cotyledon area (source tissue) in Wt and *gin2*, it supressed Wt hypocotyl growth (sink tissue) by 50%. The *gin2* mutants appear insensitive to DCMU application potentially due to its inability to process cotyledon-derived photosynthate for hypocotyl growth.

Under continuous high light conditions (Fig4.11B) *gin2* phenocopies Wt (Fig. 1). DCMU application strongly inhibited cotyledon expansion but has no effect on hypocotyl length. The *gin2* mutants appeared Wt in control and DCMU treated

conditions confirming its less significant role in nutrient resource management under high light conditions during seedling development.

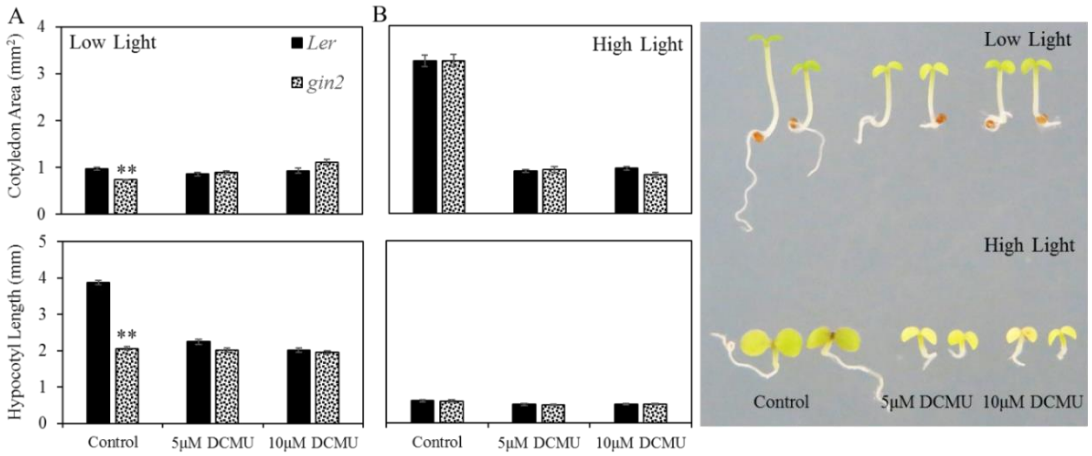

Fig. 11: Cotyledon area and hypocotyl length of 7-day-old Wt and *gin2* seedlings grown in control conditions and in the presence of 5μM and 10μM DCMU under A) Continuous low light (3μmol m^{-2} s^{-1}) and B) Continuous high light (130μmol m^{-2} s^{-1}) at 18C. Error bars indicate ±SE, **P≤ 0.01 of *gin2* relative to respective Ler in each condition (Student's t-test).

3.2.8. Hexokinase1 largely functions independent of the PIFs during seedling establishment

The HXK1 mutant *gin2* phenocopy the *pifQ* short hypocotyl in the dark/continuous low light and various photoperiods in sugar free media (Fig4.1,4.2). We initially hypothesised that PIFs and HXK1 converge at common promotor elements (G box) to co-regulate transcription during seedling development thereby integrating light and metabolic signalling. However, based on the above presented data, it is clear that the metabolic role rather than the HXK1 nuclear signalling function is required for seedling establishment.

Further, in the presence of sugar, HXK1 and PIFs appear to operate independently. In the absence of glucose (black bars), *pifQ* mutants exhibit a marked short seedling hypocotyl phenotype in SD similar to *gin2* (Fig4.12A). However, in line

with published reports, *pifQ* mutants is insensitive to 1% glucose application while *gin2* remains responsive (Simon et al. 2018; Singh et al. 2017; Zhang et al. 2016; Stewart et al. 2011). While *gin2* can germinate successfully on 6% glucose (Moore et al. 2003), *pifQ* cannot. Hence, PIFs and HXK1 appear to function in separate sugar mediated signalling pathways during seedling growth.

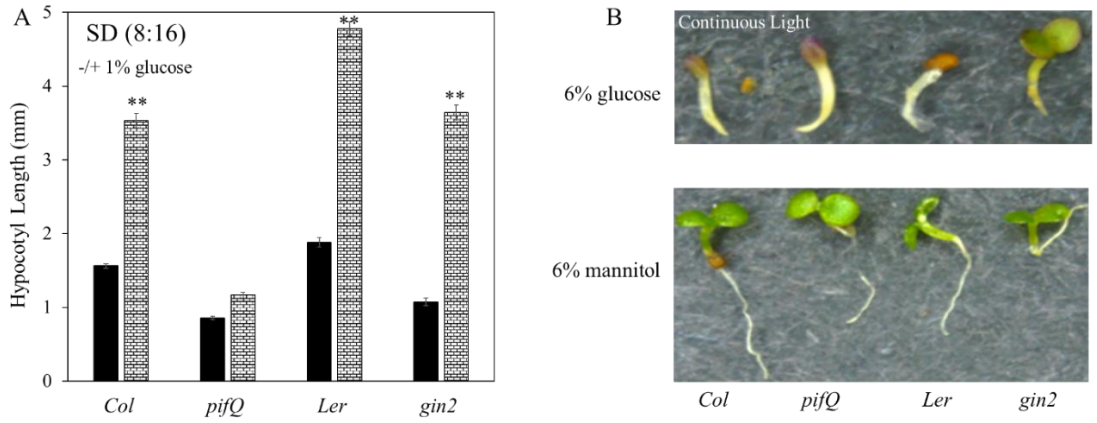

Fig4.12: Phenotypic analysis of *pifQ* and *gin2*: A) Hypocotyl length of 7-day-old Wt, *pifQ* and *gin2* seedlings grown in SD conditions (8L:16D) in the absence (black bar) and presence of 1% (w/v) glucose. B) 7-day-old seedlings grown in continuous light (130μmol m^{-2} s^{-1}) in 6% (w/v) glucose and mannitol at 18C. Error bars indicate ±SE, **P≤ 0.01 of glucose treated relative to untreated genotypes.

As the effect of both mutations are evident during skotomorphogenesis, I wanted to establish the degree of overlap between the *HXK1* and *PIF* pathways at the transcriptome level. To do this, I compared the *gin2* transcriptomic data (2353 misregulated genes) with the *pifQ* transcriptomic data (4223 misregulated genes) (Pfeiffer et al. 2014). The comparison identified 748 (11%) common genes enriched in multiple metabolic pathways (Fig4.13A,B). Interestingly, the BCAA catabolic pathway continues to be highly enriched in this subset (Fig4.13B). To investigate this

in more detail, I was interested in whether the BCAA pathway genes in the *pifQ* mutants were altered in a similar fashion to *gin2*. The *pifQ* RNAseq raw data was obtained (GSE39214; Zhang et al. 2013) from NCBI and selected genes were plotted. As observed in Fig. 13B, all 8 starvation markers significantly upregulated in *gin2* mutants are severely downregulated in the *pifQ* mutants. This is an interesting and novel observation suggesting that PIFs may promote the expression of this starvation gene set in darkness. However, based on compiled high stringency ChIP-seq data for PIF1, PIF3, PIF4 and PIF5 (Pfeiffer et al. 2014), these starvation markers are not listed as direct targets suggesting the possibility of an indirect PIF control. None-the-less PIFs and HXK1 appear to have opposing effects on modulating these key starvation genes.

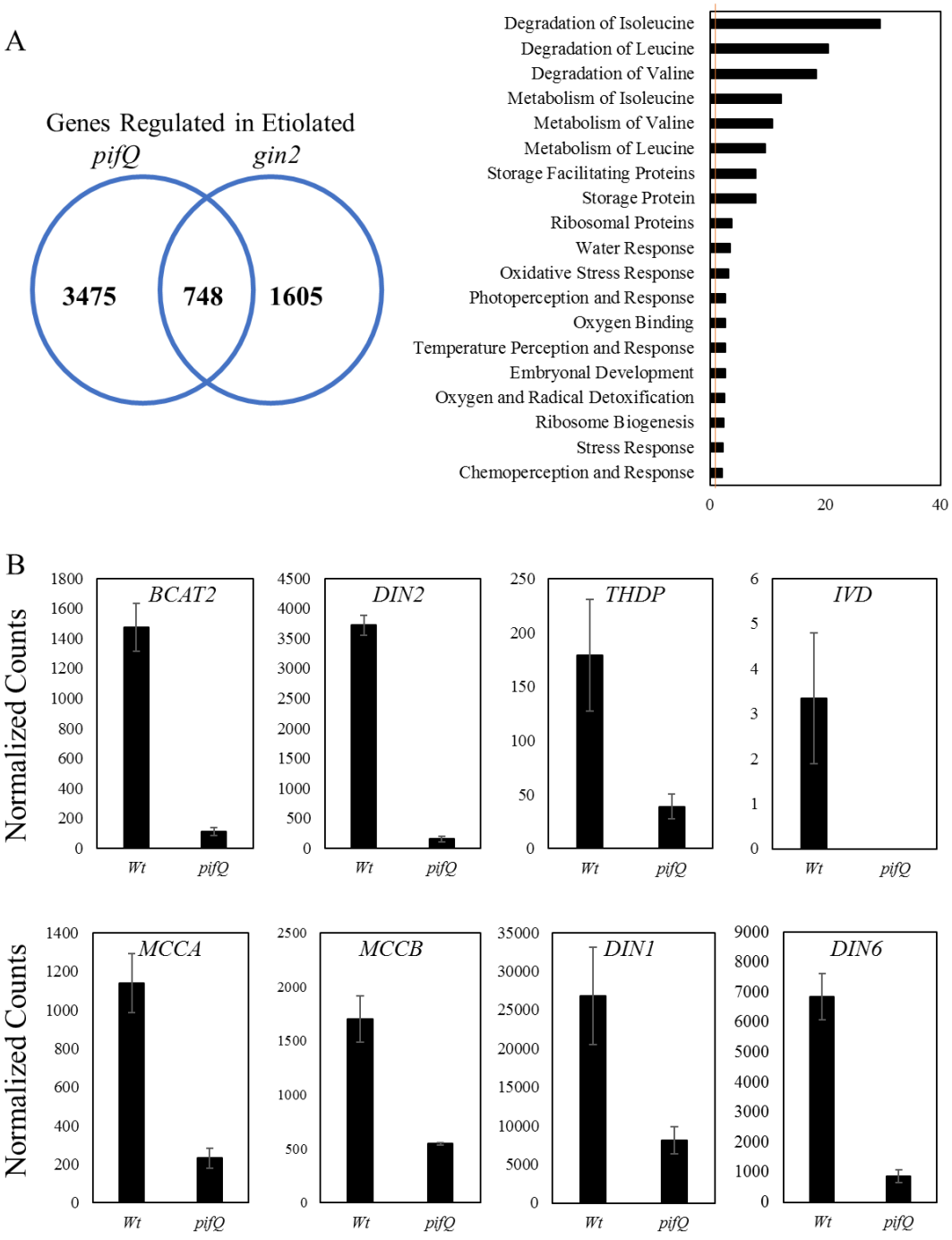

Fig4.13: Comparison of genes altered in 4-day-old etiolated gin2 mutants and 4-day-old etiolated *pifQ* mutants (data derived from Pfeiffer et al. 2014). A) Comparison and Gene Ontology (GO) analysis of overlapping genes depict pathway ratio enrichment. Pathways showing a statistically significant enrichment (>1 (orange line), $p \leq 0.01$) are shown. mRNA expression patterns of starvation markers and *HXK1* in young etiolated Wt and *pifQ* mutants. Raw data derived from Zhang et al. (2013) (NCBI GSE39214). Error bars indicate ±SE

PIF Direct Target Comparison with HXK1 Regulated Genes

Our data so far suggest that while PIFs and HXK1 contribute to skotomorphogenic growth they operate in largely separate pathways. To examine this further, I compared direct PIF targets (compiled PIF1, PIF3, PIF4, PIF5 ChIP-seq data derived from Pfeiffer et al. 2014) with genes upregulated (in principal repressed by HXK1) and downregulated (in principal activated by HXK1) in *gin2* mutants (Fig4.14). This analysis identified just 27 genes in the subset between HXK1 repressed and direct PIF targets. Of these, 16 genes (59%) are repressed by both HXK1 and PIFs and 11 genes (41%) repressed by HXK1 but PIF activated. A similar comparison was made between HXK1 activated genes and direct PIF targets (Fig4.14B). Of the 42 genes, 38 (90%) appear to be activated by both HXK1 and PIFs and 4 (10%) genes are activated by HXK1 but repressed by PIFs. Individual gene names are listed below (Fig4.14).

Both classes of genes appear enriched in metabolism, metabolism associated or hormonal pathways. Whether or not PIFs and HXK1 proteins are required for transcriptional co-regulation or opposing regulation through common cis-elements is an open question.

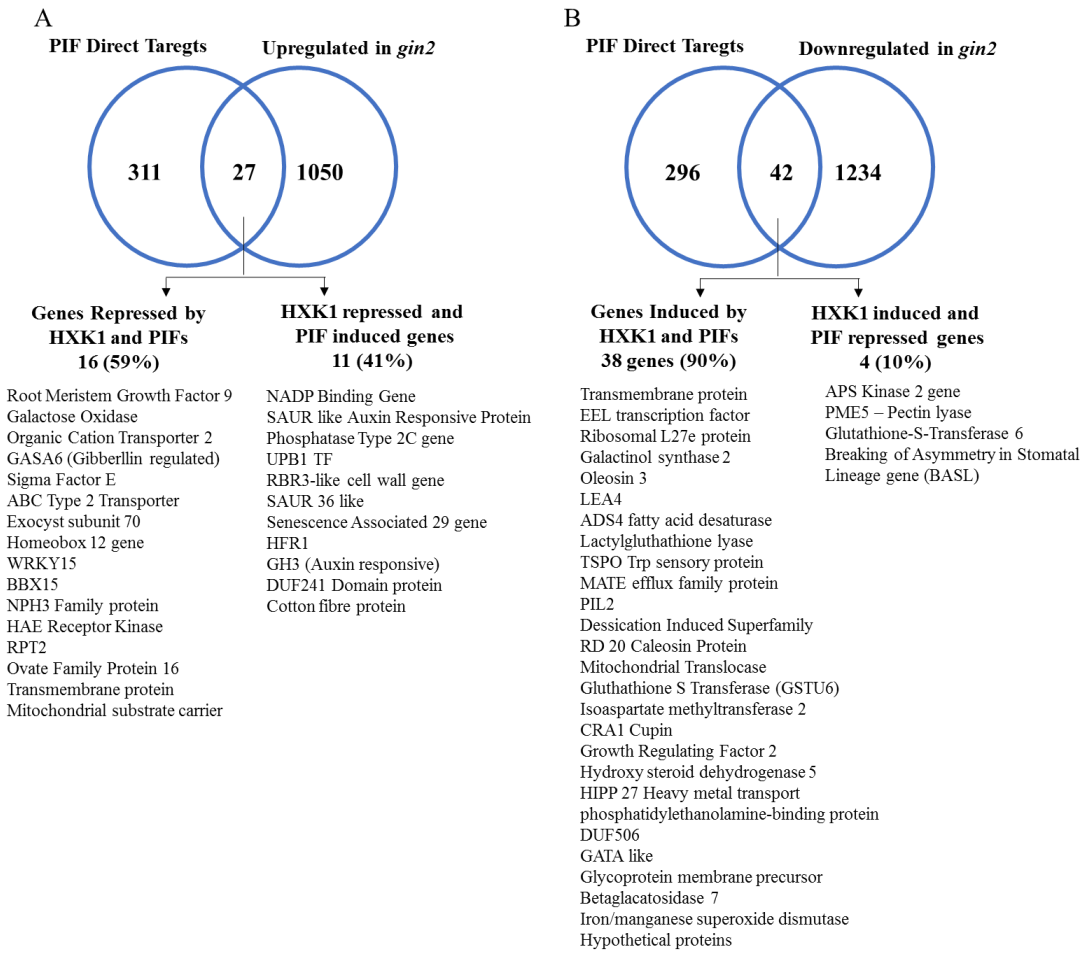

Fig4.14: Comparison between direct PIF targets (ChIP-seq data from Pfeiffer et al. 2014) and genes A) upregulated (In theory repressed by HXK1) and B) downregulated (in theory activated by HXK1) in the *gin2* mutants. Listed under the venn diagrams are individual genes regulated by PIFs and HXK1 in the same direction.

In summary, we discovered that the metabolic role of HXK1 enzyme is required for seedling establishment particularly during nutrient limited growth conditions (dark/low light). HXK1 largely operates independent to the PIF signalling during skotomorphogenesis but is rather required for nutrient reserve mobilization to fuel cellular and metabolic activities. As the collective data presented highlight the role of metabolic HXK1 in the dark, we were next interested to understand the role of HXK1 signalling in seedling development during the light phase.

3.2.9. HXK1 is not required for feedback mediated photosynthetic inhibition

In seedlings grown under continuous white light, we observed that the *Hexokinase1* transcript abundance is photosynthate regulated and fluence dependent (data not shown). *HXK1* levels are unaltered between dissected seedling cotyledons and hypocotyls grown at continuous low and high light suggesting post-transcriptional control in organ development during seedling establishment (data not shown). HXK1 is detected in nuclear fractions of Arabidopsis tissues (Yanagasawa et al. 2003; Cho et al. 2007). Cho et al. (2007) establish that nuclear HXK1 is required for feedback inhibition of photosynthesis. HXK1 in concert with VHAB1 and RPT5B function as direct transcriptional repressors of photosynthetic genes *CAB2* and *CAA* in response to exogenous glucose application. Consistent with published results (Cho et al. 2007; Moore et al. 2003; Cho et al. 2009), exogenous sugar mediated HXK1 dependent suppression of *CAB2/CAA* was observed in our SD grown seedlings harvested at ZT4. The *gin2* mutant accumulated 3 to 4.5 fold more *CAB2* and *CAA* transcript levels. G6P application however had no effect on transcript abundance of these genes in Wt and *gin2* (Fig. 15A).

In order to confirm this sugar mediated HXK1 dependent response through other means, we decided to naturally enhance endogenous sugar by growing the seedling under increasing light intensities. Surprisingly, no inhibitory effect on transcript abundance was observed in Wt at 300μmol $m^{-2}s^{-1}$ or 600μmol $m^{-2}s^{-1}$ high light. Seedlings grown at 800μmol m^{-2} s^{-1} appear chlorotic and exhibit photooxidative stress. A HXK1 dependent feedback repression was not observed by enhancing

endogenous sugar levels. Hence, exogenous sugar application may not directly correlate with endogenous sugar levels. (Fig4.15B).

We decided to test this hypothesis by measuring internal glucose (and starch) levels in Wt seedlings grown under 100, 300 and 600µmol $m^{-2}s^{-1}$ light and 100µmol $m^{-2}s^{-1}$ light supplemented with 27mM (0.5%), 54mM (1%) and 108mM (2%) exogenous glucose (Fig. 15C). The internal glucose levels measured were between 0.4 and 0.76 mg/g FW in Wt seedlings grown at 100 and 600µM $m^{-2}s^{-1}$ light. However, internal glucose concentrations far exceeded these physiological concentrations when grown in the presence of exogenous glucose (7-20 fold increase). A similar trend is observed for starch levels as a proportion of carbon during the day is utilised for starch production to support nighttime growth (Fig4.15C).

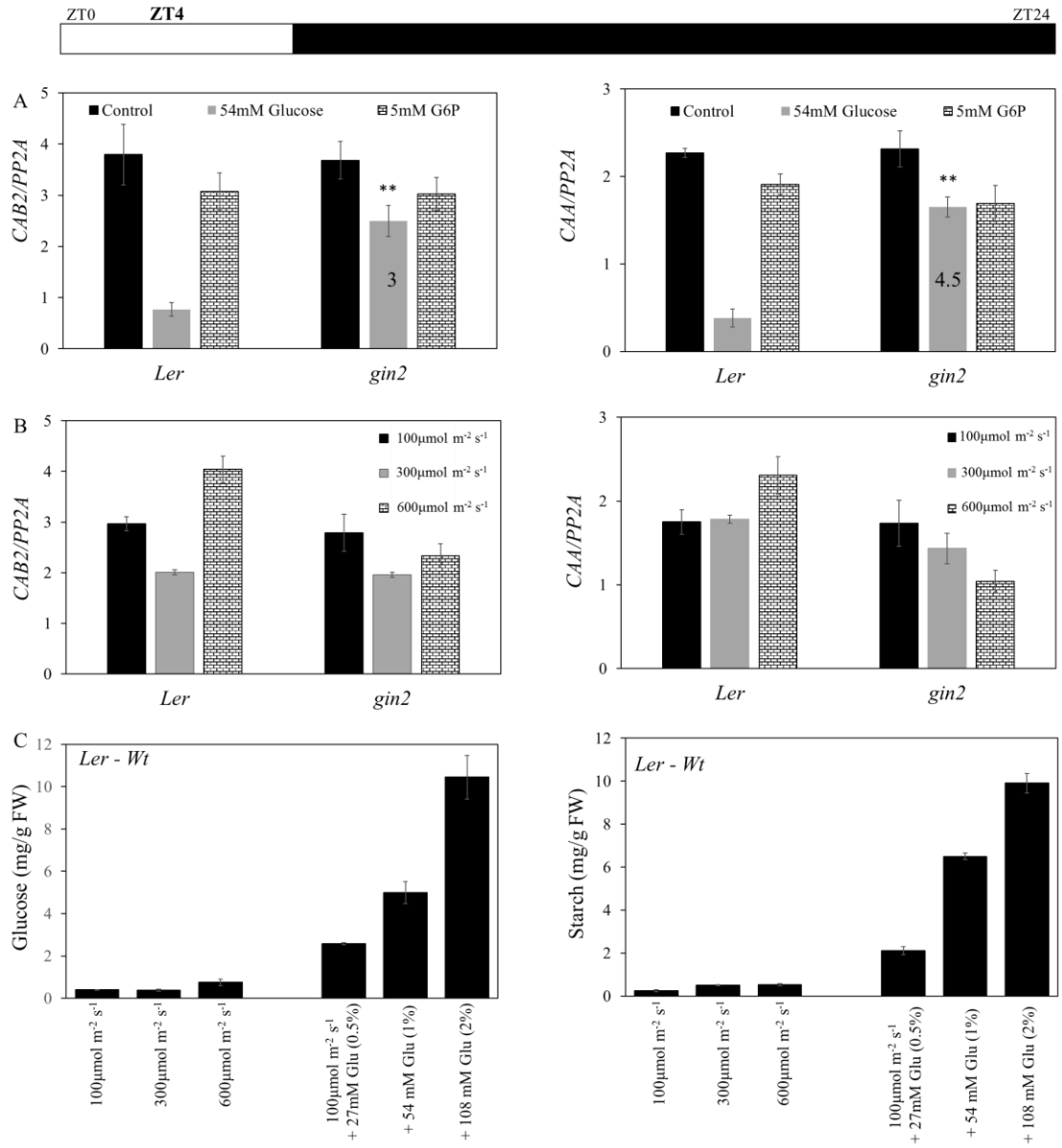

Fig4.15: Transcript abundance *CAB2/CAA* normalized to *PP2A* in *Ler* and *gin2* seedlings grown in A) the absence and presence of 54mM glucose and 5mM G6P at 100µmol $m^{-2}s^{-1}$ and B) varying light intensities. C) Glucose and starch concentrations of Wt seedlings grown under varying light intensities and exogenous glucose concentrations as stated. 4-day-old *Ler* and *gin2* seedlings grown in SD at 18C were harvested at ZT4 for all three experiments. Error bars indicate ±SE, **P≤ 0.01 of *gin2* relative to Ler in each condition (Student's t-test).

From this dataset, it is clear that enhancing endogenous sugars does not have a similar effect as exogenous sugar treatment on the transcript levels of *CAB2/CAA* in Wt seedlings. Further, exogenous application is not correlative to physiological sugar

levels. Hence, the nuclear role of HXK1 in transcriptional feedback inhibition of photosynthesis as previously described requires re-evaluation. In general, the amplified effects of exogenous sugar mediated transcriptional patterns in the light of physiologically relevant conditions must be considered.

3.3. Discussion:

In Arabidopsis, the glucose receptor HXK1 performs a dual role. The mitochondrial bound HXK1 performs a conserved enzymatic role in the respiratory pathway. It catalyses the first enzymatic step in glycolysis: glucose phosphorylation to generate Glucose-6-Phosphate (G6P). HXK1 has also been detected in nuclear fractions (Yanagasawa et al. 2003; Cho et al. 2007; Cho et al. 2009). Cho et al. (2007) demonstrate nuclear HXK1 in concert with RPT5B and VHAB1 to directly repress photosynthetic genes in response to exogenous sugar. This complex is postulated to function during negative feedback inhibition of photosynthesis. Sugar mediated HXK1 dependent repression of other developmental genes has also been demonstrated (Kunz et al. 2015; Yang et al. 2013; de Jong et al. 2014; Singh et al. 2017; Hsu et al. 2014). However, the precise role of sugar in HXK1 assembly formation and nuclear localization is unclear.

The enzymatic role of HXK1 is required for nutrient resource management

In this chapter, I have provided evidence that the metabolic role of HXK1 is required during seedling establishment. The *HXK1* mutants (*gin2, hxk1-3*) exhibit a small seedling stature in nutrient limiting conditions such as periods of darkness or low light (Fig4.1, 4.2). The mutant transcriptome enabled us to gain unprecedented insights into the role of HXK1 in nutrient resource management. Energy -demanding

and -deficit pathways are altered in the *gin2* mutants suggesting the requirement of the metabolic rather than the signalling role of HXK1 in seedling establishment (Fig.4,6). Further, the glucose accumulation in the mutant reiterate the requirement of HXK1 mediated metabolic glucose processing for ATP production to fuel energy demanding biological activities (Fig4.5A).

Energy driven microtubule and cytoskeleton based cellular components required for cell division, expansion and transport (Hashimoto, 2015) is downregulated in the *gin2* mutants consistent with the reduced epidermal cell length and number (Fig4.4, 4.5). To combat this glycolytic energy deficit, the mutants catabolize the Branched Chain Amino Acids (BCAAs) as an alternate energy source. This carbon starvation induced SnRK1 activated pathway yield intermediate compounds feeding into the TCA cycle for ATP generation (Baena-González et al. 2007; Hildebrandt et al. 2015). Hence, by supplying G6P, the HXK1 enzymatic endproduct, the *gin2* mutant phenotype is rescued and the elevated transcript abundance of BCAA catabolic enzymes is restored to Wt levels (Fig4.8,4.9). This indicates that the enzymatic role of HXK1 rather than the signalling function as previously described (Moore et al. 2003) is crucially required for seedling establishment during nutrient limiting conditions. Moore et al. (2003) show HXK1 lines impaired in catalytic activity with retained signalling function ($HXK1^{S177A}$ and $HXK1^{G104D}$) to rescue the *gin2* small seedling stature in low light (sugar free media). Considering HXK1 nuclear activity is sugar dependent, there appears to be a disconnect in their observation. Is is unclear as to how nuclear HXK1 can rescue the seedling phenotype in nutrient limiting conditions. Perhaps the phosphorylation ability in $HXK1^{S177A}$ and $HXK1^{G104D}$ is not as compromised as in *gin2*.

Although the complex signalling networks underlying seedling development is well established, little is known about the role of metabolic components. Seedling establishment is energy reserve dependent, mutations in two enzymes involved in mobilizing energy stores in the seed, *phosphoenolpyruvate carboxykinase 1 (pck1)* and *isocitrate lyase (icl)* display inhibition of etiolated hypocotyl growth. Both enzymes are key components for catabolizing fatty acids to produce sugars by gluconeogenesis and the glyoxylate cycle respectively. Hence, sugar application rescues both mutant phenotypes (Eastmond et al. 2000; Penfield et al. 2004). Similarly, *gin2* also exhibit etiolated growth inhibition (Fig4.1). G6P rescues this phenotype highlighting HXK1 metabolic role for nutrient reserve management during seedling establishment (Fig4.8). Interestingly, the effect of the mutation is visible only under low light but not high light conditions suggesting a compensatory role by other hexokinases (Karve et al. 2010).

HXK1 regulates the plastome in the dark

HXK1 also appears to play an important role in supressing the chloroplast genome (plastome) (Fig4.10) in the dark. 94% of the chloroplast genes are upregulated in the *gin2* mutant. The molecular machinery facilitating etioplast (dark) to chloroplast (light) transition is less understood (Jarvis and López-Juez, 2014), and the role of HXK1 in regulating the plastome is unknown. Although the Plastid Encoded Polymerase (PEP) gene family required for plastid transcription is highly upregulated in the *gin2* mutant, detailed investigation is required if HXK1 exerts a direct/indirect control over the PEPs or the plastome. Further, the role of plastid localized HXK3 in this response is unknown. Nevertheless, this is a highly novel finding highlighting another dimension for HXK1.

HXK1 largely operates independently of the PIFs during skotomorphogenesis

The Phytochrome Interacting Factor (PIF) TF family positively regulate skotomorphogenesis (Leivar and Monte, 2014; Gommers and Monte, 2018). Given that the metabolic role of HXK1 is required for skotomorphogenesis, our data indicates that HXK1 appears to largely operate independently of PIF signalling. A small overlap between the two mutant transcriptomes is observed (Fig4.13) so HXK1 appears to regulate only a subset of direct PIF targets (Fig4.14). However, this does not completely rule out a convergence between HXK1 and PIF signalling on common promotor elements. Further, consistent with published findings, both mutants exhibit an opposing phenotype in response to sugar suggesting HXK1 and PIFs operate in independent sugar signalling pathways (Fig4.12) (Simon et al. 2018; Singh et al. 2017; Stewart et al. 2011; Zhang et al. 2016).

HXK1 is not required for photosynthetic feedback inhibition in seedlings

Nuclear HXK1 function as a transcriptional repressor in response to exogenous sugar (Sheen, 2014; Li and Sheen, 2016). Multiple reports suggest HXK1 to function in photosynthetic feedback inhibition. Cho et al. (2006; 2009) and Moore et al. (2003) demonstrate exogenous sugar mediated transcriptional repression of two photosynthetic genes *CAB2* and *CAA* is HXK1 dependent. Although we could replicate this published result in the presence of sugar (Fig4.15A), a similar response was not observed by enhancing endogenous sugar levels (Fig4.15B). Hence, endogenous and exogenous sugar does not have a similar effect on the transcript abundance of photosynthetic genes, atleast at the seedling stage. We could try replicating the ChIP-qPCR to check for HXK1 enrichment on the *CAB2* promotor in response to sugar (Cho et al. 2007) and high light.

Further, internal glucose levels in seedlings grown in high light or in the presence of exogenous glucose are not correlative (Fig4.15C). This is a novel observation as a plethora of literature exists on the effects of exogenous sugar on Arabidopsis seedling morphology, transcriptional response and various other cellular activities believed to occur under enhanced carbon conditions. Perhaps, at the adult plant stage with increased photosynthetic capture, endogenous sugars may work in a similar capacity to exogenous sugars. However, during the cotyledonary seedling stage it certainly does not appear to hold true. Another published discrepancy is that although exogenous sugar markedly enhance seedling hypocotyl length as published in several reports (Simon et al. 2018; Singh et al. 2017; Stewart et al. 2011) the response is not mimicked by growing the seedlings in high CO_2 (Lilley et al. 2012). Detailed investigation is required to rule out the fact the exogenous sugar application in seedlings to study biological effects is not simply an artefact.

Conclusion:

In this chapter, I provide evidence that HXK1 performs an important metabolic role for seedling sustenance during nutrient limiting conditions. The transcriptome reflects the mutant phenotype. Energy -demanding and –deficit pathways are altered in the mutant. Bypassing HXK1 enzymatic function by supplying G6P rescued the mutant phenotype and carbon starvation response. Our results indicate that the enzymatic role of HXK1 rather than the signalling function as previously described (Moore et al. 2003) is required for seedling establishment. Another novel observation is that HXK1 negatively regulates the plastome in the dark and largely operate independent to PIF signalling during skotomorphogenesis. Further, we also show discrepancies concerning the sugar mediated HXK1 nuclear function in photosynthetic

gene repression as previously described (Cho et al. 2007; Moore et al. 2003). Taken together, this chapter highlights new insights into HXK1 function during seedling establishment.

CHAPTER 4

Effect of HXK1 overexpression in light signalling

4.1. Introduction

Whilst the previous chapter uncovers the role of metabolic HXK1 during skotomorphogenic growth and low light mediated seedling establishment, the current chapter provides evidence for HXK1 feedback to light signalling. In high white light, the 35S:HXK1 (HXK1OX) exhibit an enhanced photomorphogenic response (characterized by hypocotyl suppression/cotyledon expansion – Figure 1, Chapter3) It is unclear if the light pathways and HXK1 converge to co-ordinate this seedling response.

Plants have evolved multiple photoreceptors including the evolutionarily unrelated phytochromes (PHY) and cryptochromes (CRY) to perceive red/far-red light and blue/UVA light respectively. Red light activated nuclear phytochromes (Pfr) negatively regulate PIF activity. Pfr–PIF interaction facilitates PIF proteolysis (Li et al. 2011). In addition, Pfr is capable of sequestering PIFs from targets promotors rapidly inhibiting PIF signalling and hypocotyl elongation (Park et al. 2012). Therefore, under high light and high red to far-red light ratio (R/FR), seedlings exhibit a short hypocotyl phenotype. In contrast, seedlings grown in low light or low R/FR exhibit an elongated hypocotyl phenotype due to reduced nuclear Pfr abundance and enhanced PIF activity. Hence, Phy-PIF control of seedling growth is highly dynamic.

The blue light photoreceptors Cryptochromes (CRYs) also mediate seedling hypocotyl suppression. Although, CRY-PIF interaction was recently discovered, this complex formation does not facilitate PIF degradation (Pedmale et al. 2016; Liu et al.

2016). Blue light signalling largely mediates hypocotyl suppression by inactivating the COP1-SPA E3 ligase. COP1-SPA in complex with Cullin4 based E3 ligase catalyse the turnover of hypocotyl supressing signalling components (HY5, HFR1, etc) in the dark. Light activated CRY physically interact with COP1-SPA thereby disassociating complex activity (Liu et al. 2011; Lian et al. 2011). Interestingly, light activated PHYB also inhibits COP1-SPA activity through direct interactions (Sheerin et al. 2015). Hence, seedlings constitutively expressing CRY or active PhyB exhibit a 'constitutive photomorphogenic' (short hypocotyl and opened cotyledons) phenotype in the dark (Yang et al. 2000; Hu et al. 2009). Key signalling components downstream to CRY and PHY signalling positively regulating seedling photomorphogenesis include HY5 and HFR1. HY5 operates under a wide spectrum of wavelengths (FR, R, B, and UV-B) and regulates the transcription of ~4000 genes involved in various pathways (Lee et al. 2007). HY5 protein abundance is directly correlated with the extent of photomorphogenic development (Osterlund et al., 2000). HFR1, on the other hand operates exclusively as a Far-Red and Blue light signalling component in the PHYA and CRY pathways, respectively (Li et al. 2012).

Recently, Wang et al. (2016) identified a novel component, BIC1 (Blue-Light Inhibitor of Cryptochromes1) as a negative regulator of CRY signalling. BIC1 physically interact and inhibit blue light mediated CRY activation. Hence, the *cry* mutants and the *BIC1OX* seedlings exhibit a similar etiolated phenotype and transcriptome in blue light.

Intriguingly, seedlings overexpressing HXK1 in blue light also exhibit a similar etiolated phenotype. In red light, the HXK1OX seedling appear Wt. Hence, HXK1 somehow inhibits blue light mediated seedling photomorphogenesis and red

light negates this effect in a PHYB dependent manner. The HXK1OX transcriptome in both light treatments is reflective of the phenotype. I will describe my results and the hypotheses for the mechanistic basis of these responses, which is currently unknown.

4.2. Results

Exogenous sugar enhances HXK1 transcript abundance and nuclear activity (Price et al. 2004, Cho et al. 2007). Kelly et al. (2012) generated HXK1 overexpressing lines to exaggerate this nuclear signalling response without exogenous sugar application. In this section, I will present data pertaining to the differential effects of Blue (B) and Red (R) light on the HXK1OX seedling phenotype. HXK1OX inhibits B light signalling mediated seedling photomorphogenesis and R negates this effect. The transcriptome of the HXK1OX grown in B and B+R (Blue+Red) is reflective of the phenotype. Finally, I conclude with genetic evidence that PHYB signalling is required to negate the effect of B on HXK1OX.

4.2.1. Effect of monochromatic light on HXK1 during seedling photomorphogenesis

As a marked hypocotyl phenotype was observed at low light fluences in the *HXK1* mutants and OX (Chapter 3), I wanted to establish if the trend was also observed across monochromatic wavelengths.

In B and R light, *HXK1* mutants exhibited a short hypocotyl in low fluences but the effect of the mutation was lost at higher fluences. Interestingly, in red light the HXK1OX appeared Wt but a striking response was observed in B (Fig. 1 A,B).

HXK1OX appears insensitive to B mediated seedling photomorphogenesis, the seedlings exhibit an etiolated phenotype (elongated hypocotyls/small cotyledons). Hence, HXK1 overexpression strongly represses B light signalling. Complementing this observation, the mutant short hypocotyl phenotype is more severe in B than in R (-2.5 fold decrease in B and -1.3 fold decrease in red for *gin2*) (Fig. 1A,B). Hence, the effect of R light explains the phenotype of HXK1OX in increasing fluences of continuous white light (Chapter 3 – Fig. 1). The *HXK1* mutants and the OX exhibit a Wt response to FR light suggesting HXK1 does not operate in the PHYA signalling pathway (Fig. 1C). The differing responses in R and B suggested that HXK1 overexpression might exert opposing control on these distinct light pathways. To test this, I performed a red-blue competition experiment wherein the seedlings were grown in standard blue with increasing fluences of red and *vice-versa*. Increasing R fluence in the presence of B gradually supressed elongated hypocotyl length of the HXK1OX. Similarly, in the presence of R, a gradual increase in B promoted hypocotyl length (Fig. 1D). Taken together, both datasets support the hypothesis that 1) HXK1OX has opposing effects in B and R and 2) red light inhibits HXK1OX mediated negative control of blue light signalling.

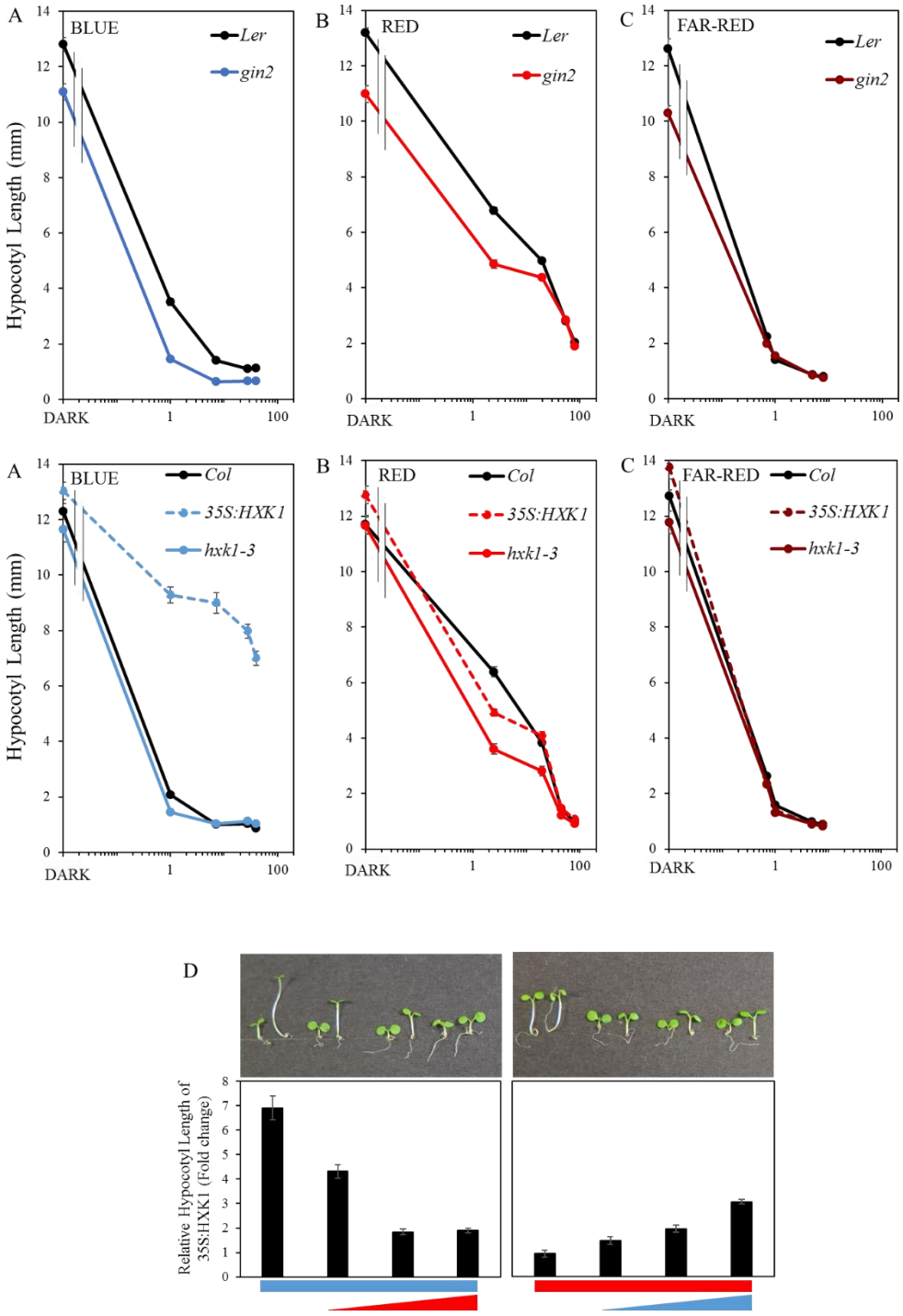

Fig5.1: Hypocotyl length of 7 day old HXK1 mutants and OX grown in A) continuous blue light (1, 7.2, 28, 40µmol $m^{-2}s^{-1}$), B) continuous red light (2.5, 19.6, 55, 80µmol $m^{-2}s^{-1}$) and C) continuous FR light (0.7, 1, 5, 8µmol $m^{-2}s^{-1}$). D) Relative hypocotyl length (Fold change) of Col and HXK1OX grown in blue (10µmol m^{-2} s^{-1}) with increasing fluences of red (10, 20 and 30µmol $m^{-2}s^{-1}$) and grown in red (10µmol m^{-2} s^{-1}) with increasing fluences of blue (5, 10 and 15µmol $m^{-2}s^{-1}$) at 18°C. Error bars indicate ±SE.

4.2.2. Effect of B and R light on HXK1 transcript and protein abundance

Given the phenotype of the *HXK1OX* in R and B, I wanted to establish if HXK1 itself was subjected to differential regulation by either light signalling pathways. Interestingly, neither light fluences influenced HXK1 transcript abundance in both Wt and 35S:HXK1. This suggests the non-involvement of R and B light signalling in *HXK1* transcription (Fig5.2A). Similarly, dark, B, R, FR or white light had no effects on HXK1 protein abundance (Fig5.2B) suggesting the absence of light mediated HXK1 turnover. This experiment does not eliminate the possibility that HXK1 may be subjected to post transcriptional/translational modification by light signalling and subsequent changes in activity.

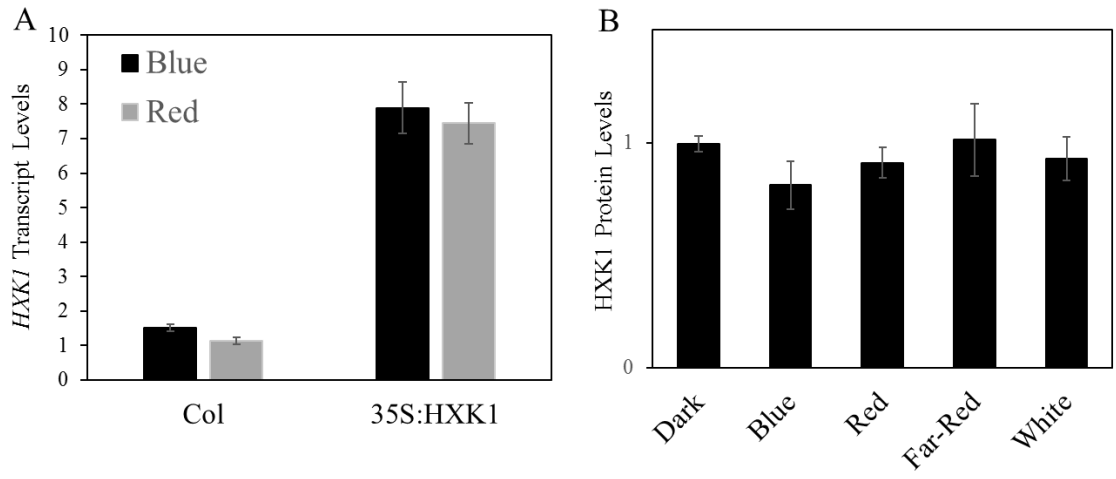

Fig5.2: A) HXK1 transcript levels in 7-day-old Wt and 35S:HXK1 (HXK1OX) seedlings grown in continuous red (40µmol $m^{-2}s^{-1}$) and blue light (10µmol $m^{-2}s^{-1}$) conditions at 18C. B) HXK1 protein abundance (relative to Actin) in 7 day old HXK1-FLAG grown in continuous dark, blue (10µmol $m^{-2}s^{-1}$), red (40µmol $m^{-2}s^{-1}$), far-red (5µmol $m^{-2}s^{-1}$) and white light (130µmol $m^{-2}s^{-1}$) at 18C. Error bars indicate ±SE.

4.2.3. HXK1OX transcriptome in B and B+R

In order to gain insights into the HXK1OX transcriptome in response to differential light treatments, a DNA affymetrix microarray was performed on triplicate samples of 4 day old HXK1OX and Wt seedlings grown in B (10µmol m^{-2} s^{-1}) and B+R (10+40µmol m^{-2} s^{-1}). This would enable us to filter candidates exclusively regulated in B and B+R and subsequently contributing to the HXK1OX phenotype. Before sampling for RNA extraction, I ensured that the seedlings used for the experiment displayed the phenotypes described above: *HXK1OX* exhibited elongated hypocotyls in B and short Wt hypocotyl phenotype in B+R. A similar enhancement in HXK1 levels was observed in the HXK1OX line in both light treatments (data not shown). Overall, 16% of the HXK1OX transcriptome was altered in B light - 8% upregulated and 8% downregulated. A comparatively smaller proportion (5%) was altered in B+R light (2% upregulated and 3% downregulated) (Fig5.3). Hence, B light exerts a larger control on the HXK1OX transcriptome and R light negates this effect. This trend is consistent with the seedling phenotype.

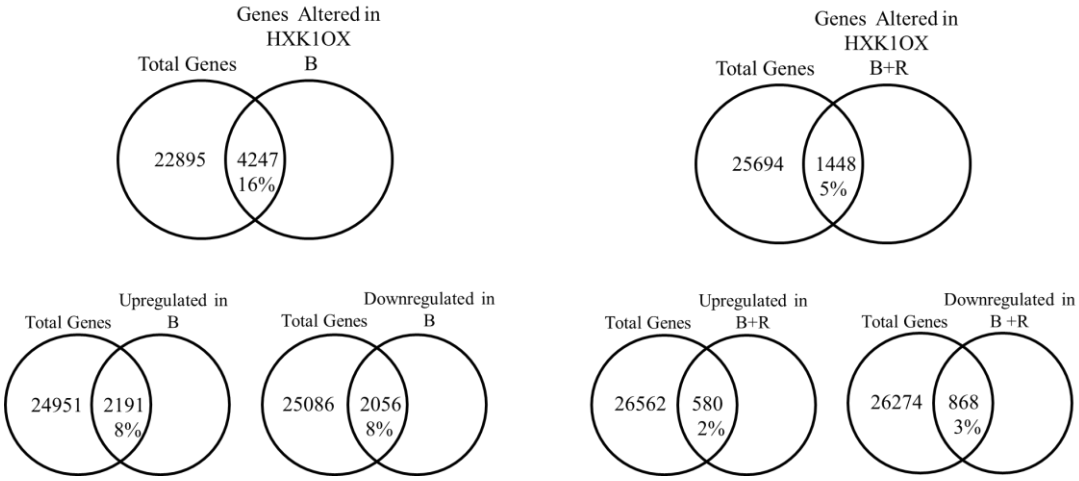

Fig5.3: Number of genes differentially altered in transcript expression in the HXK1OX in B and B+R.

Gene Ontology (GO) analysis

The 2191 genes predominantly upregulated in B grown HXK1OX seedlings are enriched in cytoskeleton/microtubule cell wall based components in addition to multiple other pathways. In contrast, the downregulated class is enriched in several energy, metabolic and aerobic respiratory pathways. Highly over-represented pathways include the Calvin cycle and CO_2 fixation amongst others (Fig5.4). Hence, consistent with the etiolated phenotype of 35S:HXK1 in blue, hypocotyl length promoting cell division/expansion associated components are upregulated and light triggered metabolic and photosynthetic components are downregulated.

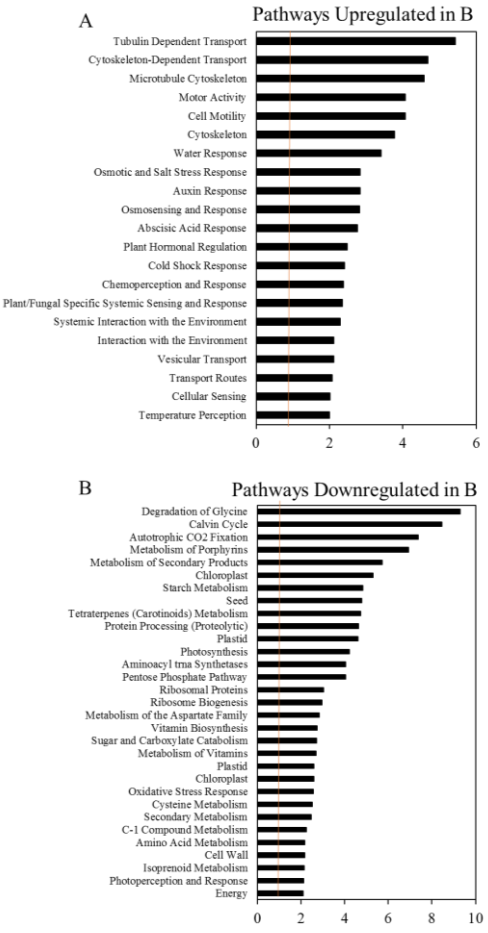

Fig5.4: Gene Ontology (GO) derived from VirtualPlant database for genes A) upregulated and B) downregulated in B gown HXK1OX. Pathways with a statistically significant enrichment (>1 (orange line), $p \leqslant 0.01$) are shown.

However, in B+R light condition where HXK1OX seedlings exhibit a Wt phenotype, a strong upregulation in sulfate transport and a modest upregulation of specific nutrient transporters is observed (Fig5.5A). Although HXK1 is implicated in N assimilation (de Jong et al. 2013), nothing is known about its role in sulfate/sulphite transport. Significant downregulation of certain oxidative stress pathways (Superoxide metabolism and UV-B stress response) is observed in the HXK1OX in B+R (Fig5.5B). Plants possess enzymatic mechanisms to regulate the damaging ROS levels. Superoxide dismutase (SOD) converts O2− into H_2O_2, which is subsequently converted into H_2O by peroxidases and catalases. These three enzymes play major roles in scavenging O2− and H_2O_2. Interestingly, only four SODs - Copper/Zinc Superoxide Dismutase 1 (CSD1), CSD2, Production of Anthocyanin Pigment 1 (PAP1) and Fe Superoxide Dismutase 2 (FSD2) and no catalases or peroxidases are downregulated in the HXK1OX in B+R. However, a role for HXK1 in ROS scavenging and stress response has not been reported.

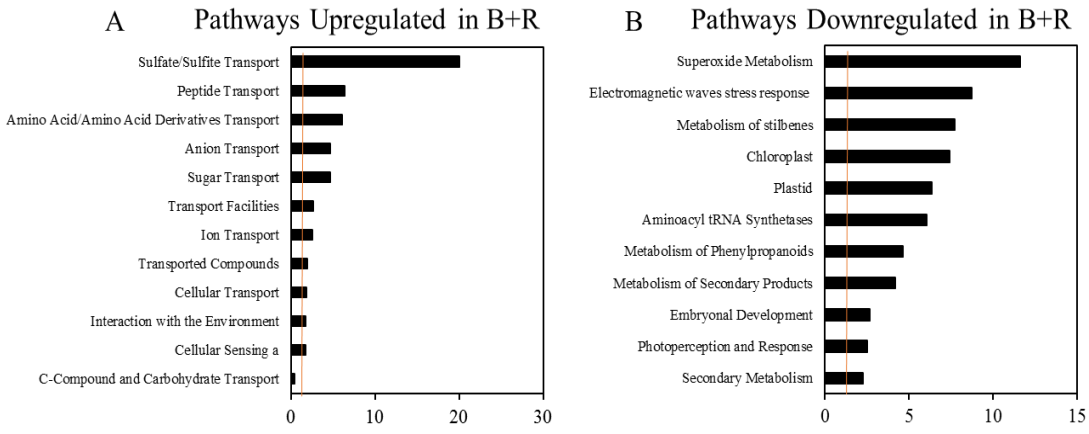

Fig5.5: Gene Ontology (GO) derived from Virtual Plant database for genes A) upregulated and B) downregulated in B+R gown HXK1OX. Pathways with a statistically significant enrichment (>1 (orange line), $p \leqslant 0.01$) are shown.

Taken the seedling phenotype, I determined the degree of overlap between genes altered in the blue light photoreceptor CRY mutants (RNAseq data derived from He et al. (2015)) and genes altered in the HXK1OX in B. A strong 25% overlap was observed. Interestingly, these 1684 CRY regulated genes altered in the HXK1OX appear to be enriched in metabolic pathways and not the energy driven microtubule/cytoskeleton class of components (Fig5.6). A comparison with CRY regulated gene lists from a different publication (Xu et al. 2018) yield identical percentage overlap and GO terms.

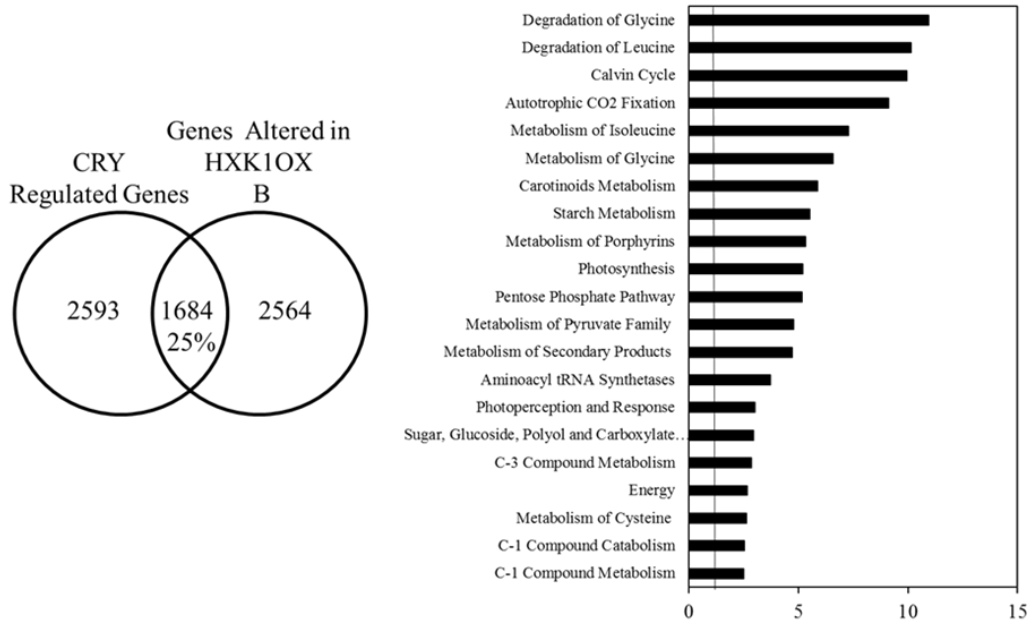

Fig5.6: Comparison between genes regulated by CRY (He et al. (2015) and HXK1OX in B. Gene Ontology (GO) derived from VirtualPlant database for the common subset (1684 genes). Pathways with a statistically significant enrichment (>1 (orange line), p $\leqslant$0.01) are shown.

I next made a three-way comparison between the genes altered in B (4247) and B+R (1448) in the HXK1OX with CRY regulated genes (3436). As depicted in the venn diagram below (Fig5.7), 613 CRY independent genes are altered by both light treatments (B and B+R) while 412 genes are exclusively altered by B+R. Similarly,

328 CRY dependent genes are altered by both light treatments while B + R exclusively alters 95 genes. These subsets are of particular interest as they are likely to give insights into key candidates mediating the differential light regulated HXK1OX phenotype. However, no subsets were enriched for particular GO terms. Transcription factors in the four subsets are enlisted below the venn-diagram (Fig5.7).

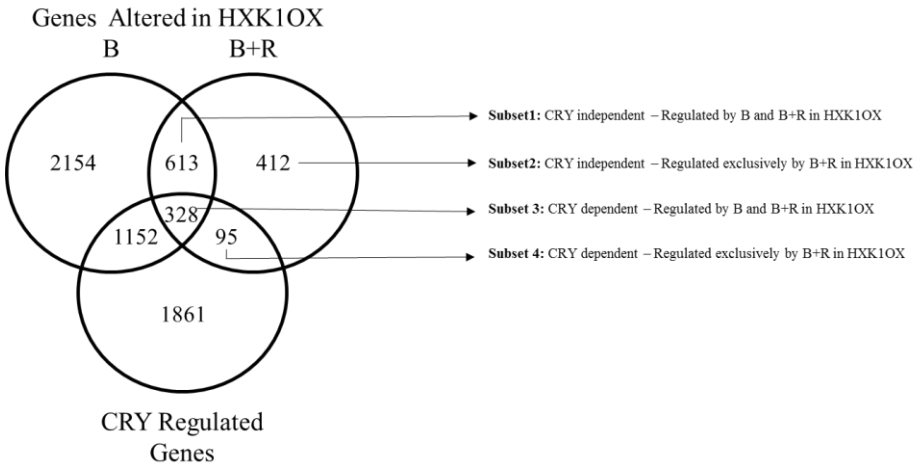

Transcription Factors (TFs)

Subset 1	Subset 2	Subset 3	Subset 4
Homeodomain-like superfamily protein	WD-40 Repeat Family Protein	Auxin Response Factor (ARF18)	Ethylene and Salt Inducible 3 (ESE3)
B Box Domain Protein 14 (BBX14)	Nuclear Factor Y Subunit 11 (NF-YB11)	Tesmin/TSO1-like protein (SOL1)	Production of Anthocyanin Pigment 1 (PAP1)
BBX18	NAC Containing Protein 3 (NAC003)	CONSTANS-like 1 (COL1)	bHLH TF Hectate 1 (HEC1)
Myb Domain Protein 13 (MYB13)	Basic-leucine zipper (bZIP) protein	SHI-related sequence 4 (SRS4)	HEC2
MYB50	Myb Domain Protein 93 (MYB93)	MYBS1	basic helix-loop-helix (bHLH) superfamily protein
MYB124	Cytokinen Response Factor 10 (CRF10)	RAD-like 3 (RL3)	BHLH100
Heat shock domain-containing protein	WRKY DNA Binding Protein33 (WRKY33)	Embryo Defective 2746 (EMB2746)	
Growth Regulating Factor 2 (GRF2)	Dehydration Response Element Protein 19 (DREB19)	Tandem Zinc Finger Protein 5 (TZP5)	
DNA-binding transcriptional regulator	AINTEGUMENTA-like 5 (AIL5)	TZP2	
Teosinte Branched 2 (TCP2)	basic region/leucine zipper transcription factor 16 (bZIP16)	Homeodomain-like superfamily protein	
TCP15	bZIP58	LOB domain-containing protein 21	
basic helix-loop-helix (bHLH) protein	B Box Domain Protein 15 (BBX15)	LOB domain-containing protein 41	
Inducer of CBF Expression 2 (ICE2)	Myb Domain Protein 54 (MYB54)	B Box Domain Protein 17 (BBX17)	
TESMIN/TSO1-LIKE CXC 2 (TCX2)	MYB16	Homeobox protein ATH1	
OBF Binding Protein 4 (OBP4)	MYB45		
BRI1-EMS-SUPPRESSOR 1 (BES1)	Agamous like 30 (AGL30)		
Response Regulator 12 (RR12)	NAC Transmembrane Motif 1 (NTM1)		
S1FA-like DNA-binding protein	TRANSPARENT TESTA 8 (TT8)		
WRKY DNA Binding Protein 31 (WRKY31)	LOB domain-containing protein 39 (LBD39)		
Integrase-type DNA-binding protein	WRKY DNA Binding Protein 36 (WRKY36)		
Homeodomain-like superfamily protein	GRAS family transcription factor		
AP2 domain transcription factor (SMZ)	WRKY family transcription factor family protein (TTG2)		

Fig5.7: A three-way comparison between genes altered in B and B+R in the HXK1OX with Cryptochrome (Cry) regulated genes. Transcription factors in the four subsets of interest are listed.

As red light negates the effect of HXK1OX on blue light signalling, I identified PHYB regulated genes in each of the four subsets. Ammad Abbas (Halliday lab) compiled the list of PHYB regulated genes with data derived from the Diurnal database (Mockler et al. 2007). Set criteria is genes with ± 2 fold change in *phyb* mutants. 130

genes in subset1, 74 genes in subset2, 146 genes in subset3 and 34 genes in subset4 are PhyB regulated (gene names not shown). Detailed investigation of these genes and TFs in the subsets is required to identify potential candidates operating downstream of HXK1OX signalling orchestrating the differential response to R and B.

4.2.4. Transcriptome clustering

For a broad analysis, genes was categorized into 10 clusters (Fig5.8A) based on expression patterns between the two light treatments. A representative visual heat map of average log Fold Change (logFC) for each cluster is shown (Fig5.8B). Fig. 10 depicts a graphical representation of the log FC normalized counts for each gene (grey lines) along with the cluster average (black line).

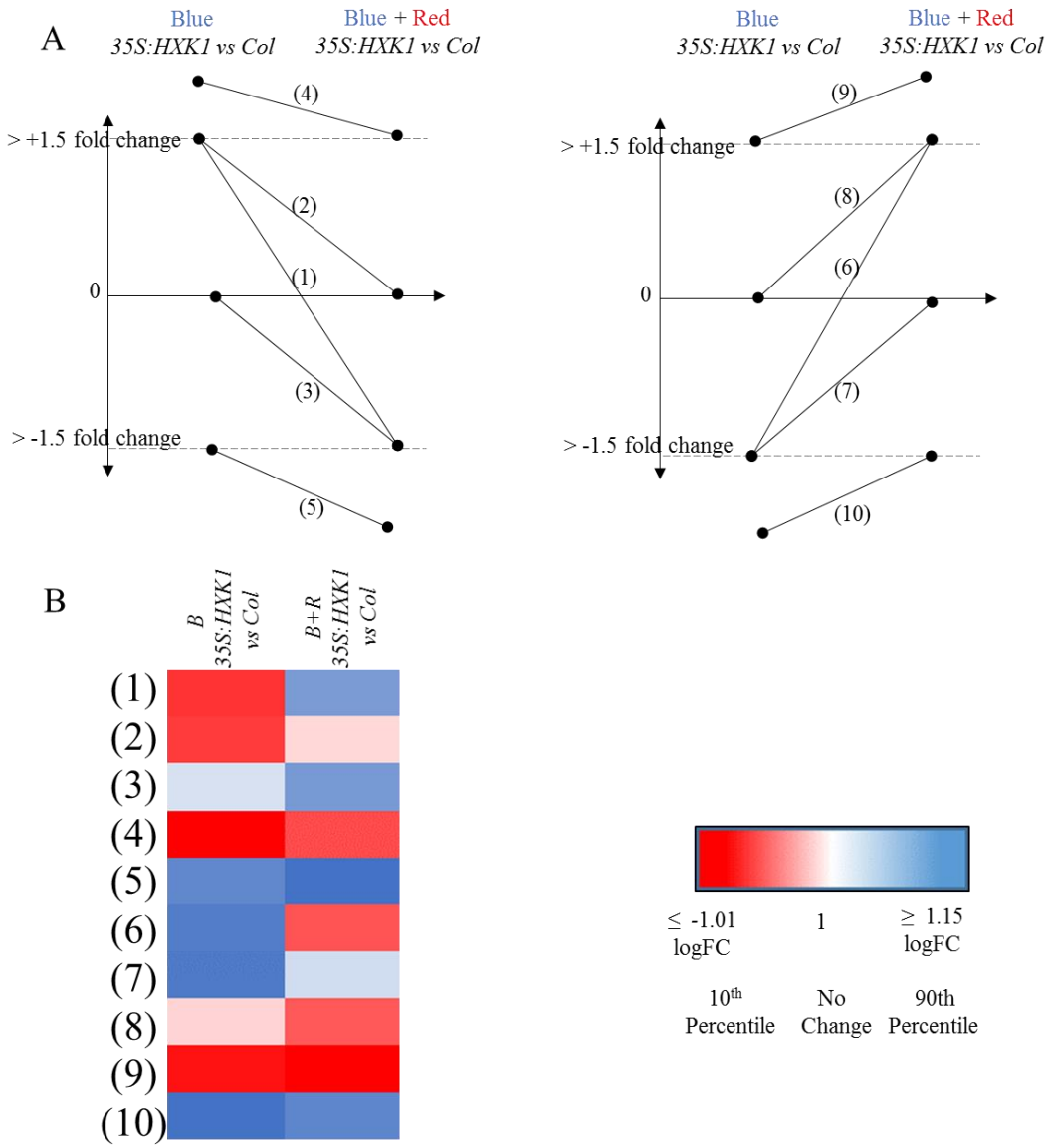

Fig5.8: Pictorial representation of gene clustering.
A) (1) Genes ⩾ 1.5 fold increase in 35S:HXK1 (relative to Col) in Blue (B) to ⩽ -1.5 fold decrease in B+Red (B+R), (2) Genes ⩾ 1.5 fold change increase in B to wildtype levels in B+R, (3) Genes with wildtype levels in B to ⩾ -1.5 fold change decrease in B +R, (4) Genes ⩾ 1.5 fold change in both treatments and ⩾ 1.5 fold change decrease between treatments, (5) Genes ⩽ -1.5 fold change in both treatments and ⩽ -1.5 fold decrease between treatments, (6) Genes ⩽ -1.5 fold change decrease in B to ⩾ 1.5 fold change increase in B+R, (7) Genes ⩾ -1.5 fold change decrease in B to wildtype levels in B+R, (8) Genes with wildtype levels in B to ⩾ 1.5 fold change increase in B+R, (9) Genes ⩾ 1.5 fold change in both treatments and ⩾ 1.5 fold change increase between treatments and (10) Genes ⩽ -1.5 fold change in both treatments and ⩾ -1.5 fold change increase between treatments.
B) Heatmap visualizing the Log Fold Change (LogFC) average between the two treatments (B and B+R in 35S:HXK1 vs Col in the 10 clusters. The values of the 10th and 90th percentiles were used as minimum (⩽ -1.01 logFC) and maximum values (⩾ 1.01 logFC).

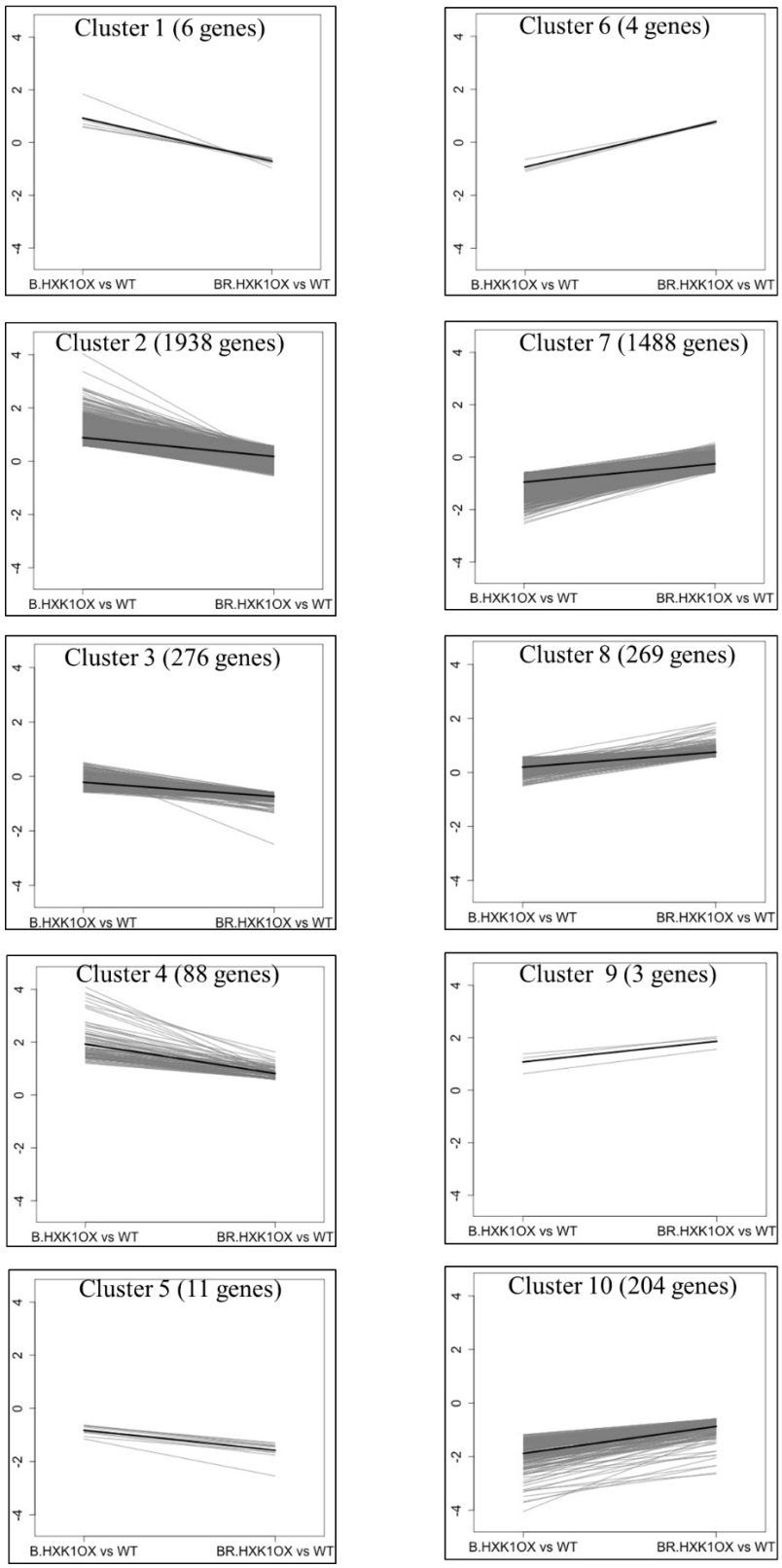

Fig5.9: Graphical representation of LogFC expression levels of individual genes (light grey lines) between the two treatments (B and B+R in 35S:HXK1 vs Col) for the 10 clusters. The solid black line represents the average of each cluster.

4.2.4.1. Cluster analysis

Although 5695 genes were altered in the HXK1OX in response to B and B+R (Fig5.4), the ten clusters included 4287 genes based on the set parameters. However, the Gene Ontology (GO) analysis between the two sets is largely similar (data not shown). Cluster 1 (≥ 1.5FC increase in B to ≤ -1.5FC decrease in B+R) and cluster 6 (≤ -1.5FC decrease in B to ≥ 1.5FC increase in B+R) fall into the extreme cluster category. The 6 genes in cluster 1 are strongly enriched in microtubule associated myosin and kinesin cytoskeleton genes in addition to a core cell cycle gene. This response is consistent with the elongated hypocotyl phenotype of the HXK1OX in blue light and the downregulation of microtubule associated genes in dark grown *gin2* mutants (RNAseq data). However, why these genes are specifically activated in B but not in R grown HXK1OX is unknown.

Cluster 1 (Genes ≥ 1.5 fold in Blue (B) and ≤ -1.5 fold in B+Red (R))

ATG	NAME	B. 35S:HXK1 vs Wt (logFC)	BR. 35S:HXK1 vs Wt (logFC)
AT5G44440	FAD-Binding Berberine Family Protein	1.84	-0.96
AT1G18370	Encodes a kinesin HINKEL - Microtubule Motor Activity	0.95	-0.65
AT5G27550	P-loop Containing NTPase - Microtubule Motor Activity	0.85	-0.80
AT1G76310	CYCLIN B2;4 - Regulation of Cell Cycle	0.71	-0.65
AT5G54280	Myosin 2 - Microtubule Motor Activity	0.61	-0.59
AT3G17360	Phragmoplast Orienting Kinesin 1 - Microtubule Motor Activity	0.59	-0.61

The 4 genes in cluster 6 enlisted below however have no specific pathway enrichment.

Cluster 6 (Genes ≤ -1.5 fold in B and ≥ 1.5 fold in B+R)

ATG	NAME	B. 35S:HXK1 vs Wt (log FC)	BR. 35S:HXK1 vs Wt (logFC)
AT4G36570	RAD Like3 (RL3) – Regulation of Transcription	-0.64	0.70
AT1G22400	UDP-Glycosyltransferase – Metabolic Process	-0.94	0.83
AT3G62150	P-Glycoprotein 21 – Auxin Influx/Efflux Transport	-1.03	0.81
AT3G45140	Lipoxygenase 2 – JA Accumulation / Volatile Biosynthesis	-1.09	0.76

Energy demanding pathways significantly altered in B are restored to Wt in B+R

Interestingly, energy demanding pathways altered in B grown HXK1OX seedlings is restored to Wt in B+R. Microtubule and cytoskeleton based genes are significantly upregulated whilst the photosynthetic metabolic pathways are downregulated in B. On supplying red light restores the transcript levels of these genes to Wt levels (Fig5.10). This trend is consistent with the seedling phenotype in the two different light treatments but the molecular mechanisms behind this action is unknown.

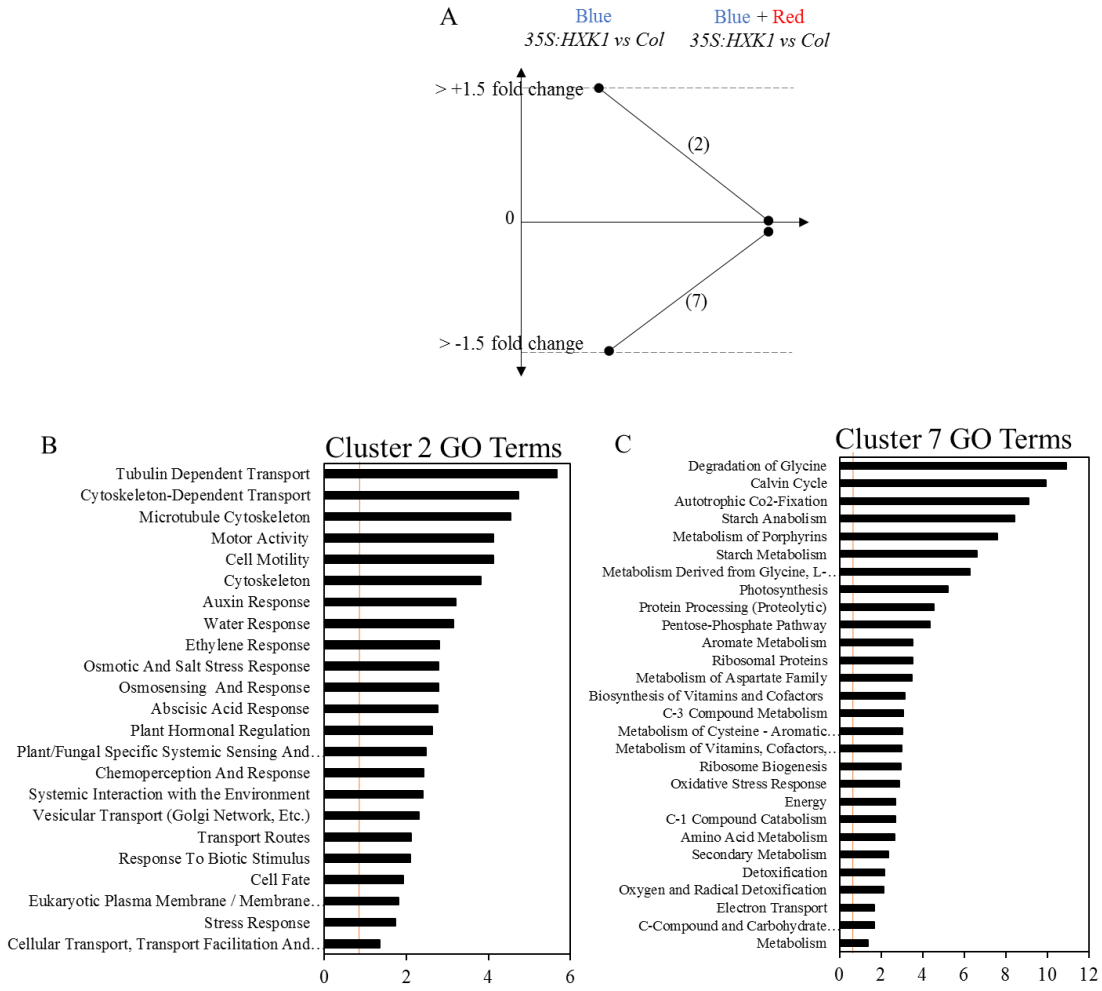

Fig5.10: A) Pictorial representation of Cluster 2 (≥ 1.5 fold change increase in B to wildtype levels in B+R) and Cluster 7 (≥ -1.5 fold change decrease in B to wildtype levels in B+R). Gene Ontology (GO) enrichment derived from VirtualPlant database for Cluster 2 (B) and Cluster 7 (C). Pathways with a statistically significant enrichment (>1 (orange line), p≤0.01) are shown.

4.2.5. Effect of PhyB loss in HXK1OX

To test if PHYB mediated red light signalling is required to supress the effect of blue light on HXK1OX, I generated the *phyb-9* HXK1OX homozygous line. Indeed, PhyB signalling is required for this suppression. In blue + red light, loss of *PHYB* in the 35S:HXK1 line obliterates red light mediated hypocotyl suppression and cotyledon expansion in the HXK1OX (Fig5.11A). Not surprisingly, the *phyb-9* 35S:HXK1 line exhibits a *phyb-9* phenotype in red and HXK1OX phenotype in B.

To understand the signalling activity of HXK1OX in monochromatic light, I measured the transcript abundance of two photosynthetic genes previously identified as direct HXK1 targets (*CAB2/CAA* Cho et al. (2007)). The transcript levels of *CAA* and *CAB2* is highly repressed in the *HXK1OX* in B (0.07 and 0.27 respectively) but appear Wt in R. In B + R light however, an intermediate fold change (0.46 and 0.55 respectively) is observed (Fig5.11 B,C).

While this trend does not explain the effect of B and R light on HXK1 transcriptional activity, it is somewhat consistent with the phenotype. The transcript abundance of photosynthetic genes *CAB2/CAA* is low in B where the HXK1OX has a small cotyledon area and Wt in R where HXK1OX exhibit a Wt phenotype.

Loss of *PHYB* in *35S:HXK1* further supresses *CAB2/CAA* transcript levels in B+R (0.29 and 0.35) (Fig5.11 B,C). Again, this is consistent with the etiolated phenotype of the *phyb-9 35S:HXK1* in B+R but the molecular interplay between red and blue light signalling on HXK1 transcriptional activity remains unclear.

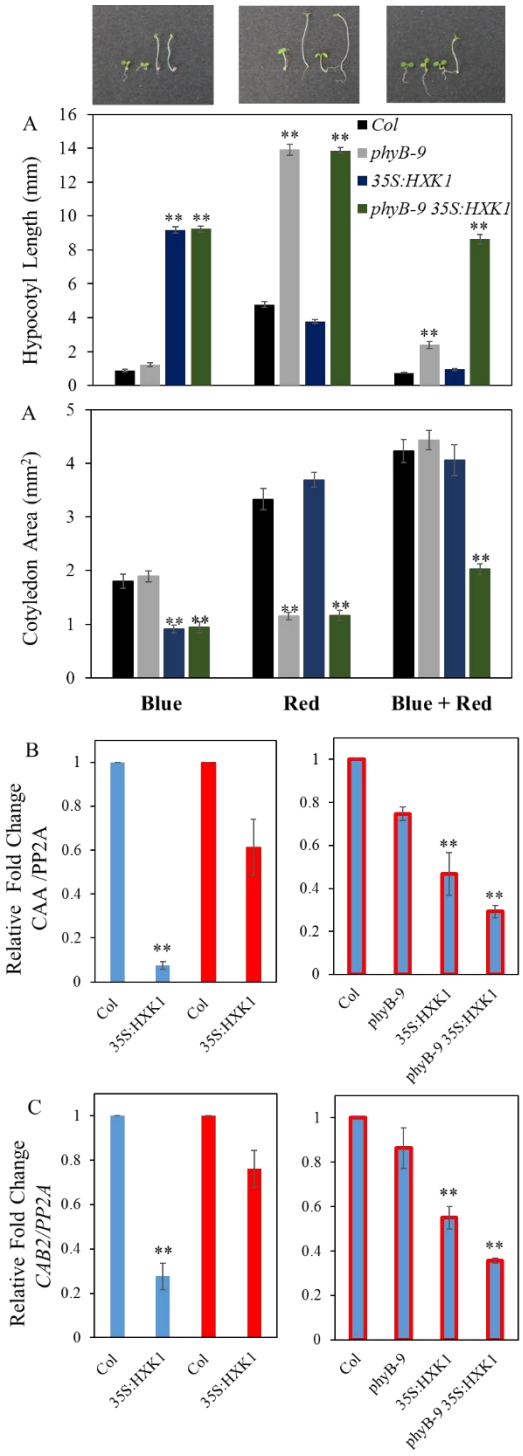

Fig5.11: Effect of red and blue light on direct HXK1 targets A) Hypocotyl length of 7-day-old seedlings grown in continuous blue (10µmol $m^{-2}s^{-1}$), red (40µmol $m^{-2}s^{-1}$) and blue + red light (10 + 40µmol $m^{-2}s^{-1}$) at 18C. Relative transcript levels (fold change relative to Wt) of B) *CAA* and C) *CAB2* in 7-day-old seedlings grown in Blue (blue bar), Red (red bar) and B+R (blue + red bar) light at 18C. Error bars indicate ±SE; and **P≤ 0.01 of *35S:HXK1*, *phyb-9* or *phyb-9 35S:HXK1* relative to Wt in each condition (Student's t-test).

I then observed the effects of *PHYB* loss in HXK1OX during white light mediated seedling photomorphogenesis. A normal photomorphogenic response (light fluence dependent hypocotyl suppression and cotyledon expansion) was observed in Wt. Consistent with published reports, the *phyB-9* mutants exhibit an elongated hypocotyl (Neff and Chory, 1998) relative to Wt at all intensities (Fig5.12). The HXK1OX seedlings exhibit an etiolated phenotype at low light (elongated hypocotyl/small cotyledon) and an exaggerated photomorphogenic phenotype at high light (characterized by hypocotyl suppression and enhanced cotyledon expansion) (Fig5.13). Loss of *PHYB* in the HXK1OX had an additive effect at low light fluences. At high light however, loss of *PHYB* obliterates the enhanced HXK1OX photomorphogenic response. Seedlings continue to exhibit a significantly elongated hypocotyl and small cotyledon phenotype (Fig5.12). Hence, our genetic data support the requirement of PHYB signalling for HXK1OX mediated seedling photomorphogenesis at high light.

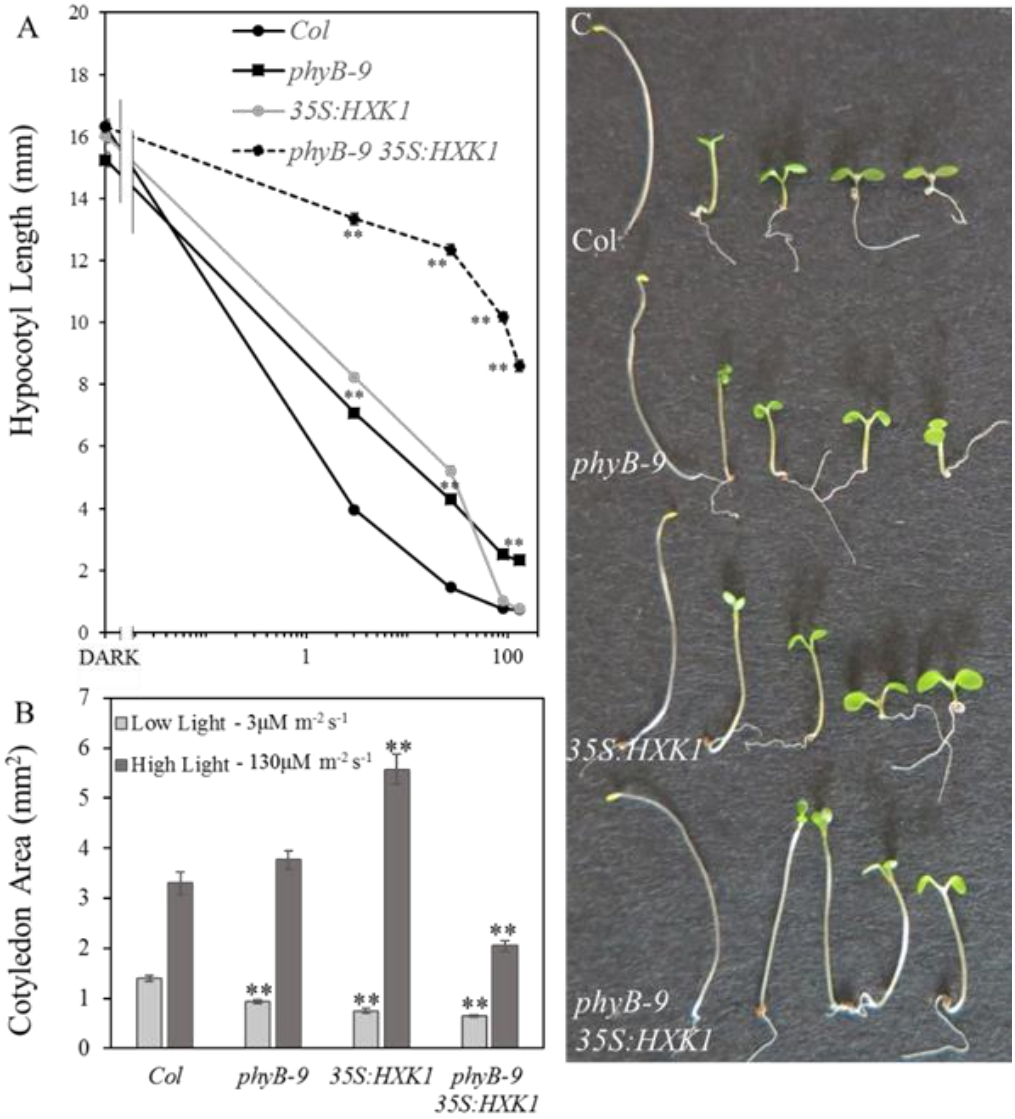

Fig5.12: Seedling morphology of the *phyb-9* HXK1OX in continuous light.
A) Hypocotyl length (in Dark, 3, 27, 90, 130µmol m^{-2} s^{-1} white light) and B) cotyledon area (in 3µmol m^{-2} s^{-1} and 130µmol m^{-2} s^{-1} white light) of 7-day-old Wt, *phyb-9*, *35S:HXK1* and *phyb-9 35S:HXK1* seedlings grown in continuous light at 18°C. Error bars indicate ±SEM; and **P≤ 0.01 of *phyb-9*, *35S:HXK1* and *phyb-9 35S:HXK1* relative to respective Wt in each condition (Student's t-test).

4.3. Discussion

Hexokinase1 function as a signalling component in response to exogenous sugar. Nuclear HXK1 in complex with partner proteins – VHAB1 and RPT5B has been shown to directly repress the transcription of photosynthetic genes *CAB2* and *CAA (*Moore et al. (2003); Cho et al. (2007)). The authors observed HXK1 enrichment on the promotor region encompassing a previously characterized G box element (Andronis et al. 2008; Maxwell et al. 2003; Cho et al. 2007). Following this observation, multiple reports show HXK1 requirement for sugar mediated transcriptional repression of other genes (Li et al. 2018; Kelly et al. 2017; Yang et al. 2013; Kunz et al. 2015; de Jong et al. 2014). Overexpressing HXK1 (*35S:HXK1*) have reduced transcript levels of *CAB2* and *CAA* even in the absence of sugar thereby amplifying the nuclear signalling response (Kelly et al. 2012).

Both blue and red light signalling pathways positively promote seedling photomorphogenesis (Arsovski et al. 2012; Nemhauser, 2002) Evident from the HXK1OX seedling phenotype in blue and red light, HXK1 exerts a strong negative control on blue light mediated seedling photomorphogenesis. This effect is negated by PHYB signalling. One hypothesis is that: HXK1 inhibits B signalling and R prevents this by targeting the same gene sets (1) or alternatively HXK1 inhibits B signalling and R prevents this through an independent pathway (2) (Fig5.13).

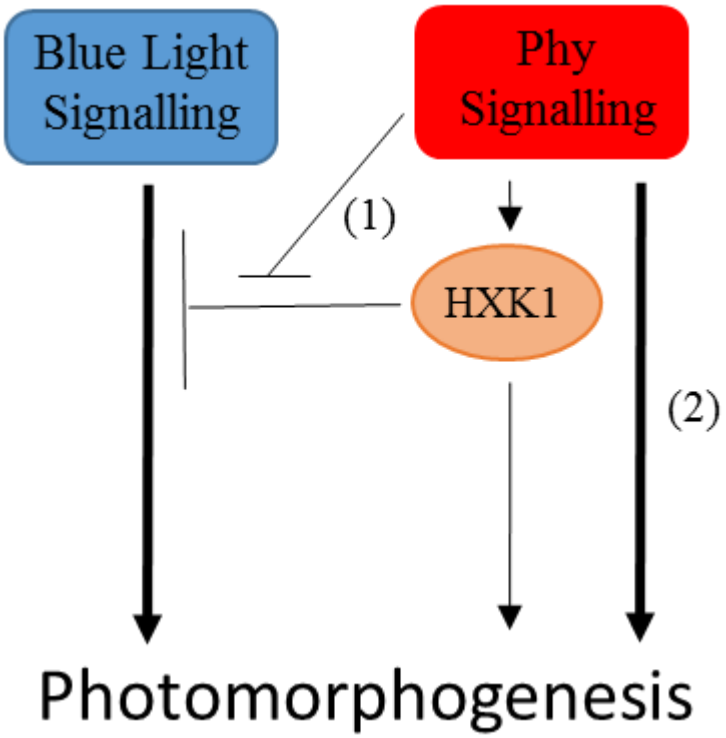

Fig5.13: Model depicting HXK1 action on B light signalling. R light negates that effect.

Transcriptional Changes in HXK1OX

B had a larger impact (16% differential regulation) than R (5% differential regulation) on the HXK1OX transcriptome (Fig5.3). The GO term enrichment is consistent with the seedling phenotype - microtubule/cytoskeleton based components are upregulated and metabolic, photosynthetic and respiratory pathways are down regulated in B grown HXK1OX. The transcript levels of these genes are restored to Wt on R light supplementation (Fig5.10). 25% of the genes altered by B light in the HXK1OX is Crytochrome (CRY) regulated. Interestingly these genes are not enriched in microtubule-based components suggesting CRY-independent HXK1 regulated gene subset. A cross to the *CRY* mutants for an epistatic genetic interaction would confirm the potential control by HXK1OX on blue light signalling.

A three-way comparison made between genes altered by B and B+R in the HXK1OX with CRY regulated genes generated four subsets of interest. These categories specifically list CRY -dependent & -independent genes exclusively altered in B and B + R grown HXK1OX (Fig5.7). Detailed investigation coupled with molecular and genetic data is required to understand the molecular mechanisms behind HXK1 control on B signalling and how R inhibits it.

Effect of PhyB loss in HXK1OX

Our genetic evidence indicate that *PHYB* loss obliterates the hypocotyl suppression and cotyledon expansion of the HXK1OX as observed in both, B+R and white light (Fig5.11A; 5.12). This is a clear indication that PHYB signalling is required to supress the effect of HXK1OX in B light. Although the well characterized HY5 is a potential candidate, it positively operates downstream to both red and blue light signalling pathways during seedling photomorphogenesis (Gangappa and Botto, 2016). Hence, HY5 may not be mediating the exclusive HXK1OX hypocotyl suppression in red light. Detailed investigations on other PHY regulated signalling components within the four subsets mentioned above might hold the answer (Fig5.7). If PHYB directly mediates this response is also an open question.

Other potential molecular mechanisms

Both red and blue light pathways synergistically mediate photomorphogenesis through common regulatory mechanisms (Arsovski et al. 2012; Li et al. 2011; Su et al. 2017). Taken that the HXK1OX exhibit a differential seedling phenotype in response to red and blue light, it is likely that HXK1 controls 1) the photoreceptors directly or 2) exclusive PHY/CRY signalling elements during photomorphogenesis.

A potential scenario is HXK1 directly inhibits the CRYs. It would be interesting to check if HXK1 operates interdependently with BIC1 (Blue-light Inhibitor of Cryptochromes1) as the BICOX exhibits a similar phenotype to HXK1OX in blue light. BIC1 inhibits CRY photoreceptor activation by interfering with CRY phosphorylation and homodimerization (Wang et al, 2016). The catalytic activity of the Phosphoregulatory Protein Kinases (PPKs) family responsible for CRY phosphorylation is suppressed by the BIC1 (Liu et al. 2017). It would be worth testing the phosphorylation status of the CRYs in the HXK1OX without and with incremental levels of BIC1 in B and B+R light. Other potential hypotheses also include HXK1 negatively regulating the PPKs or directly inhibiting CRY heterodimerization through phosphorylation or direct interaction respectively. It would be possible to test these possible scenarios.

HFR1, a key bHLH transcription factor is a positive regulator of photomorphogenesis operating downstream to CRY signalling. However, it also functions downstream of the Far-Red photoreceptor PHYA (Duek and Fankhauser, 2002; Fairchild et al. 2000). Given that the HXK1OX exhibits a Wt phenotype in FR (Fig.1C), HFR1 is an unlikely candidate in this pathway. Hence, exclusive B and R signalling components potentially mediating the response will have to be identified.

As R and B light does not affect the transcript and protein levels of HXK1 (Fig. 2), it is unclear if either light quality post-translationally modifies HXK1 thereby influencing its DNA binding ability. This could be tested through ChIP-qPCR for enrichment of HXK1 on promotors of novel gene targets in response to R, B and R+B light. All the mentioned hypotheses would enable us to gain insights into the role of HXK1 in blue and red light signalling.

Conclusion

This chapter reveals a novel role for the glucose sensor HXK1 in light signalling. Evident from the HXK1OX phenotype, HXK1 negatively controls B light signalling during seedling photomorphogenesis. Based on our genetic evidence, it is clear that PHYB signalling somehow negates this control. Detailed investigation coupled with molecular and biochemical data is required to understand the underlying molecular mechanisms behind this phenomenon. However, this exclusive phenotype in B will have to be re-examined in other independent transgenic lines for confirmatory support. If true, although the effect of the HXK1OX is amplified and may not occur to this extent in nature, it nevertheless identifies a potential link between light and metabolic signalling during seedling photomorphogenesis.

CHAPTER 5

A role for Constitutive Photomorphogenic1 (COP1) and De-etiolated1 (DET1) in sugar signalling

5.1. Introduction – COP1 and DET1

Constitutive Photomorphogenic 1 (COP1) and De-etiolated 1 (DET1) were the first group of photomorphogenesis repressors identified more than 25 years ago. These loci were identified in forward genetic screens for mutants that display light-grown phenotypes in darkness. (Chory et al. 1989; Deng and Quail, 1991). Mutations in the COP1 and DET1 loci result in seedlings exhibiting a light grown phenotype (short hypocotyls, open cotyledons and elongated roots) in complete absense of light. Both, COP1 and DET1 positively regulate the abundance of another class of negative regulators of photomorphogenesis - Phytochrome Interacting Factors (PIFs) through unknown mechanisms. Hence, mutating the *PIF* family result in a *COP1/DET1* mutant seedling phenotype in the dark. COP1 and DET1 act upstream to the PIFs, negligible levels of PIF proteins (PIF1, PIF3, PIF4, PIF5) are observed in the *cop1* and *det1* mutants (Dong et al. 2014; Ling et al. 2017; Baur et al. 2003). Subsequently, both COP1 (in complex with Supressor of PhyA (SPA family of proteins) and DET1 (in complex with COP10) were identified to function as independent substrate adaptors to the CULLIN4 based E3 ligase system (Schroeder et al. 2002; Yanagawa et al. 2004; Chen et al. 2010). Interestingly, a constitutive photomorphogenic phenotype (in the dark) is exhibited in CULLIN4 (CUL4) RNAi lines (Chen et al. 2006) confirming the role of the CUL4 complex in photomorphogenesis repression. However, both $CUL4^{COP1\text{-}SPA}$ and $CUL4^{DET1\text{-}COP10}$ complexes do not biochemically interact (Chen et

al. 2010). COP1 E3 ligase activity is dark dependent. In light, COP1 nuclear activity is inhibited by: 1) its export from the nucleus (a slow inactivation mechanism) and 2) direct inactivation of the COP1-SPA complex by photoreceptors phytochromes and cytochromes (a rapid inactivation mechanism) (Liu et al. 2011; Lian et al. 2011; Sheerin et al. 2015). However, little is know about the regulatory roles of DET1 E3 ligase and its inactivation mechanisms. The light dependent inactivation of COP1 (and DET1) E3 ligase relieves the repression on the positive regulators of photomorphogenesis to promote seedling de-etiolation.

COP1 plays a conditional role in the regulation of PHYA abundance. The light induced decline in PHYA levels appear Wt in the *cop1* mutant grown in the absence of sucrose. However, a 2% sucrose addition perturbed this response. An elevated PHYA protein abundance was observed in the *cop1* mutant relative to Wt suggesting COP1 activity maybe exogenous sugar regulated (Debrieux et al. 2013).

Over the years, discoveries on target substrates and functionalities pertaining to COP1 and DET1 based E3 ligase have been made. Mutations in *COP1* and *DET1* result in plants exhibiting pleotropic effects suggesting its crucial involvement in multiple signalling and developmental pathways (Lau and Deng, 2012). Highly conserved mammalian orthologs of this E3 ligase system mCUL4^{mCOP1} and ^{mDET1} E3 ligase system have been identified and widely implicated in cancer biology apart from lipid and glucose stimulated insulin metabolism. Unlike in plants, mCOP1 interact with mDET1 and operate as a singly complex with mCul4 based E3 ligase system. Targets of the mammalian complex include master tumor supressors such as P53, c-JUN and ETS transcription factors inaddition to multiple key components in various other pathways (Marine, 2012; Dornan et al. 2004; Vitari et al. 2011; Wertz et al. 2004).

The figure below (Fig6.1) depicts the exclusive and joint involvement of COP1 and DET1 in several plant pathways.

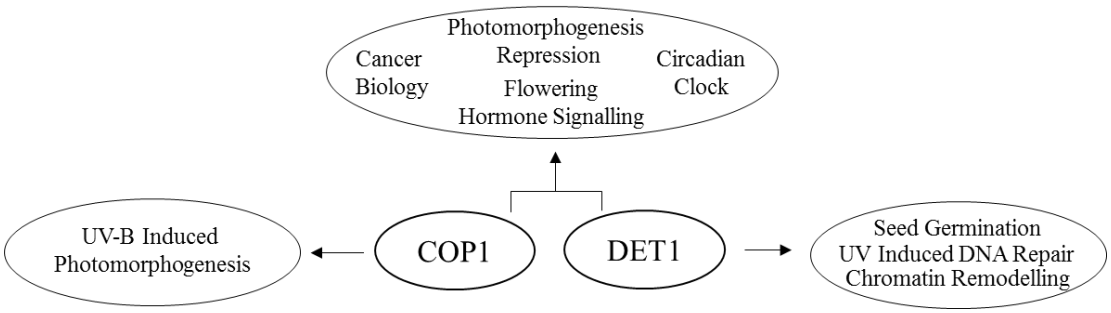

Fig6.1: Ubiquitin ligases COP1 and DET1 are independently and interdependently involved in multiple signalling pathways.

In Arabidopsis, little is known about the direct involvement of COP1 and DET1 in metabolism and sugar signalling. In this section, I provide genetic evidence for the requirement of COP1 and DET1 in sugar mediated seedling and adult plant growth. The function of both proteins in response to sugars (sucrose and glucose) appear to switch between the two developmental stages tested (seedling and adult rosettes). Based on our preliminary data and other published results, I will present mechanistic hypotheses for the phenotypes.

5.2. Results

5.2.1 *cop1* and *det1* mutant seedlings are sugar insensitive

Seedling hypocotyl growth is regulated by light signalling components and gated by the circadian clock and photoperiod. Exogenous sugar enhances hypocotyl length. Stewart et al. (2011) demonstrated that the PIF family is required for the regulation of this response as the *pifQ* mutants are insentive to sucrose induced hypocotyl elongation. Consistent with these published findings, both glucose and sucrose enhanced Wt hypocotyl length but not *pifQ*. Moreover, the sugar induced hypocotyl elongation is abolished in both the *cop1-4* and *det1-1* mutants (Fig6.2A,B) revealing a similar behavious to the *pifQ* mutant.

In darkness, seedlings exhibit an etiolated phenotype (elongated hypocotyls and closed apical hook) through a mechanism jointly co-ordinated by COP1 and DET1 E3 ligases and the PIF family of transcription factors. Mutating *COP1/DET1/PIFs* result in seedlings exhibiting a de-etiolated phenotype (short hypocotyls and open cotyledons) in the dark as observed in Fig6.2 C,D. Glucose and sucrose application appears to inhibit etiolated wildtype hypocotyl length (Hu et al. 2002). In contrast to my data in light-dark cycles, and in contrast to Wt behaviour in constant darkness, the de-etiolated *cop1, det1* and *pifQ* mutants exhibit a sugar induced hypocotyl elongation response (Fig6.2 C, D).

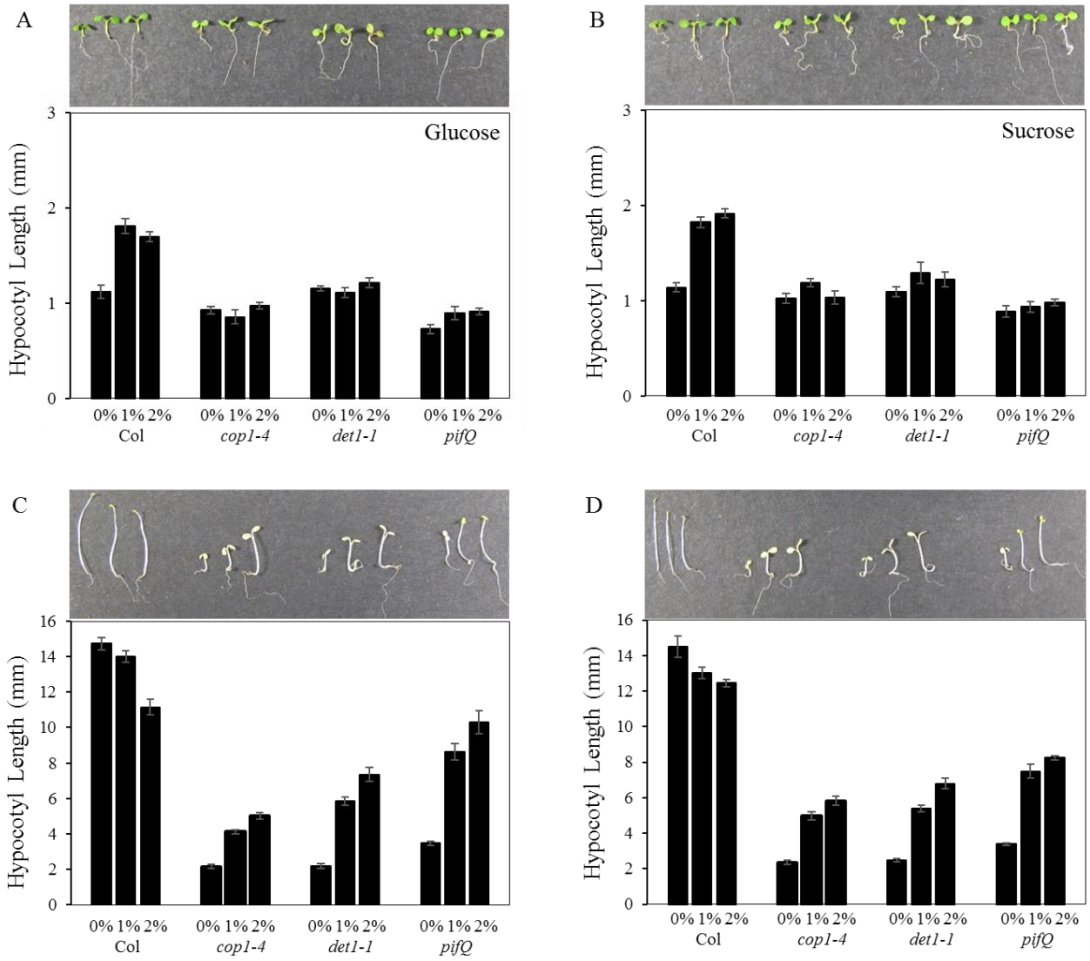

Fig6.2: *cop1/det1/pifQ* seedling hypocotyl response to sugar
A) Hypocotyl length of de-etiolated seedlings grown in the absence and presence of 1% or 2% (w/v) glucose and B) sucrose. C) Hypocotyl length of etiolated seedlings grown in the absence and presence of 1% or 2% (w/v) glucose and D) sucrose. Seedlings were grown for 7 days under 12:12 photoperiods (A,B) and constant dark (C,D), 50µmol m^{-2} s^{-1} white light at 20ºC. Error bars indicate ±SEM.

5.2.2. *cop1* and *det1* adult mutant plants are sugar hypersensitive*: cop1* and *det1* mutants display exaggerated responses to exogenous sucrose applications:

Photosynthesis derived sugars play a central role to integrate internal and external regulatory signals in driving growth and biomass. To more comprehensively investigate the role of COP1 and DET1 in sugar responses, I quantified *cop1* and *det1* mutants subjected to a range of sucrose concentrations (Fig6.3, 6.4). In the absence of

sugar, *cop1-4* and *det1-1* adult plants appear developmentally deformed and smaller in stature as previously characterized (Chory et al. 1989; Deng and Quail, 1991) (Fig. 3). According to previous studies, optimal sucrose application accelerate growth and subsequently enhance biomass (Wingnter et al. 2010). However, beyond a certain threshold, sugar application appears to have an inhibitory effect on plant growth. My data is consistent with the phenomenon, I observed that sucrose gradually enhances fresh weight (Fig. 3A), saturating at 1% (2 fold increase) beyond which sucrose has an inhibitory effect. By contrast, *cop1-4* and *det1* have a dramatically enhanced response to sucrose and this is more obvious at higher concentrations. An increase in *cop1-4* fresh weight is observed and saturated at 3% sucrose (with a 6.8 fold increase). *det1-1* on the other hand exhibits an even more exaggerated trend with a 9-fold increase fresh weight. A similar exaggerated enhancement trend for *cop1-4* and *det1-1* is observed in dry weight relative to wildtype (Fig6.3B).

A similar sugar concentration dependent trend is observed for plant rosette diameter (Fig6.3C). As observed in Col, a gradual enhancement and a dramatic reduction is seen. While fold increase in *cop1-4* appears more subtle compared to wildtype, *det1-1* mutants exhibit a more robust rosette expansion response with a 5 fold increase at 3% sucrose. Finally, we quantified the impact of sucrose application on leaf number and leaf production rate (Fig6.4). A subtle increase in leaf number and leaf production rate was observed in wildtype as the sucrose concentration increases and an inhibitory effect observed at 5% concentrations (Fig6.4). However, in *cop1-4* and *det1-1* mutants, on gradual sucrose application, the total leaf number and leaf production rate gradually increased surpassing wildtype at 5% concentrations. Hence, our data strongly emphasizes COP1 and DET1 as critical suppressors of sucrose

induced growth/biomass production thereby revealing until know unknown roles in sugar signalling.

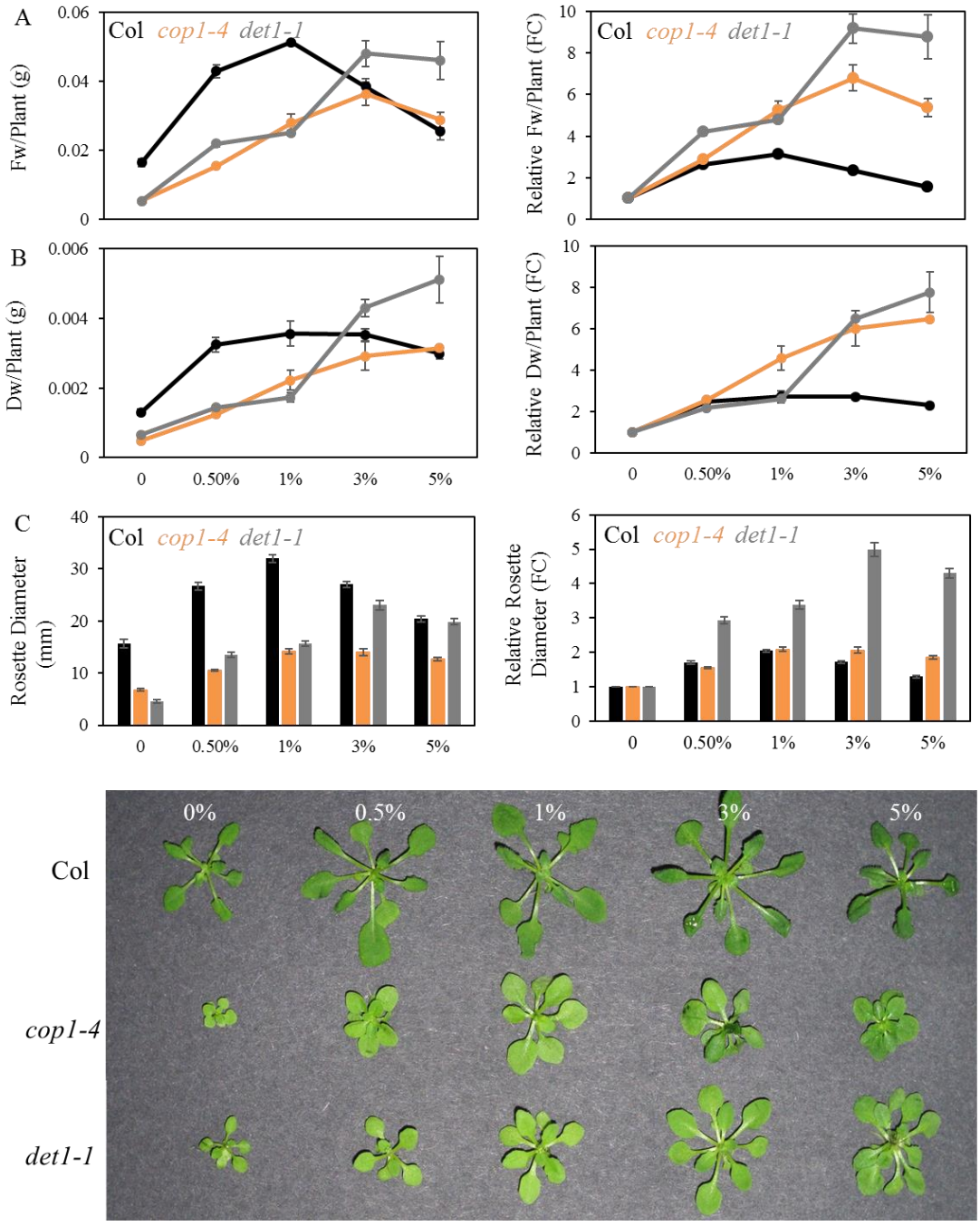

Fig6.3: *cop1/det1* adult plant response to sucrose – Growth response
A) Fresh weight and relative fresh weight (fold change), B) Dry weight and relative dry weight, C) Rosette diameter and relative rosette diameter and D) images of adult plants grown in the absence and presence of 0.5%, 1%, 3% and 5% (w/v) supplemented sucrose plates. Plants were grown for 4 weeks at 12L:12D photoperiods, 50µmol m^{-2} s^{-1} white light at 20 ºC.

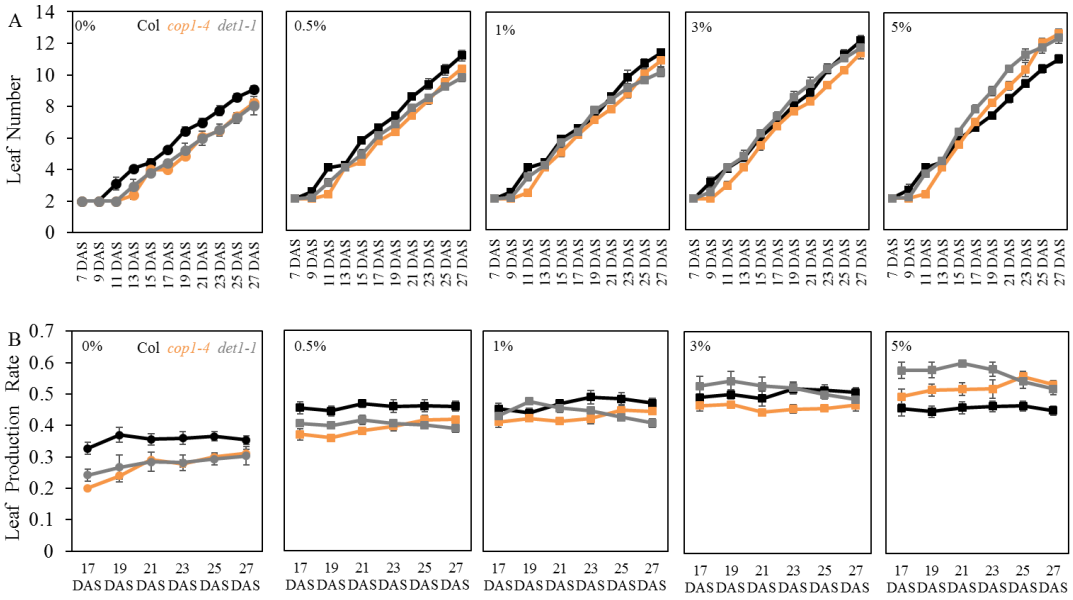

Fig6.4: *cop1/det1* adult plant response to sucrose – Leaf number and production rate A) Total leaf number and B) leaf production rate in the absence and presence of 0.5%, 1%, 3% and 5% (w/v) sucrose. Plants were grown for 4 weeks at 12L:12D photoperiods, 50µmol m^{-2} s^{-1} white light at 20 ºC.

cop1 and *det1* mutants display similar exaggerated responses to exogenous glucose applications

Photosynthetically derived sucrose is tightly coupled to sugar signalling. Sucrose or sucrose derivatives - glucose, maltose, fructose and T6P (Ruan 2014) can directly function as signalling molecules. In order to delineate the exaggerated *cop1/det1* sucrose dependent growth response from other sugar derivatives, we performed a similar growth assay on glucose supplemented media. The overall growth trend observed in glucose grown Wt, *cop1-4* and *det1-1* (Fig6.5) appear highly similar to my experiment with sucrose (Fig6.4). In Col, 1% glucose enhances biomass, an inhibitory effect was observed in higher concentrations. In *cop1-4* and *det1-1* mutants, a robust enhancement in fresh weight/dry weight, total leaf number and rosette diameter (Fig6.5) is observed in the 1-2% glucose range compared to 3-5% sucrose range. This low glucose concentration response is somewhat expected as one sucrose molecule is hydrolysed to one glucose and one fructose molecule. Hence, this exaggerated growth phenotype on exogenous sugar applications might be glucose (and sucrose) specific by activating the same pathways. Taken together, the role of COP1 and DET1 in response to sugar appears to be the opposite at the seedling compared to adult plant developmental stage.

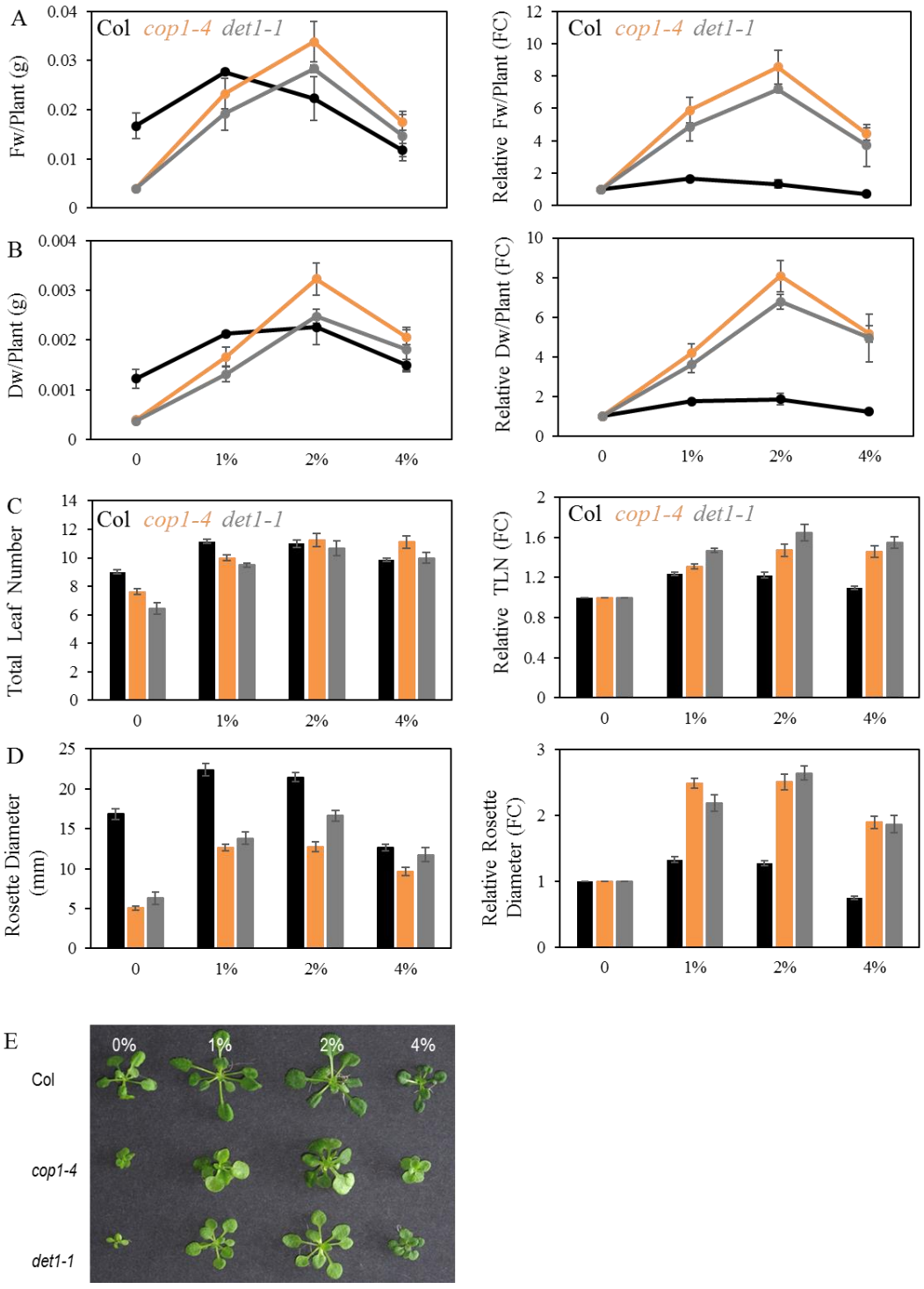

Fig6.5: *cop1/det1* adult plant response to glucose
A) Fresh weight and relative fresh weight (fold change), B) Dry weight and relative dry weight, C) Total leaf number and relative total leaf number, D) Rosette diameter and relative rosette diameter and E) Images of adult plants grown in the absence and presence of 1%, 2% and 4% (w/v) glucose. Plants were grown for 4 weeks at 12L:12D photoperiods, 50µmol m^{-2} s^{-1} white light at 20 ºC.

PIF adult mutants do not display a sugar hyper-response

In our hypocotyl assay (Fig6.2) and previously published data (Stewart et al. 2011), the *PifQ* mutant exhibits a sugar insensitive seedling hypocotyl phenotype under diurnal conditions similar to *cop1* and *det1*. Hence, we were interested to test whether if PIFs function similar to COP1 and DET1 as negative regulators of sugar induced growth in adult plants. Therefore, I tested the same growth phenotypes as we did previously for *cop1* and *det1* (see above, Fig6.4, 6.5). In Wt plants (black), 1% (w/v) sucrose (straight line) and glucose (dotted line) enhanced fresh and dry weight as before while 2% and 3% concentrations trigger an inhibitory effect (Fig6.6). The *pifQ* mutants mostly exhibit a wildtype response to both sugars suggestings PIFs are non-involved for sugar induced adult plant growth. Hence, taken together, COP1, DET1 and PIFs appear to be positively required for sugar induced seedling hypocotyl elongation but COP1 and DET1 exclusively function as negative regulators of sugar mediated adult plant growth.

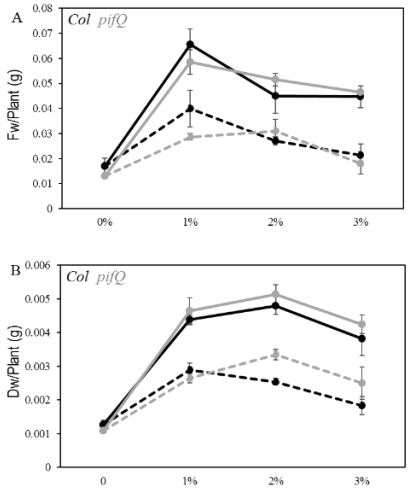

Fig6.6: pifQ adult plant response to sugar (sucrose and glucose)
A) Fresh weight and B) Dry weight of adult Col and *pifQ* mutant plants grown in the absence and presence of 1%, 2% and 3% (w/v) sucrose (straight line) and glucose (dotted line). Plants were grown for 4 weeks at 12L:12D photoperiods, 50µmol $m^{-2}s^{-1}$ white light at 20 ºC.

5.2.3. *cop1/det1* sugar hypersensitivity is mimicked under increased light conditions

To confirm our findings on the effects of exogenous sugar application, we repeated the experiment by growing the mutants in increasing light intensities. High light driven photosynthate production could possibly mimic the exogenous sugar application. *cop1*, *det1* and *pifQ* mutants were grown in increasing light fluences (low/medium/high - 130, 260 and 430μmol $m^{-2}s^{-1}$) for 4 weeks as before. A 1.9 fold increase in fresh weight was observed in Wt (high light relative to low light) and the *pifQ* mutant whereas a more subtle and significant enhancement was observed in *det1-1* (2.5 fold) and *cop1-4* (3.7 fold) mutants respectively (Fig6.7). However, a clear correlation between the physiological sugar concentrations in mutants grown under increasing light fluences on soil and sugar supplemented MS media plates would draw a better comparison for this analysis. Taken together, under natural conditions of physiologically elevated sugar levels, COP1 and DET1 function as negative regulators of growth and biomass production.

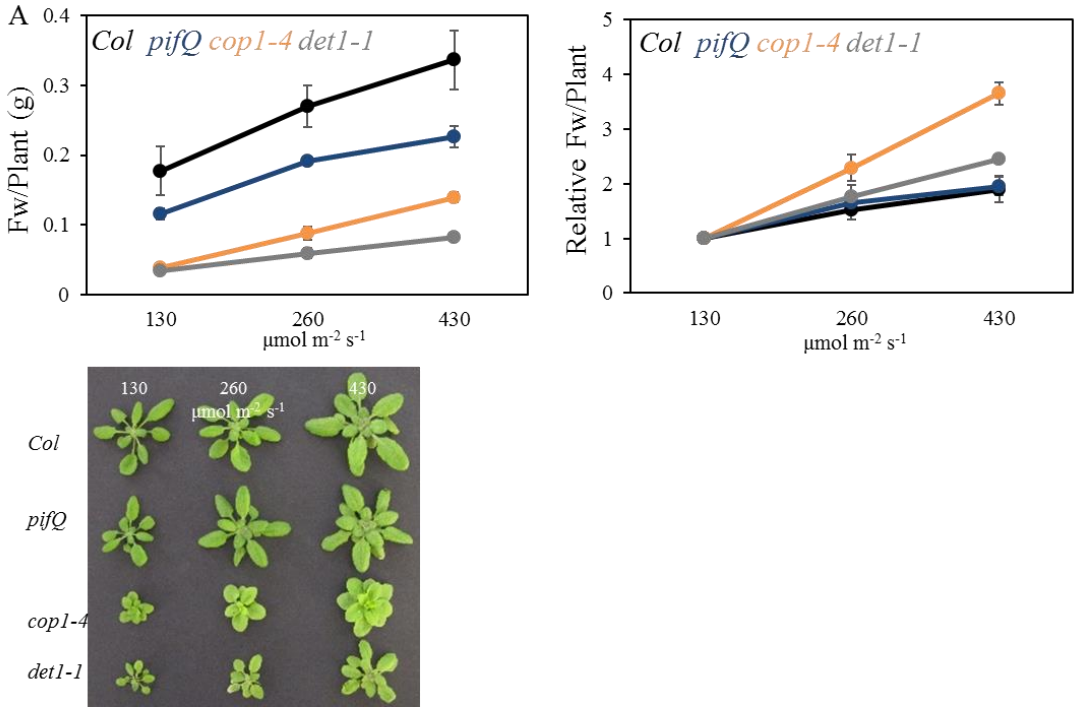

Fig6.7: *cop1/det1/pifQ* adult plant response to increasing light intensities
A) Fresh weight, relative fresh weight (Fold change) and plant images of adult Col, *pifQ*, *cop1-4* and *det1-1* mutant plants grown under increasing light fluences (130, 260 and 430µmol $m^{-2}s^{-1}$). Plants were grown for 4 weeks at 12L:12D photoperiods at 20ºC.

5.2.4. Metabolite analysis in adult mutants

To test the levels of growth promoting carbon metabolites, glucose, sucrose and starch content was measured from adult End of Night (EoN) samples of Wt, *cop1*, *det1* and *pifQ* mutants grown under low light (130µmol $m^{-2}s^{-1}$) and high light (430µmol $m^{-2}s^{-1}$) from the above experiment. In low light (130µmol $m^{-2}s^{-1}$) the metabolite levels in the mutants is somewhat similar to Wt. Hence, the exaggerated sugar mediated growth phenotypes in the *cop1/det1* mutants is not simply because the mutants accumulate less carbon. High light enhances sucrose (1.6 fold) and starch (1.3 fold) levels in wildtype, a similar fold change increase was observed in the *pifQ* mutant. However, *cop1-4* and *det1-1* mutants exhibit larger proportional increase of sucrose

(1.9 and 2.4 fold increase) and starch (1.7 and 1.8 fold increase respectively) (Fig6.8). This enhancement suggest the negative involvement of COP1 and DET1 in either glucose and starch metabolism or carbon induced growth-promoting pathways.

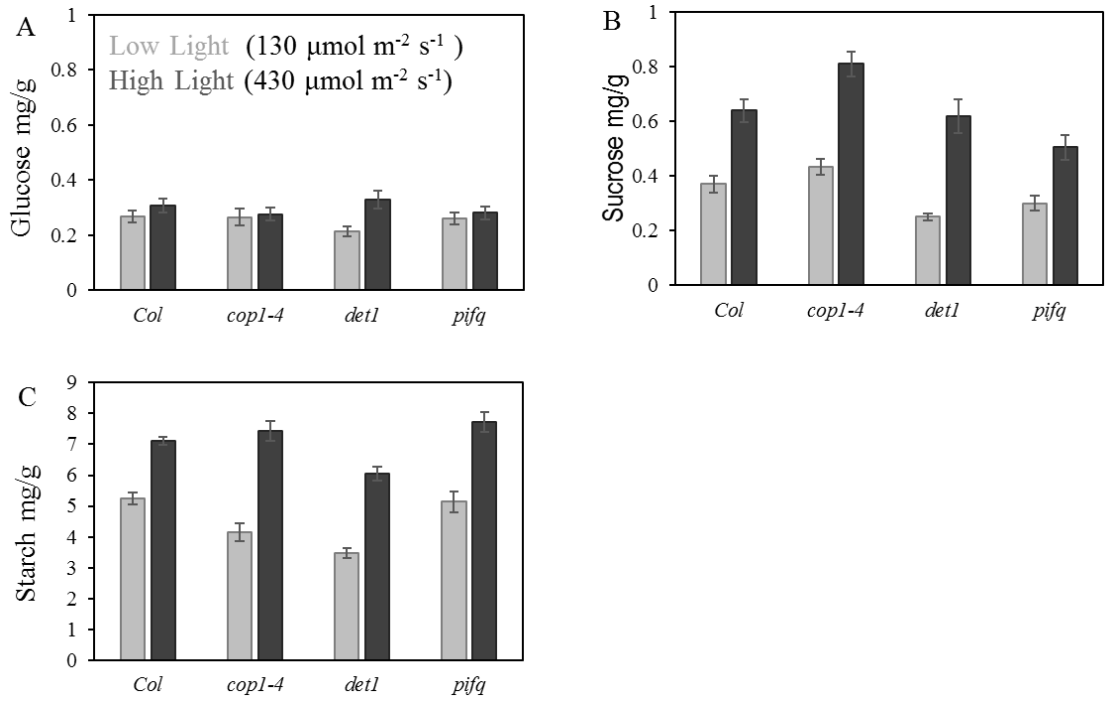

Fig6.8: Metabolite levels in wildtype, *cop1*, *det1* and *pifQ* mutants
A) Glucose, B) Sucrose and C) Starch levels (mg/g) from End of Day (EoD) samples of 4 week old rosettes grown under two light fluences (130µmol $m^{-2}s^{-1}$ and 430µmol $m^{-2}s^{-1}$) at 12:12 photoperiods and 20 ºC.

5.3. Discussion

The negative regulators of seedling photomorphogenesis - COP1, DET1 and PIFs have been implicated in multiple signalling and developmental pathways (Lau and Deng, 2012; Leivar and Monte, 2014). Amongst published data on COP1/DET1 – sugar linkage are two reports, 1) COP1 mediated proteolysis of PHYA photoreceptor was shown to be impaired by sucrose application indicating that COP1 E3 ligase activity could be sucrose regulated (Debrieux et al. 2013). 2) *det1-1* mutants have altered peroxisomal activity. Peroxisomes are sites of fatty acid conversion to sugars.

Dark grown *det1-1* mutant seedlings failed to grow after transfer to light on sugar free media (Hu et al. 2002).

Seedling phenotype:

In seedling, *cop1, det1* and *pifQ* mutants exhibit a sugar insensitive hypocotyl elongation phenotype. Stewart et al. (2011) also observed the *pifQ* seedling insensitivity to sucrose. COP1 and DET1 genetically act upstream to PIFs and are required to stabilize PIF protein levels. Bauer et al. (2004) and more recently Ling et al. (2017) demonstrate the requirement of COP1 and Dong et al. (2014) demonstrate the requirement of DET1 for PIF accumulation and stabilization in the dark. Negligible protein levels of all four PIFs (PIF1, PIF3, PIF4, PIF5) was observed in the respective mutants. Therefore, the *cop1-4* and *det1-1* seedling sugar insensitive phenotype in diurnal growth conditions may be PIF dependent (Fig6.1). Although there is some conflicting data on sucrose mediated regulation on PIF transcripts and protein abundance (Shor et al. 2017; Stewart et al. 2011), Ch-IP qPCR studies confirm that sucrose enhance PIF activity as the enrichment of PIFs on target gene promotors (Shor et al. 2017) increases in response to sugar application. Hence, the observed *cop1* and *det1* sugar insensitive seedling hypocotyl phenotype may be PIF dependent.

In constant dark conditions, Wt seedlings exhibit an etiolated response (elongated hypocotyls and closed apical hook) while the photomorphogenic repressors, *cop1, det1* and *pifQ* mutants exhibit a light grown morphology (short hypocotyl and open cotyledons) and transcriptome. In contrast to diurnal conditions, dark grown *cop1, det1* and *pifQ* mutants are sensitive to sugars and exhibit a light grown Wt like hypocotyl growth enhancement (Fig6.2 C,D). These data suggests that COP1/DET1 and PIFs may not be required for this response in the dark. The hypocotyl enhancement

in the mutants may simply be because short hypocotyls (comprising of small cells) elongate in response to sugar, whereas in Wt the elongation is saturated. Repeating the experiment in younger seedlings could answer this question, as Wt seedlings would still have smaller, less elongated cells at an earlier stage. Recent reports suggest the involvement of other signalling pathways - Target of Rapamycin (TOR) kinase, brassinosteroid and gibberellic acid hormone in mediating sugar induced hypocotyl growth in the dark (i.e. light grown seedlings transferred to dark for a period of 2-3 days). Zhang et al. (2016) demonstrated a mechanism involving Target of Rapamycin (TOR) kinase promoting sugar mediated hypocotyl elongation by activating the brassinosteroid pathway. TOR is required for sucrose stabilization of BZR1 (key brassinosteroid signalling component) in the dark. Inhibiting TOR activity result in growth arrest and reduced expression of BZR1 protein and BR responsive genes. Interestingly, in this study PIF4 was shown not to be required for sucrose induced hypocotyl elongation in the dark. In another independent study, Zhang et al. (2010) use a combination of GA_3 and PAC (GA_3 inhibitor) demonstrate GA hormone requirement for sucrose induced hypocotyl elongation in the dark. The signalling mechanism is however unknown. They also observe that the hypocotyl of *cop1* and the *pif* mutants (light grown seedlings transferred to dark) were sucrose responsive, similar to our data (Fig6.2).

Taken together, under diurnal light conditions, COP1 and DET1 function upstream to PIFs in promoting sugar induced hypocotyl elongation, whereas in the dark, other hormone signalling pathways (which may operate independent to COP/DET/PIFs) are predominantly required for this response.

Adult plant phenotype:

Contrary to the sugar insensitive seedling phenotype (Fig6.2A,B), *cop1* and *det1* mutants exhibit a sugar hyper-response later in development (Fig6.3, 6.4, 6.5). This switch in function is largely PIF independent as the *pifQ* adult mutants exhibit a Wt phenotype in response to sugar (Fig6.6). Unlike its mammalian counterpart, no physical interaction between COP1 and DET1 was observed in Arabidopsis seedlings (Wertz et al. 2004; Chen et al. 2010). However, it is an open question whether COP1 and DET1 function in concert conditionally during a later stage in development. Sugar is known to promote plant growth and biomass accumulation through at least two glucose activated signalling pathways: the HXK1 pathway and the TOR pathway (Sheen, 2014; Moore et al. 2003). Here I extrapolate from published evidence that COP1 and DET1 possibly function as potential negative regulators of both growth promoting pathways.

The mammalian TOR complex (mTORC) is directly turned over by mCOP1-mDET1 E3 ligase complex in an insulin dependent manner. Denten et al. (2007) show that under fasting conditions, mTORC2 promotes the gluconeogenic program (to generate glucose from noncarbohydrate substrates). On re-feeding, elevated blood glucose levels and insulin inhibit mTORC activity via mCOP1-mDET1 mediated proteolysis (Denten et al. 2007). Hence, could TOR turnover by COP1 and DET1 be conserved in plants? In Arabidopsis, TOR kinase is activated under increasing sugar levels to promote biomass. Moderate increase in TOR transcript abundance result in enhanced plant biomass, whereas an exaggerated increase in expression (35S:TOR lines) result in severe growth defects (Deprost et al. 2007; Ren et al. 2011) suggesting the importance of TOR dosage for growth.

Since *cop1* and *det1* mutants exhibit an exaggerated sugar driven biomass enhancement (Fig 6.3, 6.4, 6.5), could COP1 and DET1 function to keep a 'check' on plant growth by negatively regulating TOR kinase activity or TOR protein abundance conditionally? It is known that COP1 E3 ligase activity is sugar regulated (Debrieux et al. 2013). Interestingly, supporting this hypothesis, two recent papers provide indirect evidence for a negative effect COP1 on TOR kinase. Cai et al. (2017) and Pfeiffer et al. (2016) demonstrate elevated protein abundance (~6 fold increase) of phosphorylated S6K1 in the *cop1* mutant. S6K1 is a direct downstream target of TOR kinase and positively function in translation and cell cycle regulation (Xiong and Sheen, 2012). However, it is still unknown if elevated protein levels of TOR kinase is observed in the *cop1* mutant. Hence, both pieces of data strongly suggest the negative influence of COP1 on TOR activity.

Hexokinase 1 (HXK1), on the other hand, is required for growth and biomass production as the mutant exhibits a developmental deformity under high light conditions relative to Wt (Moore et al. 2003). Hexokinase1 (HXK1) in concert with partner proteins has been shown to function as a transcriptional repressor complex. Further, a ChIP-qPCR assay confirmed physical binding with maximal enrichment of HXK1 complex on the CAB2 promoter (Cho et al. 2006). Interestingly, this promotor region has been previously characterized as a DET1 regulatory element (Maxwell et al. 2003). This 40-bp DET1 dark-response element (DtRE) region comprising of a G box and CCA1 binding sites (and other elements) is required for both dark and root-specific repression of CAB2. DET1 has no DNA binding ability but capable of protein interactions (Lau et al. 2011), an intriguing question is whether DET1 associates with the HXK1 complex (or TOR) to either degrade or modify complex activity. Further,

Benvenuto et al (2004) provide evidence that DET1 binds to the nonacetylated amino-terminal tails of the core nucleosome histone H2B. They propose a possibility that DET1 may limit access to transcription factors/proteins at the promoters of photomorphogenesis promoting genes in the dark, but no follow on work has been published up to date to prove that hypothesis. Hence, it may be possible that the accessibility of HXK1/TOR/other sugar TFs targeted gene promotors is gated by DET1 in a sugar dependent manner.

However, if COP1 and DET1 negatively regulate TOR/HXK1 activity, it is unclear as to why the mutants exhibit a small stature under control conditions (i.e. absence of sugar). Carbon (C) is required for HXK1/TOR activation (Moore et al. 2330; Xiong et al. 2013), with both mutants accumulating Wt levels of glucose/sucrose, the mutant phenotype is unlikely due to internal C status mediated activation. It would be interesting to measure TOR/HXK1 protein abundance and activity in the *cop1/det1* mutants in the absence and presence of sugar. If COP1/DET1 operate independently of HXK1/TOR signalling in regulating sugar mediated biomass enhancement is a possibility.

Another interesting candidate is Trehalose-6-Phosphate (T6P), a sugar-signalling molecule. T6P levels is sugar dependent, an increase in sugar result in a concomitant raise in T6P levels (Lunn et al. 2006). T6P is biosynthesised from G6P and UDP-Glc by the enzyme Trehalose-6-P Synthase (TPS). Mutations in the TPS loci result in growth development phenotype: small rosette and reduced biomass (van Dijken et al. 2004; Gomez et al. 2010). Although the mechanistic role underlying this phenotype is unknown, no published evidence as to how COP1/DET1 could regulate T6P signalling is currently available.

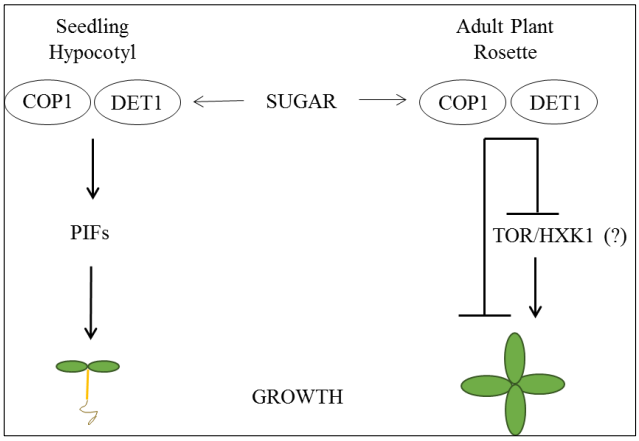

Fig6.9: Speculative working model. In seedlings, COP1 and DET1 stabilize PIF protein abundance, which positively promote sugar mediated hypocotyl elongation. In adult plants, COP1 and DET1 switch function as negative regulators of sugar-induced growth potentially inhibiting HXK1 and TOR activity or operating independently.

Hence, taken together, from preliminary data presented in this chapter, both Arabidopsis COP1 and DET1 appear to function as critical players in sugar regulation of seedling morphology and adult plant biomass, a role until know unknown. Function of COP1 and DET1 appear to switch between developmental stages in a PIF dependent and independent manner. However, the model depicted above describing the mechanism is pure speculation derived from current published understandings.

CHAPTER 6

Summary and general discussion

Here, I will summarise key findings of this thesis and discuss some intriguing questions raised by my data for future study. The unique property of the glucose receptor HXK1 is its dual capacity to function in metabolism and signalling. This study delineates the specific requirement for both roles and discovers other unknown facets of HXK1 function in seedlings.

Key findings of this thesis include:

1) HXK1 predominantly operates in the dark and low light fluences (nutrient limited conditions) during seedling development. Evident from the phenotypes, HXK1 is required for proper seedling skotomorphogenesis and photomorphogenesis (Fig4.1; 4.2).

2) A first-ever RNAseq on the HXK1 mutant *gin2* reveals that energy demanding pathways are down regulated and carbon starvation induced pathways are upregulated in the absence of *HXK1* (Fig4.4; 4.6).

3) Loss of HXK1 has a profound impact on transcripts encoding for the energy driven cytoskeleton and microtubule machinery (Fig4.4; 4.5).

4) Due to its inability to use glucose efficiently, the *gin2* mutants upregulate the carbon starvation induced Branched Chain Amino Acid (BCAA) degradation pathway as an alternate energy generation source (Fig4.6).

5) Supplying the HXK1 enzymatic end-product, G6P, restored the mutant seedling phenotype and the molecular C starvation response to Wt. This data strongly indicates

the requirement of HXK1 enzyme during nutrient limiting conditions in seedlings growth (Fig4.8).

6) HXK1 operates as a key repressor of the plastome via unknown mechanisms (Fig 4.10).

7) HXK1 operates independently of nuclear PIF signalling in the dark during skotomorphogenesis (Fig4.13)

8) HXK1 is not required for photosynthetic feedback inhibition in seedlings as widely considered. Elevated endogenous sugars did not have a similar effect as exogenous sugars on the transcript abundance of photosynthetic genes (Fig4.15).

9) Exogenous sugar application far-exceeds endogenous levels in seedlings thereby raising concerns on non-physiological carbon induced effects. (Fig4.15)

10) HXK1 exerts negative control on the blue light signalling pathway during seedling photomorphogenesis, an effect negated by PHYB (Chapter 5).

11) COP1 and DET1 function as negative regulators of sugar mediated growth and biomass productions in adult plants (Chapter 6).

Perspectives for potential future work arising from my data include:

Addressing HXK1 redundancy:

Based on the HXK1 mutant phenotypes, it is clear that HXK1 is required during seedling establishment during nutrient limiting conditions. However, the mutation does not appear to have a lethal effect on seedlings. The *gin2* mutants survived on water + agar plates even for 2 weeks under low light conditions (data not shown). As the Arabidopsis genome encodes two other HXKs with high glucose affinity and glucose phosphorylation ability (Kawai et al. 2005), it would be interesting

to generate the triple mutants and test for detrimental effects under various growth conditions.

Supporting G6P mediated rescue:

Through G6P application, I provide evidence that the enzymatic role of HXK1 is required during nutrient limited conditions in seedling establishment. G6P rescued both the mutant seedling phenotype and the starvation response to Wt (Chapter 3 – Fig. 8,9). To support this data, it would be worthy to measure glucose phosphorylation activity and G6P content in the *gin2* mutants. Also, supplementing other metabolic substrates downstream to HXK1 enzyme (Eg. Acetyl CoA, pyruvate, etc) may rescue the *gin2* phenotype and starvation response on energy restoration.

A potential co-operation between SnRK1-HXK1 signalling

As an alternate energy source, the *gin2* mutants employ the SnRK1 regulated BCAA catabolic pathway. SnRK1 recruits bZIP transcription factors to bind G box promotor elements of these genes for transcriptional induction during carbon (C) starvation. C application inhibits this response (Baena-Gonzalez et al. 2007; Pedrotti et al. 2018). Based on our data, although the C mediated suppression of these starvation genes is observed in the *gin2* mutants, an increased transcript abundance relative to Wt is still observed (Chapter 3 – Fig. 9). That asks the question: If HXK1 is required for that C mediated transcriptional repression of these genes by targeting the same G box element. It would be interesting to test if SnRK1 mediated bZIPs and HXK1 dimers co-operate as a dynamic activation-suppression transcriptional module in response to carbon starvation and restoration.

Phytochrome-PIF signalling in C starvation response

An interesting observation in chapter 3 is the significant downregulation of several SnRK1-bZIP activated starvation genes in the *pifQ* mutant in the dark. These novel observations implicate the role of Phytochrome-PIF signal transduction during C starvation conditions (such as dark). Although from ChIPseq data, these genes do not appear as direct PIF targets (Pfeiffer et al. 2014). It is worth testing if the PIFs synergistically work with the bZIPs for transcriptional co-activation of the starvation markers.

A detailed insight into HXK1 nuclear localization and assembly formation

Unlike in Arabidopsis, the nuclear-cytoplasmic shuttling of the yeast glucose sensor ScHXK2 is relatively well understood. The phosphorylation status of ScHXK2 is glucose regulated. Under high glucose conditions, the dephosphorylated ScHXK2 interact with α/β importin to facilitate nuclear import. Nuclear ScHXK2 directly interact with the core transcription repressor MIG1 for sugar mediated gene repression (Peláez et al. 2012, 2009; Fernández-García et al. 2012; Vega et al. 2016). It is currently unkown as to how exogenous sugar triggers Arabidopsis HXK1 cytoplasmic-nuclear shuttling or feeds into the complex assembly formation at the chromatin. It would also be interesting to monitor subcellular localization of pHXK1:HXK1-reporter in response to dark/white and monochromatic light and C treatments *in planta*. pHXK1:HXK1-LUC would enable us to monitor HXK1 rhythmicity in different photoperiods.

Signalling components regulating HXK1 transcription

HXK1 transcript abundance is enhanced by high light fluences, internal metabolic sugar (our data - not shown) and exogenous glucose application (Price et al.

2004). Multiple cis elements are present on the HXK1 promotor including a G box proximal to the transcriptional start site. Although, I hypothesised HY5 as a regulatory candidate (as HY5 protein abundance and activity is enhanced as light fluence increase (Osterland et al. 2000)), no altered *HXK1* transcript abundance was observed in the *hy5* mutant or overexpressor (data not shown). Other potential regulatory candidates include DELLA/BZR1/ABIs,etc. A mutant TF screen can be set up to test *HXK1 mRNA* expression to identify regulatory components integrating light and metabolic signalling.

Role of HXK1 in adult plant development

HXK1 is positively required for adult plant growth under high light conditions. The *gin2* mutants exhibit a severely reduced adult rosette phenotype and biomass (Moore et al. 2003). Spraying 10mM G6P at regular intervals did not rescue the impaired phenotype (data not shown) suggesting a metabolic HXK1 independent role. Because the *gin2* stature is reminiscent of hormone signalling mutants (*det2, ctr1*, etc) (Chory et al. 1991; Keiber et al. 1993), it would be interesting to test if hormone application (BR, auxin or ethylene) rescues the phenotype. This would give us insights into the potential role of HXK1-hormone cross talks during plant development.

Concluding remarks

My study highlights several novel facets and addresses published discrepancies pertaining to the role of HXK1 during seedling establishment. Our work provides both, a comprehensive analysis on Arabidopsis HXK1 and opens up several threads of research requiring detail investigations to discover the unknown.

CHAPTER 7 - References

Andronis C, Barak S, Knowles SM, Sugano S, Tobin EM (2008) The clock protein CCA1 and the bZIP transcription factor HY5 physically interact to regulate gene expression in Arabidopsis. Mol Plant. 1(1):58-67

Arsovski AA, Galstyan A, Guseman JM, Nemhauser JL (2012) Photomorphogenesis. The Arabidopsis Book 10:e0147

Baena-González E, Rolland F, Thevelein JM, Sheen J (2007) A central integrator of transcription networks in plant stress and energy signalling. Nature 448(7156):938-42

Bai MY, Shang JX, Oh E, Fan M, Bai Y, Zentella R, Sun TP, Wang ZY (2012) Brassinosteroid, gibberellin and phytochrome impinge on a common transcription module in Arabidopsis. Nat Cell Biol. 14(8):810-7

Balasubramanian R, Karve A, Kandasamy M, Meagher RB, Moore Bd (2007) A role for F-actin in hexokinase-mediated glucose signaling. Plant Physiol. 145(4):1423-34

Baud S, Dubreucq B, Miquel M, Rochat C, Lepiniec L (2008) Storage reserve accumulation in Arabidopsis: metabolic and developmental control of seed filling. Arabidopsis Book. 6:e0113

Bauer D, Viczián A, Kircher S, Nobis T, Nitschke R, Kunkel T, Panigrahi KC, Adám E, Fejes E, Schäfer E, Nagy F (2004) Constitutive photomorphogenesis 1 and multiple photoreceptors control degradation of phytochrome interacting factor 3, a transcription factor required for light signaling in Arabidopsis. Plant Cell 16(6):1433-45

Benvenuto G, Formiggini F, Laflamme P, Malakhov M, Bowler C (2002) The photomorphogenesis regulator DET1 binds the amino-terminal tail of histone H2B in a nucleosome context. Curr Biol. 12(17):1529-34

Bernardo-García S, de Lucas M, Martínez C, Espinosa-Ruiz A, Davière JM, Prat S (2014) BR-dependent phosphorylation modulates PIF4 transcriptional activity and shapes diurnal hypocotyl growth. Genes Dev. 28(15):1681-94

Binder S (2010) Branched-Chain Amino Acid Metabolism in Arabidopsis thaliana. Arabidopsis Book 8:e0137

Bruggeman Q, Prunier F, Mazubert C, de Bont L, Garmier M, Lugan R, Benhamed M, Bergounioux C, Raynaud C, Delarue M (2015) Involvement of Arabidopsis Hexokinase1 in Cell Death Mediated by Myo-Inositol Accumulation. Plant Cell. 27(6):1801-14

Cai W, Li X, Liu Y, Wang Y, Zhou Y, Xu T, Xiong Y (2017) COP1 integrates light signals to ROP2 for cell cycle activation. Plant Signal Behav. 12(9):e1363946

Cárdenas ML, Cornish-Bowden A, Ureta T (1998) Evolution and regulatory role of the hexokinases. Biochim Biophys Acta. 1401(3):242-64

Casal JJ (2012) Shade avoidance. Arabidopsis Book e0157

Chaiwanon J, Wang W, Zhu JY, Oh E, Wang ZY (2016) Information Integration and Communication in Plant Growth Regulation. Cell 164(6):1257-1268

Chen H, Huang X, Gusmaroli G, Terzaghi W, Lau OS, Yanagawa Y, Zhang Y, Li J, Lee JH, Zhu D, Deng XW (2010) Arabidopsis CULLIN4-damaged DNA binding protein 1 interacts with CONSTITUTIVELY PHOTOMORPHOGENIC1-SUPPRESSOR OF PHYA complexes to regulate photomorphogenesis and flowering time. Plant Cell. 22(1):108-23

Chen H, Shen Y, Tang X, Yu L, Wang J, Guo L, Zhang Y, Zhang H, Feng S, Strickland E, Zheng N, Deng XW (2006) Arabidopsis CULLIN4 Forms an E3 Ubiquitin Ligase with RBX1 and the CDD Complex in Mediating Light Control of Development. Plant Cell 18(8):1991-2004

Chen M (2008) Phytochrome nuclear body: an emerging model to study interphase nuclear dynamics and

Chen M, Schwab R, Chory J (2003) Characterization of the requirements for localization of phytochrome B to nuclear bodies. Proc Natl Acad Sci U S A. 100(24):14493-8

Chen X, Yao Q, Gao X, Jiang C, Harberd NP, Fu X (2016) Shoot-to-Root Mobile Transcription Factor HY5 Coordinates Plant Carbon and Nitrogen Acquisition. Curr Biol. 26(5):640-6

Cho JI, Ryoo N, Eom JS, Lee DW, Kim HB, Jeong SW, Lee YH, Kwon YK, Cho MH, Bhoo SH, Hahn TR, Park YI, Hwang I, Sheen J, Jeon JS (2009) Role of the rice hexokinases OsHXK5 and OsHXK6 as glucose sensors. Plant Physiol. 149(2):745-59

Cho YH, Yoo SD, Sheen J (2006) Regulatory functions of nuclear hexokinase1 complex in glucose signaling. Cell 127(3):579-89

Chory J, Peto C, Feinbaum R, Pratt L, Ausubel F (1989) Arabidopsis thaliana mutant that develops as a light-grown plant in the absence of light. Cell 58(5):991-9

Clouse SD (2011) Brassinosteroids. Arabidopsis Book. e0151
Cookson SJ, Yadav UP, Klie S, Morcuende R, Usadel B, Lunn JE, Stitt M (2016) Temporal kinetics of the transcriptional response to carbon depletion and sucrose readdition in Arabidopsis seedlings. Plant Cell Environ. 39(4):768-86

Davière JM, Achard P (2016) A Pivotal Role of DELLAs in Regulating Multiple Hormone Signals. Mol Plant. 9(1):10-20

de Jong F, Thodey K, Lejay LV, Bevan MW (2014) Glucose elevates NITRATE TRANSPORTER2.1 protein levels and nitrate transport activity independently of its HEXOKINASE1-mediated stimulation of NITRATE TRANSPORTER2.1 expression. Plant Physiol. 164(1):308-20

de Lucas M, Davière JM, Rodríguez-Falcón M, Pontin M, Iglesias-Pedraz JM, Lorrain S, Fankhauser C, Blázquez MA, Titarenko E, Prat S (2008) A molecular framework for light and gibberellin control of cell elongation. Nature 451(7177):480-4

de Lucas M, Prat S (2014) PIFs get BRright: PHYTOCHROME INTERACTING FACTORs as integrators of light and hormonal signals. New Phytol. 202(4):1126-41

Debrieux D, Trevisan M, Fankhauser C (2013) Conditional involvement of constitutive photomorphogenic1 in the degradation of phytochrome A. Plant Physiol. 161(4):2136-45
Deng XW, Caspar T, Quail PH (1991) cop1: a regulatory locus involved in light-controlled development and gene expression in Arabidopsis. Genes Dev. 5(7):1172-82

Dentin R, Liu Y, Koo SH, Hedrick S, Vargas T, Heredia J, Yates J 3rd, Montminy M (2007) Insulin modulates gluconeogenesis by inhibition of the coactivator TORC2. Nature 449(7160):366-9

Deprost D, Yao L, Sormani R, Moreau M, Leterreux G, Nicolaï M, Bedu M, Robaglia C, Meyer C (2007) The Arabidopsis TOR kinase links plant growth, yield, stress resistance and mRNA translation. EMBO Rep. 8(9):864-70
development and gene expression in arabidopsis, encodes a novel nuclear-localized protein. Cell 78(1):109-16

Dong J, Tang D, Gao Z, Yu R, Li K, He H, Terzaghi W, Deng XW, Chen H (2014) Arabidopsis DE-ETIOLATED1 represses photomorphogenesis by positively regulating phytochrome-interacting factors in the dark. Plant Cell 26(9):3630-4

Dornan D, Wertz I, Shimizu H, Arnott D, Frantz GD, Dowd P, O'Rourke K, Koeppen H, Dixit VM (2004) The ubiquitin ligase COP1 is a critical negative regulator of p53. Nature 429(6987):86-92

Dornbusch T, Michaud O, Xenarios I, Fankhauser C (2014) Differentially phased leaf growth and movements in Arabidopsis depend on coordinated circadian and light regulation. Plant Cell 26(10):3911-21

Duek PD, Elmer MV, van Oosten VR, Fankhauser C (2004) The degradation of HFR1, a putative bHLH class transcription factor involved in light signaling, is regulated by phosphorylation and requires COP1. Curr Biol. 14(24):2296-301

Duek PD, Fankhauser C (2003) HFR1, a putative bHLH transcription factor, mediates both phytochrome A and cryptochrome signalling. Plant J. 34(6):827-36

Eastmond PJ, Germain V, Lange PR, Bryce JH, Smith SM, Graham IA (2000) Postgerminative growth and lipid catabolism in oilseeds lacking the glyoxylate cycle. Proc Natl Acad Sci U S A. 97(10):5669-74

Eveland AL, Jackson DP (2012) Sugars, signalling, and plant development. J Exp Bot. 63(9):3367-77

Fairchild CD, Schumaker MA, Quail PH (2000) HFR1 encodes an atypical bHLH protein that acts in phytochrome A signal transduction. Genes Dev. 14(18):2377-91

Fankhauser C, Casal JJ (2004) Phenotypic characterization of a photomorphogenic mutant. Plant J. 39(5):747-60

Feng S, Martinez C, Gusmaroli G, Wang Y, Zhou J, Wang F, Chen L, Yu L, Iglesias-Pedraz JM, Kircher S, Schäfer E, Fu X, Fan LM, Deng XW (2008) Coordinated regulation of Arabidopsis thaliana development by light and gibberellins. Nature 451(7177):475-9

Fernández-García P, Peláez R, Herrero P, Moreno F (2012) Phosphorylation of yeast hexokinase 2 regulates its nucleocytoplasmic shuttling. J Biol Chem. 287(50):42151-64

Fox AR, Barberini ML, Ploschuk EL, Muschietti JP, Mazzella MA (2015) A proteome map of a quadruple photoreceptor mutant sustains its severe photosynthetic deficient phenotype. J Plant Physiol. 185:13-23

Fujiwara T, Nambara E, Yamagishi K, Goto DB, Naito S (2002) Storage proteins. Arabidopsis Book 1:e0020

Gangappa SN, Botto JF (2016) The Multifaceted Roles of HY5 in Plant Growth and Development. Mol Plant 9(10):1353-1365

Gómez LD, Gilday A, Feil R, Lunn JE, Graham IA (2010) AtTPS1-mediated trehalose 6-phosphate synthesis is essential for embryogenic and vegetative growth and responsiveness to ABA in germinating seeds and stomatal guard cells. Plant J. 64(1):1-13

Gommers CMM, Monte E (2018) Seedling Establishment: A Dimmer Switch-Regulated Process between Dark and Light Signaling. Plant Physiol. 176(2):1061-1074

Graf A, Schlereth A, Stitt M, Smith AM (2010) Circadian control of carbohydrate availability for growth in Arabidopsis plants at night. Proc Natl Acad Sci U S A. 107(20):9458-63

Hajdukiewicz PT, Allison LA, Maliga P (1997) The two RNA polymerases encoded by the nuclear and the plastid compartments transcribe distinct groups of genes in tobacco plastids. EMBO J. 16(13):4041-8

Hardtke CS, Gohda K, Osterlund MT, Oyama T, Okada K, Deng XW (2000) HY5 stability and activity in arabidopsis is regulated by phosphorylation in its COP1 binding domain. EMBO J. 19(18):4997-5006

Hashimoto T (2015) Microtubules in plants. Arabidopsis Book. 13:e0179

Hendriks JH, Kolbe A, Gibon Y, Stitt M, Geigenberger P (2003) ADP-glucose pyrophosphorylase is activated by posttranslational redox-modification in response to light and to sugars in leaves of Arabidopsis and other plant species. Plant Physiol. 133(2):838-49

He SB, Wang WX, Zhang JY, Xu F, Lian HL, Li L, Yang HQ (2015) The CNT1 Domain of Arabidopsis CRY1 Alone Is Sufficient to Mediate Blue Light Inhibition of Hypocotyl Elongation. Mol Plant. 8(5):822-5

Hildebrandt TM, Nunes Nesi A, Araújo WL, Braun HP (2015) Amino Acid Catabolism in Plants. Mol Plant 8(11):1563-79

Hoecker U (2017) The activities of the E3 ubiquitin ligase COP1/SPA, a key repressor in light signaling. Curr Opin Plant Biol. 37:63-69

Hu J, Aguirre M, Peto C, Alonso J, Ecker J, Chory J (2002) A role for peroxisomes in photomorphogenesis and development of Arabidopsis. Science 297(5580):405-9

Hu W, Su YS, Lagarias JC (2009) A light-independent allele of phytochrome B faithfully recapitulates photomorphogenic transcriptional networks. Mol Plant 2(1):166-82

Huang H, Nusinow DA (2016) Into the Evening: Complex Interactions in the Arabidopsis Circadian Clock. Trends Genet. 32(10):674-686

Huang JP, Tunc-Ozdemir M, Chang Y, Jones AM (2015) Cooperative control between AtRGS1 and AtHXK1 in a WD40-repeat protein pathway in Arabidopsis thaliana. Front Plant Sci. 13;6:851

Jang JC, León P, Zhou L, Sheen J (1997) Hexokinase as a sugar sensor in higher plants. Plant Cell. 9(1):5-19

Jarvis P, López-Juez E (2013) Biogenesis and homeostasis of chloroplasts and other plastids. Nat Rev Mol Cell Biol. 14(12):787-802

Johansson H, Jones HJ, Foreman J, Hemsted JR, Stewart K, Grima R, Halliday KJ (2014) Arabidopsis cell expansion is controlled by a photothermal switch. Nat Commun. 5:4848

Karve A, Rauh BL, Xia X, Kandasamy M, Meagher RB, Sheen J, Moore BD (2008) Expression and evolutionary features of the hexokinase gene family in Arabidopsis. Planta 228(3):411-25

Katari MS, Nowicki SD, Aceituno FF, Nero D, Kelfer J, Thompson LP, Cabello JM, Davidson RS, Goldberg AP, Shasha DE, Coruzzi GM, Gutiérrez RA (2010) VirtualPlant: a software platform to support systems biology research. Plant Physiol. 152(2):500-15

Kawai S, Mukai T, Mori S, Mikami B, Murata K (2005) Hypothesis: structures, evolution, and ancestor of glucose kinases in the hexokinase family. J Biosci Bioeng. 99(4):320-30

Kelly G, David-Schwartz R, Sade N, Moshelion M, Levi A, Alchanatis V, Granot D (2012) The pitfalls of transgenic selection and new roles of AtHXK1: a high level of AtHXK1 expression uncouples hexokinase1-dependent sugar signaling from exogenous sugar. Plant Physiol. 159(1):47-51

Kelly G, Sade N, Doron-Faigenboim A, Lerner S, Shatil-Cohen A, Yeselson Y, Egbaria A, Kottapalli J, Schaffer AA, Moshelion M, Granot D (2017) Sugar and hexokinase suppress expression of PIP aquaporins and reduce leaf hydraulics that preserves leaf water potential. Plant J. 91(2):325-339

Kieber JJ, Rothenberg M, Roman G, Feldmann KA, Ecker JR (1993) CTR1, a negative regulator of the ethylene response pathway in Arabidopsis, encodes a member of the raf family of protein kinases. Cell 72(3):427-41

Kircher S, Schopfer P (2012) Photosynthetic sucrose acts as cotyledon-derived long-distance signal to control root growth during early seedling development in Arabidopsis. Proc Natl Acad Sci U S A. 109(28):11217-21

Kohnen MV, Schmid-Siegert E, Trevisan M, Petrolati LA, Sénéchal F, Müller-Moulé P, Maloof J, Xenarios I, Fankhauser C (2016) Neighbor Detection Induces Organ-Specific Transcriptomes, Revealing Patterns Underlying Hypocotyl-Specific Growth. Plant Cell 28(12):2889-2904

Krahmer J, Ganpudi A, Abbas A, Romanowski A, Halliday KJ (2018) Phytochrome, Carbon Sensing, Metabolism, and Plant Growth Plasticity. Plant Physiol. 176(2):1039-1048

Kunz S, Gardeström P, Pesquet E, Kleczkowski LA (2015) Hexokinase 1 is required for glucose-induced repression of bZIP63, At5g22920, and BT2 in Arabidopsis. Front Plant Sci. 6:525

Kutschera U, Wang ZY (2012) Brassinosteroid action in flowering plants: a Darwinian perspective. J Exp Bot. 63(10):3511-22

Lau OS, Deng XW (2012) The photomorphogenic repressors COP1 and DET1: 20 years later. Trends Plant Sci. 17(10):584-93

Lau OS, Huang X, Charron JB, Lee JH, Li G, Deng XW (2011) Interaction of Arabidopsis DET1 with CCA1 and LHY in mediating transcriptional repression in the plant circadian clock. Mol Cell. 43(5):703-12

Lee J, He K, Stolc V, Lee H, Figueroa P, Gao Y, Tongprasit W, Zhao H, Lee I, Deng XW (2007) Analysis of transcription factor HY5 genomic binding sites revealed its hierarchical role in light regulation of development. Plant Cell 19(3):731-49

Leivar P and Monte E (2014) PIFs: systems integrators in plant development. Plant Cell 26(1):56-78

Leivar P, Monte E, Oka Y, Liu T, Carle C, Castillon A, Huq E, Quail PH (2008) Multiple phytochrome-interacting bHLH transcription factors repress premature seedling photomorphogenesis in darkness. Curr Biol. 18(23):1815-23

Leivar P, Quail PH (2011) PIFs: pivotal components in a cellular signaling hub. Trends Plant Sci. 16(1):19-28

Leivar P, Tepperman JM, Monte E, Calderon RH, Liu TL, Quail PH (2009) Definition of early transcriptional circuitry involved in light-induced reversal of PIF-imposed repression of photomorphogenesis in young Arabidopsis seedlings. Plant Cell. 21(11):3535-53

Li J, Li G, Wang H, Deng XW (2011) Phytochrome Signaling Mechanisms. The Arabidopsis Book 9:e0148

Li K, Yu R, Fan LM, Wei N, Chen H, Deng XW (2016) DELLA-mediated PIF degradation contributes to coordination of light and gibberellin signalling in Arabidopsis. Nat. Communications 7:11868

Li L, Ljung K, Breton G, Schmitz RJ, Pruneda-Paz J, Cowing-Zitron C, Cole BJ, Ivans LJ, Pedmale UV, Jung HS, Ecker JR, Kay SA, Chory J (2012) Linking photoreceptor excitation to changes in plant architecture. Genes Dev. 26(8):785-90

Li L, Sheen J (2016) Dynamic and diverse sugar signaling. Curr Opin Plant Biol. 33:116-125

Li X, Cai W, Liu Y, Li H, Fu L, Liu Z, Xu L, Liu H, Xu T, Xiong Y (2017) Differential TOR activation and cell proliferation in Arabidopsis root and shoot apexes. Proc Natl Acad Sci. 114(10):2765-2770

Li Y, Van den Ende W, Rolland F (2014) Sucrose induction of anthocyanin biosynthesis is mediated by DELLA. Mol Plant. 7(3):570-2

Li Y, Xu S, Wang Z, He L, Xu K, Wang G (2018) Glucose triggers stomatal closure mediated by basal signaling through HXK1 and PYR/RCAR receptors in Arabidopsis. J Exp Bot. 69(7):1471-1484

Lian HL, He SB, Zhang YC, Zhu DM, Zhang JY, Jia KP, Sun SX, Li L, Yang HQ (2011) Blue-light-dependent interaction of cryptochrome 1 with SPA1 defines a dynamic signaling mechanism. Genes Dev. 25(10):1023-8

Lilley JL, Gee CW, Sairanen I, Ljung K, Nemhauser JL (2012) An endogenous carbon-sensing pathway triggers increased auxin flux and hypocotyl elongation. Plant Physiol. 160(4):2261-70

Ling JJ, Li J, Zhu D, Deng XW (2017) Noncanonical role of Arabidopsis COP1/SPA complex in repressing BIN2-mediated PIF3 phosphorylation and degradation in darkness. Proc Natl Acad Sci U S A. 114(13):3539-3544

Liu B, Zuo Z, Liu H, Liu X, Lin C (2011) Arabidopsis cryptochrome 1 interacts with SPA1 to suppress COP1 activity in response to blue light. Genes Dev. 25(10):1029-34

Liu Q, Wang Q, Deng W, Wang X, Piao M, Cai D, Li Y, Barshop WD, Yu X, Zhou T, Liu B, Oka Y, Wohlschlegel J, Zuo Z, Lin C (2017) Molecular basis for blue light-dependent phosphorylation of Arabidopsis cryptochrome 2. Nat Commun. 11;8:15234

Lunn JE, Feil R, Hendriks JH, Gibon Y, Morcuende R, Osuna D, Scheible WR, Carillo P, Hajirezaei MR, Stitt M (2006) Sugar-induced increases in trehalose 6-phosphate are correlated with redox activation of ADPglucose pyrophosphorylase and higher rates of starch synthesis in Arabidopsis thaliana. Biochem J. 397(1):139-48

Ma D, Li X, Guo Y, Chu J, Fang S, Yan C, Noel JP, Liu H (2016) Cryptochrome 1 interacts with PIF4 to regulate high temperature-mediated hypocotyl elongation in response to blue light. Proc Natl Acad Sci U S A. 113(1):224-9

Ma L, Li J, Qu L, Hager J, Chen Z, Zhao H, Deng XW (2001) Light control of Arabidopsis development entails coordinated regulation of genome expression and cellular pathways. Plant Cell 13(12):2589-607

Marine JC (2012) Spotlight on the role of COP1 in tumorigenesis. at Rev Cancer. 12(7):455-64

Maxwell BB, Andersson CR, Poole DS, Kay SA, Chory J (2003) HY5, Circadian Clock-Associated 1, and a cis-element, DET1 dark response element, mediate DET1 regulation of chlorophyll a/b-binding protein 2 expression. Plant Physiol. 133(4):1565-77

Mockler TC, Michael TP, Priest HD, Shen R, Sullivan CM, Givan SA, McEntee C, Kay SA, Chory J (2007) The DIURNAL project: DIURNAL and circadian expression profiling, model-based pattern matching, and promoter analysis. Cold Spring Harb Symp Quant Biol. 72:353-63

Moore B, Zhou L, Rolland F, Hall Q, Cheng WH, Liu YX, Hwang I, Jones T, Sheen J (2003) Role of the Arabidopsis glucose sensor HXK1 in nutrient, light, and hormonal signaling. Science 300(5617):332-6

Neff MM, Chory J (1998) Genetic interactions between phytochrome A, phytochrome B, and cryptochrome 1 during Arabidopsis development. Plant Physiol. 118(1):27-35

Nemhauser JL (2008) Dawning of a new era: photomorphogenesis as an integrated molecular network. Curr Opin Plant Biol. 11(1):4-8

Ni W, Xu SL, González-Grandío E, Chalkley RJ, Huhmer AFR, Burlingame AL, Wang ZY, Quail PH (2017) PPKs mediate direct signal transfer from phytochrome photoreceptors to transcription factor PIF3. Nat Commun. 8:15236.

Ni W, Xu SL, Tepperman JM, Stanley DJ, Maltby DA, Gross JD, Burlingame AL, Wang ZY, Quail PH (2014) A mutually assured destruction mechanism attenuates light signaling in Arabidopsis. Science 344(6188):1160-1164

Nozue K, Covington MF, Duek PD, Lorrain S, Fankhauser C, Harmer SL, Maloof JN (2007) Rhythmic growth explained by coincidence between internal and external cues. Nature 448(7151):358-61

Nusinow DA, Helfer A, Hamilton EE, King JJ, Imaizumi T, Schultz TF, Farré EM, Kay SA (2011) The ELF4-ELF3-LUX complex links the circadian clock to diurnal control of hypocotyl growth. Nature 475(7356):398-402

Oh E, Zhu JY, Bai MY, Arenhart RA, Sun Y, Wang ZY (2014) Cell elongation is regulated through a central circuit of interacting transcription factors in the Arabidopsis hypocotyl. Elife. eLife.03031

Oh E, Zhu JY, Wang ZY (2012) Interaction between BZR1 and PIF4 integrates brassinosteroid and environmental responses. Nat Cell Biol. 14(8):802-9

Osterlund MT, Hardtke CS, Wei N, Deng XW (2000) Targeted destabilization of HY5 during light-regulated development of Arabidopsis. Nature 405(6785):462-6

Park E, Park J, Kim J, Nagatani A, Lagarias JC, Choi G (2012) Phytochrome B inhibits binding of phytochrome-interacting factors to their target promoters. Plant J. 72(4):537-46

Pedmale UV, Huang SC, Zander M, Cole BJ, Hetzel J, Ljung K, Reis PAB, Sridevi P, Nito K, Nery JR, Ecker JR, Chory J (2016) Cryptochromes Interact Directly with PIFs to Control Plant Growth in Limiting Blue Light. Cell 164(1-2):233-245

Pedrotti L, Weiste C, Nägele T, Wolf E, Lorenzin F, Dietrich K, Mair A, Weckwerth W, Teige M, Baena-González E, Dröge-Laser W (2018) Snf1-RELATED KINASE1-Controlled C/S1-

bZIP Signaling Activates Alternative Mitochondrial Metabolic Pathways to Ensure Plant Survival in Extended Darkness. Plant Cell. 30(2):495-509

Penfield S, Rylott EL, Gilday AD, Graham S, Larson TR, Graham IA (2004) Reserve mobilization in the Arabidopsis endosperm fuels hypocotyl elongation in the dark, is independent of abscisic acid, and requires PHOSPHOENOLPYRUVATE CARBOXYKINASE1. Plant Cell 2705-18

Peng C, Uygun S, Shiu SH, Last RL (2015) The Impact of the Branched-Chain Ketoacid Dehydrogenase Complex on Amino Acid Homeostasis in Arabidopsis. Plant Physiol. 169(3):1807-20

Pepper A, Delaney T, Washburn T, Poole D, Chory J (1994) DET1, a negative regulator of light-mediated

Peláez R, Fernández-García P, Herrero P, Moreno F (2012) Nuclear import of the yeast hexokinase 2 protein requires α/β-importin-dependent pathway. J Biol Chem. 287(5):3518-29

Peláez R, Herrero P, Moreno F (2009) Nuclear export of the yeast hexokinase 2 protein requires the Xpo1 (Crm1)-dependent pathway. J Biol Chem. 284(31):20548-55

Pfeiffer A, Janocha D, Dong Y, Medzihradszky A, Schöne S, Daum G, Suzaki T, Forner J, Langenecker T, Rempel E, Schmid M, Wirtz M, Hell R, Lohmann JU (2016) Integration of light and metabolic signals for stem cell activation at the shoot apical meristem. Elife e17023

Pfeiffer A, Shi H, Tepperman JM, Zhang Y, Quail PH (2014) Combinatorial complexity in a transcriptionally centered signaling hub in Arabidopsis. Mol Plant. 7(11):1598-1618

Price J, Laxmi A, St Martin SK, Jang JC (2004) Global transcription profiling reveals multiple sugar signal transduction mechanisms in Arabidopsis. Plant Cell 16(8):2128-50

Procko C, Crenshaw CM, Ljung K, Noel JP, Chory J (2014) Cotyledon-Generated Auxin Is Required for Shade-Induced Hypocotyl Growth in Brassica rapa. Plant Physiol. 165(3):1285-1301

Reed JW, Elumalai RP, Chory J (1998) Suppressors of an Arabidopsis thaliana phyB mutation identify genes that control light signaling and hypocotyl elongation. Genetics. 148(3):1295-310

Ren M, Qiu S, Venglat P, Xiang D, Feng L, Selvaraj G, Datla R (2011) Target of rapamycin regulates development and ribosomal RNA expression through kinase domain in Arabidopsis. Plant Physiol. 155(3):1367-82

Roig-Villanova I, Martínez-García JF (2016) Plant Responses to Vegetation Proximity: A Whole Life Avoiding Shade. Front Plant Sci. 7:236

Ruan YL (2014) Sucrose metabolism: gateway to diverse carbon use and sugar signaling. Annu Rev Plant Biol. 65:33-67

Sairanen I, Novák O, Pěnčík A, Ikeda Y, Jones B, Sandberg G, Ljung K (2012) Soluble carbohydrates regulate auxin biosynthesis via PIF proteins in Arabidopsis. Plant Cell 24(12):4907-16

Sasidharan R, Keuskamp DH, Kooke R, Voesenek LA, Pierik R (2014) Interactions between auxin, microtubules and XTHs mediate green shade- induced petiole elongation in arabidopsis. PLoS One 9(3):e90587

Schroeder DF, Gahrtz M, Maxwell BB, Cook RK, Kan JM, Alonso JM, Ecker JR, Chory J (2002) De-etiolated 1 and damaged DNA binding protein 1 interact to regulate Arabidopsis photomorphogenesis. Curr Biol. 12(17):1462-72

Seluzicki A, Burko Y, Chory J (2017) Dancing in the dark: darkness as a signal in plants. Plant Cell Environ. 40(11):2487-2501

Sheen J (2014) Master Regulators in Plant Glucose Signaling Networks. J. Plant Biol. 57(2):67-79

Sheerin DJ, Menon C, zur Oven-Krockhaus S, Enderle B, Zhu L, Johnen P, Schleifenbaum F, Stierhof YD, Huq E, Hiltbrunner A (2015) Light-activated phytochrome A and B interact with members of the SPA family to promote photomorphogenesis in Arabidopsis by reorganizing the COP1/SPA complex. Plant Cell 27(1):189-20

Shi H, Liu R, Xue C, Shen X, Wei N, Deng XW, Zhong S (2016b) Seedlings Transduce the Depth and Mechanical Pressure of Covering Soil Using COP1 and Ethylene to Regulate EBF1/EBF2 for Soil Emergence. Curr Biol. 26(2):139-49

Shi H, Shen X, Liu R, Xue C, Wei N, Deng XW, Zhong S (2016a) The Red Light Receptor Phytochrome B Directly Enhances Substrate-E3 Ligase Interactions to Attenuate Ethylene Responses. Dev Cell 39(5):597-610

Shor E, Paik I, Kangisser S, Green R, Huq E PHYTOCHROME INTERACTING FACTORS mediate metabolic control of the circadian system in Arabidopsis. New Phytol (1):217-228 signaling. Curr Opin Plant Biol. 11(5):503-8

Simon NML, Kusakina J, Fernández-López Á, Chembath A, Belbin FE, Dodd AN (2018) The Energy-Signaling Hub SnRK1 Is Important for Sucrose-Induced Hypocotyl Elongation. Plant Physiol 176(2):1299-1310

Singh M, Gupta A, Singh D, Khurana JP, Laxmi A (2017) Arabidopsis RSS1 Mediates Cross-Talk Between Glucose and Light Signaling During Hypocotyl Elongation Growth. Sci Rep. 7(1):16101

Soy J, Leivar P, González-Schain N, Sentandreu M, Prat S, Quail PH, Monte E (2012) Phytochrome-imposed oscillations in PIF3 protein abundance regulate hypocotyl growth under diurnal light/dark conditions in Arabidopsis. Plant J. 71(3):390-401

Soy J, Leivar P, Monte E (2014) PIF1 promotes phytochrome-regulated growth under photoperiodic conditions in Arabidopsis together with PIF3, PIF4, and PIF5. J Exp Bot. 65(11):2925-36

Stewart JL, Maloof JN, Nemhauser JL (2011) PIF genes mediate the effect of sucrose on seedling growth dynamics. PLoS One 6(5):e19894

Su J, Liu B, Liao J, Yang Z, Lin C, Oka Y (2017) Coordination of Cryptochrome and Phytochrome Signals in the Regulation of Plant Light Responses. *Agronomy 7*(1)25

Tao Y, Ferrer JL, Ljung K, Pojer F, Hong F, Long JA, Li L, Moreno JE, Bowman ME, Ivans LJ, Cheng Y, Zhao Y, Ballaré CL, Sandberg G, Noel JP, Chory J (2008) Rapid synthesis of auxin via a new tryptophan-dependent pathway is required for shade avoidance in plants. Cell 133(1):164-76

Toledo-Ortiz G, Johansson H, Lee KP, Bou-Torrent J, Stewart K, Steel G, Rodríguez-Concepción M, Halliday KJ (2014) The HY5-PIF regulatory module coordinates light and temperature control of photosynthetic gene transcription. PLoS Genet. e1004416

van Dijken AJ, Schluepmann H, Smeekens SC (2004) Arabidopsis trehalose-6-phosphate synthase 1 is essential for normal vegetative growth and transition to flowering. Plant Physiol. 135(2):969-77

Vega M, Riera A, Fernández-Cid A, Herrero P, Moreno F (2016) Hexokinase 2 Is an Intracellular Glucose Sensor of Yeast Cells That Maintains the Structure and Activity of Mig1 Protein Repressor Complex. J Biol Chem. 291(14):7267-85

Viczián A, Klose C, Ádám É, Nagy F (2016) New insights of red light-induced development. Plant Cell Environ. 10.1111

Vitari AC, Leong KG, Newton K, Yee C, O'Rourke K, Liu J, Phu L, Vij R, Ferrando R, Couto SS, Mohan S, Pandita A, Hongo JA, Arnott D, Wertz IE, Gao WQ, French DM, Dixit VM (2011) COP1 is a tumour suppressor that causes degradation of ETS transcription factors. Nature 474(7351)

Wang Q, Zuo Z, Wang X, Gu L, Yoshizumi T, Yang Z, Yang L, Liu Q, Liu W, Han YJ, Kim JI, Liu B,

Wohlschlegel JA, Matsui M, Oka Y, Lin C (2016) Photoactivation and inactivation of Arabidopsis cryptochrome 2. Science 354(6310):343-347

Wertz IE, O'Rourke KM, Zhang Z, Dornan D, Arnott D, Deshaies RJ, Dixit VM (2004) Human De-etiolated-1 regulates c-Jun by assembling a CUL4A ubiquitin ligase. Science 303(5662):1371-4

Xin R, Zhu L, Salomé PA, Mancini E, Marshall CM, Harmon FG, Yanovsky MJ, Weigel D, Huq E (2017) SPF45-related splicing factor for phytochrome signaling promotes photomorphogenesis by regulating pre-mRNA splicing in Arabidopsis. Proc Natl Acad Sci U S A. 114(33) 7018-7027

Xiong Y, McCormack M, Li L, Hall Q, Xiang C, Sheen J (2013) Glucose-TOR signalling reprograms the transcriptome and activates meristems. Nature 496(7444):181-6

Xiong Y, Sheen J (2013) Moving beyond translation: glucose-TOR signaling in the transcriptional control of cell cycle. Cell Cycle 12(13):1989-90

Xu F, He S, Zhang J, Mao Z, Wang W, Li T, Hua J, Du S, Xu P, Li L, Lian H, Yang HQ (2018) Photoactivated CRY1 and phyB Interact Directly with AUX/IAA Proteins to Inhibit Auxin Signaling in Arabidopsis. Mol Plant. 11(4):523-541

Yanagasawa S, Yoo SD, Sheen J (2003) Differential regulation of EIN3 stability by glucose and ethylene signalling in plants. Nature 425(6957):521-5

Yanagawa Y, Sullivan JA, Komatsu S, Gusmaroli G, Suzuki G, Yin J, Ishibashi T, Saijo Y, Rubio V, Kimura S, Wang J, Deng XW (2004) Arabidopsis COP10 forms a complex with DDB1 and DET1 in vivo and enhances the activity of ubiquitin conjugating enzymes. Genes Dev. 18(17):2172-81

Yang D, Seaton DD, Krahmer J, Halliday KJ (2016) Photoreceptor effects on plant biomass, resource allocation, and metabolic state. Proc Natl Acad Sci. 113(27):7667-72

Yang HQ, Wu YJ, Tang RH, Liu D, Liu Y, Cashmore AR (2000) The C termini of Arabidopsis cryptochromes mediate a constitutive light response. Cell 103(5):815-27

Yang L, Xu M, Koo Y, He J, Poethig RS (2013) Sugar promotes vegetative phase change in Arabidopsis thaliana by repressing the expression of MIR156A and MIR156C. Elife 2:e00260

Yoshida S, Mandel T, Kuhlemeier C (2011) Stem cell activation by light guides plant organogenesis. Genes Dev 25: 1439–1450

Zhang H, He H, Wang X, Wang X, Yang X, Li L, Deng XW (2011) Genome-wide mapping of the HY5-mediated gene networks in Arabidopsis that involve both transcriptional and post-transcriptional regulation. Plant J. 65(3):346-58

Zhang Y, Liu Z, Wang L, Zheng S, Xie J, Bi Y (2010) Sucrose-induced hypocotyl elongation of Arabidopsis seedlings in darkness depends on the presence of gibberellins. J Plant Physiol. 167(14):1130-6

Zhang Y, Mayba O, Pfeiffer A, Shi H, Tepperman JM, Speed TP, Quail PH (2013) A quartet of PIF bHLH factors provides a transcriptionally centered signaling hub that regulates seedling morphogenesis through differential expression-patterning of shared target genes in Arabidopsis. PLoS Genet. 9(1):e1003244

Zhang Z, Zhu JY, Roh J, Marchive C, Kim SK, Meyer C, Sun Y, Wang W, Wang ZY (2016) TOR Signaling Promotes Accumulation of BZR1 to Balance Growth with Carbon Availability in Arabidopsis. Curr Biol. 26(14):1854-60

APPENDIX

Experimental contributions towards Seaton et al. (2018), *PNAS (in press)*

Contributions

- Fig. 2D and Supp Fig. S6: ChIP-qPCR for PIF4 & PIF5 enrichment on PhyA promotor
  Dr. Gabriela Toledo-Ortiz and I performed this experiment

- Supp Fig. S7: Hypocotyl elongation in response to photoperiod and far-red light
  I performed this experiment

- Supp Fig. S9: Clock gene expression in response to photoperiod and loss of PhyA
  I performed this experiment

- Supp Fig. S10. PHYA signalling in simulated natural dawn conditions.
  Dr. Gabriela Toledo-Ortiz and I performed this experiment

m^{-2} .s^{-1}

Dawn and photoperiod sensing by phytochrome A

Daniel D. Seaton[a,1], Gabriela Toledo-Ortiz[b], Ashwin Ganpudi[a], Akane Kubota[c], Takato Imaizumi[c], and Karen J. Halliday[a,2]

[a]SynthSys, School of Biological Sciences, University of Edinburgh, EH9 3BF Edinburgh, United Kingdom; [b]Lancaster Environment Centre, Lancaster University, LA1 4YQ Bailrigg, United Kingdom; and [c]Department of Biology, University of Washington, Seattle, WA 98195-1800

Edited by Winslow R. Briggs, Carnegie Institution for Science, Stanford, CA, and approved August 28, 2018 (received for review April 8, 2018)

In plants, light receptors play a pivotal role in photoperiod sensing, enabling them to track seasonal progression. Photoperiod sensing arises from an interaction between the plant's endogenous circadian oscillator and external light cues. Here, we characterize the role of phytochrome A (phyA) in photoperiod sensing. Our metaanalysis of functional genomic datasets identified phyA as a principal regulator of morning-activated genes, specifically in short photoperiods. We demonstrate that *PHYA* expression is under the direct control of the PHYTOCHROME INTERACTING FACTOR transcription factors, PIF4 and PIF5. As a result, phyA protein accumulates during the night, especially in short photoperiods. At dawn, phyA activation by light results in a burst of gene expression, with consequences for physiological processes such as anthocyanin accumulation. The combination of complex regulation of *PHYA* transcript and the unique molecular properties of phyA protein make this pathway a sensitive detector of both dawn and photoperiod.

phytochrome | photoperiodism | systems biology | circadian rhythms | *Arabidopsis*

As photosynthetic organisms, plants are highly tuned to the external light environment. This exogenous control is exerted by photoreceptors, such as the five-member phytochrome family phyA–E that, in turn, regulate the activity of key transcription factors. An important feature of phytochrome signaling is that it can be strongly influenced by the plants' internal circadian clock, which operates as a master regulator of rhythmic gene expression (1). The interplay between phytochrome signaling and the clock aligns daily gene expression profiles to shifts in daylength. These adjustments and associated posttranscriptional events form the basis of photoperiodic sensing, coordinating molecular, metabolic, and developmental responses to the changing seasons.

Earlier work has shown that light and the clock interact through so-called "external coincidence" mechanisms to deliver photoperiodic control of responses such as flowering time and seedling hypocotyl growth (2, 3). Previously we used a modeling approach to assess the functional characteristics of these two external coincidence mechanisms (4). An important component of our study was the analysis of published genomics data that allowed us to identify network properties and to test the applicability of our model to the broader transcriptome. This work highlighted the huge potential of data mining approaches to uncover molecular mechanisms of external coincidence signaling.

A well-characterized external coincidence mechanism involves the PHYTOCHROME INTERACTING FACTOR transcription factors PIF4 and PIF5, that regulate rhythmic seedling hypocotyl growth in short photoperiods. Sequential action of the clock Evening Complex (EC) and phyB defines the photoperiodic window during which PIF4/5 can accumulate. Light-activated phyB negatively regulates PIF4/5 by triggering their proteolysis and by sequestering PIFs from their target promoters (5, 6). The EC, comprising EARLY FLOWERING 3 (ELF3), EARLY FLOWERING 4 (ELF4), and LUX ARRHYTHMO (LUX), is a transcriptional repressor that has a postdusk peak of activity. Nights longer than 10–12 h exceed the period of EC action, allowing *PIF4/5* to accumulate and regulate gene expression specifically in long nights. The period of PIF activity is abruptly terminated at dawn, following activation of phyB by light. This external coincidence module therefore delivers a diurnal control of growth that is only active in short-day photocycles and becomes more robust as the night lengthens.

The diurnal PIF growth module is a clear example of how phyB contributes to photoperiod sensing. The phytochrome family shares a set of core characteristics that enable tracking of changes in light quality and quantity, such as those that occur at dawn. The phytochrome chromoproteins exist in two isomeric forms, inactive Pr and active Pfr, that absorb in the red (R) (peak 660 nm) and far-red (FR) light (peak 730 nm), respectively. R light drives photoconversion from Pr to Pfr, while FR light reverses this process. This R/FR reversibility allows phytochromes to operate as biological light switches that respond to light spectra and intensity. Once formed, the active Pfr translocates from the cytosol to the nucleus to perform its signaling functions.

The photochemistry of phytochrome signaling is conserved across the phytochrome family. However, phyA exhibits unique signaling features, including nuclear translocation kinetics and protein stability. As a result, the responses of phyA to light are distinctive. For example, phyB–E responses are classically R/FR reversible, while phyA responses are not. Instead, phyA is tuned to detect continuous FR-rich light, indicative of close vegetation, in the so-called far-red high-irradiance responses (FR-HIRs) (7). phyA also initiates very low fluence responses that are important for activating germination and deetiolation in low-light scenarios (e.g., when shielded by vegetation). Another distinguishing feature is that unlike phyB–E, that are light stable, phyA is unstable in the presence of light. These characteristics mean that in photoperiodic

Significance

The changing seasons subject plants to a variety of challenging environments. To deal with this, many plants have mechanisms for inferring the season by measuring the duration of daylight in a day. A number of well-known seasonal responses such as flowering are responsive to daylength or photoperiod. Here, we describe how the photoreceptor protein phytochrome A senses short photoperiods. This arises from its accumulation during long nights, as happens during winter, and subsequent activation by light at dawn. As a result of this response, the abundance of red anthocyanin pigments is increased in short photoperiods. Thus, we describe a mechanism underlying a seasonal phenotype in an important model plant species.

Author contributions: D.D.S., G.T.-O., T.I., and K.J.H. designed research; D.D.S., G.T.-O., A.G., and A.K. performed research; D.D.S., G.T.-O., A.G., and K.J.H. analyzed data; and D.D.S., G.T.-O., and K.J.H. wrote the paper.

The authors declare no conflict of interest.

This article is a PNAS Direct Submission.

[1]Present address: European Molecular Biology Laboratory, European Bioinformatics Institute, Wellcome Genome Campus, CB10 1SD Hinxton, United Kingdom.

[2]To whom correspondence should be addressed. Email: karen.halliday@ed.ac.uk.

This article contains supporting information online at www.pnas.org/lookup/suppl/doi:10.1073/pnas.1803398115/-/DCSupplemental.

conditions, phyA protein levels are robustly diurnal (8), although it is not clear what drives phyA reaccumulation during the night.

Considerable progress has been made in understanding the molecular mechanisms of phyA signaling (7). Upon exposure to R or FR light, phyA is activated and moves from the cytosol to the nucleus. Nuclear import requires the nuclear localization sequence-containing helper proteins FAR-RED ELONGATED HYPOCOTYL 1 (FHY1) and FHY1-like (FHL) (9). In the nucleus, phyA Pfr negatively regulates several proteins through direct interaction, including the PHYTOCHROME INTERACTING FACTOR (PIF) transcription regulators, the E3 ligase component CONSTITUTIVE PHOTOMORPHOGENIC1 (COP1), and SUPPRESSOR OF PHYA-105 1–4 (SPA1–4) (10, 11). The COP1/SPA complex targets several transcription regulators, including LONG HYPOCOTYL 5 (HY5), LONG HYPOCOTYL IN FAR-RED 1 (HFR1), and LONG AFTER FAR-RED LIGHT 1 (LAF1), for degradation (12–14). Through the regulation of this suite of transcription factors, phyA can modulate the expression of thousands of genes (15–17).

The activity of the phyA signaling pathway is regulated at multiple levels. The timing of *PHYA* expression is controlled by the circadian clock (18) and by light, although the underlying molecular mechanisms are unknown. phyA protein is both activated and destabilized by light (19). Thus, understanding phyA signaling requires understanding the interplay between these layers of regulation. This can be achieved by analyzing dynamics of phyA regulation and action through different photoperiods where the competing regulatory signals converge at different times. Previously we have constructed mathematical models to understand photoperiodic control of flowering and PIF-mediated growth (4). This approach has been particularly useful for identifying nonintuitive pathway behaviors that arise from complex regulatory dynamics.

In this paper, we combine analysis of genome-scale datasets, mathematical modeling, and experimentation to unravel the molecular mechanisms of phyA regulation in light/dark cycles. We show that *PHYA* is directly targeted by the transcription factors PIF4 and PIF5. These transcription factors are under the dual control of light [via phytochromes (5)] and the circadian clock [via the evening complex (20)]. This results in dynamic regulation of *PHYA* transcript abundance, leading to high accumulation at night in short photoperiods. At dawn, phyA then induces the expression of hundreds of genes, including genes involved in anthocyanin biosynthesis. This firmly establishes a role for phyA as a sensor of dawn and short photoperiods.

Results

Data Mining Identifies phyA as a Potential Short-Photoperiod Sensor. Our previous work applied data mining methods to derive molecular understanding of light signaling (4). In this study we used data mining to identify gene regulatory mechanisms that respond to changing photoperiod. This approach was made possible by the high-quality transcriptomic and ChIP data available for diurnal and light-controlled gene expression (*SI Appendix*, Table S1 and Dataset S1). To do this, we developed a computational workflow combining coexpression clustering and gene set enrichment (Fig. 1*A*). First, genes were clustered on the basis of expression in a variety of conditions, focusing on different light conditions and mutants of circadian and light signaling pathways (see *SI Appendix*, Table S1 for a description of datasets). Importantly, this included gene expression in long days (LDs) [16 h light: 8 h dark (8L:16D)] and short days (SDs) (16L:8D). This procedure identified 101 coexpression clusters (Dataset S2).

To identify regulatory mechanisms, we assessed a broad range of potential regulatory pathways, consolidating 527 gene lists from the literature. This consisted of 140 gene lists from 47 papers, covering a broad range of regulatory pathways (see Dataset S1 for descriptions), combined with a further 387 transcription factor binding datasets generated in high throughput by DNA affinity purification sequencing (21). For each cluster of coexpressed genes, if there is a significant overlap between a particular gene list and the genes in a particular cluster, it can suggest regulatory mechanisms. Here, enrichment was quantified by the *P* value of overlap between gene sets and clusters (hypergeometric test; see Dataset S3 for all calculated values). Similar approaches have previously been used to identify gene regulatory networks in a variety of contexts (e.g., refs. 22 and 23). Analogous approaches include the identification of promoter motifs by enrichment in given gene sets (e.g., ref. 24). We developed a simple software tool, AtEnrich, for performing enrichment analysis of these gene lists (https://github.com/danielseaton/atenrich).

Enrichment analysis identified many significant associations, with 37 of 101 clusters enriched with at least one gene set at $P < 10^{-20}$ (Fig. 1*B*). As expected, this highlighted roles for circadian and light signaling factors in controlling the diurnal dynamics of

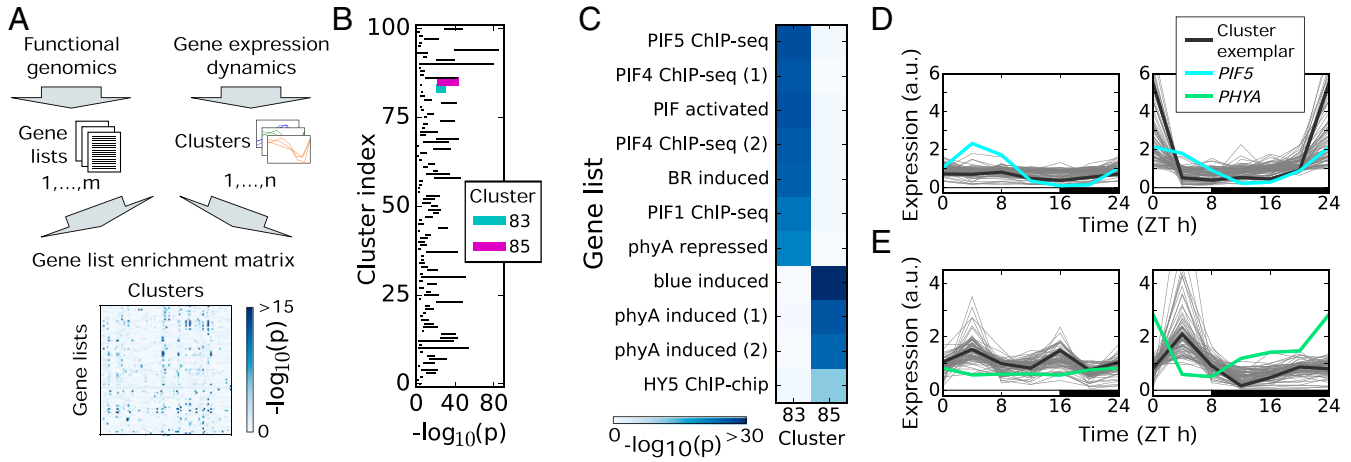

Fig. 1. Mining functional genomic data for active gene regulatory networks. (*A*) Flowchart of data integration. Genes were clustered together according to their dynamics in a range of conditions. Functional genomic datasets (e.g., ChIP-Seq, RNA-Seq) were curated from literature in the form of gene lists. Each cluster was then tested for overenrichment of each gene list (hypergeometric test). (*B*) Top gene list enrichment scores across all clusters. Horizontal lines indicate the range spanned by the three top-scoring enrichments. (*C*) Highlighted enrichment tests for clusters 83 and 85, which are enriched for distinct subsets of phytochrome-related gene lists. (*D*) Short-day, night-specific expression of cluster 83 and its relationship with *PIF5* expression. (*E*) Short-day, morning-specific expression of cluster 85 and its relationship with *PHYA* expression. Expression of each gene is mean normalized.

gene expression. For example, cluster 83 is regulated by the *PIF4*/*PIF5* pathway, that controls changes in hypocotyl elongation with photoperiod (4, 25) (Fig. 1 *C* and *D*). Targets of the PIF family of transcription factors have been identified by ChIP-Seq (26–28), as have targets of PIF-interacting proteins AUXIN RESPONSE FACTOR 6 (ARF6) and BRASSINAZOLE-RESISTANT 1 (BZR1) (29). Cluster 83 is strongly enriched for all of these gene lists ($P < 10^{18}$; hypergeometric test; Fig. 1*C* and Dataset S3). The expression profile of cluster 83 genes in long days (16L:8D) and short days (8L:16D) is consistent with regulation by the PIF4 and PIF5 transcription factors. This is illustrated in Fig. 1*D*, with higher night-time levels of *PIF5* transcript in short photoperiods and higher night-time expression of genes in this cluster. As expected, this cluster includes well-known markers of PIF activity, including *ATHB2*, *IAA29*, *HFR1*, and *CKX5* (30).

Phytochrome signaling, and in particular phyA, is also implicated in the regulation of cluster 85. This cluster is enriched for genes responding rapidly to red light in a phyA-dependent manner (16), and for genes responding to far-red light in a phyA-dependent manner (15) (Fig. 1*C*). Furthermore, it is enriched for genes bound by the transcription factor HY5 (31), which is stabilized by phyA via its interaction with COP1 (32). This cluster also displays a pattern of gene expression consistent with sensitivity to light, with a peak in expression following dawn (Fig. 1*E*). The size of this peak changes with photoperiod, and is especially pronounced in short photoperiods (Fig. 1*E*). Interestingly, the expression of these genes in the morning is correlated with expression of *PHYA* during the preceding night, which is higher during the night in short photoperiods (Fig. 1*E*). Therefore, we proceeded to investigate the photoperiodic regulation of *PHYA* expression and the implications of this for the seasonal control of gene expression of this set of genes.

A Model of PIF Activity Predicts *PHYA* Expression Dynamics. Previous reports have indicated that phyA protein accumulates in etiolated seedlings and during the night in a diurnal cycle through an unknown process (8, 33). As highlighted by earlier studies and our clustering analysis, the PIF family of transcription factors displays a similar pattern of activity (3, 4, 25). Furthermore, our previous analysis of gene expression dynamics identified *PHYA* as a putative target of PIF4 and PIF5 (4).

To assess the plausibility of PIF4/5 regulation of *PHYA* expression, we tested whether our model of PIF4/5 activity could explain *PHYA* dynamics in different photoperiods and circadian clock mutants, as measured by microarray experiments in a previous study (24). In short days (8L:16D), both model and data exhibited rhythmic *PHYA* expression with an end of night peak (Fig. 2*A*). In long days (16L:8D), however, expression was low throughout the day and night (Fig. 2*A*). The model also matched the measured response of *PHYA* expression at end of night and end of day across multiple photoperiods (*SI Appendix*, Fig. S1). Finally, the model matched the exaggerated nocturnal rise in *PHYA* observed in two circadian clock mutants: *lux* and *LHYox* (Fig. 2*B* and *SI Appendix*, Fig. S3*A*). These mutants are notable for exhibiting weak evening complex activity, with a resultant increase in *PIF4* and *PIF5* expression during the night. Interestingly, the *PHYA* cofactor *FHL* (also identified as a likely PIF4/5 target in ref. 4) showed similar patterns of expression across the microarray datasets inspected here, and its expression was also explained by the model (*SI Appendix*, Figs. S2 and S3). This suggests that PIF4/5 regulate both *PHYA* and *FHL*, and therefore may exert significant influence on the activity of the phyA signaling pathway.

PIF4 and PIF5 Directly Regulate *PHYA* Expression. To further establish a role for PIF4 and PIF5 in regulating *PHYA* and *FHL* expression, we measured mRNA levels by qPCR in Columbia-0 (Col-0) [wild type (WT)] and *pif4 pif5* plants, in short (8L:16D) and long (16L:8D) photoperiods. This revealed the expected *PHYA* expression profile, with transcript levels rising to much higher levels during the night in a short day compared with in a long day, and markedly reduced in the *pif4 pif5* mutant specifically in short photoperiods (Fig. 2*C*). This was reduced further in the *pifQ* mutant, that lacks PIF1 and PIF3 in addition to PIF4 and PIF5 (*SI Appendix*, Fig. S4). Furthermore, a similar pattern was observed for *FHL* (*SI Appendix*, Fig. S4). As for transcript, phyA protein accumulated to higher levels in short days compared with long days (*SI Appendix*, Fig. S5*A*), and its levels at zeitgeber time zero (ZT0) in short days were reduced in the *pif4 pif5* and *pifQ* mutants (*SI Appendix*, Fig. S5*B*). These data suggest that PIFs may act collectively to regulate phyA abundance.

The strong coordination between *PHYA* expression and PIF activity across many conditions suggested that this regulation

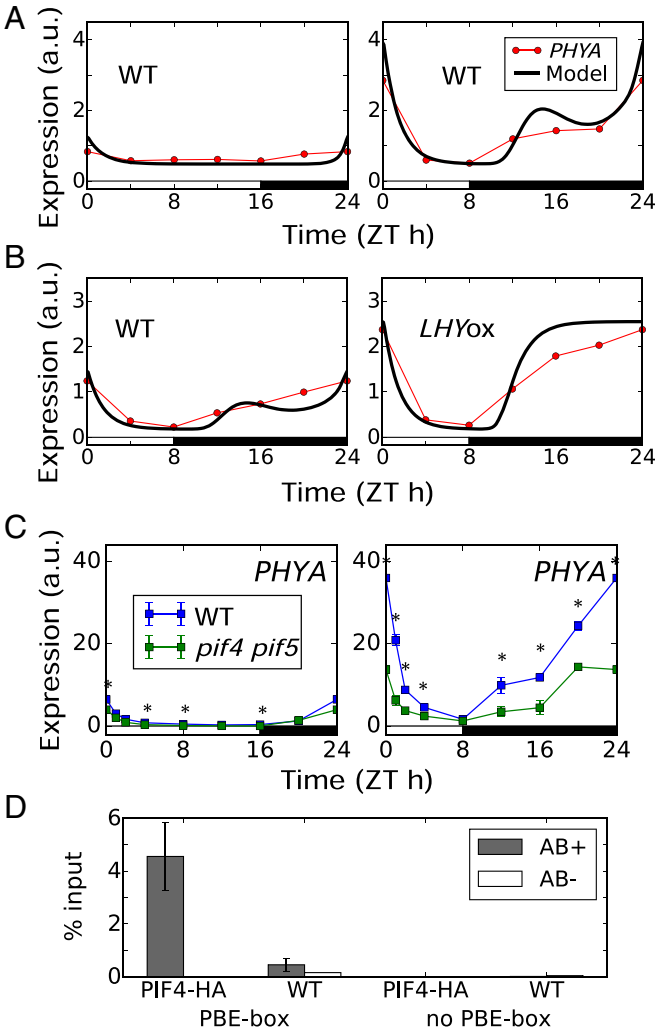

Fig. 2. *PHYA* expression is directly regulated by PIF4 and PIF5. (*A* and *B*) Comparison of model simulations and microarray data for *PHYA* in short compared with long photoperiods (*A*) and WT (L*er*) compared with *LHYox* in 8L:16D light/dark cycles (*B*) (data from ref. 24). (*C*) PHYA expression in short and long photoperiods, in the WT (Col-0) and the *pif4 pif5* mutant. Plants were grown for 2 wk in the given photoperiod. Expression was measured relative to *ACT7* (* indicates a difference from WT at $P < 0.05$, two-tailed *t* test, $n = 3$, error bars represent SEM, ZT0 timepoint replotted at ZT24). (*D*) ChIP-qPCR of PIF4 binding to the *PHYA* promoter. Plants were grown for 2 wk in short days (8L:16D white light, 100 μmol $m^{-2}{\cdot}s^{-1}$) at 22 °C, and samples were collected at the end of the 2 wk at ZT0 ($n = 3$, error bars represent SEM).

might be direct. Several ChIP-Seq analyses of the PIF family have been performed across a range of conditions (26–28, 34). Among these, only Oh et al. (34) found direct binding of a PIF (PIF4) to the *PHYA* promoter, in deetiolated seedlings. To test direct regulation of *PHYA* by PIFs in our conditions, we performed ChIP for PIF4-HA and PIF5-HA on the *PHYA* promoter in plants grown in short days, focusing on a region with a PIF-binding E-box (PBE) element (CACATG; ref. 28). This revealed enrichment of PIF4-HA (Fig. 2*D*) and PIF5-HA (*SI Appendix*, Fig. S6) at the *PHYA* promoter. Thus, PIF4 and PIF5 appear to regulate *PHYA* expression by direct binding to its promoter in short days.

PIFs Regulate phyA Action Specifically in Short Days. Additional support for PIF4 and PIF5's role as short day regulators of *PHYA* comes from a hypocotyl elongation experiment. When supplied continuously, far-red light activates phyA in a HIR mode (19). We used this unique photochemical property to provide a readout for phyA activity through the night of short-day- and long-day-grown seedlings. Our data showed that 4 h of FR light [delivered at the end of the night (EON)] suppressed hypocotyl elongation in a phyA and PIF-dependent manner specifically in short days (*SI Appendix*, Fig. S7). To rule out any potential influence of phyB and other light stable phytochromes on phyA action, we also provided brief end-of-day (EOD) far-red treatments that switch these phytochromes to their inactive Pr conformer. As expected, this enhanced hypocotyl elongation in WT and *phyA* seedlings, and this response was more marked in short days. Delivery of prolonged EON far-red– to EOD far-red–treated seedlings led to phyA suppression of hypocotyl elongation, a response that was markedly reduced in *pif4pif5* and *pifQ* mutants. These photophysiological experiments provide robust support for our central hypothesis that the photoperiodic phyA regulation is largely conferred by short-day PIF action.

phyA Mediates a Photoperiod-Dependent Acute Light Response. Differences in phyA accumulation during the night are expected to affect phyA activity during the following day. To assess this, we developed a mathematical model of phyA signaling mechanisms, combining our model of PIF regulation with a simplified version of the model of Rausenberger et al. (35) (see *SI Appendix* for details; Fig. 3*A*). In this model, phyA signaling activity is high when light is present and phyA protein is abundant. The rapid decrease in the level of phyA protein after dawn means that phyA activity peaks in the early morning. This pulse in the expression of downstream genes is termed an "acute light response" (36). This is illustrated in Fig. 3*B*, showing simulations of the combined clock–PIF–phyA model in short and long photoperiods.

The model predicted that the changing activity of PIFs across different photoperiods and genotypes changes the amplitude of the acute light response (Fig. 3*B*). In particular, it predicted that the amplitude of the acute light response at dawn is increased in short photoperiods, as well as in the *LHYox* and *lux* mutants (i.e., conditions with high *PHYA* expression during the night). The genes in the putative phyA-regulated cluster (cluster 85) display these dynamics (Fig. 3 *C* and *D*). The model also matched gene expression dynamics during seedling deetiolation, in which dark-grown seedlings are exposed to red light (*SI Appendix*, Fig. S8*A*). Here, the model predicted a diminished amplitude of response in the *pifQ* mutant during deetiolation in red light (*SI Appendix*, Fig. S8*B*). Again, the model correctly predicted the expression of genes in cluster 85 across these conditions in microarray data from plants grown in darkness and treated with red light for 1 h, or grown in continuous red light (37) (*SI Appendix*, Fig. S8*C*). Together, these results demonstrate that our molecular understanding of this pathway is consistent with phyA regulation of cluster 85, as expected based on its enrichment for phyA-associated terms in our metaanalysis of functional genomic datasets (Fig. 1*C*).

To further test the model predictions of phyA activity, we investigated the regulation of the dawn-induced circadian clock gene *PSEUDO RESPONSE REGULATOR 9* (*PRR9*), a known target of phyA signaling (35). Measurement of *PRR9* expression in *pif4 pif5* and *phyA* demonstrated that *PRR9* is indeed regulated by phyA, with reduced expression in both mutants, specifically in short photoperiods (*SI Appendix*, Fig. S9*A*). Given the effect of phyA on *PRR9* expression, we hypothesized that this regulation would affect the expression of other circadian clock genes. However, the expression of core clock genes *PRR7*, *TOC1*, *GI*, *LUX*, and *ELF4* displayed limited changes in *phyA* and *pif4 pif5* mutants in short and long days (*SI Appendix*, Fig. S9*B*).

In summary, this cluster of putative phyA targets displays expression dynamics consistent with our mathematical model. This further implicates phyA as a key regulator of these genes.

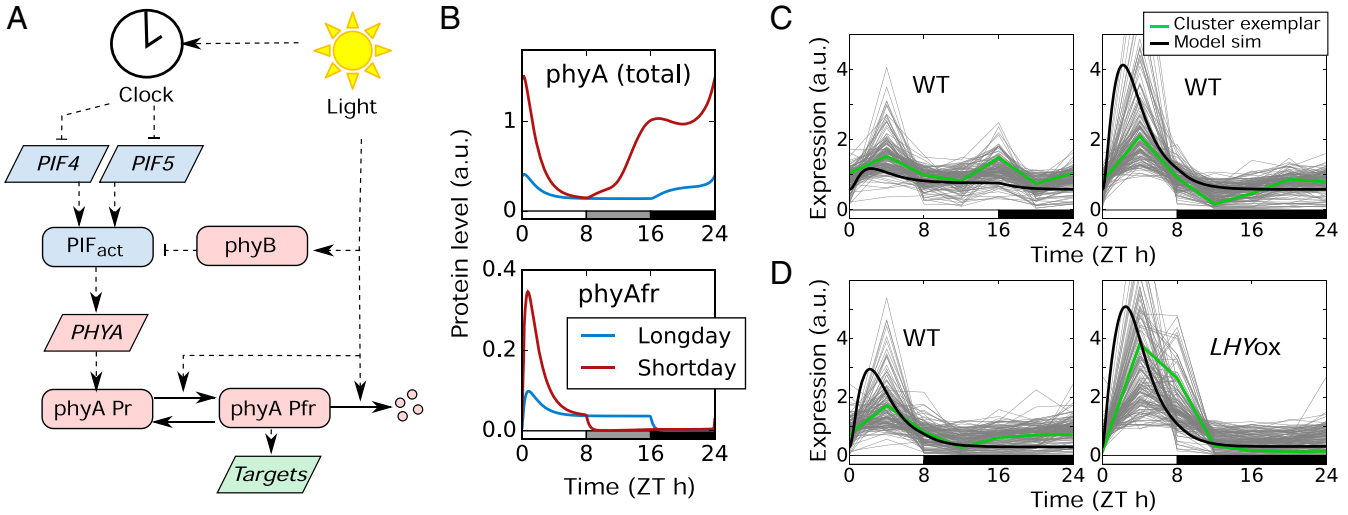

Fig. 3. A model of phyA signaling predicts gene expression dynamics. (*A*) Model schematic. Solid lines represent mass transfer; dashed lines represent regulatory effects. Transcripts are represented by trapezoids, proteins by rectangles. (*B*) Simulation of the phyA signaling model in short and long photoperiods. (*C* and *D*) Gene expression of the putative phyA-regulated cluster of coexpressed genes, compared with model simulations, in photoperiods (*C*), and *LHYox* (*D*) (data from ref. 24; model simulations rescaled to match arbitrary scaling of normalized microarray data).

phyA Confers Photoperiodic Control of Anthocyanin Accumulation. Our results demonstrate that phyA-mediated acute light responses are amplified in short photoperiods. Therefore, we expect short photoperiods to exaggerate *phyA* mutant phenotypes. To identify potential phenotypes of interest, we assessed enrichment of gene ontology (GO) terms within the cluster of putative phyA targets. This identified highly significant enrichment for anthocynanin and flavonoid biosynthesis (GO:0046283, GO:0009812; *SI Appendix*, Table S2). This is consistent with the observation that phyA is involved in anthocyanin accumulation in far-red light (38) and regulates expression of *CHALCONE SYNTHASE* (*CHS*), an enzyme involved in the synthesis of flavonoid and anthocyanin precursors.

To test the phyA photoperiodic link, we measured expression of *FLAVANONE 3-HYDROXYLASE* (*F3H*) and *CHS* in short and long days, in WT (Col-0), *pif4 pif5*, and *phyA*. Although *CHS* was not identified in the phyA-regulated cluster (cluster 85), it is a well-known target of phyA signaling and displays several of the expected features of induction by phyA in available microarray data, including a photoperiod-modulated dawn peak. Our time series qPCR data showed that in short days, *CHS* and *F3H* transcript levels rose rapidly postdawn in WT, but this response was markedly reduced in *phyA* and *pif4 pif5* (Fig. 4*A*). Contrasting with this, expression of *CHS* and *F3H* was similar in *phyA* and *pif4 pif5* through a long day (Fig. 4*A*). This comparison was similar in experiments where natural dawn was simulated based on weather data (*SI Appendix*, Fig. S10; see *SI Appendix* for details), with a fast dawn (reaching 100 μmol $m^{-2}{\cdot}s^{-1}$ after 50 min), and a slow dawn (reaching 100 μmol $m^{-2}{\cdot}s^{-1}$ after 90 min). While the amplitude varied slightly, the expression profiles of *PHYA*, *F3H*, and *CHS* in WT, *phyA*, *pif4 pif5*, and *phyA pif4 pif5* were qualitatively similar in abrupt, fast, and slow dawns. This response consistency most likely results from the inherent photosensory properties that enable phyA to detect very low fluence rate light. These data are consistent with phyA being most active during the day in short photoperiods.

To test whether these differences in gene expression result in differences in metabolic phenotype, we measured anthocyanin accumulation in plants grown in short and long days. As expected, anthocyanin levels were highest in the WT in short days and were reduced in the *phyA*, *pif4 pif5*, and *pifQ* mutants, specifically in short days (Fig. 4*B*). These results demonstrate how the PIF–phyA module mediates seasonal changes in anthocyanin levels.

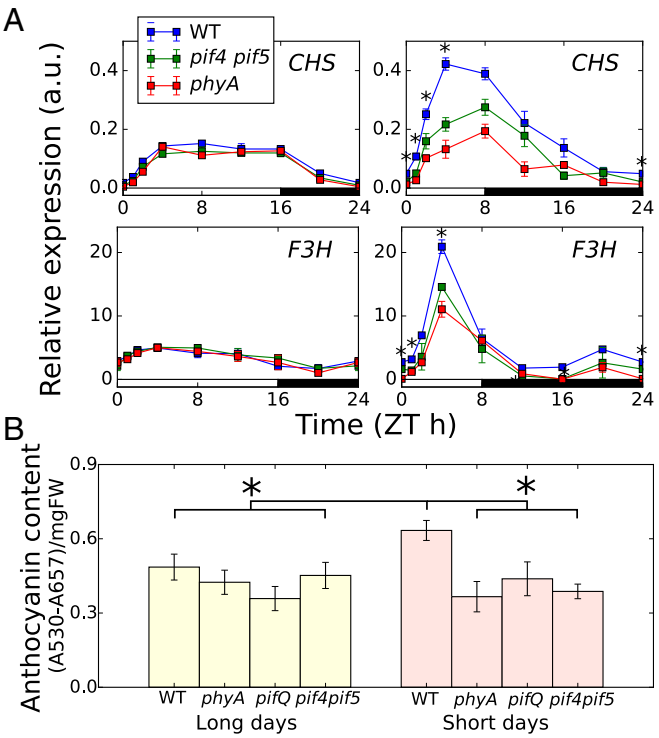

Fig. 4. Anthocyanin accumulation is regulated by phyA in a photoperiod-specific manner. (*A*) qPCR timecourse data for *F3H* and *CHS* in LD and SD, respectively, in WT (Col-0), *pif4 pif5*, and *phyA*. Expression is relative to *ACT7*. Plants were grown for 2 wk at 22 °C under 100 μmol $m^{-2}{\cdot}s^{-1}$ white light in the specified photoperiod (* indicates significant difference at $P < 0.05$ between WT and both *pif4 pif5* and *phyA*, two-tailed *t* test, $n = 3$, error bars represent SEM). (*B*) Anthocyanin accumulation in the same conditions as *A*, also including the *pifQ* mutant (* indicates difference from WT in short days at $P < 0.01$, one-tailed *t* test, $n = 3$, error bars represent SD).

Discussion

Perception of light allows plants to prepare for the predictable daily and seasonal rhythms of the natural environment. We have delineated a role for the light photoreceptor phyA in both daily and seasonal responses. On a daily timescale, phyA acts as a precise sensor of dawn, peaking in activity following first light. On a seasonal timescale, the amplitude of this dawn peak in activity changes, and is especially pronounced in short photoperiods.

The ability of phyA to respond sensitively to dawn relies on two key properties: its ability to sense very low levels of light (39) and its accumulation in darkness (8, 33). It is well established that the active Pfr form of phyA is light labile and degrades fairly rapidly following light exposure. However, inactive phyA Pr accumulates in seedlings that are kept in prolonged periods of darkness (8). A night-time rise in phyA protein levels has also been reported for seedlings grown in short days (33). Here, we have identified the PIF transcription factors as regulators of this nocturnal elevation in phyA and linked this accumulation to the induction of hundreds of transcripts at dawn.

This cycle of accumulation and repression of photosensitivity across a dark-to-light transition is reminiscent of responses in the mammalian eye. A combination of physiological and molecular mechanisms heighten photosensitivity during prolonged darkness, but this sensitivity gradually diminishes during prolonged exposure to light (40). Such systems have been shown to enable sensitive responses to fold changes in stimuli (41). This may be especially important in the case of phyA, as it allows a high-amplitude response at dawn, when there is a transition from darkness to low-intensity light. Furthermore, phyA is not the only light-labile photoreceptor: Cryptochrome 2 shows similar patterns of accumulation in darkness (33, 42). Thus, our analysis of phyA signaling may have implications for other light signaling pathways. In particular, it highlights the importance of studying such pathways in conditions that approximate the natural environment, i.e., in photoperiods.

Our analysis suggests that nocturnal accumulation of phyA results in photoperiodic responses. In short photoperiods, higher levels of phyA are present during the night, leading to an enhanced sensitivity to light at dawn. Inspection of transcriptomic and functional genomic datasets revealed that this expectation is met in hundreds of phyA-induced genes. Furthermore, these changes in gene expression have consequences for plant metabolism and growth. For example, induction of genes involved in flavonoid and anthocyanin biosynthesis in short photoperiods is reflected in changes in anthocyanin accumulation in these conditions. A role for phyA in regulating anthocyanin metabolism has previously been demonstrated under far-red light (38). Here, we extend this role to plants grown under white light in short photoperiods. The potential relevance of increased anthocyanin accumulation to growth in short photoperiods remains to be understood, but may involve protection from photoperiod-specific stresses. For example, anthocyanins protect from oxidative stress (43), which is higher in short photoperiods (44).

Previously, substantial focus has been placed on the role of phyA in seedling establishment (19, 45). We recently demonstrated a role

for phyA, alongside other phytochromes, in biomass production (46), while others have shown that phyA regulates flowering (33). The precise regulatory mechanisms involved in each process are likely to be context dependent. For example, in seedlings grown in constant far-red light, loss of PIF4 and PIF5 does not affect phyA protein abundance (45). These conditions differ substantially from the conditions used in this study, where a change in photoperiod is required to promote transcription of *PIF4*, *PIF5*, and their target *PHYA*. This illustrates the potential for the same regulatory network to be deployed in different ways, depending on the developmental and environmental context.

In summary, our study firmly positions phyA as a photoperiodic dawn sensor that is tuned to detect the very low light levels that signify dawn onset in the natural environment. This property ensures that phyA is a very reliable sensor of dawn transition in nature, where weather, local and seasonal changes, can profoundly affect the intensity of morning light.

Materials and Methods

Col-0 (wild type) and mutants in this background, were used for all experiments. See *SI Appendix, Materials and Methods* for detailed descriptions of the plant materials and growth conditions. Experimental methods (qPCR, ChIP, Western blotting, and anthocyanin measurement), data analysis methods (coexpression clustering and enrichment analysis), and the mathematical modeling methods are also provided in *SI Appendix, Materials and Methods*.

ACKNOWLEDGMENTS. We thank James Furniss and Ammad Abbas for assistance with plant growth, Christian Fankhauser for kindly providing *phyA pif4 pif5* seeds, Akira Nagatani for kindly providing phyA antibody, and members of the K.J.H. laboratory for comments on the manuscript. This work was supported by Biotechnology and Biological Sciences Research Council Grants BB/M025551/1 and BB/N005147/1 (to K.J.H.); NIH Grant GM079712, National Science Foundation Grant IOS-1656076, and Next-Generation BioGreen 21 Program (Grant PJ013386, Rural Development Administration, Republic of Korea) (to T.I.); and Royal Society Grant RG150711 (to G.T.-O.). A.K. is supported by the Japan Society for the Promotion of Science Postdoctoral Fellowships for Research Abroad.

1. Greenham K, McClung CR (2015) Integrating circadian dynamics with physiological processes in plants. *Nat Rev Genet* 16:598–610.
2. Yanovsky MJ, Kay SA (2002) Molecular basis of seasonal time measurement in Arabidopsis. *Nature* 419:308–312.
3. Nozue K, et al. (2007) Rhythmic growth explained by coincidence between internal and external cues. *Nature* 448:358–361.
4. Seaton DD, et al. (2015) Linked circadian outputs control elongation growth and flowering in response to photoperiod and temperature. *Mol Syst Biol* 11:776.
5. Leivar P, Quail PH (2011) PIFs: Pivotal components in a cellular signaling hub. *Trends Plant Sci* 16:19–28.
6. Park E, et al. (2012) Phytochrome B inhibits binding of phytochrome-interacting factors to their target promoters. *Plant J* 72:537–546.
7. Possart A, Fleck C, Hiltbrunner A (2014) Shedding (far-red) light on phytochrome mechanisms and responses in land plants. *Plant Sci* 217–218:36–46.
8. Sharrock RA, Clack T (2002) Patterns of expression and normalized levels of the five Arabidopsis phytochromes. *Plant Physiol* 130:442–456.
9. Hiltbrunner A, et al. (2006) FHY1 and FHL act together to mediate nuclear accumulation of the phytochrome A photoreceptor. *Plant Cell Physiol* 47:1023–1034.
10. Krzymuski M, et al. (2014) Phytochrome A antagonizes PHYTOCHROME INTERACTING FACTOR 1 to prevent over-activation of photomorphogenesis. *Mol Plant* 7:1415–1428.
11. Yoo J, Cho M-H, Lee S-W, Bhoo SH (2016) Phytochrome-interacting ankyrin repeat protein 2 modulates phytochrome A-mediated PIF3 phosphorylation in light signal transduction. *J Biochem* 160:243–249.
12. Osterlund MT, Hardtke CS, Wei N, Deng XW (2000) Targeted destabilization of HY5 during light-regulated development of Arabidopsis. *Nature* 405:462–466.
13. Seo HS, et al. (2003) LAF1 ubiquitination by COP1 controls photomorphogenesis and is stimulated by SPA1. *Nature* 423:995–999.
14. Jang IC, Yang JY, Seo HS, Chua NH (2005) HFR1 is targeted by COP1 E3 ligase for post-translational proteolysis during phytochrome A signaling. *Genes Dev* 19:593–602.
15. Chen F, et al. (2014) Arabidopsis phytochrome A directly targets numerous promoters for individualized modulation of genes in a wide range of pathways. *Plant Cell* 26:1949–1966.
16. Tepperman JM, Hwang Y-S, Quail PH (2006) phyA dominates in transduction of red-light signals to rapidly responding genes at the initiation of Arabidopsis seedling deetiolation. *Plant J* 48:728–742.
17. Tepperman JM, Zhu T, Chang HS, Wang X, Quail PH (2001) Multiple transcription-factor genes are early targets of phytochrome A signaling. *Proc Natl Acad Sci USA* 98:9437–9442.
18. Hall A, Kozma-Bognár L, Tóth R, Nagy F, Millar AJ (2001) Conditional circadian regulation of PHYTOCHROME A gene expression. *Plant Physiol* 127:1808–1818.
19. Casal JJ, Candia AN, Sellaro R (2014) Light perception and signalling by phytochrome A. *J Exp Bot* 65:2835–2845.
20. Nusinow DA, et al. (2011) The ELF4-ELF3-LUX complex links the circadian clock to diurnal control of hypocotyl growth. *Nature* 475:398–402.
21. O'Malley RC, et al. (2016) Cistrome and epicistrome features shape the regulatory DNA landscape. *Cell* 165:1280–1292, and erratum (2016) 166:1598.
22. Kuleshov MV, et al. (2016) Enrichr: A comprehensive gene set enrichment analysis web server 2016 update. *Nucleic Acids Res* 44:W90–W97.
23. Kulkarni SR, Vaneechoutte D, Van de Velde J, Vandepoele K (2018) TF2Network: Predicting transcription factor regulators and gene regulatory networks in Arabidopsis using publicly available binding site information. *Nucleic Acids Res* 46:e31.
24. Michael TP, et al. (2008) A morning-specific phytohormone gene expression program underlying rhythmic plant growth. *PLoS Biol* 6:e225.
25. Kunihiro A, et al. (2011) Phytochrome-interacting factor 4 and 5 (PIF4 and PIF5) activate the homeobox ATHB2 and auxin-inducible IAA29 genes in the coincidence mechanism underlying photoperiodic control of plant growth of Arabidopsis thaliana. *Plant Cell Physiol* 52:1315–1329.
26. Hornitschek P, et al. (2012) Phytochrome interacting factors 4 and 5 control seedling growth in changing light conditions by directly controlling auxin signaling. *Plant J* 71:699–711.
27. Pfeiffer A, Shi H, Tepperman JM, Zhang Y, Quail PH (2014) Combinatorial complexity in a transcriptionally centered signaling hub in Arabidopsis. *Mol Plant* 7:1598–1618.
28. Zhang Y, et al. (2013) A quartet of PIF bHLH factors provides a transcriptionally centered signaling hub that regulates seedling morphogenesis through differential expression-patterning of shared target genes in Arabidopsis. *PLoS Genet* 9:e1003244.
29. Oh E, et al. (2014) Cell elongation is regulated through a central circuit of interacting transcription factors in the Arabidopsis hypocotyl. *eLife* 3:e03031.
30. Nomoto Y, Kubozono S, Yamashino T, Nakamichi N, Mizuno T (2012) Circadian clock- and PIF4-controlled plant growth: A coincidence mechanism directly integrates a hormone signaling network into the photoperiodic control of plant architectures in Arabidopsis thaliana. *Plant Cell Physiol* 53:1950–1964, and erratum (2013) 54:643.
31. Lee J, et al. (2007) Analysis of transcription factor HY5 genomic binding sites revealed its hierarchical role in light regulation of development. *Plant Cell* 19:731–749.
32. Hardtke CS, et al. (2000) HY5 stability and activity in arabidopsis is regulated by phosphorylation in its COP1 binding domain. *EMBO J* 19:4997–5006.
33. Mockler T, et al. (2003) Regulation of photoperiodic flowering by Arabidopsis photoreceptors. *Proc Natl Acad Sci USA* 100:2140–2145.
34. Oh E, Zhu J-Y, Wang Z-Y (2012) Interaction between BZR1 and PIF4 integrates brassinosteroid and environmental responses. *Nat Cell Biol* 14:802–809.
35. Rausenberger J, et al. (2011) Photoconversion and nuclear trafficking cycles determine phytochrome A's response profile to far-red light. *Cell* 146:813–825.
36. Anderson SL, et al. (1997) Attenuation of phytochrome A and B signaling pathways by the Arabidopsis circadian clock. *Plant Cell* 9:1727–1743.
37. Leivar P, et al. (2009) Definition of early transcriptional circuitry involved in light-induced reversal of PIF-imposed repression of photomorphogenesis in young Arabidopsis seedlings. *Plant Cell* 21:3535–3553.
38. Neff MM, Chory J (1998) Genetic interactions between phytochrome A, phytochrome B, and cryptochrome 1 during Arabidopsis development. *Plant Physiol* 118:27–35.
39. Shinomura T, et al. (1996) Action spectra for phytochrome A- and B-specific photoinduction of seed germination in Arabidopsis thaliana. *Proc Natl Acad Sci USA* 93:8129–8133.
40. Lamb TD, Pugh EN, Jr (2004) Dark adaptation and the retinoid cycle of vision. *Prog Retin Eye Res* 23:307–380.
41. Shoval O, et al. (2010) Fold-change detection and scalar symmetry of sensory input fields. *Proc Natl Acad Sci USA* 107:15995–16000.
42. El-Din El-Assal S, Alonso-Blanco C, Peeters AJM, Raz V, Koornneef M (2001) A QTL for flowering time in Arabidopsis reveals a novel allele of CRY2. *Nat Genet* 29:435–440.
43. Ramakrishna A, Ravishankar GA (2011) Influence of abiotic stress signals on secondary metabolites in plants. *Plant Signal Behav* 6:1720–1731.
44. Pétriacq P, et al. (2017) Photoperiod affects the phenotype of mitochondrial complex I mutants. *Plant Physiol* 173:434–455.
45. Lorrain S, Trevisan M, Pradervand S, Fankhauser C (2009) Phytochrome interacting factors 4 and 5 redundantly limit seedling de-etiolation in continuous far-red light. *Plant J* 60:449–461.
46. Yang D, Seaton DD, Krahmer J, Halliday KJ (2016) Photoreceptor effects on plant biomass, resource allocation, and metabolic state. *Proc Natl Acad Sci USA* 113:7667–7672.

Supporting Information Appendix

Dawn and photoperiod sensing by phytochrome A

Daniel D Seaton, Gabriela Toledo-Ortiz, Ashwin Ganpudi, Akane Kubota, Takato Imaizumi, Karen J Halliday

www.pnas.org/cgi/doi/10.1073/pnas.1803398115

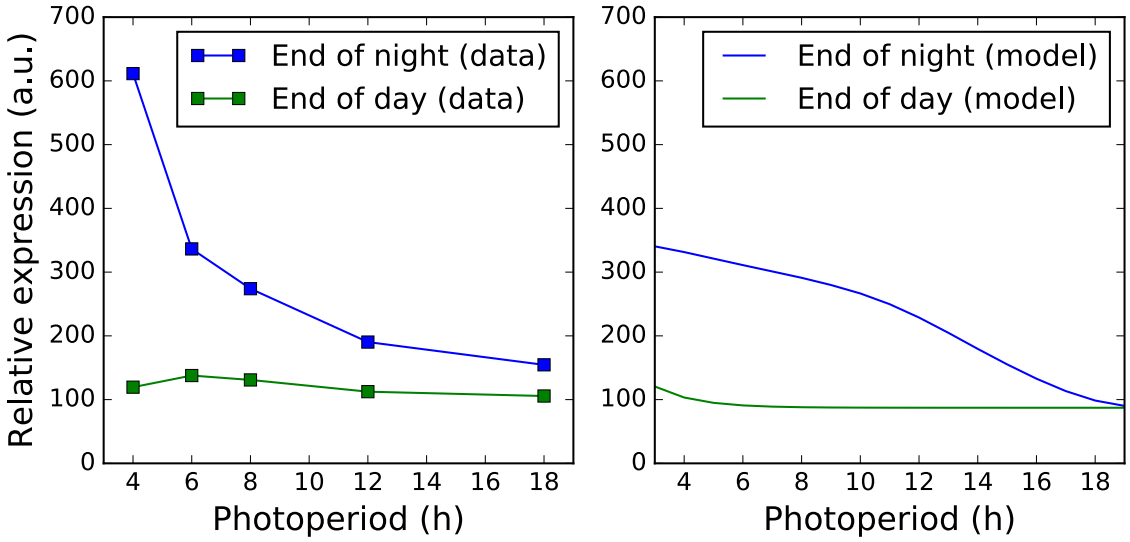

Supplementary Figure S1. Comparison of microarray data and model simulations for *PHYA* expression at the end of night and end of day across 5 photoperiods (data from Flis et al, 2016).

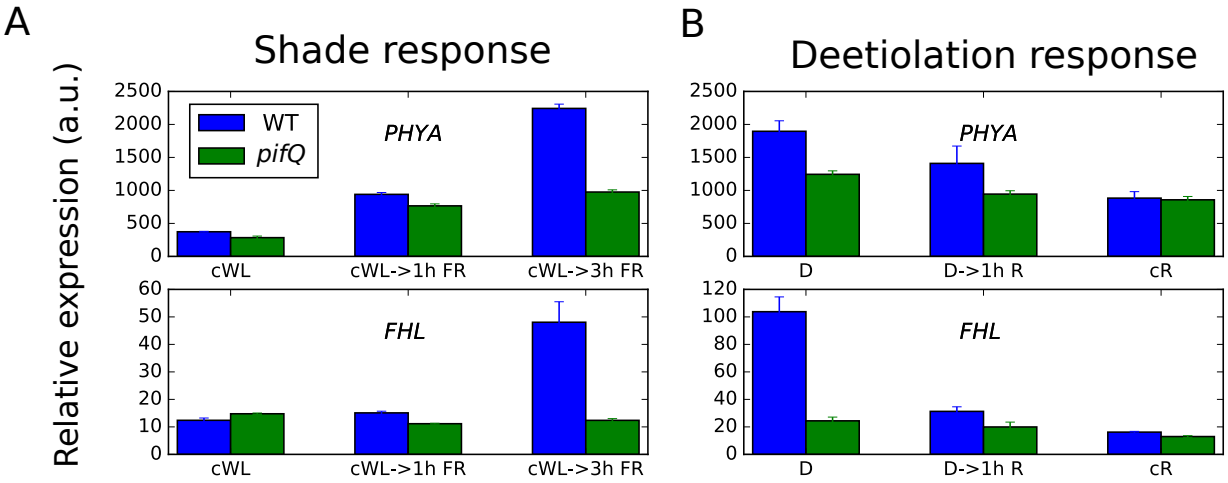

Supplementary Figure S2. Expression of *PHYA* and *FHL* in response to shade and deetiolation.

(A) Shade response microarray data are from Leivar et al, 2012. WT and *pifQ* seedlings were grown for 2 days in white light (cWL), supplemented by far red light for 1 h (cWL-> 1h R), or supplemented by far red light for 3h (cWL->3h FR). (B) Deetilation response microarray data are from Leivar et al, 2009. WT and *pifQ* seedlings were grown for 2 days in the dark (D), followed by 1 h in red light (D-> 1h R), or grown for 2 days in red light (cR).

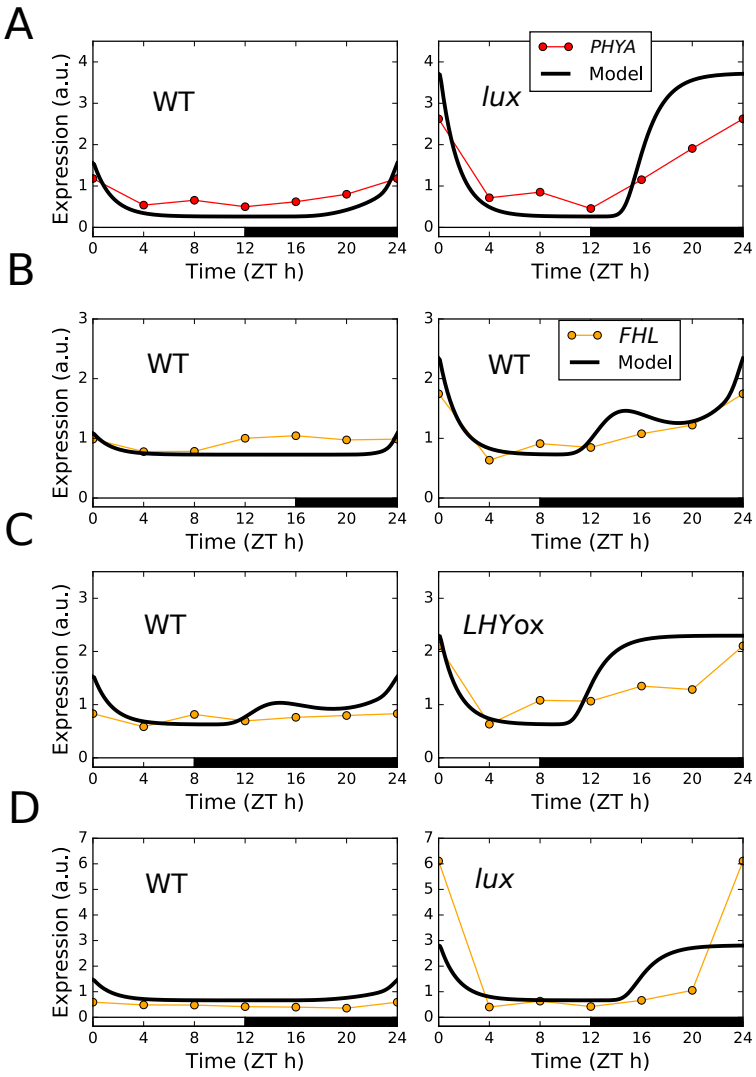

Supplementary Figure S3. Comparison of model simulations and microarray data for *PHYA* and *FHL* expression.

(A) *PHYA* expression in WT (Col-0) compared to the *lux* mutant in 12L:12D light/dark cycles. (B) *FHL* expression in WT (Ler) in short compared to long photoperiods. (C) *FHL* expression in WT (Ler) compared to *LHY*ox in 8L:16D light/dark cycles. (D) *FHL* expression in WT (Col) compared to the *lux* mutant in 12L:12D light/dark cycles.

A

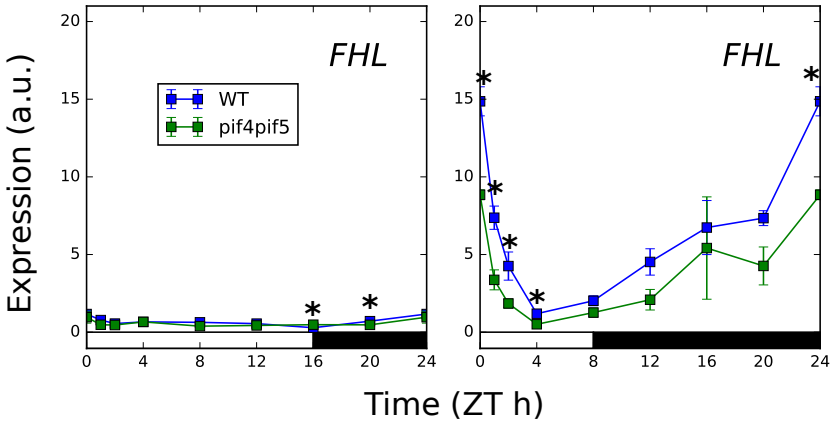

B

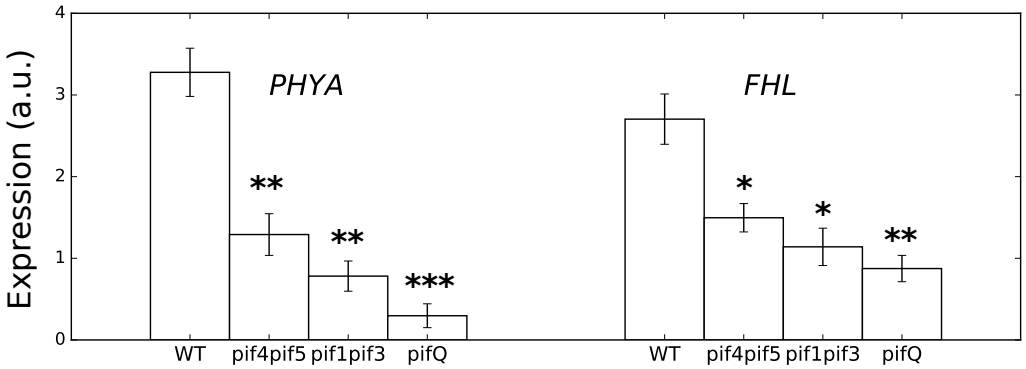

Supplementary Figure S4. (A) *FHL* expression in long and short days, in the WT (Col-0) and the *pif4 pif5* mutant. * indicates a difference from WT at $p < 0.05$ (two-tailed t-test, n=3, error bars represent SEM). (B) *FHL* and *PHYA* expression in short days at ZT0, in the WT (Col-0), and the *pif4 pif5*, *pif1 pif3*, and *pifQ* mutants. Plants were grown for 2 weeks in the stated photoperiod. Expression was measured relative to *ACT7*. *,**,*** indicates a difference from WT at $p < 0.05,0.01,0.001$ respectively (two-tailed t-test, n=3, error bars represent SEM).

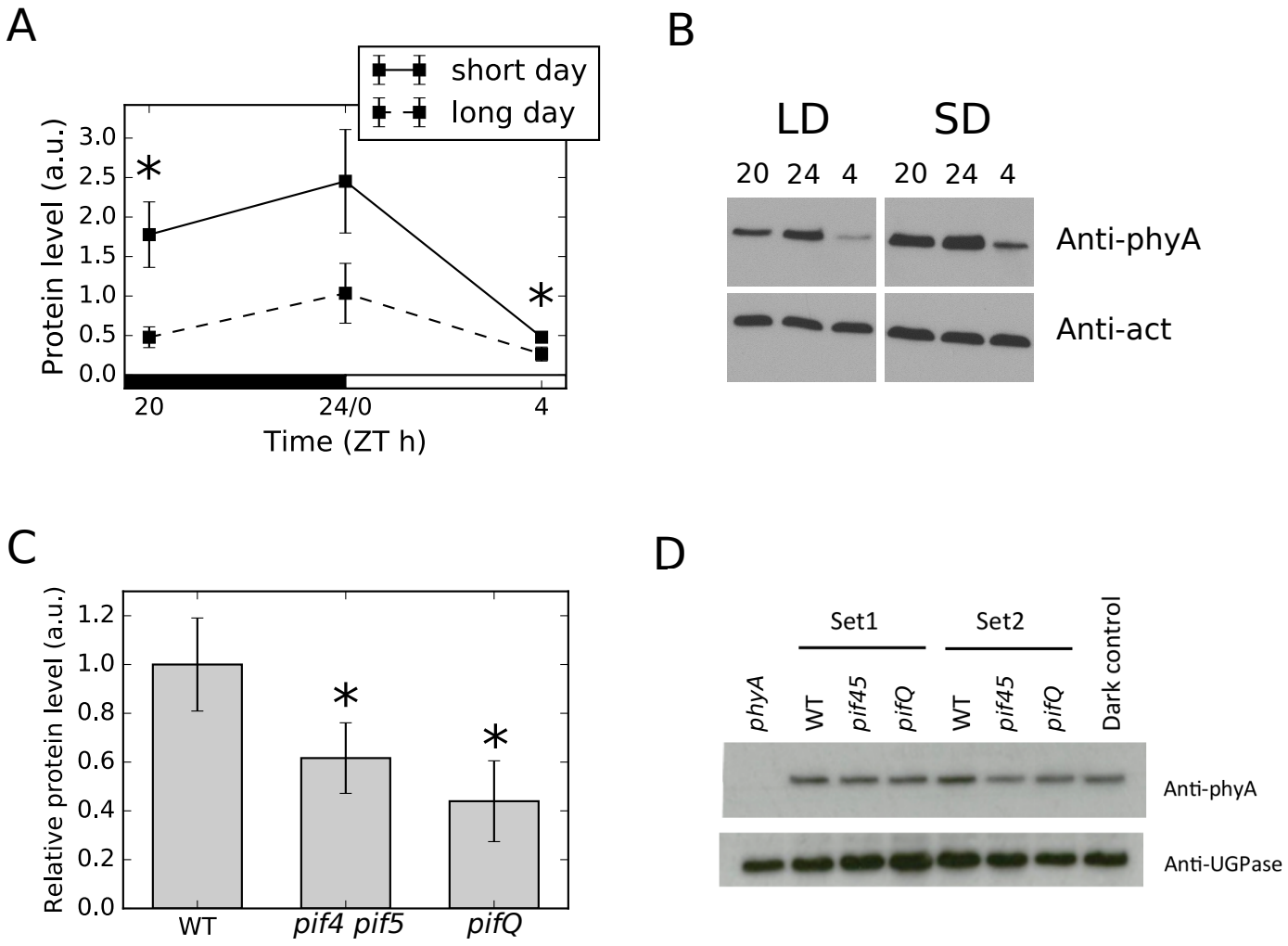

Figure S5. phyA protein quantification.

(A) Quantified Western blot data for phyA at three timepoints spanning dawn, in WT (Col-0), for two-week old plants grown in short and long days, normalised to actin loading standard (error bars represent SEM, n=3, * $p<0.05$, one-sided t-test). (B) Representative Western blot of data plotted in (A). Note that images shown are taken from the same blot. (C) Quantified Western blot data for phyA at ZT0 (before lights on), in WT (Col) and the *pifQ* and *pif4 pif5* mutants, for plants grown in short days, normalised to a UGPase loading standard (error bars represent SEM, n=4, * $p<0.05$, one-sided t-test for paired samples). (D) Representative Western blot of data plotted in (C).

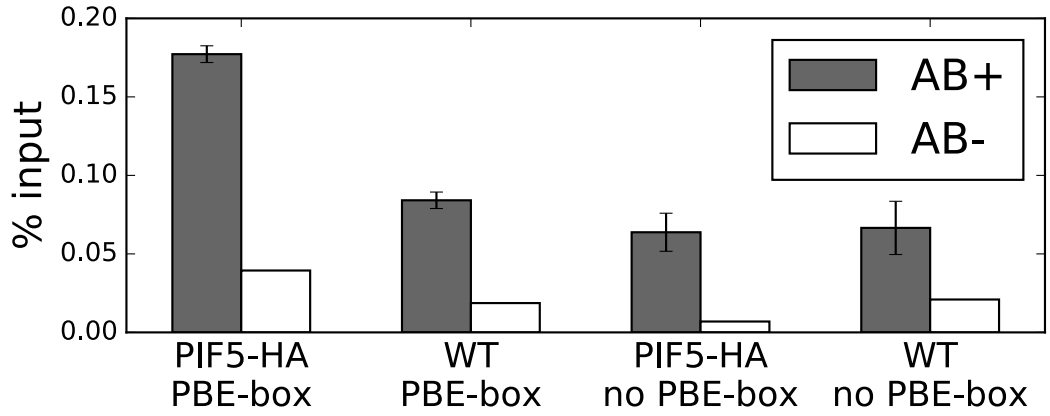

Supplementary Figure S6. PIF5 ChIP at the *PHYA* promoter, in regions with and without PBE-box elements. Plants were grown for two weeks in short days (8L:16D white light, 100 µmol $m^{-2}s^{-1}$) at 22°C, and samples were collected at the end of the two weeks at ZT0 (n=3, error bars represent SEM).

A

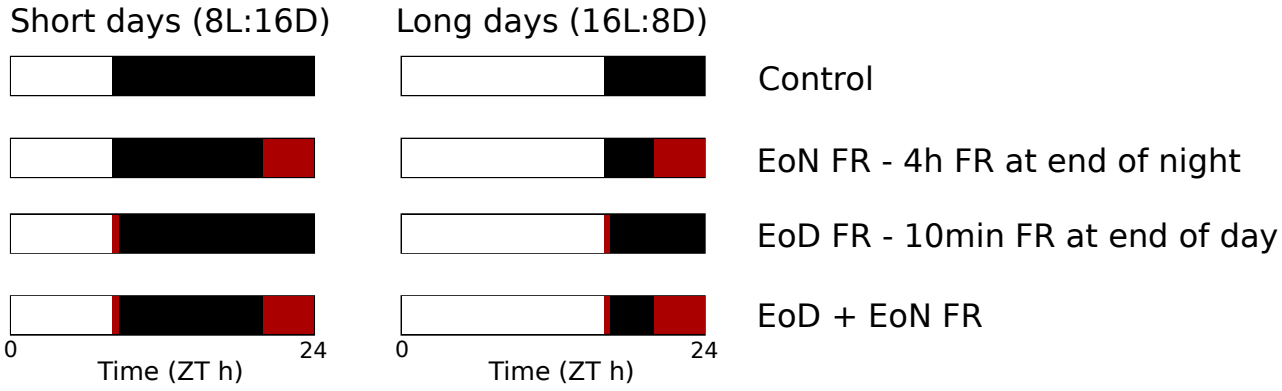

B

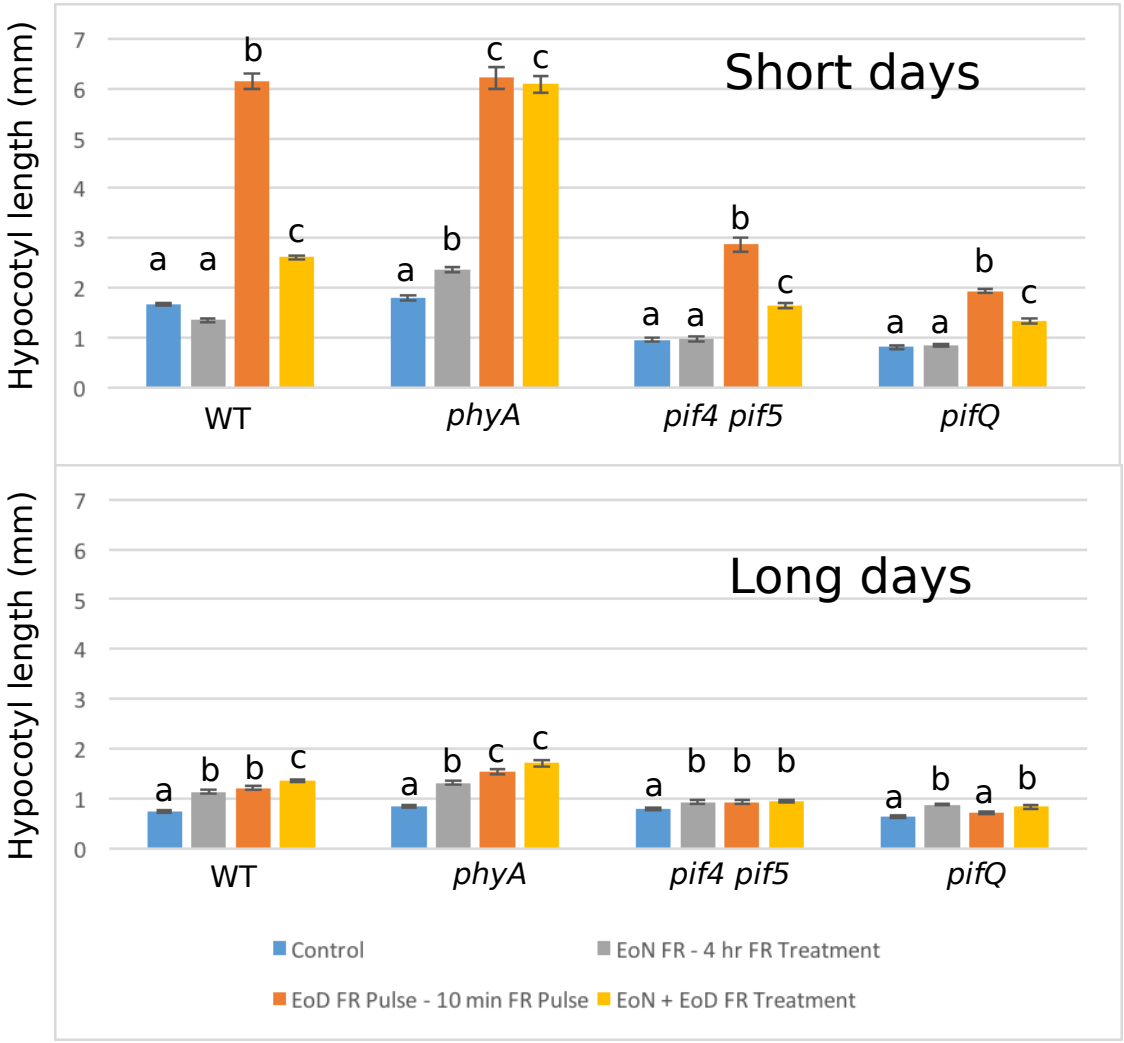

Supplementary Figure S7. Hypocotyl elongation in response to photoperiod and far-red light. (A) Schematic of light treatments, with intensities of 100 µmol $m^{-2}s^{-1}$ for white light and 40 µmol $m^{-2}s^{-1}$ for far-red light). (B) Hypocotyl measurements for WT (Col-0), *phyA*, *pif4 pif5*, and *pifQ*. Plants were grown for 7 days at 22°C in the specified light conditions. Differences in hypocotyl elongation across light treatments were evaluated independently for each genotype, and groups of treatments spanning significant differences are indicated for an adjusted p-value threshold of 0.05 (Tukey's multiple comparison test). Error bars represent SEM. N>12.

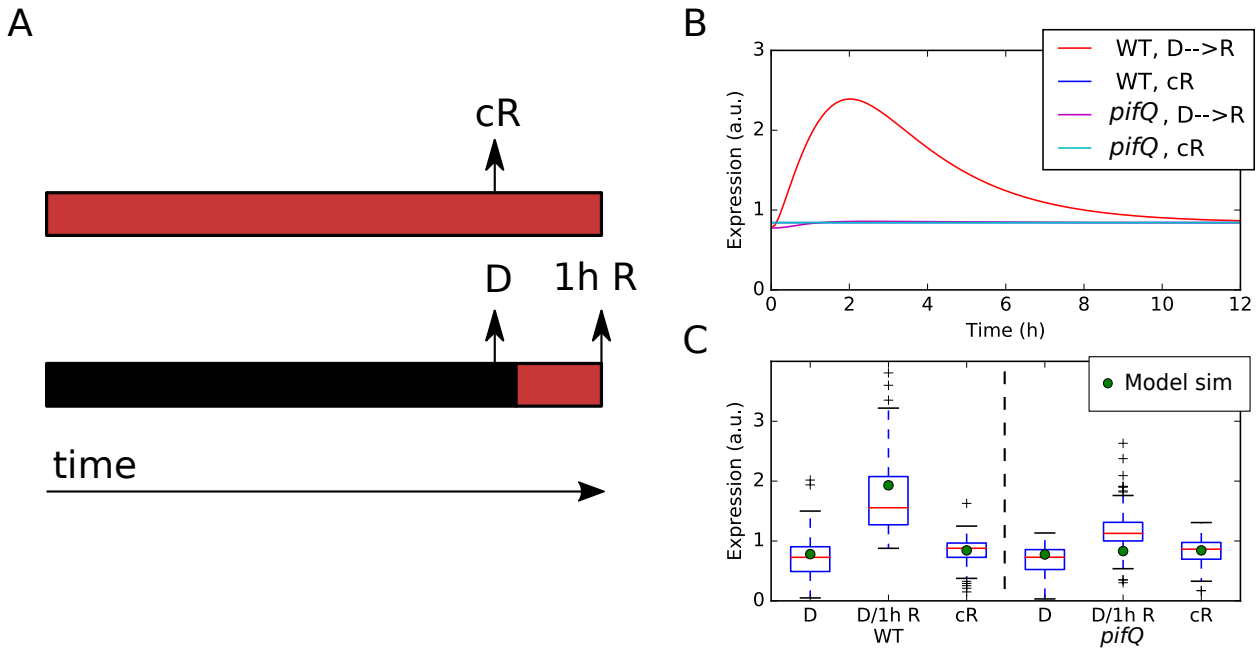

Figure S8. A model of phyA signalling predicts gene expression dynamics in a deetiolation experiment.

(A) Schematic of the deetiolation protocol, involving deetiolation either in continuous red light (cR, top) or darkness (D) followed by 1h of red light (1h R). (B) Simulated expression of a target of phyA, following a transition from darkness to continuous red light (D-->R), compared to plants grown continuously in red light (cR). (C) Gene expression of the putative phyA-regulated cluster of co-expressed genes following a transition from darkness to continuous red light (data from Leivar et al, 2009). Model simulation results from (B) are replotted for comparison.

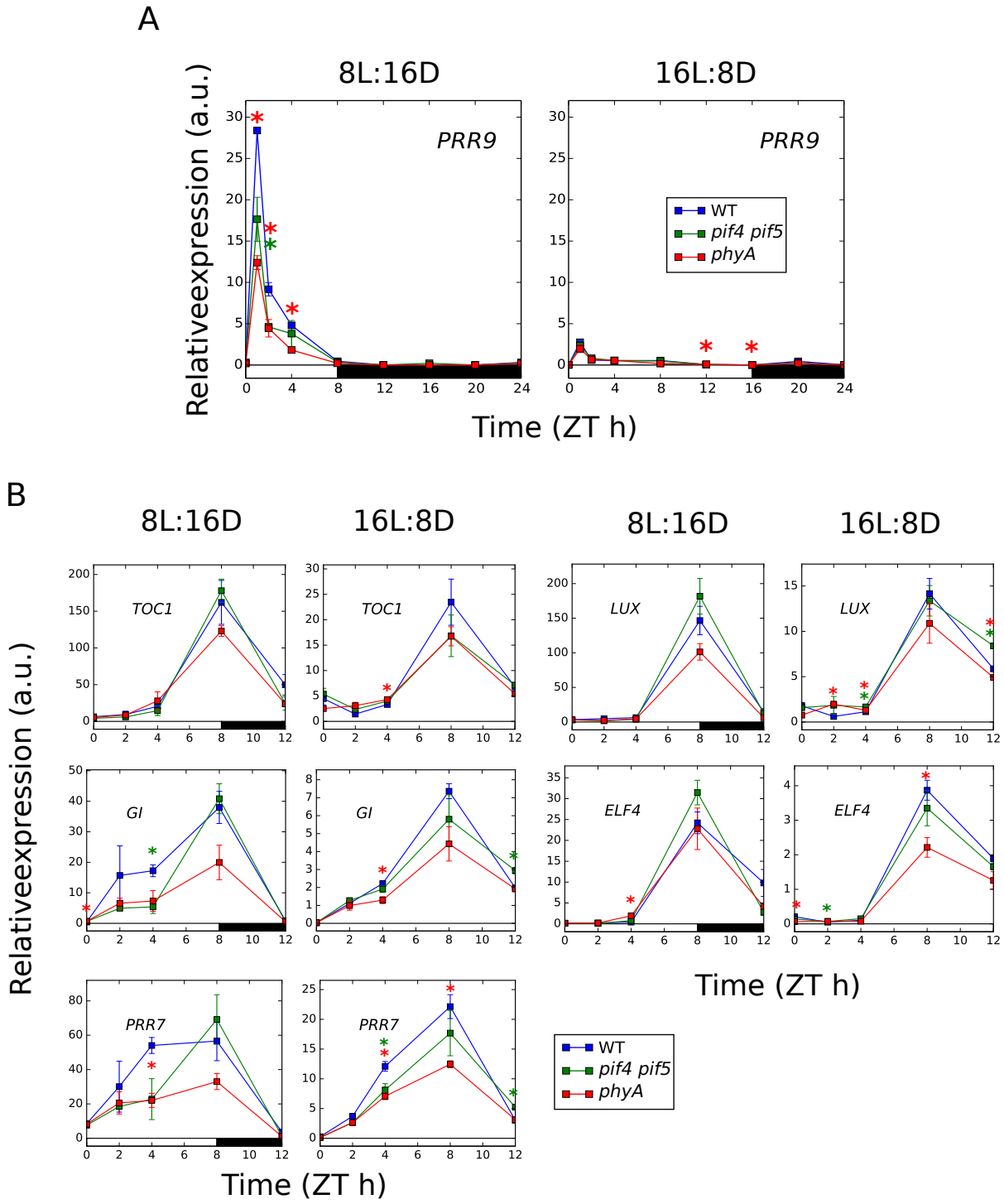

Supplementary Figure S9. Clock gene expression in response to photoperiod and loss of phyA.

(A) qPCR timecourse data for *PRR9* in short (left) and long (right) photoperiods, in WT (Col-0), *pif4 pif5*, and *phyA* (B) qPCR timecourse data for core clock genes at a subset of timepoints between ZT0 and ZT12, in short (left) and long (right) photoperiods, in WT (Col-0), *pif4 pif5*, and *phyA*. Expression is relative to *ACT7*. Plants were grown for 2 weeks at 22°C under 100 µmol $m^{-2}s^{-1}$ white light in the specified photoperiod (n = 3, error bars represent SEM, green and red *s indicates significant difference between WT and *pif4 pif5* and *phyA*, respectively, $p < 0.05$, two-tailed t-test).

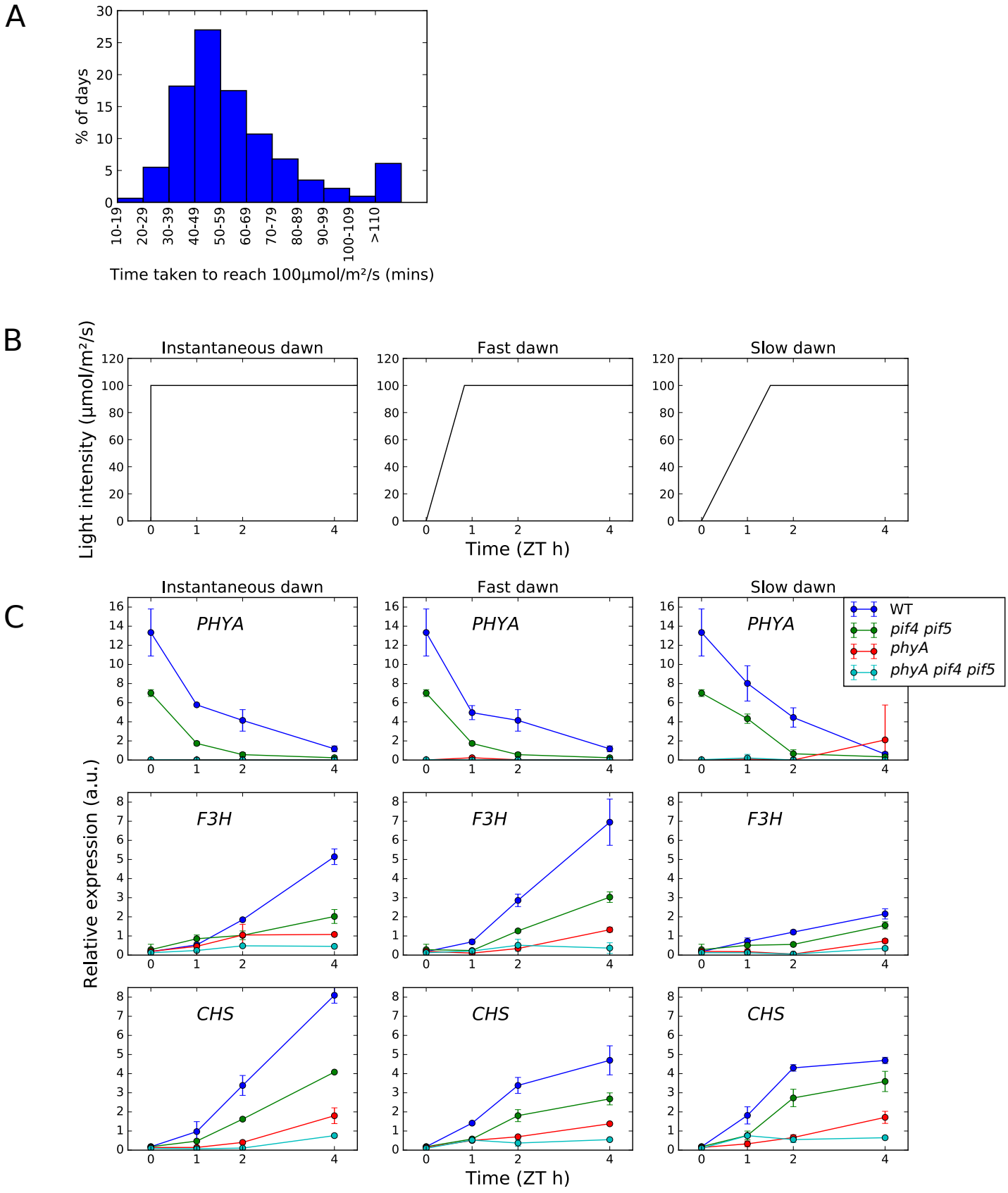

Supplementary Figure S10. phyA signalling in simulated natural dawn conditions.

(A) Histogram of the time taken for the light intensity to reach 100 µmol $m^{-2}s^{-1}$ on days with short photoperiods in Edinburgh, UK (see Supporting Information for details). (B) Schematic of the experimental protocol to simulate natural dawn based on weather data. (C) qPCR timecourse data for *PHYA*, *F3H*, and *CHS* in the three light conditions shown in (B), in WT (Col-0), *pif4 pif5*, *phyA*, and phyA *pif4 pif5* mutants. Expression is relative to ACT7. Plants were grown for 2 weeks at 22°C under 100 µmol $m^{-2}s^{-1}$ white light in the short photoperiods (n = 3, error bars represent SEM).

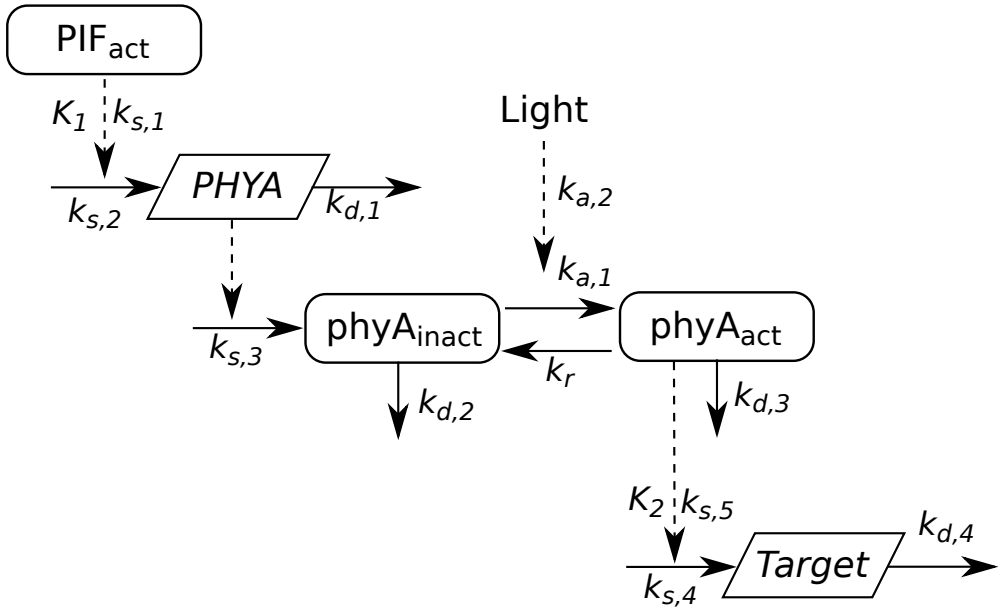

Supplementary Figure S11. Schematic of phyA model.

Rectangles indicate protein species. Trapezoids indicate transcripts. Solid lines indicate mass transfer (synthesis and turnover of molecules, and conversion of phyA between inactive and active forms). Dashed lines indicate regulatory influences.

Tables

Table S1, gene expression dataset descriptions. List of gene expression datasets used.

Dataset	Type	Description	Reference
shortday_vs_longday	ATH1 microarray	WT (Ler) seedlings grown in long(8h) and short (16h) photoperiods, sampled at 4h timepoints over 2 days.	Michael et al, 2008; DIURNAL database
WT_vs_lux	ATH1 microarray	WT (Col) and *lux* seedlings grown in 12L:12D, sampled at 4h timepoints over 2 days	Michael et al, 2008; DIURNAL database
WT_vs_LHYox	ATH1 microarray	WT (Ler) and LHYox (*lhy-1*) seedlings grown in 8L:16D, sampled at 4h timepoints over 2 days	Michael et al, 2008; DIURNAL database
red_light_deetiolation	ATH1 microarray	WT (Col) and pifQ seedlings grown in constant darkness, or constant red, or transferred from darkness to red light	Leivar et al, 2009
WT_vs_lnk1lnk2	RNA-seq	WT (Col) and lnk1;lnk2 seedlings grown in 16L:8D, sampled at 4h intervals	Rugnone et al, 2013

Table S2, cluster 85 GO enrichment. Top-scoring GO enriched terms of the genes in cluster 85.

GO.ID	Term	Annotated	Significant	Expected	classicFisher
GO:0009812	flavonoid metabolic process	178	22	2.56	5.1E-15
GO:0009813	flavonoid biosynthetic process	163	21	2.34	9.7E-15
GO:0010224	response to UV-B	78	16	1.12	1E-14
GO:0009411	response to UV	158	19	2.27	7.2E-13
GO:0046283	anthocyanin-containing compound metaboli...	59	11	0.85	5.4E-10
GO:0009744	response to sucrose	144	14	2.07	0.000000015
GO:0034285	response to disaccharide	145	14	2.08	0.000000017
GO:0009416	response to light stimulus	719	30	10.33	0.000000063
GO:0009314	response to radiation	742	30	10.66	0.00000013
GO:0009718	anthocyanin-containing compound biosynth...	43	8	0.62	0.00000014

Table S3, primers. PCR primer sequences for qPCR and ChIP-PCR analyses.

Primer	Sequence
JF16-ACT7-QPCR-F	CAGTGTCTGGATCGGAGGAT
JF17-ACT7-QPCR-R	TGAACAATCGATGGACCTGA
JF149-PHYA-F	AATCTAGAGATCAGGTTAACGC
JF150-PHYA-R	CTTCTTCTGACACATCTTCCT
JF-797-FHL-F	TTATCACGACTCCGAATTTGC
JF-798-FHL-R	TCTTTGGAATCTTGGTTGCTG
JF240-CHS-F	GGACTAAAGGAAGAGAAGATGAG
JF241-CHS-R	TCTAGTATGAAGAGAACGCAC
GT-1479-F3H-F	CAGATCGTTGAGGCTTGTGAGA
GT-1480-F3H-R	GACGAGTCATATCCGCCACTAAGT
JF266-PRR9-F	CTGCGTGGGAGGTTCTAAAG
JF267-PRR9-R	GCAGCACCTCTCAGCATACA
JF118-CCA1-F	CTGTGTCTGACGAGGGTCGAA
JF119-CCA1-R	ATATGTAAAACTTTGCGGCAATACCT
JF262-ELF4-F	CGACAATCACCAATCGAGAATG
JF263-ELF4-R	AATGTTTCCGTTGAGTTCTTGAATC
JF329-GI-F	GGTCGACGGTTTCTCCAATCTA
JF330-GI-R	CGGACTATTCATTCCGTTCTTC
JF321-TOC1-F	TCTTCGCAGAATCCCTGTGAT
JF322-TOC1-R	GCTGCACCTAGCTTCAAGCA
JF311-LUX-F	TGCTCATCATCTTCACAAACC
JF312-LUX-R	CTTCCTCTCCCATTTCAAACTC
JF304-PRR7-F	CTTTCTCAAGGTATAATCCAGCC
JF305-PRR7-R	ACAATCATATGCTGCTTCAGTC

Table S4, model parameters. Parameters for the ODE model of phyA signalling.

Parameter name	Value	Units	Description
k_s1	0.1	conc/h	Basal rate of synthesis of PHYA mRNA
k_s2	2	conc/h	PIF-dependent rate of synthesis of PHYA mRNA
k_s3	1	1/h	Rate of phyA_R translation
k_s4	0.04	conc/h	Basal rate of synthesis of X mRNA
k_s5	0.24	conc/h	phyA_FR-dependent rate of synthesis of X mRNA
k_d1	0.7	1/h	Rate of degradation of PHYA mRNA
k_d2	0.5	1/h	Rate of degradation of phyA_R
k_d3	2.5	1/h	Rate of degradation of phyA_FR
k_d4	0.5	1/h	Rate of degradation of X mRNA
k_r	0.3	1/h	Dark reversion rate of phyA_FR
k_a1	0.01	1/h	Basal activation rate of phyA_R
k_a2	1	1/h	Light-dependent activation of phyA_R
K_1	0.7	conc	Michaelis-menten constant for activation of PHYA mRNA synthesis by PIFs
K_2	0.3	conc	Michaelis-menten constant for activation of X mRNA synthesis by phyA_FR

Datafiles

Datafile 1, gene list descriptions. Short descriptions of all curated gene lists taken from literature.

Datafile 2, gene clustering. Tab-separated file listing gene IDs (left-hand column) and their corresponding cluster (right-hand column).

Datafile 3, cluster enrichment scores. -log10(pval) for the overenrichment of each gene list (rows) in each cluster (columns).

Materials and Methods

Coexpression clustering

The gene expression datasets used for clustering were microarray timeseries from short days vs long days in WT (Ler) (1), WT (Col) vs lux (1), WT (Ler) vs LHYox (1), and WT (Col) vs *pifQ* (2), and RNA-seq timeseries from WT (Col) vs lnk1;lnk2 (3).

The subset of 10,297 transcripts chosen for clustering were selected on the basis of their identification as being rhythmically expressed in diurnal conditions in the microarray experiments of (4). Clustering was performed in Python using the scikit-learn affinity propagation clustering algorithm (parameters: damping = 0.5, preference = -14). Similarities between genes were defined by calculating Pearson's correlation coefficient across each dataset listed above, and then summing these coefficients. This measure of similarity allows genes to cluster by similarity of their dynamics in a particular experiment, rather than by changes in average expression across experiments in different growth conditions, developmental stages etc., processed by different labs.

Plant material and growth conditions

Columbia-0 (Col-0) wild type and mutants were used for experiments. The mutant alleles corresponded to: *phyA* (*phyA-211*), *pif4 pif5* (*pif4-2*, *pif5-2*), *pifQ* (*pif1-1*, *pif3-3*, *pif4-2*, *pif5-2*), *phyA pif4 pif5* (*phyA-211*, *pif4-101, pif5-3*). Over expressing plants included 35S::PIF4-HA and 35S::PIF5-HA. All have been previously described (5-7). Seeds were surface sterilized, sown in GM-agar media and stratified in darkness for 3 days at 4°C before given a 3 h white light pulse to induce germination. Seedlings were kept in the dark for 2 days at 22°C and transferred to Short Days (8L:16D) or Long Days (16L:8D) (22°C, white light 100 μmol m^{-2} s^{-1}) for two weeks before harvesting at the indicated time. All samples were processed in biological triplicates.

RNA isolation and transcript levels analysis by qPCR

For quantitative PCR (qPCR) experiments seedlings were prepared and sown as previously described. In brief, seedlings were grown for 2 weeks at 22°C in SD or LD photoperiods (white light 100 μmol m^{-2} s^{-1}). Samples were collected in liquid nitrogen and RNA was extracted with RNeasy Plant Mini kit (Qiagen). cDNA synthesis was performed using the SuperScript VILO cDNA synthesis kit (Invitrogen). The qPCR was performed with a LightCycler 480 (Roche). All samples were processed in biological triplicates. Primers used for qPCR gene expression analyses

are listed in Supplementary Table S3.

Chromatin Immunoprecipitation assays

ChIP assays were conducted according to (8) except that 2 week old plants were used for the assay. Plants were grown for two weeks in short days (8L:16D white light, 100 µmol m^{-2} s^{-1}) at 22°C, and samples were collected at the end of the two weeks at ZT0. The sequences of the primers used in these experiments to amplify PBE-box containing promoter region of phyA are shown in Table S3.

phyA Immunoblots

Total proteins were extracted from 100 mg of tissue from plants grown under short or long days for two weeks (see plant material and growth conditions) and harvested at the indicated times on day 14. Two separate experiments were performed for Supplementary Fig S5A and B.

For Supplementary Fig S5A (phyA quantification in short and long days): Total protein was extracted from seedlings grown under short days or long days for 2 weeks, and harvested at each time point on day 14. Whole protein extract was extracted using a buffer containing 50 mM Na-phosphate (pH 7.4), 100 mM NaCl, 10% (v/v) glycerol, 5 mM EDTA, 1 mM DTT, 0.1% Triton X-100, 50 µM MG-132, 2mM Na3VO4, 2 mM NaF, and Pierce Protease Inhibitor Tablets, EDTA-free (Thermo Fisher Scientific). All extraction procedure was performed under dim white light in 4°C. 30 µg protein in each sample was run in 8% SDS-PAGE gels, and transferred to Nitrocellulose membranes (Bio-rad). phyA protein was detected by using anti-PHYA antibody (a kind gift from Dr. Akira Nagatani, Kyoto Univ.) at a dilution of 1:3000, whereas actin protein was detected by anti-actin antibody (MA1-744, Life Technologies) at a dilution of 1:5000, followed by a HRP-condugated goat anti-mouse antibody (Thermo Fisher Scientific) at a dilution of 1:10,000. Immunoreactive proteins were visualized with SuperSignal West Pico Chesmiluminescent Substrate (Thermo Fisher Scientific) and Amersham ECL Select Western Blotting Detection Reagent (GE healthcare). For protein quantification, signals from immunoblottted membranes incubated in chemiluminescent detection reagents were imaged and quantified by a high sensitivity cooled CCD camera system (NightOWL, Berthold) and the IndiGo program (Berthold). Actin was used for normalization of a protein in whole extract.

For Supplementary Fig S5B (phyA quantification in PIF mutants): Protein was extracted in a buffer containing 100 mM Tris-HCl pH 8, 50 mM EDTA, 150 mM NaCl, 10% glycerol, 5,M MgCl2, 1 mM DTT, 1mM PMSF, 50 uM MC132 and 1% protease complete inhibitor cocktail with no EDTA (Roche). Extraction was conducted under green safe light at 4°C. Samples were ground in liquid nitrogen and powder resuspended by vortexing. Samples were incubated at 4°C with rotation in darkness for 15 min, centrifuged in darkness at 4°C for 5 min at maximum speed. Supernatant was recovered and used to measure total protein by Bradford. 30 µg of total protein were loaded. Samples were run in a 10% PAGE-SDS gel, followed by wet transfer to nitrocellulose. phyA protein was detected using the AA01antibody (from Akira Nagatani, Kyoto University) at a dilution of 1:1000 (working solution 1 mg/ml) and probing with mouse-anti horseradish peroxidase antibody (1:5000 dilution). Loading was confirmed by reprobing the membranes with an anti-goat UGP-ase antibody (Agrisera) at 1:1000 dilution followed by a HRP-conjugated sheep anti-goat antibody

(Biorad) at a 1:5000 dilution. Signal was detected with Amersham ECL kit (GE Health care) according to the manufacturer's protocol. Quantification was performed using Image-J software.

Anthocyanin measurements

For the anthocyanin measurements, samples were grown under our standard SD and LD conditions for two weeks, and anthocyanin measurement was performed as described in (9). For anthocyanin extraction, 50 mg of seedling tissue were incubated with gentle mixing in 300 ul of extraction buffer (methanol containing 1% HCl) overnight at 4C in the dark. After extraction, 200 ul of water and 200 ul of chloroform were added to each sample, and absorbances read at 530 and 657 nm. Anthocyanin content was determined using the formula: absorbance at 530 nm (A530) – 0.33A657. Each sample was extracted and measured in biological triplicates.

Mathematical model of phyA signalling

The model of phyA signalling is an ODE model based on a simplification of the model by Rausenberger et al (10), integrated with ODE models of the circadian clock and PIF signalling pathways (11, 12). A schematic is shown in Fig S11. Here, the model equations are presented and justified in detail. Parameter values are provided in Table S4. MATLAB code is available from https://github.com/danielseaton/seaton2018_phyA_photoperiod_model.

PHYA transcript is governed by the equation:

$$\frac{d[PHYA_m]}{dt} = k_{s1} + k_{s2}\frac{[PIF_{act}]^2}{[PIF_{act}]^2 + K_1} - k_{d1}[PHYA_m]$$

phyA protein in the inactive (R) form is then given by:

$$\frac{d[phyA_R]}{dt} = k_{s3}[PHYA_m] + k_r[phyA_{FR}] - (k_{d2} + k_{a1} + k_{a2}L)[phyA_R]$$

phyA protein in the active (FR) form is given by:

$$\frac{d[phyA_{FR}]}{dt} = (k_{a1} + k_{a2}L)[phyA_R] - (k_{d3} + k_r)[phyA_{FR}]$$

Levels of a downstream transcript are then given by:

$$\frac{d[X]}{dt} = k_{s4} + k_{s5}\frac{[phyA_{FR}]^2}{K_2^2 + [phyA_{FR}]^2} - k_{d4}[X]$$

Data mining of functional genomics datasets

140 gene lists were consolidated from 47 publications, and are listed and described in Datafile 1. These do not include the 387 transcription factor DAP-seq datasets described in (13), and available therein. All gene lists are available for download by downloading the AtEnrich software through PyPI (see https://github.com/danielseaton/AtEnrich for details).

Simulation of natural dawn

Natural dawns in short photoperiods were simulated based on weather data from Edinburgh, UK.

Light intensity data were obtained for 15-30th November and 15-30th January, from 2006 to 2015. These dates correspond to when the photoperiod is ~8h i.e. the short photoperiod condition which is being simulated. We calculated the distribution of times taken to reach 100 μmol m^{-2} s^{-1}. This showed a clear peak around 50min (Fig S10A), which was taken as the 'fast dawn' condition. A 'slow dawn' (90 min duration) was chosen to represent the tail of the distribution of dawn durations (Fig S10A). These dawns were simulated in the growth chamber by increasing the light intensity in 10μmol $m^{-2}s^{-1}$ increments, to reach 100 μmol $m^{-2}s^{-1}$ at the specified time.

1. Michael TP, Breton G, Hazen SP, Priest H, Mockler TC, Kay SA, et al. A morning-specific phytohormone gene expression program underlying rhythmic plant growth. PLoS biology. 2008;6:e225.
2. Leivar P, Tepperman JM, Monte E, Calderon RH, Liu TL, Quail PH. Definition of Early Transcriptional Circuitry Involved in Light-Induced Reversal of PIF-Imposed Repression of Photomorphogenesis in Young Arabidopsis Seedlings. The Plant Cell. 2009;21:3535-53.
3. Rugnone ML, Faigón Soverna A, Sanchez SE, Schlaen RG, Hernando CE, Seymour DK, et al. LNK genes integrate light and clock signaling networks at the core of the Arabidopsis oscillator. Proceedings of the National Academy of Sciences of the United States of America. 2013;110:12120-5.
4. Bläsing OE, Gibon Y, Günther M, Höhne M, Morcuende R, Osuna D, et al. Sugars and Circadian Regulation Make Major Contributions to the Global Regulation of Diurnal Gene Expression in Arabidopsis. The Plant Cell. 2005;17:3257-81.
5. Hornitschek P, Kohnen MV, Lorrain S, Rougemont J, Ljung K, López-Vidriero I, et al. Phytochrome interacting factors 4 and 5 control seedling growth in changing light conditions by directly controlling auxin signaling. The Plant Journal: For Cell and Molecular Biology. 2012;71:699-711.
6. Leivar P, Tepperman JM, Cohn MM, Monte E, Al-Sady B, Erickson E, et al. Dynamic Antagonism between Phytochromes and PIF Family Basic Helix-Loop-Helix Factors Induces Selective Reciprocal Responses to Light and Shade in a Rapidly Responsive Transcriptional Network in Arabidopsis. The Plant Cell. 2012;24:1398-419.
7. Lorrain S, Trevisan M, Pradervand S, Fankhauser C. Phytochrome interacting factors 4 and 5 redundantly limit seedling de-etiolation in continuous far-red light. Plant J. 2009;60(3):449-61.
8. Moon J, Zhu L, Shen H, Huq E. PIF1 directly and indirectly regulates chlorophyll biosynthesis to optimize the greening process in Arabidopsis. Proceedings of the National Academy of Sciences of the United States of America. 2008;105:9433-8.
9. Shin J, Park E, Choi G. PIF3 regulates anthocyanin biosynthesis in an HY5-dependent manner with both factors directly binding anthocyanin biosynthetic gene promoters in Arabidopsis. Plant J. 2007;49(6):981-94.
10. Rausenberger J, Tscheuschler A, Nordmeier W, Wüst F, Timmer J, Schäfer E, et al. Photoconversion and nuclear trafficking cycles determine phytochrome A's response profile to far-red light. Cell. 2011;146:813-25.
11. Seaton DD, Smith RW, Song YH, MacGregor DR, Stewart K, Steel G, et al. Linked circadian outputs control elongation growth and flowering in response to photoperiod and temperature. Molecular Systems Biology. 2015;11.
12. Pokhilko A, Fernández AP, Edwards KD, Southern MM, Halliday KJ, Millar AJ. The clock gene circuit in Arabidopsis includes a repressilator with additional feedback loops. Molecular Systems Biology. 2012;8:574.
13. O'Malley RC, Huang S-sC, Song L, Lewsey MG, Bartlett A, Nery JR, et al. Cistrome and Epicistrome Features Shape the Regulatory DNA Landscape. Cell. 2016;165:1280-92.

Phytochrome, Carbon Sensing, Metabolism, and Plant Growth Plasticity[1][CC-BY]

Johanna Krahmer, Ashwin Ganpudi, Ammad Abbas, Andrés Romanowski, and Karen J. Halliday[2]

Institute for Molecular Plant Sciences, School of Biological Sciences, University of Edinburgh, Edinburgh EH9 3BF, United Kingdom

ORCID IDs: 0000-0001-7728-5110 (J.K.); 0000-0002-9515-3899 (A.G.); 0000-0003-1678-9985 (A.A.); 0000-0003-0737-2408 (A.R.); 0000-0003-0467-104X (K.J.H.).

Plants continuously monitor fluctuations in their environment and actively adjust their metabolism to cope with variations in light and carbon resource availability. However, the links between photoreceptor signaling pathways and central metabolism are poorly understood. Emerging evidence suggests that phytochrome photoreceptor signaling and carbon resource management are strongly coupled. In this review, we outline the current understanding of how phytochrome-dependent light signaling interfaces with metabolism and carbon resource management.

The ability to sense and react to the light environment enables plants to adapt to and thrive in a changing environment. Post germination, seedlings adopt either a skotomorphogenic or photomorphogenic developmental program, depending on whether light is available. The skotomorphogenic strategy is adopted by dark-grown seedlings, which exhibit elongated hypocotyls and closed cotyledons that are folded against the hypocotyl in a so-called apical hook. This growth program relies on seed reserves to seek light through rapid hypocotyl extension. By contrast, when exposed to light, seedlings undergo photomorphogenic growth, which typically prevents hypocotyl elongation and, instead, promotes cotyledon expansion and greening, processes that enable seedlings to begin photoautotrophic growth. To support photomorphogenic development, plants have evolved multiple families of photoreceptors that capture a wide range of the light spectrum. These include UVB-RESISTANCE8, which detects UV-B light, cryptochromes (crys), phototropins, and the ZEITLUPE/FLAVIN-BINDING, KELCH REPEAT, F BOX 1/LOV KELCH PROTEIN2 family of photoreceptors, which absorb UV-A and blue light, and the phytochromes (phys), which sense red (R) and far-red (FR) light (Galvão and Fankhauser, 2015). This review will focus on the phy photoreceptors, whose unique photosensory properties can profoundly influence plant growth and development.

The phys are a multigene family; for instance, the Arabidopsis (*Arabidopsis thaliana*) genome encodes five *PHY* genes, designated *PHYA* to *PHYE*. These photoreceptors are synthesized in the cytosol in their inactive Pr form. R light exposure drives Pr photoconversion to the biologically active Pfr form (Li et al., 2011). Pfr is then translocated into the nucleus, where it negatively regulates transcription through direct binding to PHYTOCHROME INTERACTING FACTORS (PIFs), basic helix-loop-helix (bHLH) transcription factors that are negative regulators of photomorphogenesis. Phy interaction with PIFs has the dual effect of sequestering PIFs from their cognate promoters and promoting PIF phosphorylation and proteolysis (Leivar and Quail, 2011; Park et al., 2012). In parallel, phys indirectly suppress the COP1 E3 ubiquitin ligase/SPA complex (Sheerin et al., 2015), which mediates the turnover of PHYA and PHYB and positive regulators of photomorphogenesis, such as HY5, HYH, LAF1, and LONG HYPOCOTYL IN FAR RED (HFR1; Wang and Wang, 2015). In darkness, these transcription factors are targets of 26S proteasome-mediated degradation by the COP1 E3 ligase component (Lau and Deng, 2012).

As light exposure elicits distinct and quantifiable growth and molecular changes post germination, the seedling system has proved to be invaluable in delineating the photoreceptor roles and signaling events.

ADVANCES

- Phytochrome depletion targets a wide range of photosynthetic processes and transcriptionally regulates various photosynthetic components, such as chlorophyll and carotenoid biosynthetic genes.
- Phytochrome signaling affects the abundance of a wide range of primary metabolites, such as organic acids, amino acids, sugars, and starch.
- Photoreceptor-related signaling components help transduce metabolic signals.

[1] This work was funded by studentships from the Darwin Trust to A.A. and A.G., the BBSRC (BB/M025551/1 and BB/N005147/1), and the Leverhulme Trust (RPG-2015-293).

[2] Address correspondence to karen.halliday@ed.ac.uk.

J.K., A.G., A.A., A.R., and K.J.H. wrote and revised the article; J.K. composed the figure; J.K. and K.J.H. did the editing.

www.plantphysiol.org/cgi/doi/10.1104/pp.17.01437

Such experiments have established that phys are important sensors of irradiance quality and quantity in early development (Strasser et al., 2010; Hu et al., 2013). However, phys also operate postseedling establishment, ensuring that plant development continues to react to local and seasonal changes. Many of these light-driven responses elicit alterations in growth and architecture that may necessitate concomitant changes in carbon resource distribution and management. This review highlights studies that are beginning to uncover connections between phys and central metabolism. The new research is revealing that phy action is not confined to molecular signaling but also strongly impacts metabolism, while the plant's carbon status is relayed back to the phy pathway. This integrated system enables plants to simultaneously adjust growth, resources, and metabolism to a changing environment.

PHYTOCHROMES, MEDIATORS OF PLANT GROWTH PLASTICITY

The general body plan of plants is genetically encoded, but plant architecture can be modified to adjust to the environment that surrounds it. In this sense, external cues, such as light, have a profound effect on the way a plant grows and develops, ultimately affecting a plant's fitness, disease resistance, and productivity (Li et al., 2012). Phys are able to modulate plant plasticity because of their exquisite sensitivity to both fluence rate (light intensity) and light quality (spectral composition). The competing reactions of rapid light-induced photoreceptor activation to Pfr and slower inactivating thermal relaxation to Pr deliver a graded response to fluence rate (Rausenberger et al., 2010; Johansson et al., 2014; Jung et al., 2016; Legris et al., 2016).

This characteristic allows seedlings to calibrate deetiolation and subsequent vegetative growth with the available light levels. Sensitivity to spectral composition arises from the unique photochemical properties that allow phys to detect small changes in the R-FR ratio caused by nearby plants. The neighbor-sensing system allows plants to reprogram their growth and metabolism such that they can cope better with potential shading and competition for resources. This suite of changes in plant physiology and development is collectively referred to as the shade avoidance response (SAR). While several phys contribute to SAR, phyB plays a particularly prominent role. Indeed, *phyB* mutants display classical SAR phenotypic traits, but additional mutations increase the severity of the phenotype (Franklin and Whitelam, 2005; Martínez-García et al., 2010; Leivar and Quail, 2011; Casal, 2012). In Arabidopsis, SAR characteristics include perturbed seedling deetiolation (the switch to photomorphogenic growth), altered leaf architecture, typified by elongated petioles and small leaf blades, reduced biomass, and early flowering (Li et al., 2012; Galvão and Fankhauser, 2015; Yang et al., 2016; Fig. 1A). Phys, therefore, provide a versatile sensory system that can detect intrusive vegetation, shading, or persistent cloud cover and elicit adaptive changes (Galvão and Fankhauser, 2015).

A series of studies have shown that PIFs operate antagonistically to phys, as positive regulators of the SAR response. Although seven members of the PIF family can interact with PHYs, only PIF4, PIF5, and PIF7 have unambiguously been shown to mediate this response, with PIF1 and PIF3 playing minor roles (Leivar and Quail, 2011; Casal, 2012; Leivar and Monte, 2014; de Wit et al., 2015, 2016). As PIFs are phosphorylated by phyB Pfr and targeted for degradation, under low R-FR ratio conditions that switch phyB Pfr to its inactive Pr form, PIF4 and PIF5 proteins accumulate (Lorrain et al., 2008). Interestingly, while phyB also induces PIF7 phosphorylation, this does not trigger PIF7 degradation; rather, it inactivates it, blocking the transcriptional regulation of target genes. A low R-FR ratio, therefore, strongly promotes PIF action by boosting PIF4 and PIF5 levels and by allowing for PIF7 action (Li et al., 2012).

PIF4, PIF5, and PIF7 are known to mediate SAR by directly targeting genes involved in auxin biosynthesis and other hormone signaling pathways, including GA, brassinosteroid (BR), jasmonate, and ethylene (Leivar and Monte, 2014).

The SAR is negatively regulated by the atypical bHLH transcription factors HFR1 and PHY RAPIDLY REGULATED1 (PAR1) and PAR2 (Galstyan et al., 2011). These proteins suppress PIF action by binding to their DNA-binding domain and affecting their biological activity (Hao et al., 2012; Zhou et al., 2014). Interestingly, PIFs induce the expression of these genes, which suggests that HFR1 and PARs operate in a negative feedback loop that may be important to moderate the SAR response. These studies have shown that the phy-PIF regulatory mechanism provides a means to directly couple light sensing with transcriptional regulation and growth. This system is a central driver of plastic growth responses enabling plants to adapt to changeable light conditions.

PHYTOCHROME CONTROL OF PHOTOSYNTHETIC CAPACITY

A very prominent feature of seedling establishment conditions is the development of chloroplasts and their preparation for photosynthetic function. This section will review the expanding body of evidence that links phy to photosynthetic competence.

Several studies have shown that phys are important regulators of photosynthetic pigment abundance. R light treatment of wild-type seedlings has been shown to induce the formation of chlorophyll within hours (Ghassemian et al., 2006), while sequential phy depletion in R-grown *phyB*, *phyABDE*, and *phyABCDE* mutant seedlings leads to concomitant reductions in chlorophyll levels (Hu et al., 2013). In older plants, severe phy deficiency or a low R-FR ratio also lowers chlorophyll levels per biomass unit, but not to the same

A

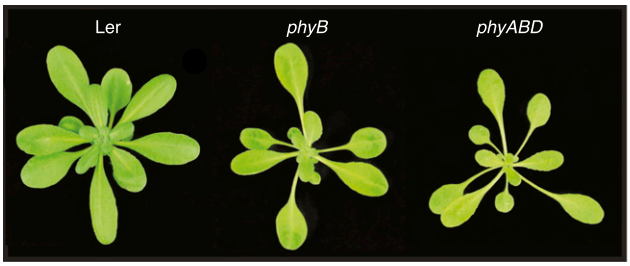

≤ 0.6 (5th percentile) — 1 (no change) — ≥ 4.6 (95th percentile)

B

Publication	Jumtee et al 2008		Jumtee 2009		Yang et al 2016		Han et al 2017	Fukushima et al 2009							Publication
Species	*Arabidopsis*		rice		*Arabidopsis*		*Arabidopsis*	*Arabidopsis*							Species
Experiment	Etiolated seedlings FR or W treated at 0h, sampling after 24h. (*phyA*/D) / (WT/D)		Young and mature leaf		EOD and EON		EOD and EON, different lights	Time course in LD							Experiment
Genotypes	*phyA* vs WT		*phyABC* vs WT		*phyABDE* and *phyABCDE* vs WT		*phyAB* vs WT	*prr975* vs WT							Genotypes
Plant age	4 days		25 to 30 days		35 days		20 days	18 to 19 days							Plant age
Light regime	etiolated, then FR or W		LD 14.5:9.5		2 weeks LD8:16, 3 weeks LD12:12		LD16:8	LD12:12							Light regime
Temperature	21°C		28°C (day) 23°C (night)		18°C		20°C (day), 16°C (night)	22°C							Temperature
Samples	FR	W	YL	ML	EON	EOD	*phyAB*	7	9	11	13	15	17	19	Samples
Glucose	+		+	+		+			-	-	-	-	-	-	Glucose
Fructose	+		+	+				-	-	-	-	-	-	-	Fructose
Galactose	+		+	+			-	na	na	na	na	na	na	na	Galactose
Sucrose	+					+									Sucrose
Maltose	na	na	-	-				na	na	na	na	na	na	na	Maltose
Trehalose	na	na		-	+									-	Trehalose
Raffinose	na	na	+	+	+	+		+	+	+	+	+	+	+	Raffinose
Succinate			-	-	+	+	-	+	+	+	+	+	+	+	Succinate
Fumarate			+		+	+		+	+	+	+	+	+	+	Fumarate
Malate			+	+	+	+	na	+	+	+	+	+	+	+	Malate
Citrate			+		+	+	-	+	+	+	+	+	+	+	Citrate
2-Oxo-glutarate	na	na	+	-	na	na	na	+	+	+	+	+	+	-	2-Oxo-glutarate
Alanine			+	-	-					+		-	+	-	Alanine
Valine	+		+	-	+	+	-				+		+	+	Valine
Leucine	+		+		+		-								Leucine
Isoleucine	+		+	-	na	na	-	+	+	+	+		+		Isoleucine
Proline	+		+		+	+		+	+	+	+	+	+	+	Proline
Glycine	+		+		na			+	+	+	+	+	+		Glycine
Serine	+									-			+		Serine
Threonine	+		+	-		-	-			-		-	+	-	Threonine
Aspartate			-	-	+	+	-				+	+	+		Aspartate
Methionine	+	+	+		na	na		+	+		+		+		Methionine
Glutamate			+	-	+	+	-	+	+	+	+	+	+	+	Glutamate
Phenylalanine	+	+		-	+	+			-	-	-	+	+	+	Phenylalanine
Lysine	+		+	-	na	na	-	-	-						Lysine
Tyrosine	+		+		na	na									Tyrosine
Tryptophan			na	na	na	na		-	-	-			+		Tryptophan
Asparagine			+					+		+	+		+		Asparagine
Glutamine	na	na			+	+	na	+	+	+	+	+	+	+	Glutamine
Homoserine	na	na	na	na	na	na	-		+		+	-	+		Homoserine
Arginine	na	na	na	na	na	na		-	-	-	-		+		Arginine
Putrescine	+		na	na	na	na						+	+		Putrescine
Ornithine			na	na	na	na									Ornithine
Glycerate			-		na		-	+	+	+	+	+	+		Glycerate
Pyruvate			+		na	na									Pyruvate
Lactate			-	-			na		-						Lactate
Shikimate	na	na	-	-	na	na	na	+	+	+	+	+	+	+	Shikimate
Ascorbate	na	na	na	na	na	na		+	+		+	+	+	+	Ascorbate
Nicotinate	na	na	na	na	na	na		+	+	+	+	+	+	+	Nicotinate

Figure 1. Phytochrome affects biomass, plant architecture, and carbon metabolism. A, Images of Arabidopsis Landsberg *erecta* wild type (Ler) and the phytochrome mutants *phyB* and *phyABD*. B, Lack of phytochrome signaling leads to enhanced levels of several organic acids, sugars, and amino acids in most studies. The heat map visualizes fold changes in soluble metabolite content in phytochrome mutants and the *prr975* mutant compared with wild-type (WT) controls, or in response to low R-FR ratio, as seen in gas chromatography-mass spectrometry (GC-MS) data sets (Jumtee et al., 2008, 2009; Fukushima et al., 2009; Yang et al., 2016;

extent as in seedlings (Hu et al., 2013; Patel et al., 2013; Yang et al., 2016). In tomato (*Solanum lycopersicum*), phy effects on chlorophyll levels also are quite evident in adult plants (Kharshiing and Sinha, 2016).

Over the years, a solid body of work has strongly implicated phys in the transcriptional regulation of photosynthesis-related genes. *CAB* and *RBCS* were among the first known phy-regulated genes (Silverthorne and Tobin, 1984; Mösinger et al., 1985; Nagy et al., 1986; Otto et al., 1988; Dean et al., 1989; Wehmeyer et al., 1990; Thompson and White, 1991). These early studies implicated phy in the rapid accumulation of *CAB* and *RBCS* mRNA following exposure to R light. Later research provided genetic evidence for phy control of the chlorophyll biosynthesis gene *HEMA1* and the light-harvesting complex component *LHCB2* (McCormac and Terry, 2002). This role was confirmed by microarray studies illustrating that R light treatment of etiolated seedlings led to broad changes in the expression of genes involved in photosynthesis or chloroplast development (Leivar et al., 2009). Moreover, in darkness, about 60% of these genes also are significantly up-regulated in *pifQ* mutants, which lack PIF1, PIF3, PIF4, and PIF5. This indicates that, in the dark, PIFs have an important role in suppressing photosynthetic gene expression (Leivar et al., 2009).

In addition to these observations, the molecular mechanisms leading to the reduction in chlorophyll levels have been investigated. Two reports (Toledo-Ortiz et al., 2010, 2014) showed that PIFs and the bZip transcription factor HY5 antagonistically regulate chlorophyll and carotenoid biosynthesis. Carotenoids assist photosynthesis by acting as auxiliary antennae for light absorption. These studies demonstrated that both PIFs and HY5 can bind to and potentially compete for G-boxes on the promoters of carotenoid and chlorophyll biosynthetic genes, such as *PHYTOENE SYNTHASE*, *VIOLAXANTHIN DEEPOXIDASE* or *PROTOCHLOROPHYLLIDE OXIDOREDUCATASE C*, *GENOMES UNCOUPLED5* (*GUN5*), and *LIGHT-HARVESTING CHLOROPHYLL-PROTEIN COMPLEX I SUBUNIT A4*. Pigment and transcript levels for these genes are accordingly low in the *hy5* mutant and elevated in the quadruple *pifQ* mutant. As phys negatively regulate PIFs but promote HY5 action, this dual-control transcriptional mechanism conveys exquisite light control of photosynthesis-related genes.

Interestingly, other studies have shown that chloroplast status can feedback to influence the photomorphogenic pathways through chloroplast retrograde signaling (for review, see Chan et al., 2016). Earlier studies hinted that this might be the case (McCormac and Terry, 2004; Nott et al., 2006). A recent study has shown that the *GOLDEN2-LIKE1* (*GLK1*) transcription factor plays a critical role in this process in seedlings (Martín et al., 2016). In darkness, PIFs repress *GLK1* expression, while light inactivates this process, allowing gene regulation and photomorphogenic development to proceed. At high light intensities that may be damaging for the chloroplast, *GLK1* is repressed, this time through *GUN1*-mediated retrograde signaling from the chloroplast. This signal halts photomorphogenic gene expression and development, which serve to protect the seedlings from high-light damage.

In summary, there is ample evidence for transcriptional regulation of photosynthetic genes by phytochromes, especially genes involved in photosynthetic pigment synthesis, and we are now also beginning to understand the role of phytochrome in retrograde signaling and the interplay between both signaling systems.

FINE-TUNING OF PHOTOSYNTHETIC PROCESSES BY PHYTOCHROME

Molecular studies have hardwired the links between phy and photosynthetic gene expression, but photophysiological analysis is required to understand the advantages and disadvantages of altered photosynthetic capacity in phy-dependent adaptive responses (e.g. SAR). A recent study analyzed the contribution of phys and crys to the regulation of proteins involved in chloroplast metabolism and the Calvin cycle, including Rubisco and Rubisco activase (Fox et al., 2015). First, the quadruple *phyA;phyB;cry1;cry2* mutant was shown to have reduced chlorophyll levels, harvesting complex, and Calvin cycle proteins. Then, reduced maximum CO_2 fixation in this quadruple mutant confirmed the impaired activity of the Calvin cycle and electron transport components. These data suggest that phy and cry signaling may not affect simply photosynthetic capacity but the efficiency of the Calvin cycle. Notably, this study also showed that, despite the deficiencies of *phyA;phyB;cry1;cry2* mutants, these were not limiting

Figure 1. (*Continued.*)
Han et al., 2017). Fold changes were calculated by dividing the metabolite content of the mutant (or low R-FR ratio-treated plants) by that of the wild type (or high R-FR-treated plants). For Jumtee et al. (2008), values at 24 h after the start of FR or white light treatment were first normalized by the respective dark control of each genotype at the same time point, and then fold change of *phyA* over the wild type was determined from these values. Experimental setup, samples, and conditions for each study are indicated above the heat map. Fold changes are indicated in colors, with dark blue representing the largest decrease and dark orange representing the largest increase in the mutant over the wild type, or low R-FR over high R-FR ratio. The values of the 5th and 95th percentiles were used as minimum and maximum values, respectively. + and − indicate statistically significant increase and decrease, respectively, according to the statistics employed in each study. EOD, End of day; EON, end of night; LD, light-dark; D, dark; YL, young leaf; ML, mature leaf; na, data are not available for this metabolite. Numbers for Fukushima et al. (2009) indicate time of sampling after light onset in the morning in hours.

for photosynthesis at low light levels but were very restrictive at high fluence rates. Other studies observed reductions in CO_2 uptake in *phyB* and multiallele *phy* mutants at medium and high light levels (Boccalandro et al., 2009; Yang et al., 2016). Conversely, cotton (*Gossypium hirsutum*) plants that overexpress *PHYB* were shown to have higher photosynthetic rates per unit of leaf area and higher biomass (Rao et al., 2011). These data collectively indicate that phy action is important for regulating carbon fixation and biomass production, particularly at high fluence rates. They also suggest that, even though the photosynthetic machinery may be impaired by phy deactivation, it is not necessarily limiting for photosynthesis in low-light environments.

An additional observation was made by Boccalandro et al. (2009), who showed that phyB also increases stomatal density, which is postulated to enhance photosynthetic rate at the expense of water use efficiency. Leaf thickness is another phy-controlled architectural trait that may affect photosynthetic performance. Thiele et al. (1999) showed that potato (*Solanum tuberosum*) plants overexpressing *PHYB* achieve higher photosynthetic rates per plant and per leaf area but have similar rates to wild-type plants when normalized to chlorophyll content. The authors suggested that the thicker palisade tissue and the resulting higher chlorophyll content per unit of leaf area allowed the plants to reach a higher overall photosynthetic rate. Thinner leaves are part of the shade avoidance syndrome (McLaren and Smith, 1978; Franklin and Whitelam, 2005), which necessarily entails a larger leaf area-to-biomass ratio. Therefore, carbon uptake should be normalized to the existing biomass to determine its contribution to growth, and this information is lacking in most studies.

Taken together, these mechanistic and physiological studies are uncovering an important role of phys in managing photosynthetic capacity. In SAR conditions that can be light limiting, reduced investment in the photosynthetic machinery does not appear to impair CO_2 uptake and may relieve the demand on energy reserves, liberating resources for other processes.

PHYS HAVE WIDE-RANGING EFFECTS ON CORE METABOLITES

Following assimilation by photosynthesis, the newly acquired carbon is distributed into different metabolic pathways to either provide energy for maintenance and growth or to biosynthesize metabolites for other components, such as amino acids for protein synthesis. Evidence is emerging that phy signaling has sizable effects on the majority of such primary carbon metabolic pathways and a subset of secondary metabolites. Studies published over the last 11 years reported metabolomics experiments comparing phy mutants with wild-type controls in Arabidopsis and rice (*Oryza sativa*; Ghassemian et al., 2006; Jumtee et al., 2008, 2009; Patel et al., 2013; Yang et al., 2016; Han et al., 2017). One of these studies analyzed metabolic changes during the first 24 h of FR- or white-light induced deetiolation of dark-germinated wild-type and *phyA* seedlings (Jumtee et al., 2008), while Ghassemian et al. (2006) investigated changes due to deetiolation in R light. The other reports (Patel et al., 2013; Yang et al., 2016; Han et al., 2017) focused on metabolic changes in low R-FR ratio or *phy* single and multiallele mutant whole rosettes (more than 2.5 weeks old), while the rice study distinguished between young and mature leaves (Jumtee et al., 2009). Although the results differ, as expected for different experiments, species, and conditions, the general trend indicates that a large number of metabolites, especially sugars and tricarboxylic acid cycle components, accumulate to higher levels in *phy* mutants compared with wild-type plants (for cross-comparison of most of these studies, see Fig. 1B). Interestingly, a large subset of these changes are observed in the *prr975* mutant (Fig. 1B) that lacks the circadian clock genes PSEUDO RESPONSE REGULATOR9 (PRR9), PRR7, and PRR5 (Fukushima et al., 2009). This may not be surprising as, like the *phyB* mutant, *prr975* seedlings have a similar elongated hypocotyl phenotype in R light, suggesting that PRRs may be positive regulators of the phyB pathway (Kato et al., 2007). Indeed, epistasis analysis positions *PRR7* and *PRR5* downstream of phytochrome in this response (Ito et al., 2007). Furthermore, as TOC1 was shown to bind to and repress the activity of PIF3 and PIF4, it is possible that other PRRs suppress PIF signaling in a similar manner (Soy et al., 2016; Zhu et al., 2016). Because of the strong connections between phy signaling and PRRs, we have included the metabolic changes in the *prr975* mutant in this review (Fukushima et al., 2009). The following section will review phy control of sugars and starch, followed by tricarboxylic acid cycle intermediates and amino acids.

Starch and Sugars

Suc is the major sugar used to transport excess carbon from source leaves to sink tissues (Kölling et al., 2013), where it is broken down into Glc and Fru, which are then used by different pathways including respiration. Starch is synthesized during the day and is used as a carbon resource during the night to sustain maintenance and growth in the absence of light (Zeeman et al., 2010).

Jumtee et al. (2008) reported that exposure of etiolated seedlings to FR light led to a phyA-dependent fall in the levels of sugars (including Suc, Glc, Fru, and Gal). Interestingly, white light treatment appeared to be less effective in depleting sugars. As FR light activates deetiolation, but not the greening of cotyledons, under these conditions, the carbon resources may be used for growth but not replenished through photosynthesis.

An intriguing finding is that, even though phy depletion tends to impair photosynthesis, particularly at higher light levels (see above), Arabidopsis phyBD and phyABDE mutants sampled at day 35 overaccumulate daytime sugars and starch (Yang et al., 2016). The rice phyABC triple mutant also has higher daytime sugar

levels compared with the wild type, and this is particularly evident in younger triple mutant leaves that contain excessive levels of the reducing sugars Glc, Fru, and Gal. Like the Arabidopsis phyBD and phyABDE mutants, the rice phyABC mutant has altered starch levels compared with the wild type. However, in rice phyABC, starch is more abundant at night, indicating incomplete usage during the dark period.

Two studies (Fukushima et al., 2009; Han et al., 2017) that sampled around 18 to 20 d (as opposed to 35 d in Yang et al., 2016) reported reduced sugar levels in prr975, phyA, phyB, and phyAB when compared with the wild type. Reflecting this, the phy mutants in the study by Han et al. (2017) also have lower starch. This is interesting, as it illustrates that the impact of phy and PRR signaling on sugar and starch abundance may be dependent on the developmental stage and/or experimental conditions. In fact, Patel et al. (2013) show that rosettes accumulate significantly more soluble sugars (especially Suc) at low R-FR ratios compared with high R-FR ratios at 16°C but not at 22°C. This is a possible explanation for the different results reported by Han et al. (2017; 20°C daytime) and Yang et al. (2016; 18°C), in addition to age, photoperiod, choice of mutant, and light intensity. A consistent finding across studies is that phy deficiency alters sugar levels. Whether this leads to a rise or fall in sugars will potentially depend on the collective effects of phy on carbon uptake and resource use in different conditions or phases of development. More in-depth metabolic flux analysis will be required to decipher the regulatory processes that underlie the sometimes dramatic phy-controlled changes in sugar metabolite levels. Transcriptome studies showed that ~30% of R-induced genes are involved in cellular metabolism (Leivar et al., 2009); therefore, it appears that metabolic changes may result at least in part from transcriptional regulation.

Tricarboxylic Acid Cycle Components and Amino Acids

Photosynthetic carbon is used either for growth and biosynthetic processes or to create ATP, involving glycolysis and the tricarboxylic acid cycle. The intermediates of these processes are used not only in respiration but also in the biosynthesis of other metabolites, such as amino acids (for review, see Fernie et al., 2004). It appears that the majority of tricarboxylic acid cycle organic acids and amino acids are regulated by phy. During FR-induced deetiolation, amino acid concentrations drop in wild-type but not in *phyA* seedlings (Liu et al., 2012). The authors hypothesize that this phyA-mediated effect may arise from an increase in protein synthesis to support growth, which would deplete the amino acid pool. Likewise, the abundance of amino acids drops in response to deetiolation in constant red light within only a few hours (Ghassemian et al., 2006). Han et al. (2017) also record reductions in amino acid and tricarboxylic acid cycle intermediates in *phyA*, *phyB*, and *phyAB* plants long after deetiolation. However, other studies report elevated levels of amino acids and tricarboxylic acid cycle components in adult multiallele *phy* mutants, *prr975*, and young *phyABC* rice leaves (Fukushima et al., 2009; Jumtee et al., 2009; Yang et al., 2016). Among the metabolites measured by Patel et al. (2013), Gly exhibited the largest increase under low R-FR ratio compared with high R-FR ratio at 16°C, but no change was seen at 22°C. Therefore, as for sugars, temperature (but also photoperiod, age, choice of mutants, and light intensity) provides a possible explanation for the differences seen by Yang et al. (2016) and Han et al. (2017).

In cases where organic and amino acids accumulate, it is currently unclear whether this is because of increased production or slower consumption. Transcript profiles of enzymes catalyzing the synthesis of fumarate and citrate reveal that these genes are down-regulated in *phyABDE* mutants (Yang et al., 2016), suggesting that these metabolites are not elevated through transcriptional up-regulation. An alternative hypothesis is that tricarboxylic acid cycle intermediates accumulate due to decreased synthetic processes that use these metabolites. For example, reduced throughput to chlorophyll (which can be low in phy mutants) would increase the pool of chlorophyll biosynthesis precursors, including Glu (Tanaka and Tanaka, 2007). Another possibility is that high levels of amino acids may arise from reduced rates of protein synthesis. The challenge ahead will be to establish whether the metabolic changes observed in phy-deficient plants are an accidental consequence of misregulated growth or whether they are adaptive for light-limiting or FR-rich canopy shade conditions. The apparent conditionality of the phy-dependent metabolic profile suggests that phys may have an important role in ensuring that the metabolic response is aligned with the plant growth strategy (Jumtee et al., 2008, 2009; Yang et al., 2016; Han et al., 2017).

PHY CONTROL OF GROWTH AND BIOMASS

Another open question is whether and how the changes in cellular metabolic processes by phy depletion are linked to biomass accumulation. There is evidence that phy can have a positive effect on biomass accumulation in some conditions. For example, *phyA* tomato mutants, as well as 5-week-old Arabidopsis *phyBD* and *phyABDE* mutants, have substantially less biomass than the respective wild-type controls (Kharshiing and Sinha, 2016; Yang et al., 2016). As discussed above, reduction in photosynthetic rates often is accompanied with a reduction in biomass, and this would be a plausible mechanism leading to a reduction in biomass in phy mutants. Alternatively, inefficient metabolism in phy-deficient plants could contribute to their decreased biomass. To resolve these questions, more quantitative data are needed in order to estimate the contribution of the photosynthetic machinery or metabolic misregulation to biomass accumulation.

CARBON SENSING BY PHY SIGNALING COMPONENTS

Recent studies have shown that, as well as adjusting metabolism, phytochrome signaling responds to endogenous carbon status. In fact, if phytochrome signaling is involved in sensing carbon availability, this opens the question of whether the changes in metabolism and growth in phytochrome mutants and *prr975* arise at least in part from altered carbon reserve sensing. Several studies have delineated close links between central light signaling components, including HY5 and PIFs, and carbon-activated signaling.

HY5 has emerged as a key phytochrome signaling component that links light signal transduction to carbon resource management. Earlier chromatinimmunoprecipitation (ChIP)-chip analysis identified more than 3,500 direct HY5 target genes with a significant enrichment in metabolic, nutrient signaling, and photosynthetic genes (Lee et al., 2007). HY5 was subsequently shown to regulate the expression of chlorophyll biosynthesis and photosynthesis-related genes through direct binding to G-box promoter elements (Toledo-Ortiz et al., 2014). More recently, HY5 was shown to directly enhance the expression of TREHALOSE-6-PHOSPHATE SYNTHASE1 (TPS1) and the Suc efflux transporters SWEET11 and SWEET12. TPS1 elevates levels of trehalose-6-phosphate, a metabolic signaling molecule that controls growth, flowering, and shoot-to-root transport of Suc (Chen et al., 2016). However, HY5 action is not confined to the shoot; it translocates to the root and induces the expression of root-located *HY5*, which, in turn, activates *NRT2.1* transcription and root nitrate uptake. Furthermore, the HY5-induced *NRT2.1* expression in the root appears to be dependent on the shoot metabolic carbon status. Thus, HY5 appears to play a pivotal role in coordinating carbon uptake and growth in the shoot with nitrogen uptake in roots (Chen et al., 2016). Interestingly, COP1-mediated proteolysis of PHYA was shown to be impaired by Suc application, indicating that COP1 could be Suc regulated (Debrieux et al., 2013). It will be interesting to establish if other COP1 targets such as HY5 are regulated by internal carbon status.

The PIF transcription factors were recently implicated in sugar signaling. Suc-induced hypocotyl elongation appears to be PIF dependent, and this response is abolished in the *pifQ* mutant (Stewart et al., 2011). Although Suc only moderately alters *PIF* transcription, PIF5 protein was shown to accumulate in response to Suc (Stewart et al., 2011). A different study by Shor et al. (2017) did not observe Suc effects on the protein stability of PIF1, PIF3, PIF4, and PIF5 but demonstrated through ChIP-quantitative PCR (qPCR) that Suc enhances PIF enrichment at the promoters of the clock genes *LHY* and *CCA1*. This Suc-dependent regulation appears to enhance the peak of *LHY* and *CCA1* expression at dawn. The authors propose that this mechanism may allow PIFs to participate in Suc entrainment of the oscillator. A number of earlier studies demonstrated that PIFs target promoter elements of multiple auxin biosynthetic and signal transduction genes (Franklin et al., 2011; Nozue et al., 2011; Hornitschek et al., 2012). PIFs also have been shown to be required for the Suc regulation of several of these auxin-related rates (Lilley et al., 2012; Sairanen et al., 2012).

The PIF-interacting proteins DELLA and BZR1, master regulators in the GA and BR pathways, respectively, also have been implicated in sugar responses. DELLAs are potent growth suppressors that are known to operate, in part, by directly sequestering PIFs and BZR1 from target promoters (Davière and Achard, 2016). The binding of GA to GID receptors increases GID affinity for DELLAs and initiates their degradation by the 26S proteasome (Davière and Achard, 2016). Recently, Suc (but not Glc) was shown to stabilize the DELLA RGA protein and inhibit its GA-mediated turnover. This stabilized DELLA is necessary for both the Suc-induced up-regulation of the anthocyanin biosynthetic genes and the Suc-induced hypocotyl growth repression in dark-grown seedlings (Li et al., 2014). A separate study using paclobutrazol (PAC) treatment (a GA biosynthesis inhibitor) implicated GA in the Suc induction of hypocotyl elongation in dark-adapted seedlings (Zhang et al., 2010). The BR-regulated transcription factor BZR1 also has been implicated in this dark-dependent Suc response (Zhang et al., 2016). Interestingly, BZR1 has been shown to complex with PIF4 to coregulate light- and hormone-responsive genes (Oh et al., 2012). Zhang et al. (2016) demonstrated that Suc increased the stability of BZR1 in a mechanism proposed to involve Target of Rapamycin (TOR) kinase. TOR is a central component in energy sensing and the regulation of biosynthetic processes such as ribose biogenesis and protein synthesis. Inhibiting TOR activity results in growth arrest and reduced expression of BR-responsive genes (Zhang et al., 2016). Hence, carbon availability controls a growth program through a TOR-dependent BZR1 pathway. Together, this analysis indicates that the PIF-BZR1-DELLA regulatory hub integrates light, carbon, and hormonal signals.

TOR also has been implicated in the integration of carbon and light signaling in the control of leaf initiation at the shoot apical meristem. For some time, phytochrome signaling has been known to control the rate at which leaves develop in Arabidopsis (Halliday et al., 2003). Light was shown to promote leaf initiation and meristematic activity by triggering the localization of the polar auxin transporter PIN1 and cytokinin signaling (Yoshida et al., 2011). More recently, an elegant study in seedlings demonstrated that light signals are relayed to shoot apical meristem cells through a long-distance cytokinin, most likely from the cotyledons (Pfeiffer et al., 2016). Furthermore, TOR kinase conveys both light signaling and energy information to control the expression of *WUSCHEL*, a gene that keeps stem cells in an active state. This finding has advanced our

OUTSTANDING QUESTIONS

- What are the regulatory processes targeted by phytochrome signaling that lead to the changes in metabolite abundance?
- What causes the severe biomass deficiency observed in multi-allele phytochrome mutant plants and how does this tie in with photosynthetic capacity?
- What are the mechanisms of metabolic signal sensing by phytochrome signaling components?

thinking on how light signaling and carbon availability jointly coordinate growth.

CONCLUSION AND FUTURE PERSPECTIVES

We have given an overview of the interrelation of carbon resource management and metabolism and phy signaling. Owing to considerable scientific efforts, a picture is emerging where phys play important roles in driving growth plasticity and biomass production as well as controlling photosynthetic capacity and metabolite levels. However, we are far from fully understanding most of the underlying mechanisms. It is unclear how the known phy signaling mechanisms are connected to the metabolite profiles observed in phy mutants (see Outstanding Questions). Systems or modeling approaches could be used to help delineate these links and to understand the interplay between light signaling, carbon signaling, metabolism, and growth. The Arabidopsis Framework model integrates information from external light inputs, carbon resource production, and allocation to leaves and growth (Chew et al., 2014). This type of modular model could be used to predict the dual action of phytochrome and photosynthesis on resource management and biomass production. A long-term goal will be to understand how light-induced changes in molecular signaling and metabolism control plant plasticity.

Received October 4, 2017; accepted December 11, 2017; published December 18, 2017.

LITERATURE CITED

Boccalandro HE, Rugnone ML, Moreno JE, Ploschuk EL, Serna L, Yanovsky MJ, Casal JJ (2009) Phytochrome B enhances photosynthesis at the expense of water-use efficiency in Arabidopsis. Plant Physiol **150:** 1083–1092

Casal JJ (2012) Shade avoidance. The Arabidopsis Book **10:** e0157,

Chan KX, Phua SY, Crisp P, McQuinn R, Pogson BJ (2016) Learning the languages of the chloroplast: retrograde signaling and beyond. Annu Rev Plant Biol **67:** 25–53

Chen X, Yao Q, Gao X, Jiang C, Harberd NP, Fu X (2016) Shoot-to-root mobile transcription factor HY5 coordinates plant carbon and nitrogen acquisition. Curr Biol **26:** 640–646

Chew YH, Wenden B, Flis A, Mengin V, Taylor J, Davey CL, Tindal C, Thomas H, Ougham HJ, de Reffye P, et al (2014) Multiscale digital Arabidopsis predicts individual organ and whole-organism growth. Proc Natl Acad Sci USA **111:** E4127–E4136

Davière JM, Achard P (2016) A pivotal role of DELLAs in regulating multiple hormone signals. Mol Plant **9:** 10–20

Dean C, Pichersky E, Dunsmuir P (1989) Structure, evolution, and regulation of rbcS genes in higher plants. Annu Rev Plant Physiol Plant Mol Biol **40:** 415–439

Debrieux D, Trevisan M, Fankhauser C (2013) Conditional involvement of constitutive photomorphogenic1 in the degradation of phytochrome A. Plant Physiol **161:** 2136–2145

de Wit M, Keuskamp DH, Bongers FJ, Hornitschek P, Gommers CMM, Reinen E, Martínez-Cerón C, Fankhauser C, Pierik R (2016) Integration of phytochrome and cryptochrome signals determines plant growth during competition for light. Curr Biol **26:** 3320–3326

de Wit M, Ljung K, Fankhauser C (2015) Contrasting growth responses in lamina and petiole during neighbor detection depend on differential auxin responsiveness rather than different auxin levels. New Phytol **208:** 198–209

Fernie AR, Carrari F, Sweetlove LJ (2004) Respiratory metabolism: glycolysis, the tricarboxylic acid cycle and mitochondrial electron transport. Curr Opin Plant Biol **7:** 254–261

Fox AR, Barberini ML, Ploschuk EL, Muschietti JP, Mazzella MA (2015) A proteome map of a quadruple photoreceptor mutant sustains its severe photosynthetic deficient phenotype. J Plant Physiol **185:** 13–23

Franklin KA, Lee SH, Patel D, Kumar SV, Spartz AK, Gu C, Ye S, Yu P, Breen G, Cohen JD, et al (2011) Phytochrome-interacting factor 4 (PIF4) regulates auxin biosynthesis at high temperature. Proc Natl Acad Sci USA **108:** 20231–20235

Franklin KA, Whitelam GC (2005) Phytochromes and shade-avoidance responses in plants. Ann Bot **96:** 169–175

Fukushima A, Kusano M, Nakamichi N, Kobayashi M, Hayashi N, Sakakibara H, Mizuno T, Saito K (2009) Impact of clock-associated Arabidopsis pseudo-response regulators in metabolic coordination. Proc Natl Acad Sci USA **106:** 7251–7256

Galstyan A, Cifuentes-Esquivel N, Bou-Torrent J, Martinez-Garcia JF (2011) The shade avoidance syndrome in Arabidopsis: a fundamental role for atypical basic helix-loop-helix proteins as transcriptional cofactors. Plant J **66:** 258–267

Galvão VC, Fankhauser C (2015) Sensing the light environment in plants: photoreceptors and early signaling steps. Curr Opin Neurobiol **34:** 46–53

Ghassemian M, Lutes J, Tepperman JM, Chang HS, Zhu T, Wang X, Quail PH, Lange BM (2006) Integrative analysis of transcript and metabolite profiling data sets to evaluate the regulation of biochemical pathways during photomorphogenesis. Arch Biochem Biophys **448:** 45–59

Halliday KJ, Salter MG, Thingnaes E, Whitelam GC (2003) Phytochrome control of flowering is temperature sensitive and correlates with expression of the floral integrator FT. Plant J **33:** 875–885

Han X, Tohge T, Lalor P, Dockery P, Devaney N, Esteves-Ferreira AA, Fernie AR, Sulpice R (2017) Phytochrome A and B regulate primary metabolism in Arabidopsis leaves in response to light. Front Plant Sci **8:** 1394

Hao Y, Oh E, Choi G, Liang Z, Wang ZY (2012) Interactions between HLH and bHLH factors modulate light-regulated plant development. Mol Plant **5:** 688–697

Hornitschek P, Kohnen MV, Lorrain S, Rougemont J, Ljung K, López-Vidriero I, Franco-Zorrilla JM, Solano R, Trevisan M, Pradervand S, et al (2012) Phytochrome interacting factors 4 and 5 control seedling growth in changing light conditions by directly controlling auxin signaling. Plant J **71:** 699–711

Hu W, Franklin KA, Sharrock RA, Jones MA, Harmer SL, Lagarias JC (2013) Unanticipated regulatory roles for Arabidopsis phytochromes revealed by null mutant analysis. Proc Natl Acad Sci USA **110:** 1542–1547

Ito S, Nakamichi N, Nakamura Y, Niwa Y, Kato T, Murakami M, Kita M, Mizoguchi T, Niinuma K, Yamashino T, et al (2007) Genetic linkages between circadian clock-associated components and phytochrome-dependent red light signal transduction in Arabidopsis thaliana. Plant Cell Physiol **48:** 971–983

Johansson H, Jones HJ, Foreman J, Hemsted JR, Stewart K, Grima R, Halliday KJ (2014) Arabidopsis cell expansion is controlled by a photothermal switch. Nat Commun **5:** 4848

Jumtee K, Bamba T, Okazawa A, Fukusaki E, Kobayashi A (2008) Integrated metabolite and gene expression profiling revealing phytochrome

A regulation of polyamine biosynthesis of Arabidopsis thaliana. J Exp Bot **59:** 1187–1200

Jumtee K, Okazawa A, Harada K, Fukusaki E, Takano M, Kobayashi A (2009) Comprehensive metabolite profiling of phyA phyB phyC triple mutants to reveal their associated metabolic phenotype in rice leaves. J Biosci Bioeng **108:** 151–159

Jung JH, Domijan M, Klose C, Biswas S, Ezer D, Gao M, Khattak AK, Box MS, Charoensawan V, Cortijo S, et al (2016) Phytochromes function as thermosensors in Arabidopsis. Science **354:** 886–889

Kato T, Murakami M, Nakamura Y, Ito S, Nakamichi N, Yamashino T, Mizuno T (2007) Mutants of circadian-associated PRR genes display a novel and visible phenotype as to light responses during de-etiolation of Arabidopsis thaliana seedlings. Biosci Biotechnol Biochem **71:** 834–839

Kharshiing E, Sinha SP (2016) Deficiency in phytochrome A alters photosynthetic activity, leaf starch metabolism and shoot biomass production in tomato. J Photochem Photobiol B **165:** 157–162

Kölling K, Müller A, Flütsch P, Zeeman SC (2013) A device for single leaf labelling with CO_2 isotopes to study carbon allocation and partitioning in Arabidopsis thaliana. Plant Methods **9:** 45

Lau OS, Deng XW (2012) The photomorphogenic repressors COP1 and DET1: 20 years later. Trends Plant Sci **17:** 584–593

Lee J, He K, Stolc V, Lee H, Figueroa P, Gao Y, Tongprasit W, Zhao H, Lee I, Deng XW (2007) Analysis of transcription factor HY5 genomic binding sites revealed its hierarchical role in light regulation of development. Plant Cell **19:** 731–749

Legris M, Klose C, Burgie ES, Rojas CC, Neme M, Hiltbrunner A, Wigge PA, Schäfer E, Vierstra RD, Casal JJ (2016) Phytochrome B integrates light and temperature signals in Arabidopsis. Science **354:** 897–900

Leivar P, Monte E (2014) PIFs: systems integrators in plant development. Plant Cell **26:** 56–78

Leivar P, Quail PH (2011) PIFs: pivotal components in a cellular signaling hub. Trends Plant Sci **16:** 19–28

Leivar P, Tepperman JM, Monte E, Calderon RH, Liu TL, Quail PH (2009) Definition of early transcriptional circuitry involved in light-induced reversal of PIF-imposed repression of photomorphogenesis in young Arabidopsis seedlings. Plant Cell **21:** 3535–3553

Li J, Li G, Wang H, Deng XW (2011) Phytochrome signaling mechanisms. The Arabidopsis Book **9:** e0074,

Li L, Ljung K, Breton G, Schmitz RJ, Pruneda-Paz J, Cowing-Zitron C, Cole BJ, Ivans LJ, Pedmale UV, Jung HS, et al (2012) Linking photoreceptor excitation to changes in plant architecture. Genes Dev **26:** 785–790

Li Y, Van den Ende W, Rolland F (2014) Sucrose induction of anthocyanin biosynthesis is mediated by DELLA. Mol Plant **7:** 570–572

Lilley JL, Gee CW, Sairanen I, Ljung K, Nemhauser JL (2012) An endogenous carbon-sensing pathway triggers increased auxin flux and hypocotyl elongation. Plant Physiol **160:** 2261–2270

Liu MJ, Wu SH, Chen HM, Wu SH (2012) Widespread translational control contributes to the regulation of Arabidopsis photomorphogenesis. Mol Syst Biol **8:** 566

Lorrain S, Allen T, Duek PD, Whitelam GC, Fankhauser C (2008) Phytochrome-mediated inhibition of shade avoidance involves degradation of growth-promoting bHLH transcription factors. Plant J **53:** 312–323

Martín G, Leivar P, Ludevid D, Tepperman JM, Quail PH, Monte E (2016) Phytochrome and retrograde signalling pathways converge to antagonistically regulate a light-induced transcriptional network. Nat Commun **7:** 11431

Martínez-García JF, Galstyan A, Salla-Martret M, Cifuentes-Esquivel N, Gallemí M, Bou-Torrent J (2010) Regulatory components of shade avoidance syndrome. Adv Bot Res **53:** 65–116

McCormac AC, Terry MJ (2002) Light-signalling pathways leading to the co-ordinated expression of HEMA1 and Lhcb during chloroplast development in Arabidopsis thaliana. Plant J **32:** 549–559

McCormac AC, Terry MJ (2004) The nuclear genes Lhcb and HEMA1 are differentially sensitive to plastid signals and suggest distinct roles for the GUN1 and GUN5 plastid-signalling pathways during de-etiolation. Plant J **40:** 672–685

McLaren JS, Smith H (1978) Phytochrome control of the growth and development of Rumex obtusifolius under simulated canopy light environments. Plant Cell Environ **1:** 61–67

Mösinger E, Batschauer A, Schäfer E, Apel K (1985) Phytochrome control of in vitro transcription of specific genes in isolated nuclei from barley (Hordeum vulgare). Eur J Biochem **147:** 137–142

Nagy F, Kay SA, Boutry M, Hsu MY, Chua NH (1986) Phytochrome-controlled expression of a wheat Cab gene in transgenic tobacco seedlings. EMBO J **5:** 1119–1124

Nott A, Jung HS, Koussevitzky S, Chory J (2006) Plastid-to-nucleus retrograde signaling. Annu Rev Plant Biol **57:** 739–759

Nozue K, Harmer SL, Maloof JN (2011) Genomic analysis of circadian clock-, light-, and growth-correlated genes reveals PHYTOCHROME-INTERACTING FACTOR5 as a modulator of auxin signaling in Arabidopsis. Plant Physiol **156:** 357–372

Oh E, Zhu JY, Wang ZY (2012) Interaction between BZR1 and PIF4 integrates brassinosteroid and environmental responses. Nat Cell Biol **14:** 802–809

Otto B, Grimm B, Ottersbach P, Kloppstech K (1988) Circadian control of the accumulation of mRNAs for light and heat-inducible chloroplast proteins in pea (*Pisum sativum* L.). Plant Physiol **88:** 21–25

Park E, Park J, Kim J, Nagatani A, Lagarias JC, Choi G (2012) Phytochrome B inhibits binding of phytochrome-interacting factors to their target promoters. Plant J **72:** 537–546

Patel D, Basu M, Hayes S, Majláth I, Hetherington FM, Tschaplinski TJ, Franklin KA (2013) Temperature-dependent shade avoidance involves the receptor-like kinase ERECTA. Plant J **73:** 980–992

Pfeiffer A, Janocha D, Dong Y, Medzihradszky A, Schöne S, Daum G, Suzaki T, Forner J, Langenecker T, Rempel E, et al (2016) Integration of light and metabolic signals for stem cell activation at the shoot apical meristem. eLife **5:** e17023

Rao AQ, Bakhsh A, Nasir IA, Riazuddin S, Husnain T (2011) Phytochrome B mRNA expression enhances biomass yield and physiology of cotton plants. J Biotechnol **10:** 1818–1826

Rausenberger J, Hussong A, Kircher S, Kirchenbauer D, Timmer J, Nagy F, Schäfer E, Fleck C (2010) An integrative model for phytochrome B mediated photomorphogenesis: from protein dynamics to physiology. PLoS ONE **5:** e10721

Sairanen I, Novák O, Pěnčík A, Ikeda Y, Jones B, Sandberg G, Ljung K (2012) Soluble carbohydrates regulate auxin biosynthesis via PIF proteins in *Arabidopsis*. Plant Cell **24:** 4907–4916

Sheerin DJ, Menon C, zur Oven-Krockhaus S, Enderle B, Zhu L, Johnen P, Schleifenbaum F, Stierhof YD, Huq E, Hiltbrunner A (2015) Light-activated phytochrome A and B interact with members of the SPA family to promote photomorphogenesis in *Arabidopsis* by reorganizing the COP1/SPA complex. Plant Cell **27:** 189–201

Shor E, Paik I, Kangisser S, Green R, Huq E (2017) PHYTOCHROME INTERACTING FACTORS mediate metabolic control of the circadian system in Arabidopsis. New Phytol **215:** 217–228

Silverthorne J, Tobin EM (1984) Demonstration of transcriptional regulation of specific genes by phytochrome action. Proc Natl Acad Sci USA **81:** 1112–1116

Soy J, Leivar P, González-Schain N, Martín G, Diaz C, Sentandreu M, Al-Sady B, Quail PH, Monte E (2016) Molecular convergence of clock and photosensory pathways through PIF3-TOC1 interaction and co-occupancy of target promoters. Proc Natl Acad Sci USA **113:** 4870–4875

Stewart JL, Maloof JN, Nemhauser JL (2011) PIF genes mediate the effect of sucrose on seedling growth dynamics. PLoS ONE **6:** e19894

Strasser B, Sánchez-Lamas M, Yanovsky MJ, Casal JJ, Cerdán PD (2010) Arabidopsis thaliana life without phytochromes. Proc Natl Acad Sci USA **107:** 4776–4781

Tanaka R, Tanaka A (2007) Tetrapyrrole biosynthesis in higher plants. Annu Rev Plant Biol **58:** 321–346

Thiele A, Herold M, Lenk I, Quail PH, Gatz C (1999) Heterologous expression of Arabidopsis phytochrome B in transgenic potato influences photosynthetic performance and tuber development. Plant Physiol **120:** 73–82

Thompson WF, White MJ (1991) Physiological and molecular studies of light-regulated nuclear genes in higher plants. Annu Rev Plant Physiol Plant Mol Biol **42:** 423–466

Toledo-Ortiz G, Huq E, Rodríguez-Concepción M (2010) Direct regulation of phytoene synthase gene expression and carotenoid biosynthesis by phytochrome-interacting factors. Proc Natl Acad Sci USA **107:** 11626–11631

Toledo-Ortiz G, Johansson H, Lee KP, Bou-Torrent J, Stewart K, Steel G, Rodríguez-Concepción M, Halliday KJ (2014) The HY5-PIF regulatory module coordinates light and temperature control of photosynthetic gene transcription. PLoS Genet **10:** e1004416

Wang H, Wang H (2015) Phytochrome signaling: time to tighten up the loose ends. Mol Plant **8:** 540–551

Wehmeyer B, Cashmore AR, Schäfer E (1990) Photocontrol of the expression of genes encoding chlorophyll a/b binding proteins and small subunit of ribulose-1,5-bisphosphate carboxylase in etiolated seedlings of *Lycopersicon esculentum* (L.) and *Nicotiana tabacum* (L.). Plant Physiol **93:** 990–997

Yang D, Seaton DD, Krahmer J, Halliday KJ (2016) Photoreceptor effects on plant biomass, resource allocation, and metabolic state. Proc Natl Acad Sci USA **113:** 7667–7672

Yoshida S, Mandel T, Kuhlemeier C (2011) Stem cell activation by light guides plant organogenesis. Genes Dev **25:** 1439–1450

Zeeman SC, Kossmann J, Smith AM (2010) Starch: its metabolism, evolution, and biotechnological modification in plants. Annu Rev Plant Biol **61:** 209–234

Zhang Y, Liu Z, Wang L, Zheng S, Xie J, Bi Y (2010) Sucrose-induced hypocotyl elongation of Arabidopsis seedlings in darkness depends on the presence of gibberellins. J Plant Physiol **167:** 1130–1136

Zhang Z, Zhu JY, Roh J, Marchive C, Kim SK, Meyer C, Sun Y, Wang W, Wang ZY (2016) TOR signaling promotes accumulation of BZR1 to balance growth with carbon availability in Arabidopsis. Curr Biol **26:** 1854–1860

Zhou P, Song M, Yang Q, Su L, Hou P, Guo L, Zheng X, Xi Y, Meng F, Xiao Y, et al (2014) Both PHYTOCHROME RAPIDLY REGULATED1 (PAR1) and PAR2 promote seedling photomorphogenesis in multiple light signaling pathways. Plant Physiol **164:** 841–852

Zhu JY, Oh E, Wang T, Wang ZY (2016) TOC1-PIF4 interaction mediates the circadian gating of thermoresponsive growth in Arabidopsis. Nat Commun **7:** 13692